SELECTIVE OXIDATIONS AND CARBON-CARBON BOND FORMING REACTIONS USING TRANSITION METAL CATALYSTS

A THESIS

SUBMITTED TO THE

UNIVERSITY OF PUNE

FOR THE DEGREE OF

DOCTOR OF PHILOSOPHY

IN

CHEMISTRY

BY

TIMMANNA H. BENNUR

CATALYSIS DIVISION

NATIONAL CHEMICAL LABORATORY

PUNE - 411 008, INDIA

April 2003

dedicated to ....

My beloved Parents

&

Guide

CERTIFICATE

Certified that the work incorporated in the thesis entitled **"*Selective oxidations and Carbon-Carbon Bond Forming Reactions Using Transition Metal Catalysts*"** for the degree of Doctor of Philosophy in Chemistry, was carried out by the candidate under our supervision in the Catalysis Division, National Chemical Laboratory, Pune. Such material as has been obtained from other sources has been duly acknowledged in the thesis.

(Dr. S. Sivasanker)   **(Dr. D. Srinivas)**

Research Guide   Research Co-guide

ACKNOWLEDGEMENT

CONTENTS

4. SELECTIVE OXIDATIONS WITH Mn-TMTACN-H$_2$O$_2$ SYSTEM: INFLUENCE OF CARBOXYLATE BUFFER AND ACTIVE Mn SPECIES

5. CARBON-CARBON BOND FORMING REACTIONS OVER Pd CONTAINING HYDROTALCITES

1.1. GENERAL BACKGROUND

Transition metal catalyzed reactions are already established as an important part of synthetic chemistry involving organic transformations like oxidation, reduction and carbon-carbon bond forming reactions [1]. Transition metal complexes of ligands such as porphyrins and salens are capable of catalyzing the oxidation of hydrocarbons even under mild conditions [2-4]. Palladium is the prime metal used in various carbon-carbon coupling reactions like Heck, Suzuki and others [5, 6]. In biological systems, harmful organic molecules like hydrocarbons are metabolized to give water-soluble compounds or biologically important materials by metallo-enzymes. Fe containing Cytochrome P-450 is an important oxygenase enzyme, which catalyzes many oxidations [7]. Manganese ions are involved in a number of fundamental biochemical processes, for example, the photosynthetic conversion of CO_2 into carbohydrate and dioxygen in green plants, algae and some bacteria is known to occur on the active sites of tetranuclear manganese clusters in photosystem II (PS II) [8-12]. Copper is another abundant trace metal in biological systems and is often found as a co-factor in proteins spanning over a wide range of functions. Heme/copper terminal oxidases catalyze the four electron reduction of dioxygen to water [13, 14]. In view of this, model Fe and Mn-porphyrin complexes (Fig. 1.1a) have been investigated for their ability to transfer oxygen atom from different oxygen sources (H_2O_2, ROOH, PhIO etc.) to hydrocarbons [15-19]. Synthetic non-porphyrin transition metal complexes like metal salens are also gaining importance as model systems for non-heme enzymatic oxidation reactions [20-37]. Metal phthalocyanine complexes (Fig. 1.1b) have been extensively studied as biological analogues [38]. The coordination chemistry of cyclic aliphatic amines with

transition metals is well known. These complexes have been investigated for their catalytic behavior in the selective epoxidation of hydrocarbons.

(a)

(b)

M(porphyrin)

M(phthalocyanine)

R = aryl
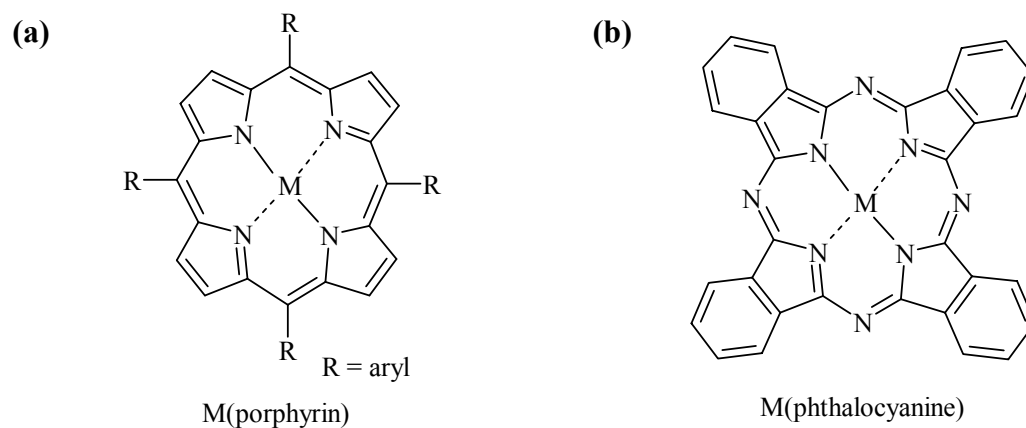
Figure 1.1. *Molecular structures of metal porphyrins (a) and phthalocyanines (b) (M = iron, manganese, etc.).*

Immobilization of transition metal catalysts on solid supports facilitates easy handling and recovery and could result in improved activities and selectivities through support effects [39-41]. Many approaches aimed at heterogenizing precious palladium catalysts for carbon-carbon bond formation reactions have been reported [42]. Metal complexes of porphyrins, salens, phthalocyanines, etc. have been heterogenized using various supports like clays [41], microporous silica [43, 44], mesoporous zeolites [45-52] and polymers [53, 54]. Metal complexes encapsulated in zeolites are called by the acronym, *zeozymes* (zeolite based enzyme mimics). Zeolite lattices with their net negative charge can serve as anions to complexes of metal ions and provide a different environment as well. As a result, catalytic properties of encapsulated metal complexes have been found to be different from those of neat complexes. Besides, the acid-base properties of the zeolite may also influence the products obtained [45].

1.2. HOMOGENEOUS COPPER AND MANGANESE CATALYSTS IN OXIDATION REACTIONS

1.2.1. Schiff Base Complexes

Schiff bases are a class of acyclic ligands that are known to form stable metal complexes due to their *"chelating effect".* In 1889 Combes prepared the copper complex of the Schiff base ligand (Fig. 1.2), for the first time, while studying the effect
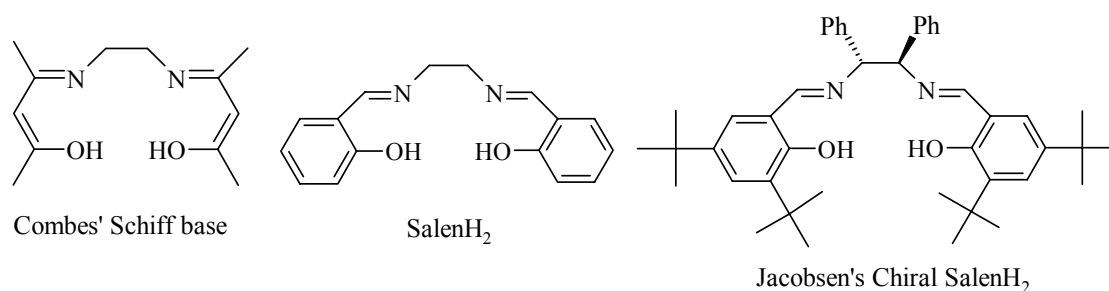
Figure 1.2. *Molecular structures of Schiff base ligands.*

of diamines on diketones [55]. Later on reports appeared on metal salen complexes in 1933 and since then many complexes have been synthesized [56]. At present, metal-salens constitute a standard system in coordination chemistry. The investigation on metal salens took new turn since last decade especially following the discovery of salen catalyzed enantioselective epoxidation of olefins by Jacobsen and Katsuki groups (Fig. 2) [57, 58]. Srinivasan et al. [24] isolated Mn(II)-salen complexes for the first time and used them for epoxidation. There are scattered reports on the use of homogeneous Cu(II) salen complexes in oxidation reactions [59]. The development of chiral salen metal complexes and catalysts has stimulated a rapid growth in the chemistry and application of metal salen complexes.

3

1.2.2. Peraza Macrocyclic Complexes

The peraza crowns or peraza macrocycles are also an important class of cyclic complexing agents for transition metal ions [60]. They form more stable complexes with a variety of metal ions than do the open chain polyamines containing the same number of nitrogen atoms. This extra stability of the metal complexes involving macrocyclic ligands over those with non-cyclic counterparts is called the *"macrocyclic effect"* [61]. The enhanced complexing ability of aza macrocycles for transition-metal ions has made them interesting to researchers in many areas [62-65]. The most important macrocycles are 1,4,7-triazacyclononane (tacn) - a nine membered macrocycle ($[9]aneN_3$), 1,4,7,10-tetraazacyclododecane (cyclen) - a twelve membered macrocycle ($[12]aneN_4$), 1,4,8,11-tetrazacyclotetradecane (cycalm) - a fourteen membered macrocycle ($[14]aneN_4$) and their N-alkylated derivatives (Fig. 1.3). The important N-alkylated derivatives are 1,4,7-trimethyl-1,4,7-triazacyclononane (tmtacn), 1,4,7,10-tetramethyl-1,4,7,10-tetraazacyclododecane (tmcyclen) and 1,4,8,11, tetramethyl-1,4,8,11-tetrazacyclotetradecane (tmcyclam). These macrocycles can be synthesized either "free" or bound to a given metal ion [66, 67]. The preparation of the

M(tacn), R=H   M(cyclen), R=H   M(cyclam), R=H
M(Me₃tacn), R=Me   M(Me₄cyclen), R=Me   M(Me₄cyclam), R=Me

M =Cu^{+2}, Mn^{+2} etc.

Figure 1.3. Molecular structures of copper and manganese perazamacrocyclic complexes.

free macrocycle has many advantages. The macrocycles are usually prepared by Richman-Atkins procedure [68]. In the last two decades metal complexes of these amines (Fig. 1.3) have been extensively studied [61, 69].

1.2.2.1. Copper Complexes

In general, the study of copper complexes as homogeneous oxidation catalysts is not as widely reported as those of the other first row transition metals. Bunce et al. [70] have investigated copper complexes as homogeneous catalysts. Many copper complexes of macrocyclic amines have been designed in order to prepare low molecular weight biomimics of copper(II) containing metalloprotiens. Bis(μ-O) dicopper complexes of N-alkylated tacn have been synthesized and characterized by various spectroscopic techniques [71]. The preparation, spectroscopic properties and crystal structure have been reported for a monomeric Cu(II) compound containing the cyclic triamine tacn [72]. Binuclear Cu(II) complexes of tmtacn (1,4,7-trimethyl-1,4,7-triazacyclononane) bridged by anions like oxalate have also been reported [73]. Kinetic and thermodynamic stabilities of copper triaza macrocyclic complexes have been studied [74, 75]. The dissociation of $[Cu(cyclen)]^{+2}$ in acid solution has been investigated by Hay and Pujari [76]. The copper complex of tetramethylcyclen has also been prepared [77]. Of the several tetradentate macrocyclic ligands known, cyclam is the most studied. Copper cyclam complexes have been prepared and characterized by many researchers [78]. However, the study of copper macrocyles as catalysts for oxidation reactions remains to be explored fully.

1.2.2.2. Manganese Complexes

Since recently, much research is being carried out on the catalytic activity of binuclear manganese complexes with tacn and its N-methyl derivative tmtacn [79-82]. A large number of crystalline structures of complexes like the thermodyanamically

stable tetranuclear complex $[(tacn)_4Mn^{IV}_4O_6(Br)_{3.5}(OH)_{0.5}].6H_2O$ and $[(tmtacn)_2Mn^{III}_2(m\text{-}O)(m\text{-}CH_3CO_2)_2](ClO_4)_2$ dimers have been studied in detail by Wieghardt et al. [83, 84]. Synthesis, crystal structure and biological relevance of the complex $[(tmtacn)Mn^{IV}(\mu\text{-}O)_3Mn^{IV}(tmtacn)](PF_6)_2.H_2O$ and a series of related binuclear manganese complexes have been studied by them [82]. Very recently, De Vos et al. [85, 86] reported that Mn-tmtacn complexes are extremely active catalysts for oxidations with H_2O_2. They also found that *in situ* prepared Mn-tmtacn exhibited efficient and selective catalytic activity for the epoxidation of olefins at ambient conditions using H_2O_2 as the oxidant in the presence of a carboxylic acid buffer [86]. The activity of this catalyst was found to be remarkably high in the presence of oxalate buffer and the reaction was found to be stereospecific for *cis* olefins. The oxalate ligand is believed to act as a co-ligand. In another investigation, Mn-tmtacn-ascorbate buffer was found to surpass the activity of Mn-tmtacn-oxalate buffer in epoxidation and alcohol oxidation [87]. Attempts to induce asymmetry to the epoxide using these catalysts have, however, not been successful. Shulpin et al. [88] activated the C-H bond of saturated alkanes at ambient temperatures using the binuclear Mn(IV) complex $[LMn^{IV}(O)_3Mn^{IV}L]^{2+}$. The synthesis, characterization and the crystal structure of di-μ-oxo-dimanganese(III, IV) and (IV, IV) complexes employing the tetra-dentate ligands 1,4,7,10-tetraazacyclododecane (cyclen) and 1,4,8,11-tetraazacyclotetradecane (cyclam) have also been reported [89, 90]. However, reports on mononuclear complexes of manganese with these polycyclic amines are scarce [91]. It appears that substantial scope exists for studying the catalytic activity of *in situ* prepared Mn-tmtacn complexes in various hydrocarbon oxidations as analogues of biomimic manganese and iron porphyrins.

1.3. HETEROGENIZATION OF HOMOGENEOUS OXIDATION CATALYSTS

Immobilizing the metal complex catalysts by anchoring, incorporating or encapsulating into an organic (polymer / dendrimer) or an inorganic support (metal oxide, zeolite etc.) is an active area of research [92-94]. Many polymer and silica supported porphyrins have been prepared [95, 96]. The process not only allows the separation of the catalyst from the reaction mixture but also sometimes improves its activity and selectivity. Many strategies have been adopted to heterogenize metal complexes.

1.3.1. Heterogenization *via* covalent linking

The metal complex can be anchored to the support material such as SiO_2 through a ligand. For e.g., modified salen ligands have been tethered to polymeric supports/SiO_2 [51, 97, 98]. Mn-tacn and Mn-dmtacn (dmtacn = 1,4-dimethyl-1,4,7-triazacyclononane) anchored to a silica support have been found to possess very good catalytic activity [50, 99]. Subba Rao et al. [50] tethered the copper and manganese complexes of tacn to silica or MCM-41 through glycidylation (Fig. 1.4).
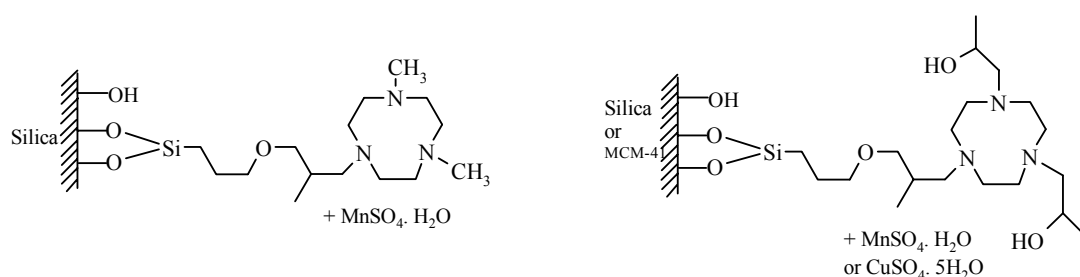
Figure 1.4. Tacn-type ligands covalently bonded on silica.

1.3.2. Heterogenization by encapsulation

It was Herron et al. who encapsulated the Ni(CO)L, complexes entrapped in zeolite X for the first time and referred to such a zeolite guest molecule as *"ship-in-bottle"* complexes [100]. This means that all of the individual components (metal ion and the various ligands) may easily pass in and out of the zeolite but the final assembled coordination complex is too large and rigid to pass out once assembled inside. In later years, cobalt salen was encapsulated in the supercages of zeoite-Y in an attempt to prepare the analogue of hemoglobin and myoglobin following the same principle [101]. As a support, zeolites have the advantage that a metal complex can be physically trapped in the pores (cages) and not necessarily bound to the oxide surface (Fig. 1.5a). So the metal complex is free to move within the confines of the supercages acting as small reaction vessels.

The microporus zeolites X and Y possess large supercages of 12-13 Å diameter with pore openings of ~ 7 Å. Ligands with molecular dimensions smaller than 7Å can easily diffuse inside the zeolite pores. The metal complex once formed is too large to diffuse out. Therefore, usually a method that involves the diffusion of the ligands into the M-zeolites (M = transition metal) and complexation with the metal ion (called the "flexible ligand method") is used to encapsulate metal complexes. Various coordinations are possible in neat complexes but due to geometric restrictions inside the zeolite, the complexes are formed inside the zeolite matrix with certain coordinations only. Mesoporous materials possess pore diameters greater than 20Å. In these systems there is no need to construct metal complexes as in flexible ligand or template synthesis method. They can be directly introduced inside the mesopores of these materials. The metal complexes, however, may be leached out during the preparation itself. In order to achieve better encapsulation, these mesoporous materials have to be modified.
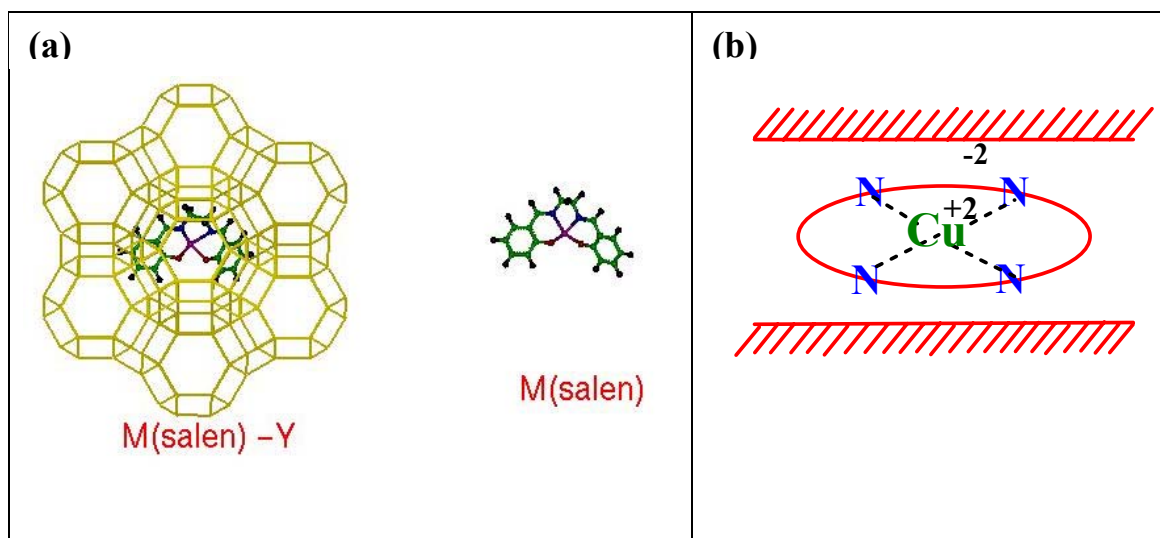
Figure 1.5. *Model diagrams for metal salen complex encapsulated in zeolite-Y (a) and [Cu(cyclen)]$^{+2}$ inside the layers of montmorillonite clay (b).*

The synthesis and characterization of Cu(II) salen encapsulated in zeolite-Y and its catalytic properties in the oxidation of cyclohexanol to cyclohexanone at ambient conditions using H_2O_2 as the oxidant has been reported by Ratnasamy et al. [102]. Later on, the encapsulation of copper and manganese complexes and their application as oxidation catalyst was reported by the same authors [103, 104]. EPR characterization of neat and zeolite encapsulated copper salen complexes have also been reported by them [105]. Mn(II) and Mn(III) salens encapsulated in zeolite matrices have been used in various oxidations [39, 106, 107]. Among the other oxidants, TBHP was found to be the best alternative to PhIO during oxidation with Mn schiff base encapsulated complexes.

Encapsulation can also be achieved by chelation of metal ions exchanged in zeolites by adsorbed ligands. Here, the zeolite lattice itself functions as a charge compensating anion. The complex can still be moving in the pores from one site to another. For e.g., EPR and UV-visible spectroscopic studies of the complexation of exchanged Mn^{+2} or Cu^{+2} with absorbed triamines have revealed the non-stationary

nature of these complexes [108, 109]. Many complexes of cyclic and acyclic amines with manganese have been encapsulated by this method by Knops-Gerrits et al. [110]. They studied the physicochemical behavior of manganese complexes with polypyridines, polyamides, salens and polyamines and their catalytic behavior in selective oxidations with H_2O_2 as oxidant. Both the ligands tacn and tmtacn chelate with intrazeolite Mn. With tacn as the ligand, only decomposition was the main process with little epoxidation. But with tmtacn as the ligand selective epoxidation was the major process. This difference between the ligands may be due to the formation of a hydrogen bond between the N-H group and H_2O_2 increasing the concentration of hydrogen peroxide on the Mn site resulting in its disproportionation. The catalytic activity of Mn(tmtacn) encapsulated in NaY has been found to be comparable to that of homogeneous Mn(tmtacn) catalyst [112]. Yet another example is $[Cu(cyclam)]^{+2}$ intercalated into the layers of montmorillonite cationic clay by Choy et al. (Fig. 1.5b) [111]. However, there are no reports on the encapsulation of copper and manganese complexes of tetraaza macrocycles in zeolites.

1.4. HYDROTALCITES AS HETEROGENEOUS CATALYSTS

In recent years, layered double hydroxides (LDH) or more conveniently called as hydrotalcite (HT) like anionic clays are gaining interest as catalysts, catalyst supports, ion-exchangers and composite materials [113, 116]. They belong to the class of anionic, basic clays having the general formula, $[M^{(II)}_{(1-x)} M^{(III)}_x (OH)_2]^{x+} [(A^{n-})_{x/n} yH_2O]^{x-}$ where x = 0.1-0.33, $M^{(II)}$ = Mg, Cu, Ni, Co, and Mn, $M^{(III)}$ = Al, Fe, Cr, and Ga and A^{n-} is an interlayer anion such as CO_3^{2-}, NO_3^- and SO_4^{2-} [113]. Their calcination at 723 K gives rise to the decomposition of the layer structure and formation of basic mixed oxides having high surface area. These 'spinel type' oxides have shown promise

as catalysts [117, 118]. The characteristic double-layered structure can be associated with different cations and offers a pronounced versatility with regard to the elemental composition. Transition metals, that are expected to act as active sites of catalysts can also be introduced in the brucite layer [114]. Hydrotalcites containing metals like Ni, Cu, Co, Pd etc., have already been reported in the literature [113, 115]. Hydrotalcites with zirconium incorporated into the layers have been used for the selective oxidation of phenol to catechol with H_2O_2 [116]. Kaneda et al. [119] reported the use of Ru-Co-Al-CO_3 HT for the oxidation of alcohols. Choudhary and co-workers [120] have found out that Ni-Al hydrotalcite is active in the oxidation of alcohols using molecular oxygen. They also investigated the application HTs for asymmetric C-C bond-forming reactions [121]. Narayanan et al. [122] studied the hydrogenation of phenol to cyclohexanone over Pd(II) containing Mg-Al hydrotalcites. Very recently, a single-pot biomimic synthesis of chiral diols mediated by a newly developed trifunctional solid catalyst consisting of active palladium, tungsten, and osmium species embedded in a single layered double-hydroxide matrix has been achieved by Choudary et al. [123]. Another important development in LDH catalysis is the nano-palladium immobilized layered double hydroxide (LDH-Pd(0)) catalyzed Heck olefination, Suzuki coupling and Sonogashira reactions of chloroarenes [124]. Unlike other supported Pd catalysts, hydrotalcites incorporated with palladium in their structure could be good catalysts with minimal leaching.

1.5. SELECTIVE OXIDATION OF HYDROCARBONS

The selective oxidation of hydrocarbons, comprising alkanes, olefins and aromatics has far-reaching practical implications [125]. The activation of the inert C–H bond of alkanes at transition-metal centers, under mild conditions and with high selectivity is

extremely important. Although profitable practical applications have not yet been developed, the understanding of how these organometallic reactions occur, and what their inherent advantages and limitations are, has progressed considerably. A variety of enzymes efficiently and selectively catalyze alkane oxidation at body temperatures and pressures. The direct use of biological organisms for industrial alkane oxidation under such benign conditions has not yet been possible in practice. Hence, the numerous inorganic biomimic analogues of these enzymes have been under investigation for some time [126].

1.5.1. Choice of an Oxidant

It is essential that the oxidant is cheap and generates no side products that need additional investment for their separation. Molecular oxygen (or air) is the primary oxidant used in the industry for economic and environmental reasons [127]. However, O_2 has a tendency to oxidize the substrate by mechanisms that are not readily or rationally controlled and hence it is difficult to control product selectivity. H_2O_2 is environmentally friendly as the only waste product resulting from using it for oxidation is water [127, 128]. The "active oxygen" content of hydrogen peroxide, 47 % of its weight, is much higher than that of other oxidants. Also, aqueous hydrogen peroxide is a stable reagent, provided it is handled and stored in the correct manner [129]. Therefore, H_2O_2 is the second best oxidant for catalytic liquid phase oxidations. The problem, however, is its reactivity in the presence of transition metal catalysts leading to homolytic cleavage of the weak O-O bond ($\Delta H = 50$ kcal/mole) generating hydroxy radicals that perform non-selective oxidations or cause its decomposition into molecular oxygen. Other oxidants generally used for oxidation reactions include NaOCl, organic hydroperoxides, PhIO and percarboxylic acids. For both aqueous and non-aqueous reaction conditions, TBHP (*tert*-butylhydroperoxide) is often found to be the more

selective oxidant [130, 131]. Compared to other organic oxidants it is not expected to be a persistent environment pollutant. The byproduct *t*-butanol is a valuable chemical. TBHP has been found to be by far the most preferred oxidant for epoxidation reactions [132].

1.5.2. Epoxidation of Olefins

The catalytic oxidation of olefins to epoxides is an important transformation in organic synthesis [133, 134]. Much attention has been given to develop transition metal catalysts with various synthetic ligands such as porphyrins [135], Schiff bases [133, 136, 137] and cyclic amines [138]. All transition metal catalyzed epoxidations are one oxygen transfer (oxo transfer) reactions [139]. Salen complexes have been investigated the most as they have many advantages over porphyrin complexes and titanium tartarate catalysts [140]. Although many metal ions form complexes with salen, only chromium [141], manganese [24], nickel [142], and ruthenium have been used in epoxidation reactions [143]. Among them, Mn^{III}(salen) reported by Kochi and co-workers are found to be the most efficient. A new chapter in epoxidation was opened in 1990 when Jacobsen and co-workers reported chiral Mn^{III}(salen) catalysts for epoxidation [144]. However, reports on the use of hydrogen peroxide with manganese catalysts are not many [85-87, 145, 146]. Iron-cyclam has been reported for epoxidation of olefins with H$_2$O$_2$ [138]. Nickel cyclam complexes are again well known as epoxidation catalysts. The *in situ* prepared, Mn-tmtacn was found to be very efficient for the epoxidation of electron deficient, terminal and non-terminal alkenes with H$_2$O$_2$ (Scheme 1.1) and its catalytic activity was enhanced in the presence of carboxylic acid buffers [85-87]. The mechanism of Mn-tmtacn-catalysed epoxidation has been the subject of much research. However, little is known about the mechanisms or the nature of the active intermediates in these catalytic systems.
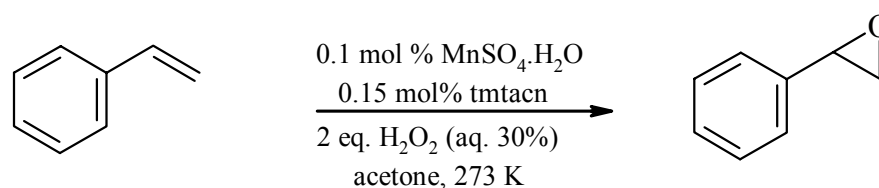
Scheme 1.1. *Epoxidation of styrene catalyzed by in situ formed Mn-tmtacn complex in acetone (Ref. 18).*

Various successful attempts to fine-tune catalyst selectivity for epoxidation have been reported. The encapsulation of Mn-tmtacn complex in zeolites increased the epoxidation selectivity [109]. By immobilisation of the triazacyclononane ligand on an inorganic support, a new group of active heterogeneous manganese tacn epoxidation catalysts were introduced [85]. Improved selectivities were found but the conversions obtained were lower than with the homogenous catalysts. Epoxidation of olefins with heterogeneous chiral and achiral salen complexes of manganese have also been explored [39, 147, 148]. The oxidation of alkenes over some transition metal exchanged zeolites has also been reported [149, 150]. However, investigations related to the epoxidation of olefins with copper complexes are not many in the literature.

1.5.3. Oxidation of C-H Bond of Alkanes

1.5.3.1. Cyclohexane Oxidation

The selective oxidation of cyclohexane under mild conditions is a topic of great interest [151]. Many biomimetic catalyst systems that can catalyze the selective oxidation of alkanes at room temperature with different oxidants have been developed. The ability of cytochrome *P*-450 enzyme to transfer oxygen to unreactive hydrocarbons led synthetic chemists to mimic these catalysts [152]. Recently, Shulpin et al. [88] reported the use of a binuclear manganese(IV) complex ([LMn^{IV}(O)$_3$Mn^{IV}L]$_2$C, L: 1,4,7-trimethyl-1,4,7-triazacyclononane) as the catalyst, in the presence of acetic acid

which results in decreased decomposition of H_2O_2 to water and oxygen. The reaction initially forms cyclohexyl hydroperoxide (CHHP), as the predominant product, which is later decomposed to cyclohexanone and cyclohexanol. Many homogeneous and heterogeneous catalysts have been developed for cyclohexane oxidation using different oxidants [153, 154]. Reports on the use of H_2O_2 as oxidant are not many.

1.5.3.2. *Benzylic Oxidation*

Benzylic oxidation of aromatics is an important reaction from industrial and synthetic organic chemistry angles [155, 156]. Commercial processes involve the use of cobalt and bromide ion catalysts in acetic acid medium at 473 K and oxygen pressure of 30 bars. Many homogeneous and heterogeneous transition metal catalysts have been reported to effect this transformation, and many of them are Cr- based [157-159]. Benzylic oxidations using cerium ammonium nitrate in hot acetic acid, HNO_3 and $HClO_4$ and Ce(IV)-triflate with water that are akin to the industrial processes have also been reported [159, 160]. In biomimic catalysis, manganese porphyrins are known to perform benzylic oxidation using H_2O_2 as oxidant (Scheme 1.2) [161]. Oxo-Ru-porphyrins have been reported to be useful in chiral catalysis [162]. Asymmetric
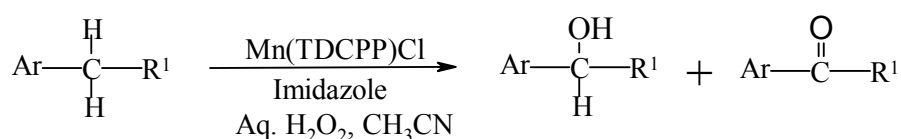
Ar= Aryl, R^1 = H, CH_3, Aryl, etc.

TDCPP = Tetrakis (2,6-dichlorophenyl) porphyrin

Scheme 1.2. *Benzylic oxidation in the presence Mn-porphyrin-imidazole catalyst system using H_2O_2.*

benzylic oxidation has also been carried out using Mn-salen catalysts and PhIO as oxidant [163]. However, the efficiency of these catalysts is not significant.

1.6. CARBON-CARBON BOND FORMING REACTIONS OVER HETEROGENOUS PALLADIUM CATALYSTS

Heterogeneous palladium catalysts possess very good activity and selectivity in C-C bond forming reactions such as Heck reaction, Suzuki coupling etc., apart from their easy separation from the reaction medium and reuse [164]. Generally, these involve palladium metal dispersed onto the surface of the support or modifying the support in order to anchor the active homogeneous palladium catalysts. Numerous reports are available in the literature on palladium containing heterogeneous catalysts.

1.6.1. Heck Reaction

Heck olefination or simply the "Heck reaction" was discovered independently by T. Mizorki and R. F. Heck in 1973 [165, 166], although Heck is mainly remembered for his initial work on noncatalytic (stoichiometric) reactions, and subsequent work to establish its generality. In general, the Heck reaction involves the C-C bond formation reaction between aryl halides and olefins catalyzed by palladium in the presence of a base (Scheme 1.3) [167-172].

$$Ar-X \ + \ \diagup\!\!\!=\!\!W \quad \xrightarrow[\text{Base}]{\text{Pd}} \quad Ar\diagup\!\!\!=\!\!\!\sim\!W$$

Ar = Aryl
X = I, Br, Cl
W = CO$_2$Me, Ph etc.   Base= Et$_3$N, K$_2$CO$_3$, NaOAc etc
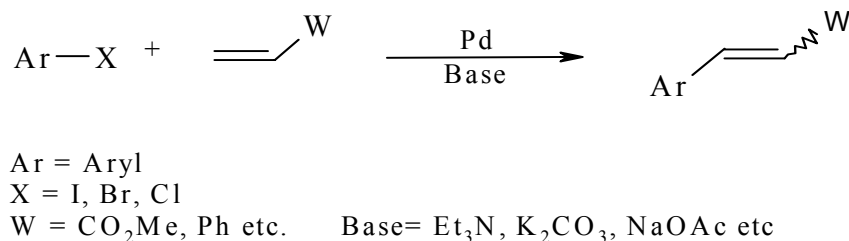
Scheme 1.3. *Heck reaction between aryl halides and olefins.*

Typical catalysts are Pd(0)-phosphine complexes, e.g. Pd(PPh$_3$)$_4$, or *in situ* catalysts such as Pd(OAc)$_2$/PPh$_3$. The bases may be either organic, such as Et$_3$N and *t*-Bu$_3$N or inorganic, such as K$_2$CO$_3$ and NaOAc. Aryl halides will be normally aryl iodides or aryl bromides. However, attempts are on to utilize the cheap aryl chlorides in the reaction. Many homogeneous catalysts/catalyst systems are known for the Heck reaction [173]. The first reports on the employment of heterogeneous catalysts for the Heck reaction followed its discovery soon. Mizoroki [174] observed that catalytic activity was independent of the amount of Pd black. In the same year Julia et al. [175] reported the use of Pd/C as heterogeneous catalyst for Heck reaction. In 1990's, heterogeneous Heck Reaction (HETHR) was extensively studied due to its popularity and its applicability in the industry. It is practiced on an industrial scale in the manufacture of (a) the agrochemical Prosulfuron-^{TM} and the sunscreen agent octyl *p*-methoxycinnamte by Novartis, (b) Naproxin by Albemarle and (c) anti-asthma agent (Singulair) by Merk [176, 177]. Important advantages of this reaction are the broad availability of aryl halides and tolerance of the reaction for a wide variety of functional groups. Augustine and O' Leary [178], Zhuangyu and co-workers [179, 180], Ying and co-workers [181, 182], Arai and co-workers [183] and Köhler and co-workers [42] studied the action of heterogeneous catalysts thoroughly. To name a few of the heterogeneous catalysts, polymer/dendrimer supported palladium catalysts [184], palladium on carbon [185] and palladium supported on metal oxides [186], clays [187], and molecular sieves [182, 188] have been used in the Heck reaction. Yet another recent development is the use of palladium nanoclusters [189]. Recently, novel Ni, Co, Cu and Mn heterogeneous catalysts have been reported [190]. Very recently, Pd(0) supported on hydrotalcite like anionic clays has been found to act as a good catalyst for the Heck C-C coupling [123]. Unlike all other supports, Pd(II)-containing hydrotalcites

are believed to undergo minimum leaching due to its incorporation into the layers of the hydrotalcite structure. The fact that no inert atmosphere and no ligands are necessary, the easy catalyst separation and the potential to increase the existing catalyst activity makes supported Pd catalysts an important alternative to homogeneous catalysts for industrial applications.

1.6.2. Suzuki Coupling

Suzuki reaction is another Pd catalyzed C-C coupling reaction that involves the reaction of an aryl boronic acid with an aryl halide, diazonium salt or trifalte to produce a biaryl (Scheme 1.4) [191]. A base is necessary to neutralize the liberated acid. Suzuki reaction is much favored in the pharmaceutical industry due to non-toxicity and
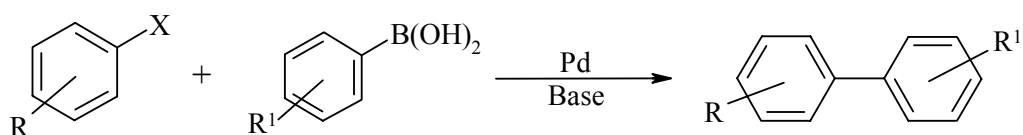
Scheme 1.4. *Suzuki coupling of aryl halides with aryl boronic acids.*

non-moisture sensitivity of the organoboranes. Biaryls are important as building blocks for biologically active substances [192]. Many developments in homogeneous catalysts have been reported for Suzuki coupling [193]. However, the use of heterogeneous catalysts has not been explored much [194-196]. The Suzuki coupling reactions mediated by a heterogeneous palladium catalyst are confined to bromo- and iodoarenes. However, very recently, Choudary et al. reported Pd(0)-supported on Mg-Al hydrotalcite as a heterogeneous catalyst for Suzuki reaction with chlororarenes [124].

1.6.3. Sonogashira Reaction

Similar to the Heck reaction, the Sonogashira reaction is also a C-C bond forming reaction, which involves the coupling of terminal alkynes with aryl or alkyl

halides [197]. This reaction generally involves the use of a palladium catalyst in conjunction with copper iodide, the copper reacting with the alkyne to form an alkynylcuprate (Scheme 1.5).

$$R-X \quad + \quad H\text{———}R^1 \quad \xrightarrow[\text{Base}]{\text{Pd/CuI}} \quad R\text{———}R^1$$

X = I, Br, Cl
R = Aryl
R' = Aryl, Alkyl
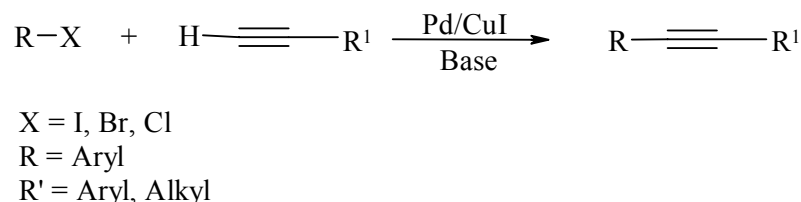
Scheme 1.5. *Example of Sonogashira reaction.*

If the reaction is performed on an alkene, the geometry about the double bond is usually reserved, making this an extremely useful reaction for the synthesis of ene-yne molecules with specific geometry (Scheme 1.6).
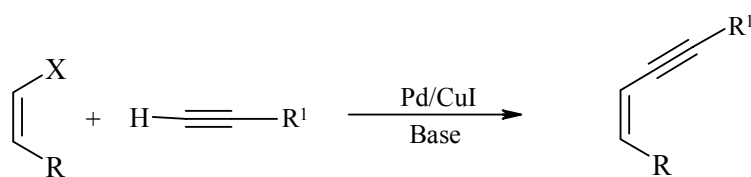
Scheme 1.6. *Sonogashira reaction of alkenyl halides.*

Though homogeneous catalysts are well known for this reaction, there are few reports on the use of heterogeneous catalysts [196, 124].

1.6.4. Recovery and leaching of the catalyst

Though supported catalysts have the advantage of easy recovery, the problem of metal leaching from the catalyst under liquid-solid conditions is well known. It is reported that the supported catalysts are just reservoirs of soluble *active species*, generated under reaction conditions [197]. Many people have argued that the reaction involves leached *homogeneous species* in the solution, the leached palladium re-depositing onto the support at the end of the reaction on cooling. The extent of re-

deposition depends on several factors including the nature of solvent and base employed, the reaction temperature and the nature of the support [165]. In general, it is just the *"release and recapture"* principle that has been proposed to explain the mechanism and higher activity of the supported catalyst in heterogeneous C-C bond forming reactions [198]. However, it must be pointed out that homogeneous catalytic reactions with the same ppm level of Pd are not efficient. Therefore, it is possible that in some cases the catalysts may be truly heterogeneous in that the active species remains attached to the surface during the reaction.

1.7. SCOPE OF THE THESIS

The aim of the present investigation is to develop novel transition metal catalysts for selective oxidations and carbon-carbon bond forming reactions. The processes involving these catalysts are expected to lead to green chemistry/technology.

1.7.1. Objectives of the thesis

The objectives of the thesis are as follows:

1. To synthesize and characterize neat Cu and Mn of Schiff base and perazamacrocylic ligands complexes and to evaluate their catalytic activities in epoxidation of olefins and benzylic oxidation of aromatics.

2. To heterogenize Cu and Mn complexes by encapsulating them inside the pores of zeolite-Y and to evaluate their catalytic activities.

3. To study the effect of molecular confinement, size of the macrocyclic ligand, N-substitution and buffer on the catalytic activity of the complexes.

4. To synthesize and characterize palladium-containing hydrotalcites and to evaluate their catalytic activity for carbon-carbon bond forming reactions viz., Heck reaction, Suzuki coupling and Sonogashira reaction.

1.7.2. Organization of the work

The *introduction chapter (this chapter)* presents an overview on metal catalyzed hydrocarbon oxidations and carbon-carbon bond forming reactions. Literature reports on Schiff base and perazamacrocyclic complexes of copper and manganese, their synthesis, characterization and the catalytic activities as biomimic homogeneous and heterogeneous catalysts for oxidation of hydrocarbons is briefly described. It also presents a brief discussion on hydrotalcites and transition metal incorporated hydrotalcites as heterogeneous catalysts for important organic transformations such as C-C bond forming reactions. Finally the scope of the thesis is discussed.

Chapter 2 deals with the synthesis of Schiff base and tri- and tetraaza macrocyclic ligands. Richman-Atkins synthesis of peraza macrocyclic ligands has been simplified and generalized for all tri- and tetraaza ligands prepared in this work. It describes the preparation of Cu and Mn complexes of these ligands and encapsulation of these complexes in zeolite Na-Y. This chapter also describes the various physicochemical techniques and methods of sample pre-treatment.

Chapter 3 presents the characterization and catalytic activities of Mn and Cu complexes of tri- and tetraaza macrocycles and quadridentate Schiff base ligands (salen and saloph). It also presents the characterization and activities of these complexes encapsulated in zeolite-Y. The formation of different complexes of manganese with 1,4,7-triazacyclononane was observed at different pH of the reaction medium. Activities of these metal complexes have been investigated in the epoxidation of styrene and ethyl benzene oxidations with H_2O_2 and TBHP oxidants.

Chapter 4 gives an account of the epoxidation of olefins and benzylic oxidation of aromatics using *in situ* prepared Mn-tmtacn-oxalate buffer-H_2O_2 system at ambient temperatures (273 − 333 K). The influence of buffers (acetate, oxalate, tartarate,

malonate, citrate and ascorbate) on the catalytic activity of Mn-tmtacn during epoxidation of allyl acetate and terminal/non-terminal olefins and benzylic oxidation of aromatics is investigated. The structure of the active Mn species (in situ formed) is determined by EPR, UV-visible and FT-IR-ATR spectroscopies.

Chapter 5 reports the synthesis and characterization of Pd containing Mg/Al hydrotalcites with different Mg/Al and Pd/Mg ratios (Mg/Al = 2-3 and Pd/Mg = 0.01-0.05) and their application as catalysts in carbon-carbon bond forming reactions viz. Heck reaction, Suzuki coupling and Sonogashira reaction.

Chapter 6 presents the overall summary of the work.

1.8.   REFERENCES

1.   Beller, M; Balm, C (Eds.), *Transition Metals for Organic Synthesis,* Wiley-VCH, **1998,** *Vol. 1 and Vol. 2.*

2.   Sheldon R. A.; Kochi, J. K. *Metal-Catalyzed Oxidations of Organic Compounds*, Academic Press: New York, **1981**.

3.   Sheldon R. A., Ed.; *Metalloporphyrin in Catalytic Oxidations,* Marcel Dekker New York, **1994**.

4.   Kautsuki, T. *Coord. Chem. Rev*. **1995**, *140*, 189.

5.   Diederich, F.; Stang, P. J. (Eds.) *Metal Catalyzed Cross-Coupling Reactions,* Wiley-VCH, Weinheim, **1997**.

6.   Heck, R. F. *Palladium Reagents in Organic Synthesis*, Acadamic Press, London, **1985**.

7.   Ortiz de Montellino, P. R. (Ed.) *Cytochrome P-450. Structure, Mechanism and Biochemistry,* 2nd ed., Plenum Press New York, **1995**.

8.   Pecoraro, V.L. (Ed.) *Manganese Redox Enzymes*, VCH, New York, **1992**.

9.   Dismukes, G.C. *Chem. Rev.* **1996**, *96,* 2909.

10.   Styler, L. *Biochemistry,* W. H. Freeman, (Ed.) VCH, New York, **1988**.

11.   Yachendra, V. K.; Sauer, K.; Klien, M. P. *Chem. Rev.* **1996**, *96,* 2927.

12.   Kono, Y.; Fridiwitch, I. *J. Biol. Chem.* **1983**, *258*, 6015.

13. Ferguson Miller, S.; Babcock, G.T. *Chem. Rev.* **1996**, *96*, 2889.

14. Delroth, P.; Mitchell, D.M.; Gennis, R.B.; Brzezinski, P. *Biochemistry*, **1997,** *36,* 11787.

15. Groves, J. T.; Nemo, T. E.; Myers, R. S. *J. Am. Chem. Soc.* **1979**, *101*, 1032.

16. Groves, J. T.; Watanabe, Y. *J. Am. Chem. Soc.* **1986**, *108*, 7834.

17. Groves, J. T.; St, M. K. *J. Am. Chem. Soc.* **1987**, *109*, 3812.

18. Bortolini, O.; Ricci, M.; Meunier, B.; Ascone, I.; Goulon, J. *New. J. Chem.* **1986**, *10,* 39.

19. Lee, W. A.; Bruice, T. C. *J. Am. Chem. Soc.* **1985**, *107*, 513.

20. Van Atta, R.B.; Franklin, C.C.; Valentine, J.S. *Inorg. Chem.* **1984**, 23, 4121.

21. Franklin, C.C.; Van Atta, A.F.T.; Valentine, J.S. *J. Am. Chem. Soc.* **1984**, *106*, 814.

22. Tai, A.F.; Margerum, L.D.; Valentine, J.S. *J. Am. Chem. Soc.* **1986**, *108*, 5006.

23. Che, C.-M.; Yam, V.W.-W. *J. Am. Chem. Soc.* **1989**, *109*, 1262.

24. Srinivasan, K.; Michaud, P.; Kochi, J.K. *J. Am. Chem. Soc.* **1986**, *108,* 2309.

25. Samsel, E.G.; Srinivasan, K.; Kochi, J.K. *J. Am. Chem. Soc.* **1985**, *107,* 7606.

26. Leung, U.H.; Che, C.-M. *Inorg. Chem.* **1989**, *28*, 4619.

27. Kimura, E.; Shionoya, M.; Yamauchi, T.; Shiro, M. *Chem. Lett.* **1991**, 1217.

28. Kinneary, J.F.; Albert, J.S.; Burrows, C.J. *J. Am. Chem. Soc.* **1988**, *110*, 6124.

29. Jorgensen, K.A. *Chem. Rev.* **1989**, *89*, 3.

30. Yoon, H.; Burrows, C.J. *J. Am. Chem. Soc.* **1988**, *110,* 4087.

31. Koola, J.D.; Kochi, J.K. *Inorg. Chem.* **1987**, *26,* 908.

32. Yamada, M.; Ochi, S.; Suzuki, H.; Hisazumi, A.; Kuroda, S.; Shimao, I.; Araki, K. *J. Mol. Catal.* **1994**, *87*, 195.

33. Yoon, H.; Wagler, T.R.; O'Connor, K.J.; Burrows, C.J. *J. Am. Chem. Soc.* **1990**, *112*, 4568

34. Kinneary, J.F.; Wagler, T.R.; Burrows, C.J. *Tetrahedron Lett.* **1988**, *29*, 877.

35. Wagler, T.R.; Fang, Y.; Burrows, C.J. *J. Org. Chem.* **1989**, *54,*1584.

36. Wagler, T.R.; Burrows, C.J. *Tetrahedron Lett.* **1988**, *40,*5091.

37. Wonwoo, N.; Raymond, H.; Valentine, J.S. *J. Am. Chem. Soc.* **1991**, *113,* 7052.

38. Eckert, H.; Fabry, G.; Kiesel, Y.; Raudaschl, G.; Seidel, C. *Angew. Chem. Int. Ed. Engl.* **1983**, *22*, 881.

39. Kumar, K.R.; Choudary, B.M.; Jamil, Z.; Thyagarajan, G. *J. Chem. Soc. Chem.*

Commun. **1986**, 130.

40. Balkas, K.J.; Gabrielor, A.G.; Bell, S.L.; Bedioui, F.; Roue, L.; Devyank, J. *Inorg. Chem.* **1994**, *33*,67.

41. Barloy, L.; Battioni, P.; Mansuy, D. *J. Chem. Soc., Chem. Commun.* **1990**, 1365.

42. Köhler, K.; Wagner, M.; Djakovitch, L. *Catal. Today* **2001**, *66*, 105.

43. Bowers, C.; Dutta, P.K. *J. Catal.* **1990**, *122*, 271.

44. Knops-Gerrits, P.P.; Abbe, M.L.; Jacobs, P.A. *Stud. Surf. Sci. Catal.* **1997**, *108*, 445.

45. Knops-Gerrits, P.P.; De Vos, D.E.; Jacobs, P.A. *J. Mol. Catal*. **1997**, *117*, 57.

46. Pinnavaia, T.; Tzou, M.; Laundau, S.; Raythatha, R. *J. Mol. Catal.* **1984**, *27*, 195.

47. Frunza, L.; Kosslick, H.; Landmesser, H.; Hoft, E.; Fricke, R. *J. Mol. Catal.* **1997**, *123*, 179.

48. Kim, G.-J.; Kim, S.-H. *Catal. Lett.* **1999**, *57*, 139.

49. Kim, S.-S.; Zhang, W.; Pinnavaia, T.J. *Catal. Lett.* **1997**, *43*,149.

50. Subba Rao, Y.V.; De Vos, D.E.; Bein, T.; Jacobs, P.A. *Chem. Commun.* **1997**, 355.

51. Sutra, P.; Brunel, D. *J. Chem. Soc., Chem. Commun.* **1996,** 2485.

52. Choudhary, B. M.; Kantam, M. L.; Rahman, A.; Sreekanth. P.; Bharathi, B. *J. Mol. Catal.* **1994**, *87*, 195.

53. Mimitolo, F.; Pini, D.; Salvadori, P.; *Tetrahedron Lett.* **1996**, *37*, 3375.

54. De, B.B.; Lohray, B.B.; Sivaram, S.; Dhal, P.K. *Tetrahedron: Asymm.* **1995**, *6*, 2105.

55. Combes, A.*C. R. Acad. Fr.*, **1889**, *108*, 1252.

56. Pfieiffer, P.; Brieth, E.; Lübbe, E.; Tsumaki, T. *Liebigs Ann. Chem.* **1933**, *503*, 84.

57. Zhang, W.; Loebach, J.L.; Wilson, S.R.; Jacobsen, E.N. *J. Am. Chem. Soc.* **1990**, *112,* 2801.

58. Irie, R.; Noda, K.; Ito, Y.; Matsumoto, N.; Katsuki, T. *Tet. Lett.* **1990**, *31*, 7345.

59. Canali, L.; Sherrington, D.C. *Chem. Soc. Rev.* **1999**, *28,* 85.

60. Bunce, S.; Cross, R.J.; Farrugia, L.J.; Kunchandy, S.; Meason, L.L.; Muir, K.W.; O'Donnell, M.; Peacock, R.D.; Stirling, D.; Teat, S.J. *Polyhedron,* **1998**, *17*, 4179.

61. Bianchi, A; Micheloni, M.; Paoletti, P. *Coord. Chem. Rev.* **1991**, *110*, 17.

62. Cabbiness, D.K.; Morgerum, D.W. *J. Am. Chem. Soc.* **1969**, *91,* 2801.

63. Izgat, R.M. *Chem. Rev.* **1991**, *91*, 1721.

64. Lindory, L. F.; Baldwin, D.S. *Pure. Appl. Chem.* **1989**, *61*, 909.

65. Kimura, E. *J. Coord. Chem.* **1986**, *15*, 1.

66. Poon, C. K.; Tobe, M. L. *J. Chem. Soc. A.* **1968**,1549.

67. Barefield, E.K.; Wagner, F.; Herlinger, A.W.; Dahl, A.R. *Inorg. Synth.* **1976,** *16*, 220.

68. Richman, J. E.; Atkins, T.J. *J. Am. Chem. Soc.* **1974**, *96*, 2268.

69. Christenson, J.J.; Eatough, D.J.; Izgat, R.M. *Chem. Rev.* **1974**, *74*, 351.

70. Bunce, S.; Cross, R.J.; Farrugia, L.J.; Kunchandy, S.; Meason, L.L.; Muir, K.W.; O'Donnell, M.; Peacock, R.D.; Stirling, D.; Teat, S.J. *Polyhedron,* **1998**, *17,* 4179.

71. Mahapatra, S.; Halfen, J.A.; Wilkinson, E.C.; Pan, G.; Wang, X.; Young, V.G., Jr.; Cramer, C.J.; Que, L., Jr.; Tolman, W.B. *J. Am. Chem. Soc.* **1996**, *118*, 11555.

72. Schwindinger, W.F.; Fawcett, T.G.; Lalancette, R.A.; Potenza, J.A.; Schugar, H.J. *Inorg. Chem.* **1980**, *19,* 1379.

73. Chaudhuri, P.; Oder, K. *J. Chem. Soc.Dalton Trans.* **1990**, 1597.

74. Zompa, L.J. *Inorg. Chem.* **1978**, *17*, 2531.

75. Riedo, T.J.; Kaden, T.A. *Helv. Chim. Acta,* **1979**, *62*, 1089.

76. Hay, R.W.; Pujari, M.P. *Helv. Chim. Acta.* **1985**, *100*, L1-L3.

77. Coates, J.H.; Hadi, D.A.; Lincoln, S.F. *Aust. J. Chem.* **1982**, *35*, 903.

78. Shane, A.M.; Taylor, N. J.; Carty, A.J. *Inorg. Chem.* **1983**, *22*, 1411.

79. Hage, R.; Krijnen, B.; Waarber, J.B.; Hartl, F.; Stufkens, D.J.; Snoeck, T.L. *Inorg. Chem.* **1995**, *34*, 4973.

80. Koek, J.H.; Russel, S.W.; van der Wolf, L.; Warnaar, J.B.; Speck, A.L.; Kerscher, J.; DelPizzo, L. *J. Chem. Soc. Dalton Trans.* **1996**, 353.

81. Shulpin, G.B.; Süss-Fink,G.; Shulpina, L.S. *J. Mol. Catal. A:Chem.* **2001**, *170*, 17.

82. Hage, R.; Iburg, J.E.; Kerschner, J.; Koek, J.H.; Lempers, E.L.M.; Martens, R.J.; Racherla, U.S.; Russel, S.W.; Swarthoff, T.; van Vilet, M.R.P.; van der Wolf, L.; Krinjen, B. *Nature,* **1994**, *369*, 637.

83. Wieghardt, K.; Bossek, U.; Nuber, B.; Weiss, J.; Bonvoisin, J.; Corbella, M.; Vitols, S.E.; Girerd, J.J. *J. Am. Chem. Soc.* **1988**, *110,*7398.

84. Wieghardt, K. *Angew. Chem., Int. Ed. Engl.* **1989**, *28,* 1153.

85. De Vos, D. E; Bein, T. *Chem. Commun.* **1996**, 917.

86. De Vos, D.E.; Sels, B.F.; Reynaers, M.; Subba Rao, Y.V.; Jacobs, P.A. *Tetrahedron Lett.,* **1998**, *39,* 3221.

87 Berkssell, A.; Sklorz, C.A. *Tetrahedron Lett.,* **1999**, *40,* 7965.

88. Shulpin, G.B.; Süss-Fink,G.; Smith, J.R.L. *Tetrahedron* **1999,** *55,* 5345.

89. Goodson, P.A.; Hodgson, D. J.; Glerup, J.; Michelsen K.; Weihe, H. *Inorg. Chim. Acta* **1992**, *197,* 141.

90. Brewer, K.J.; Liegeois, A.; Otvos, J.W.; Calvin, M.; Spreer, L.O. *J. Chem. Soc. Chem. Comm.* **1988**, 1219.

91. Létumier, F.; Broeker, G.; Barbe, J-M.; Guilard, R.; Lucas, D.; Dahaoui-Gindrey, V.; Lecomte, C.; Thouin, L.; Amatore, C. *J. Chem. Soc.*, *Dalton Trans*. **1998**, 2233.

92. Cooke, P.R.; Smith, J.R.L. *J. Chem. Soc. Perkin Trans. 1* **1995**, 243.

93. Sabater, M.J.; Corma, A.; Domenech, A.; Fornes, V.; Garcia, H. *Chem. Comm.* **1995**, 1285.

94. Pugin, B.; Blaser, H-U. in *Comprehensive Asymmetric Catalysis,* Jacobsen, E.N.; Pfaltz, A.; Yamamato, H. (Edts) **1999**, *Vol 3,*1367.

95. Miki, K.; Sato, Y. *Bull. Chem. Soc. Jpn.* **1993,** *66,* 2385.

96. Canali, L.; Cowan, E.; Deleuze, H.; Gibson, C. L.; Sherrington, D.C. *Chem. Comm.* **1998,** 2561.

97. Minutolo, F.; Pini, D.; Salvadori, P. *Tetrahedron Lett.* **1996**, *37,* 3375.

98. Carlos, B.; Barbara, G; Sabater, M.J.; Garcia, H.; Corma, A. *Appl. Catal.A: General* **2002**, *228,* 279.

99. De Vos, D.E.; De Wildeman, S.; Sels, B.; Grobet, P.J.; Jacobs, P.A. *Angew. Chem.* **1999**, 38, 1033.

100. Herron, N.; Stucky, G. D.; Tolman, C. A. *Inorg. Chim. Acta* **1985**, *100,* 135.

101. Herron, N.; *Inorg. Chem.* **1986,** *25,* 4115.

102. Ratnasamy, C.; Murugkar, A.; Padhye, S.; Pardhy, S.A. *Ind. J. Chem.: A* **1995**, *35,* 1

103. Jacob, C.R.; Varkey, S.P.; Ratnasamy, P. *Micropor. Mesopor. Mater.* **1998**, *22,* 465.

104. Raja, R.; Ratnasamy, P. *Appl. Catal. A: General.* **1997**, *156*, L-7.

105. Deshpande, S.; Srinivas, D.; Ratnasamy, P. *J. Catal.* **1999**, *188,* 261.

106. Choudary, B.M.; Kantam, M.L.; Bharathi, B.; Sreekanth, P.; Figueras, F. *J. Mol. Catal. A:Chem.* **2000**, *159*, 417.

107. Kumar, K.R.; Choudary, B.M.; Kantam, M.L. *J. Catal.* **1991**, *130,* 41.

108. De Vos, D.E.; Bein, T. *J. Am. Chem. Soc.* **1997**, *119*, 9460.

109. De Vos, D.E.; Meinershagen, L.; Bein, T. *Angew. Chem., Int. Ed. Engl.* **1996**, *25,* 2211.

110. Knops-Gerrits, P.-P.; De Vos, D.E.; Jacobs, P.A. *J. Mol. Catal. A:Chem.* **1997**, *117*, 57.

111. Choy, J-H.; Kim, D-K.; Park, J-C.; Choi, S-N.; Kim, Y-J. *Inorg. Chem.* **1997**, *36,* 189.

112. Sauer, M.V.C.; Edwards, J.O. *J. Phys. Chem.* **1971**, *75,* 3004.

113. Cavani, F.; Trifiro, F.; Vaccari, A. *Catal. Today* **1991**, *11*, 173.

114. Basile, F.; Fernasar, G.; Gazzane, M. Vaccari, A. *Appl. Clay Sci.* **2000**, *16*, 185.

115. Chen, Z.; Hwang, C.M.; Liaw, C.W. *Appl. Catal. A: General* **1998**, *169*, 207.

116. Velu, S.; Veda Ramaswamy, Ramani, A.; Chanda, B.M.; Sivasanker, S. *Chem. Comm.* **1997**, 2107.

117. Parida, K.; Das, J. *J. Mol. Catal. A:Chem.* **1997**, *117*, 57.

118. Takahiro, N.; Nobuyaki, K.; Masashi, I.; Sakae, U. *Chem. Commun.* **2000**, 1245.

119. Kaneda, K.; Yamashita, T.; Matsushita, T.; Ebitani, K. *J. Org. Chem.* **1998**, *63*, 1750.

120. Choudhary, B. M.; Kantam, M. L.; Rahman, A.; Reddy, Ch. V.; Rao, K. K. *Angew. Chem. Int. Ed. Engl.* **2001**, *40,* 763.

121. Choudary, B. M.; Kavita, B.; Chowdari, N. S.; Sreedhar, B.; Kantam, M. L. *Catal. Lett.* **2002**, *78,* 373.

122. Narayanan, S.; Krishna, K. *Chem. Commun.* **1997**, 1991.

123. Choudary, B.M.; Chowdari, N.S.; Madhi, S.; Kantam, M.L. *Angew. Chem. Int. Ed. Engl.* **2001**, *40,* 4617.

124. Choudary, B.M.; Madhi, S.; Chowdari, N.S.; Kantam, M.L.; Sreedhar, B. *J. Am. Chem. Soc.* **2002**, *124*, 14127.

125. Sheldon, R.A.; van Santen, R.A. Edts. *Catalytic Oxidation; Principle and Applications,* World Scientific Publishing Co. Ltd.**1995**.

126. Groves, J. T. *Nature* **1997**, *389*, 329.

127. Edwards, J.O.; Curci, R. in: Strukul, G. (Ed.) *Catalytic Oxidations with Hydrogen Peroxide as Oxidant,* Kluwer Academic Publishers, Dordrecht, **1992**.

128. Moiseev, I.I. *J. Mol. Catal. A: Chem.* **1997**, *127*, 1.

129. Clerici, M.G. *Stud. Surf. Sci. Catal.* **1993**, *78*, 21.

130. Sharpless, K. B.; Verhoeven, T. R. *Aldrichimica Acta* **1979**, *12*, 63.

131. Hill, J. G.; Rossiter, B.E.; Sharpless, K.B. *J. Org. Chem.* **1983**, 48, 3607.

132. Sharpless, K. B.; Behrens, C. H.; Katsuki, T.; Lee, A. W. M.; Martin, V. S.; Takatani, M.; Viti, S. M.; Walker, F. J.; Woodard, S. S. *Pure Appl. Chem.* **1983**, *55,* 589.

133. Sheldon, R.A.; in Cornils, B.; Hermann, W.A. (Eds) *Applied Homogeneous Catalysis with Organometallic Compounds,* VCH, Weinheim, **1996**.

134. Jacobsen, E.N.; in Ojima, I. Ed. *Catalytic Asymmetric Synthesis,* VCH, New York, **1993**, 159.

135. Battioni, P; Renaud, J.P.; Bartoli, J.F.; Riena-Artlies, Ford, M.; Mansuy, D. *J. Am. Chem. Soc.* **1988**, *110*, 8462.

136. Jacobsen, E.N.; Zhang, W.; Muci, A.R.; Ecker, J.R.; Deng, L. *J. Am. Chem. Soc.* **1991**, *113*, 7063.

137. Bernardo, K.; Leppard, S.; Robert, A.; Commenges, G.; Dahan, F.; Meunier, B. *Inorg. Chem.* **1996**, *35*, 387.

138. Nam, W.; Ho, R.; Valentine, J.S. *J. Am. Chem. Soc.* **1991**, *113*, 8462.

139. Katsuki, T.; *Coord. Chem. Rev.* **1995**, *140*, 189.

140. Katsuki, T.; Sharpless, K.B. *J. Am. Chem. Soc.* **1980**, *102*, 5974.

141. Samuel, E.G.; Srinivasan, K.; Kochi, J.K. *J. Am. Chem. Soc.* **1985,** *107*, 7606.

142. Yoon, H.; Burrows, C.J. *J. Am. Chem. Soc.* **1988**, *110*, 4087.

143. Taqui Khan, M.M.; Mirza, S.A.; Sreelatha, C.; Abdi, S.H.R.; Shaikh, Z.A. *Stud. Org. Chem.* (Amsterdam), **1988**, *33,* 211.

144. Zang, W.; Loebach, J.L.; Wilson, S.R.; Jacobsen, E.N. *J. Am. Chem. Soc.* **1990**, *112*, 2801.

145. Lee, N.H.; Muci, A.R.; Jacobsen, E.N. *Tetrahedron Lett.* **1991**, *32,* 5065.

146. Groves, J. T.; Watanabe, Y.; McMurry, T. J. *J. Am. Chem. Soc.* **1983**, *105*, 4489.

147. Bowers, C.; Dutta, P.K. *J. Catal.* **1990**, *122*, 271.

148. Sabater, M.J.; Corma, A; Domenech, A.; Vicente, F.; García, H. *J. Chem. Soc.*

Chem. Comm. **1997**, 1285.

149. Schuchardt, U.; Carvalho, W.A.; Spinacé, E.V. *Synlett,* **1993**, *10,* 713.

150. Farzaneh, F.; Sadeghi, S.; Turkian, L.; Ghandi, M. *J. Mol. Catal. A: Chem.* **1998**, *132*, 255.

151. Can-Cheng, G.; He-Ping, L.; Jian-Bing, X. *J. Catal.* **1999**, *185,* 345.

152. Bedioui, F. *Coord. Chem. Rev.* **1995**, *144*, 39.

153. Schuchardt, U.; Cardoso, D.; Sercheli, R.; Pereira, R.; da Cruz, R.S.; Guerreiro, M.C.; Mandelli, D.; Spinacé, E.V.; Pires, E.L. *Appl. Catal. A: General,* **2001**, *211*, 1.

154. Armengol, E.; Corma, A.; Vicente, F.; Hermenegildo, G.; Primo, J. *Appl. Catal. A: General,* **1999**, *181*, 305.

155. O' Donnel, M. J.; Boniece, J.M.; Earp, S.E. *Tetrahedron Lett.* **1978**, 2641.

156. Fasth, K.-J.; Antoni, G.; Lanstrom, B. *J. Chem. Soc.*, *Perkin Trans*. **1998**, 3081.

157. Muzart, J. *Chem. Rev.* **1992**, *92*, 113.

158. Choudary, B.M.; Durga Prasad, A.; Bhuma, V.; Swapna, V. *J. Org. Chem.* **1992,** *57,* 5841.

159. Nair, V.; Mathew, J.; Prabhakaran, J. *Chem. Soc. Rev.* **1997**, 127.

160. Laali, K.K.; Herbert, M.; Cushnyr, B.; Bhatt, A.; Terrano, D. *J. Chem. Soc.*, *Perkin Trans. I.* **1998**, 3081.

161. Battioni, P.; Renaud, J. P.; Bartoli, J. F.; Reina-Artiles, M.; Fort, M.; Mansuy, D. *J. Am. Chem. Soc.* **1988,** *110*, 8462.

162. Zhang, R.; Yu, W.-Y.; Lai, T.-S.; Che, C.M. *Chem. Commun.* **1999**, 1791.

163. Hamachi, K.; Irie, R.; Katsuki, T. *Tet. Lett.* **1996**, *37*, 4979.

164. Biffis, A.; Zecca, M.; Basato, M. *J. Mol. Catal. A:Chem.* **2001**, *173*, 249.

165. Heck, R.F. *Acc. Chem. Soc.* **1979**, 12, 146.

166. Mizoroki, T.; Mori, K.; Ozaki, A. *Bull. Chem. Soc. Jpn.* **1971,** *44*, 581.

167. De Meijer, A.; Meyer, F. E. *Angew. Chem. Int. Ed. Engl.* **1994**, *33*, 2379.

168. Herrmann, W.A.; Brossmer, C.; Reisinger, C.-P.; Riemeier, T. H.; Ofele, K.; Beller, M. *Chem. Eur. J.* **1997**, *3,* 1357.

169. Cornils, B.; Herrmann, W.A. *Applied Homogeneous Catalysis with Organometallic Compounds,* VCH. Wienheim, **1996**.

170. Reetz, M. T.; Lohmer, G.; Schwickardi, R. *Angew. Chem. Int. Ed. Engl.* **1998**, *37*, 481.

171. Reetz, M. T.; Wastermann, E. *Angew. Chem. Int. Ed. Engl.* **2000**, *39*, 165.

172. Herrmann, W.A.; Elison, M.; Fisher, J.; Köcher, C.; Artus, G.R.J. *Angew. Chem. Int. Ed. Engl.* **1995**, *34*, 2371.

173. Beletskaya, I. P.; Cheperkov, A.V. *Chem. Rev.* **2000**, *100,* 3009.

174. Mizoroki, T.; Mori, K.; Ozaki, A. *Bull. Chem. Soc. Jpn.* **1973,** *46*, 1505.

175. Julia, M.; Duteil, M. *Bull. Soc. Chim. Fr.* **1973**, 2790.

176. De Uries, J.G. *Can. J. Chem.* **2001**, *79*, 1086.

177. Sheldon, R.A. *J. Mol. Catal. A:Chem.* **1996**, *107*, 75.

178. Augustine, R.L.; O'Leary, S.T. *J. Mol. Catal. A:Chem.* **1995**, *95*, 277.

179. Zhuangyu, Z.; Hongwen, H.; Tsi-Yu, K. *Synthesis* **1991**, 539.

180. Yi, P.; Zhuangyu, Z.; Hongwen, H. *J. Mol. Catal.* **1990**, *62*, 297.

181. Menhert, C.P.; Ying, J.Y. *Chem. Comm.* **1997**, 2215.

182. Menhert, C.P.; Weaver, D.W.; Ying, J.Y. *J. Am. Chem. Soc.* **1998**, *120*, 12289.

183. Bhange, B.M.; Arai, M. *Catal. Rev.* **2001**, *43*, 315.

184. Anderson, C. M.; Korebelas, K.; Awasti, A. K. *J. Org. Chem.* **1985**, *50*, 3891.

185. Augustine, R.L.; O'leary, S. T. *J. Mol. Catal.* **1992**, *72*, 229.

186. Wagner, M.; Köhler, K.; Djakovitch, L.; Weinkauf, S.; Hagen, V.; Muhler, M. *Topic. Catal.* **2000**, *13,* 319.

187. Ramachandani, R.K.; Uphade, B.S.; Vinod, M.P.; Wakharkar, R.D.; Choudhary, V.R.; Sudalai, A. *Chem. Commun.* **1997**, 2071.

188. Djakovitch, L.; Köhler, K. *J. Am. Chem. Soc.* **2001**, *123,* 5995.

189. Yeung, L. K.; Crooks, R. M. *Nano Lett.* **2000**, *1,* 14.

190. Iyer, S.; Thakur, V. *J. Mol. Cat. A: Chemical* **2000**, *157*, 275.

191. Sonogashira, K.; Tohda, Y.; Hagihara, N. *Tetrahedron Lett.* **1975**, 4467.

192. Szmant, H.H. *Organic Builiding Blocks of the Chemical Industry,* John Wiley & Sons, New York, **1989**.

193. Andreu, M.G.; Zapf, A.; Beller, M. *Chem. Commun.* **2000**, 2475 and reference there in.

194. LeBlond, C.R.; Andrews, A.T.; Sun, Y.; Sowa, J.R. Jr. *Org. Lett.* **2001**, *3,* 1555.

195. Fenger, I.; Drian, C. L. *Tetrahedron Lett.* **1998**, *39*, 4287.

196. Heidenreich, R.G.; Köhler, K.; Krauter, J.G.E.; Pietsch, J. *Synlett,* **2002**, 1118.

197. Sheldon, R.A.; Wallau, M.; Arends, I.W.C.E.; Schuchardt, U. *Acc. Chem. Res.* **1998**, *31*, 485.

198. Zhao, F.; Murakami, K.; Shirai, M.; Arai, M. *J. Catal.* **2000**, *194*, 479.

Chapter 2. SYNTHESIS OF METAL COMPLEXES AND

CHARACTERIZATION METHODOLOGIES

_____

2.1. INTRODUCTION

This chapter describes the synthetic methodologies adopted for the preparation of the various ligands and their Cu and Mn complexes used in the study. It also presents the different techniques employed for the characterization of the prepared materials. The complexes studied are categorized into two groups viz., Schiff bases and peraza macrocycles. These systems have been widely investigated for the past several decades due to their relevance to metalloenzymes [1 - 4]. The encapsulation of these complexes in the supercages of zeolite Y to develop inorganic mimics of enzymes is reported.

Schiff bases were prepared according to reported procedures [5-7] by condensing salicylaldehyde with ethylenediamine (to prepare N,N'-ethylenebis(salicylidinamine); salenH$_2$) or *o*-phenylenediamine (to prepare N,N'-*o*-phenylenebis(salicylidinamine); salophH$_2$) in alcohol. Molecular structures of these ligands are shown in Fig. 2.1.

Peraza macrocycles can be synthesized either "free" or bound to a given metal ion [8, 9]. Preparation of the "free" macrocycles has, however, several advantages. The H forms of the ligands (i.e., "free" macrocycles) were prepared by a modified Richman-Atkins synthesis [10, 11], which is an improved method of Stetter and Roos [12]. N-methylated forms were prepared according to the reported procedure [13]. Three types of peraza macrocycles viz., 1,4,7-triazacyclononane ([9]ane-N$_3$; tacn), 1,4,7,10-tetraazacyclododecane ([12]ane-N$_4$; cyclen) and 1,4,8,11-tetraazacyclotetradecane ([14]ane-N$_4$; cyclam), and the N-methylated derivatives, 1,4,7-trimethyl-1,4,7-

triazacyclononane (Me$_3$[9]ane-N$_3$; tmtacn) and 1,4,7,10-tetramethyl-1,4,7,10-tetraazacyclododecane (Me$_4$[12]ane-N$_4$; tmcyclen) were prepared in this study. Molecular structures of these macrocycles are also shown in Fig. 2.1. Variation is made in the size of macrocyclic ring, number of N-donor atoms and substitution to examine their influence on the molecular structure and catalytic activity.

Acetate salts of Cu and Mn were used in the preparation of Schiff base salen and saloph complexes. However, these salts did not yield the desired complexes with peraza macrocycles and hence, the nitrate and chloride salts were used in their preparation. Detailed synthesis procedure of these ligands and metal complexes is given in the following section.

SalenH$_2$ SalophH$_2$

R=H (tacn)   R=H (cyclen)   R=H (cyclam)
R=Me (tmtacn)   R=Me(tmcyclen)   R=Me (tmcyclam)
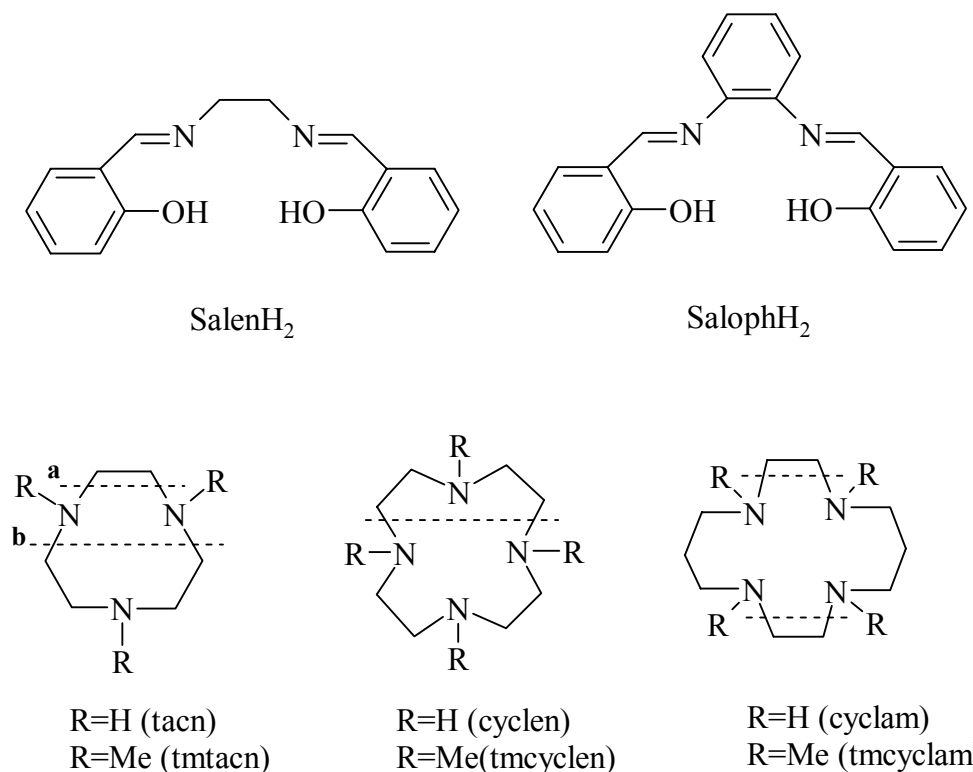
Figure 2.1. *Molecular structures of Schiff base and peraza macrocycle ligands. Dotted lines indicate the bonds formed during the cyclization of the macrocyclic ligands.*

2.2. SYNTHESIS

2.2.1. Materials

The solvents methanol, chloroform, N,N-dimethylformamide (DMF) and acetonitrile used in this work were of A.R. grade and procured from s. d. fine Chem., India. All the other chemicals used in the synthesis were obtained from Merck, India. The solvents were purified and dried according to standard purification procedures [14].

2.2.2. Synthesis of Schiff Base Complexes

2.2.2.1. Synthesis of Schiff Bases (Fig. 2.1)

SalenH₂. To prepare N,N'-ethylenebis(salicylidenamine) (salenH₂), salicylaldehyde (40 mmol, 4.26 ml) was added to a solution of ethylenediamine (20 mmol, 1.33 ml) in absolute ethanol (40 ml). The mixture was heated to reflux for 1 h and the bright yellow crystalline solid salenH₂ formed was collected by filtration. Yield 92% (4.98 g). Melting point (m. p.) 128°C.

Anal. (wt %): Found - C: 71.2, H: 6.0, N: 10.3. Calcd - C: 71.6, H: 6.0, N: 10.4.

^{1}H NMR (CDCl₃), δppm: 3.73 (s, 4H), 6.47-7.20 (m, 8H), 8.07 (s, 2H), 12.0 (br s, 2H)

IR (Nujol) cm^{-1}: 2854-2924, 1633, 1577, 1417, 1375, 1282, 1197, 1150, 1020, 1041, 975, 858.

SalophH₂. N,N'-*o*-phenylenebis(salicylidenaminate) (salophH₂) was prepared in a similar manner as described above using *o*-phenylenediamine and salicylaldehyde. Yield 88 %. m. p. 161°C.

Anal. (wt %): Found - C: 71.2, H: 6.0, N: 10.3. Calcd. - C: 71.6, H: 6.0, N: 10.4.

^{1}H NMR (CDCl₃) δppm: 6.47-7.22 (m, 12H), 8.3 (s, 2H), 12.2 (br s, 2H).

IR (Nujol) cm^{-1}: 2854-2924, 1649, 1560, 1375, 1275, 1191, 1149, 1103, 908.

2.2.2.2.. Synthesis of Neat Cu and Mn Schiff Base Complexes

Cu(salen) and Cu(saloph). In the preparation of Cu(salen) and Cu(saloph), the corresponding Schiff base ligand (5 mmol) was taken in 20 ml of methanol. To a boiling solution of this, $Cu(CH_3COO)_2.H_2O$ (5 mmol) dissolved in 15 ml of methanol was added slowly, over a period of 30 min. The reaction mixture was refluxed for 3 - 4 h and allowed to cool to room temperature. The solid complexes thus obtained were filtered and recrystallized from methanol/chloroform.

Cu(salen). Anal. (wt %): Found - C: 56.0, H: 4.7, N: 7.5. Calcd. - C: 56.4, H: 5.0, N: 7.7. IR (Nujol) cm^{-1}: 2854-2924, 1647, 1629, 1596, 1541, 1377, 1304, 1190, 1141, 980.

Cu(saloph). Anal. (wt %): Found - C: 62.4, H: 4.4, N: 7.2. Calcd. - C: 62.4, H: 4.1, N: 7.1. IR (Nujol) cm^{-1}: 2926, 1608, 1577, 1521, 1460, 1339, 1284, 1188, 1145, 1126, 920, 856.

Mn(salen) and Mn(saloph). The Mn complexes were prepared in a similar manner using $Mn(CH_3COO)_2.4H_2O$ and the corresponding Schiff base ligand. Synthesis was carried out under argon atmosphere.

Mn(salen). Anal. (wt %): Found - C: 60.0, H: 4.4, N: 8.2. Calcd. - C: 59.8, H: 4.4, N: 8.7. IR (Nujol) cm^{-1}: 2854-2924, 1627, 1598, 1541, 1496, 1377, 1284, 1199, 1149, 1126, 908.

Mn(saloph). Anal. (wt %): Found - C: 61.1, H: 4.4, N: 6.4. Calcd. - C: 60.0, H: 4.5, N: 6.9. IR (Nujol) cm^{-1}: 2924, 1627, 1597, 1541, 1496, 1377, 1284, 1199, 1149, 1126, 1022, 856.

2.2.2.3. Synthesis of Encapsulated Schiff Base Complexes

Preparation of Cu(II) and Mn(II)-exchanged NaY. To prepare the Cu (1.2%)-exchanged NaY, 0.024 g of $Cu(CH_3COO)_2.H_2O$ was dissolved in 10 ml of distilled water. To this, 2 g of NaY was added and stirred for 12 h. The solid was filtered and

washed repeatedly with distilled water. Cu-Y thus obtained by the ion exchange method was dried at 120°C for 12 h. Powder XRD showed no structural change of zeolite Y. The amount of Cu (1.2%) loading was estimated by atomic absorption spectroscopy (AAS).

Mn-Y (with 1.2% Mn) was prepared in a similar manner using NaY and $Mn(CH_3COO)_2.4H_2O$.

Preparation of Cu(salen)-Y, Cu(saloph)-Y, Mn(salen)-Y and Mn(saloph)-Y. The encapsulated Schiff based complexes were prepared by the "flexible ligand synthesis method." In a typical preparation of these materials, the copper or manganese exchanged NaY samples were initially evacuated at 100°C. They were then mixed thoroughly with the corresponding Schiff base ligand (3 times excess). The mixture was heated to 100°C for 1 h and then, the temperature was raised to 250°C. Heating was continued for 5 - 6 h. A change in the color from cream to brown indicated the formation of the Schiff base complexes inside the zeolite cages. The free ligand was removed by Soxhlet extraction with chloroform, acetonitrile and finally, with acetone for 2 days each. The characteristics of these materials are given in Chapter 3.

2.2.3. Synthesis of Peraza Macrocyclic Complexes

2.2.3.1. Synthesis of Peraza Macrocyclic Ligands (Fig.2.1)

A generalized method for the synthesis of tacn, cyclen and their methylated compounds is shown in Scheme 22 and of cyclam is shown in Scheme 23. The details of the synthesis of different peraza macrocycles and their intermediates are described in the following section.

<u>**1,4,7,-Triazacyclononane (tacn)**</u>

The ligand tacn was prepared initially as a tosylated compound using N,N'-bis(*p*-tolylsulfonyl)ethylenediamine, N,N',N-tris(*p*-toluenesulfonyl) diethylenetriamine,
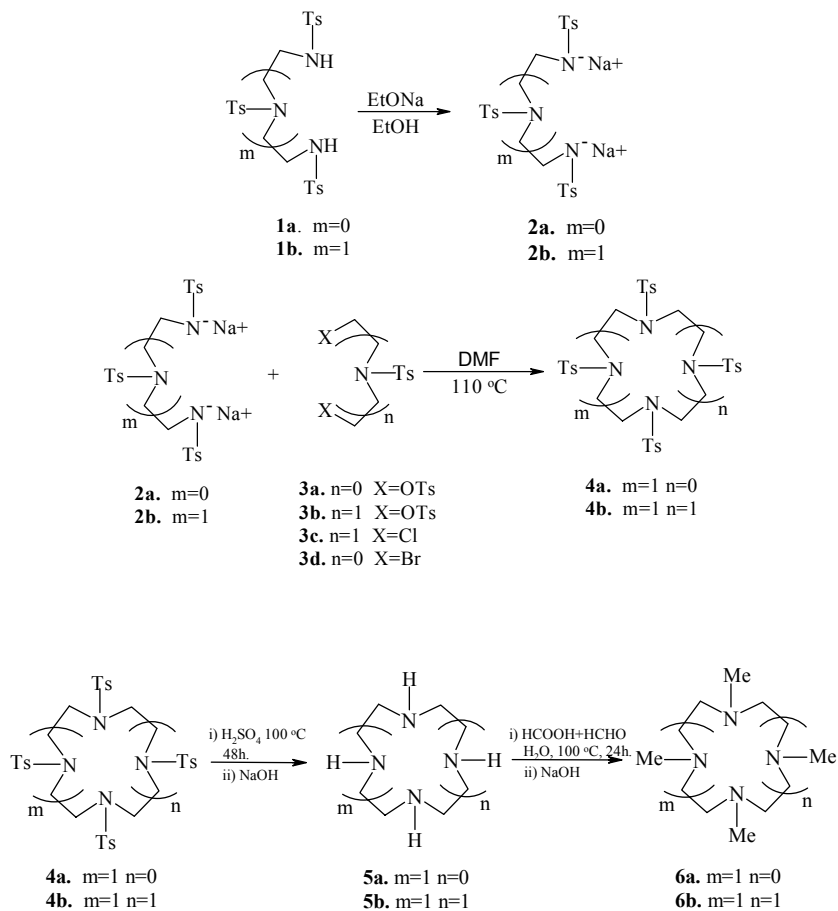
Scheme 2.1. *Synthesis of tmtacn and tmtcyclen ligands.*
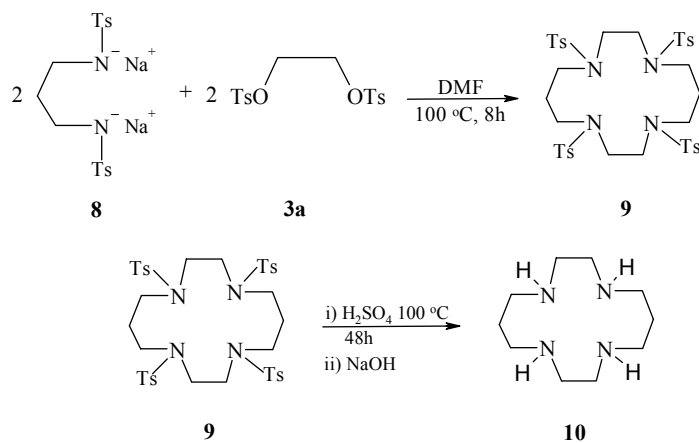
Scheme 2.2. *Synthesis of cyclam ligand*

N,N'-ditosyl-1, 2-disodiumethylenediamine, 1,4,7-tritosyl-1, 7-disodium-1, 4, 7-triazaheptane, 1,2-di(toluene-*p*-sulfonyloxy)ethane, N, O, O'-tris (*p*-tolylsulfonyl) diethanol amine and N-tosyl-2,2'-dichloethylamine. It was then detosylated by different methods. Details of the preparation of tacn and the starting materials used are as follows.

Preparation of N, N'-bis(p-tolylsulfonyl)ethylenediamine (1a) (Scheme 2.3).

A solution of ethylenediamine (1.8 g, 30 mmol) in pyridine (Py; 30 ml) was added slowly to a stirred solution of toluene-*p*-sulfonyl chloride (TsCl; 11.4 g, 60 mmol) in pyridine (30 ml) keeping the temperature below 50°C. The solution was then heated at $50\text{-}60^{\circ}$C for 6 h. The reaction mixture was cooled and added to a beaker containing 350 g of ice and stirred well. The precipitate obtained was filtered after attaining the room temperature, washed with cold ice-cold water and 50% aq. ice-cold ethanol. It was dried at room temperature and recrystallized form ethanol to get 89.4% yield of product **1a** (9.86 gm). m.p.163°C (lit. [15] 165 $^{\circ}$C).

Anal. (wt %): Found - C: 52.4, H: 5.2, N: 7.6, S: 17.3. Calcd. C: 5.4, H: 5.4, N: 7.6, S:16.9.

^{1}H NMR (CDCl$_3$) δppm: 1.66 (s, 6H), 2.44 (s, 2H), 3.07 (s, 2H), 5.0 (br s, 2H), 7.34 (d, 4H, J = 8.3 Hz), 7.7 (d, 4H, J = 8.5 Hz).

IR (Nujol) cm^{-1}: 3288, 2926, 1596, 1446, 1323, 1157, 1089, 913.

$$H_2N \diagup\diagdown NH_2 \xrightarrow[\text{50-60 °C}]{\text{TsCl, Py}} Ts-NH \diagup\diagdown HN-Ts$$

1a
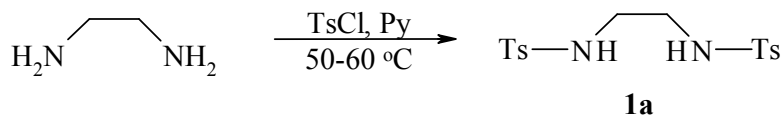
Scheme 2.3

Preparation of N,N',N-tris(*p*-toluenesulfonyl)diethylenetriamine (1b) (Scheme 2.4). A solution of diethylenetriamine (3.01 g, 30 mmol) in pyridine (30 ml)

was added slowly to a solution of toluene-*p*-sulfonyl chloride (17.2 g, 90 mmol) in pyridine (30 ml) with constant stirring and cooling so as to keep the temperature below 50°C. When the addition was over, the reaction mixture was heated at 50-60°C for additional 4 hours and poured into a beaker containing 300 g of ice and stirred well. The solid obtained was filtered, washed repeatedly with water and then with 50% aq. cold ethanol and dried at 100°C to obtain a pale yellow solid. The solid was purified by crystallization from acetonitrile. Yield 93% (15.8 g). m.p. 177-178°C (lit. [16] 175°C). Anal. (wt %): Found - C: 52.8, H: 5.3, N: 7.3, S: 16.9. Calcd.; C: 53.0, H: 5.3, N: 7.4, S: 16.9.

^{1}H NMR (CDCl$_3$) δppm: 2.43 (s, 9H), 3.16 (s, 8H), 3.33(br, 2H), 7.29 (d, 6H, J = 8 Hz), 7.59 (d, 2H, J = 10 Hz), 7.74 (d, 4H, J = 8 Hz).

IR (Nujol) cm^{-1}: 3288, 2926, 1596, 1446, 1323, 1157, 1089, 913, 725.

1b
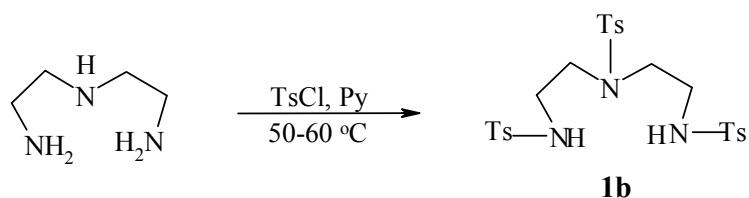
Scheme 2.4

Preparation of N,N'-ditosyl-1,2-disodiumethylenediamine (2a) (Scheme 2.5).

A solution of sodium ethoxide (prepared from 0.23 g of Na in 10 ml of dry ethanol) was

1a   **2a**
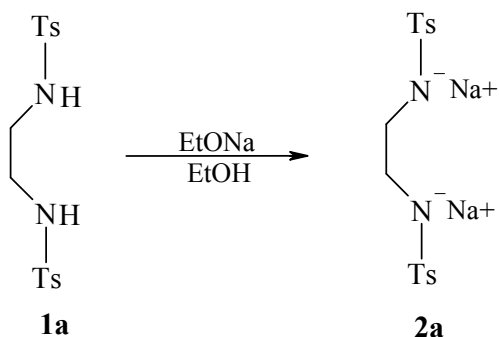
Scheme 2.5

added under dry conditions to slurry of **1a** (1.84 g, 5 mmol) in dry ethanol (50 ml) at 80°C. The mixture was refluxed for 4 h with vigorous stirring and left at room temperature overnight. Excess ethanol was decanted and the solid was dried to get 99% of the highly hygroscopic sodium salt (1.98 g). m.p. > 290°C.

Preparation of 1,4,7-tritosyl-1, 7-disodium-1,4,7-triazaheptane (2b) (Scheme 2.6). A solution of sodium ethoxide (prepared from 0.92 g of sodium in 30 ml of dry ethanol) was added under dry conditions to a slurry of **2a** (11.3 g, 20 mmol) at 80°C and stirred for half an hour at that temperature. Then the reaction mixture was left at room temperature overnight to get 98% (11.9 g) yield of crystalline **2b**, which is highly hygroscopic. m.p. > 290°C.
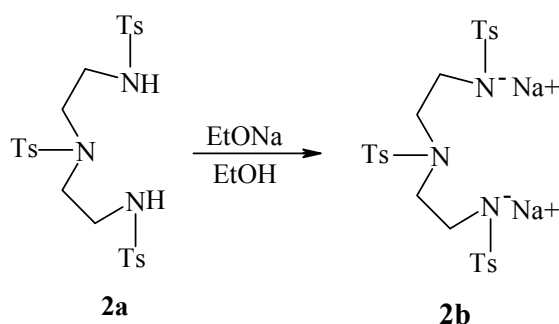
Scheme 2.6

Preparation of 1,2-di(toluene-*p*-sulfonyloxy)ethane (3a) (Scheme 5). To a stirred solution of ethane-1,2-diol (1.86 g, 30 mmol) and toluene-*p*-sulfonyl chloride (11.44 g, 60 mmol) in dichloromethane (60 ml) was added triethylamine (66 mmol, 9.2 ml) dropwise with constant stirring and cooling at 0°C under argon atmosphere. The reaction mixture was stirred overnight at room temperature. The white precipitate obtained was filtered off and washed with dichloromethane. The filtrate was washed with water, 1N HCl, 1N NaHCO$_3$ and brine and dried over Na$_2$SO$_4$. The solvent was evaporated to get the crude product, which was crystallized from ethanol/acetone. Yield 91% (10.1 g). m.p. 125°C (lit [17] 126°C).

Anal. (wt%): Found - C: 51.9, H: 5.4, S: 17.5 Calcd.- C: 51.8, H: 4.9, S: 17.3.

^{1}H NMR (CDCl$_3$) δppm: 2.46 (s, 6H), 4.18 (s, 4H), 7.37 (d, 4H, J = 4 Hz), 7.32 (d, 4H, J = 4 Hz).

IR (Nujol) cm^{-1}: 2924-2854, 1596, 1361, 1180, 1093, 918.

3a
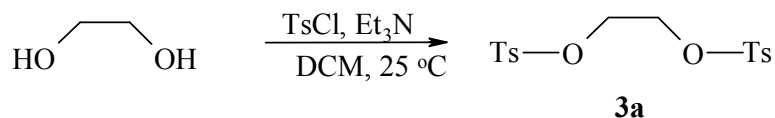
Scheme 2.7

Preparation of N, O, O'- tris(*p*-tolylsulfonyl) diethanol amine (3b) (Scheme 2.8). To a stirred solution of toluene-*p*-sulfonyl chloride (8.5 g, 45 mmol) in dichloromethane (40 ml) was added diethanolamine (1.58 g, 15 mmol) and triethylamine (7.5 ml, 54 mmol) dropwise with constant stirring and cooling to 0°C under dry conditions. The reaction mixture was stirred overnight at room temperature. The white precipitate obtained during the reaction was filtered off and washed with dichloromethane. The dichloromethane layer was washed with water, 1N HCl, 1N NaHCO$_3$ and brine and was dried over Na$_2$SO$_4$. After solvent evaporation, the thick viscous liquid was allowed to stand several hours to obtain a solid that was crystallized from ethanol. Yield 94% (8.0 g). m.p. 93°C (lit. [18] 93-94°C).

^{1}H NMR (CDCl$_3$) δppm: 2.42 (s, 6H), 2.45 (s, 3H), 3.36 (t, 4H J = 6Hz), 4.10 (t, 4H, J = 6 Hz), 7.34 (d, 6H, J = 8 Hz), 7.58 (d, 2H, J = 8 Hz), 7.73 (d, 4H, J = 8 Hz).

IR (Nujol) cm^{-1}: 2924-2854, 1598, 1456, 1361, 1093, 1176,1159, 1097, 979, 813.

3b
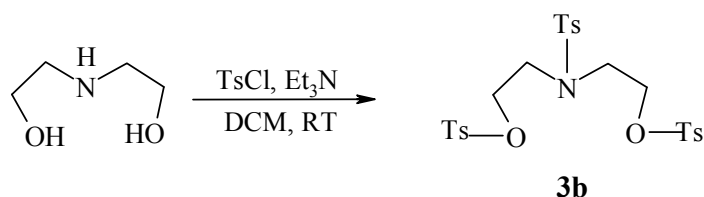
Scheme 2.8

Preparation of N-tosyl-2,2'-dichloroethylamine (3c) (Scheme 2.9). To a solution of the HCl salt of 2,2'-dichloroethylamine (4.46 g, 25 mmol) dissolved in pyridine (20 ml) was added slowly a solution of toluene-*p*-sulfonyl chloride (4.75 g, 25 mmol) with constant stirring and keeping the temperature below 60°C. When the addition was over the reaction mixture was heated at 60-70°C for 4 hours and poured into a beaker containing 300 g of ice and stirred well. The solid obtained was filtered, washed with cold water and dried at room temperature. The sample was purified by crystallization from pet. ether / ethyl acetate. Yield 65.4% (4.1 g). m.p. 48°C (lit. [19], 49°C).

Anal. (wt%): Found - C: 44.4, H: 5.1, N: 4.6, S: 1.8. Calcd. - C: 44.6 H: 5.0, N: 4.7, S: 10.8.

^{1}H NMR (CDCl$_3$) δppm: 2.45 (s, 3H), 3.46 (d, 2H, J = 8 Hz), 3.69 (s, 2H, J = 8 Hz), 7.33 (d, 2H, J = 8 Hz), 7.70 (d, 2H, J = 8 Hz).

IR (Nujol) cm^{-1}: 2854-2924, 1660, 1456, 1375, 1155, 1092, 966, 760.
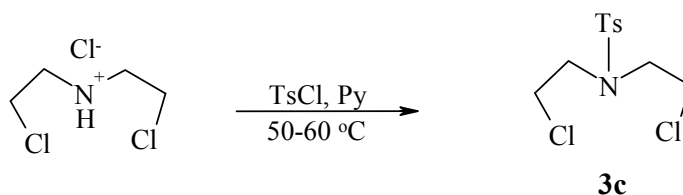
Scheme 2.9

Preparation of 1,4,7-tritosyl-1,4,7-triazacyclononane (4a); Route-1 (Scheme 2.10). To the solution of **2b** (6.09 g, 10 mmol) in dry DMF (25 ml) heated at 100°C was added slowly through a syringe a solution of **3a** (3.7 g, 10 mmol) in dry DMF (15 ml) with stirring over a period of 1h. After the addition was over the heating was continued for another 4 hrs and the reaction mixture was cooled to room temperature. The solution was then added to vigorously stirred water (400 ml), the precipitate was filtered-off,

washed with water (50 ml) and dried at 100ºC. The solid was crystallized from acetone/water. Yield 96% (5.6 g).
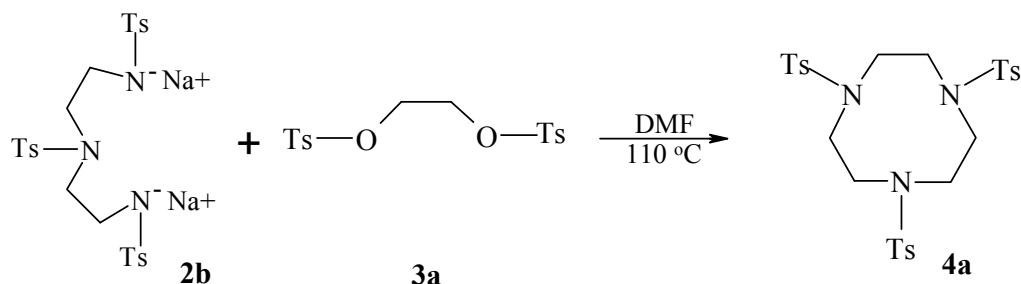
Scheme 2.10

Route-2 (Scheme 2.11). To the solution of **2a** (6.09 g, 10 mmol) in dry DMF (25 ml) heated at 100ºC was added a solution of **3c** (2.96 g, 10 mmol) in dry DMF (15 ml) slowly through a syringe with stirring over a period of 1h. After the addition was over the heating was continued for 12 h and cooled to room temperature. The solution was then added to vigorously stirred water (400 ml), the precipitate was filtered-off, washed with water (50 ml), dried at 100ºC and crystallized from acetone/water (90:10 v/v). Yield 47% (2.74g).
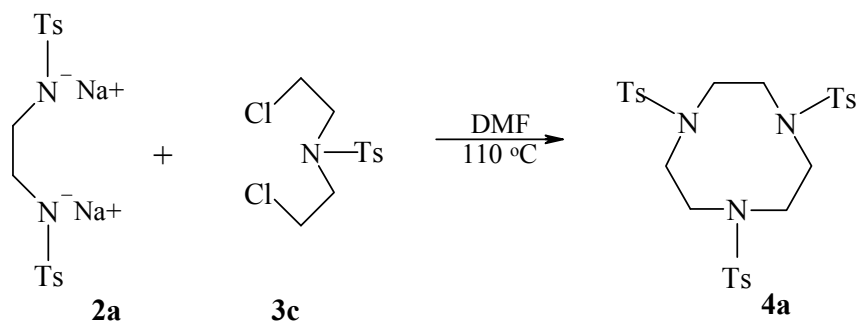
Scheme 2.11

Route-3 (Scheme 2.12). This route of preparation is a modified procedure of ref. [20]. To the solution of **2b** (6.09g, 10 mmol) in dry DMF (60 ml) heated at 100°C was added **3d** (0.86 ml, 10 mmol) slowly through a syringe with stirring. The reaction was monitored by TLC. After the reaction was over (15 - 16 h), it was cooled to room temperature and the reaction mixture was added to vigorously stirred water (400 ml), the precipitate was filtered-off, washed with water (50 ml) and dried at 100°C and crystallized from acetone/water. Yield 64% (3.7 g).
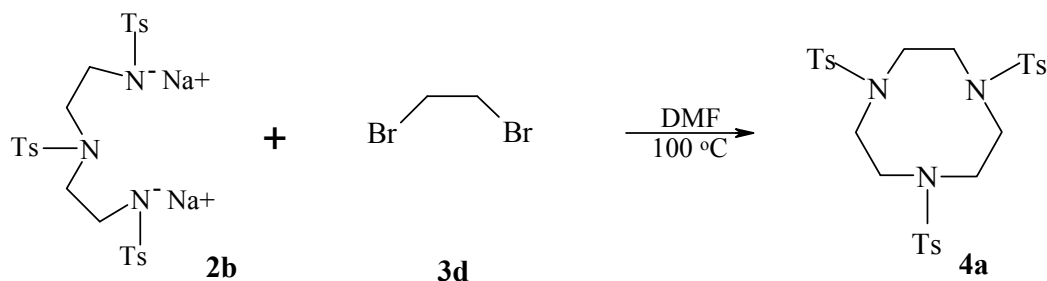
Scheme 2.12

Route-4 (Scheme 2.13). The procedure is similar to route-3, except **2a** and **3b** are used as sodium salt and coupling reagent respectively. Yield 55 % (3.2 g). m.p. 222-223°C (lit. [21] 223°C).

Anal. (wt %): Found - C: 54.6 H: 6.1, N: 7.2, S: 15.9. Calcd. C: 54.8, H: 5.6, N: 7.1, S: 16.3.
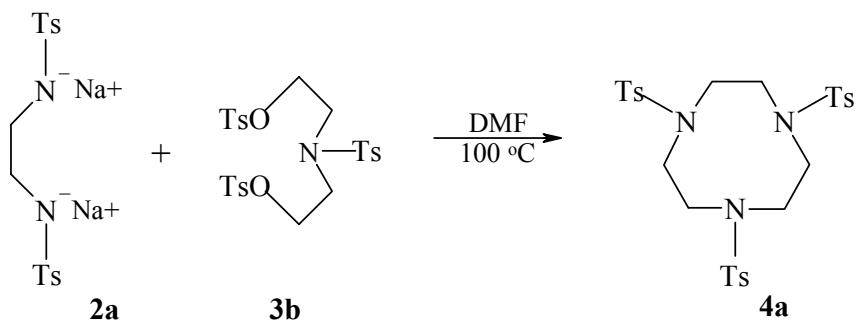
Scheme 2.13

NMR (CDCl$_3$) δppm: 2.42 (s, 9H), 3.40 (d, 12H), 7.29 (d, 6H, J = 8 Hz), 7.76 (d, 6H, J = 8.3 Hz).

IR (Nujol) cm^{-1}: 2854-2924, 1596, 1454, 1321, 1153, 1089, 997.

Preparation of 1,4,7-triazacyclononane (tacn) (5a) (Scheme 2.14). 4a (4.42 g, 7.5 mmol) was dissolved in conc. H$_2$SO$_4$ (4 - 5 ml) and stirred at 110°C for 48 h. The mixture was then cooled to 0°C and 15-20 ml of ether was added slowly with constant stirring. The brown solid obtained was filtered, dissolved in minimum amount of water and the pH was adjusted to 10 with 10N NaOH at 0°C. (If necessary the sodium sulphate precipitated was filtered off and washed repeatedly with chloroform). The tacn was extracted repeatedly with equal volumes of chloroform (5 x 10 ml). The extracts were dried over Na$_2$SO$_4$ and evaporated to get a light yellow viscous liquid, which on standing at 0°C gave crystals of **5a.** Yield 68.5% (0.65 g). m. p. 42 ^{o}C.

^{1}H NMR (CDCl$_3$) δppm: 2.79 (s, 6H), 2.63 (br, 3H).

IR (Neat) cm^{-1}: 3306, 2854-2928, 1660, 1157, 1032, 997.

MS: M$^+$ 126, 112, 99, 85, 73, 56, 44 (base peak).
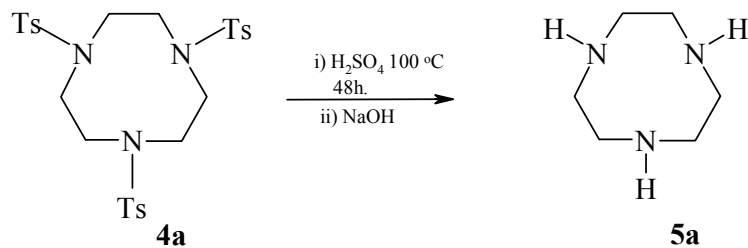
Scheme 2.14

1,4,7-Trimethyl-1,4,7-triazacyclononane(tmtacn) (6a) (Scheme 2.15)

5a (0.65 g, 5 mmol) was dissolved in 98% aqueous formic acid (4 ml) 37-40% aqueous formaldehyde (4 ml) and water (2 ml). The solution was heated at 100°C for 24 h. The reaction mixture was cooled to 0°C and the pH was adjusted to 10-12. The 1,4,7-trimethyl-1,4,7-triazacyclononane (tmtacn) in solution was extracted repeatedly with

chloroform. The tmtacn (**6a**) thus obtained was purified by a small filter column (silica

60-120 and pet. ether /methanol = 80: 20). Yield 80 % (0.68g).

^{1}H NMR (CDCl$_3$) δppm: 2.38 (s, 9H), 2.70 (s, 12H).

IR (Neat) cm^{-1}: 2802-2900, 1666, 1600, 1454, 1373, 1290, 1076, 1031, 999.

MS: M[+] 171, 154, 147, 127, 115, 99, 84, 70, 58, 42 (base peak).

5a   **6a**
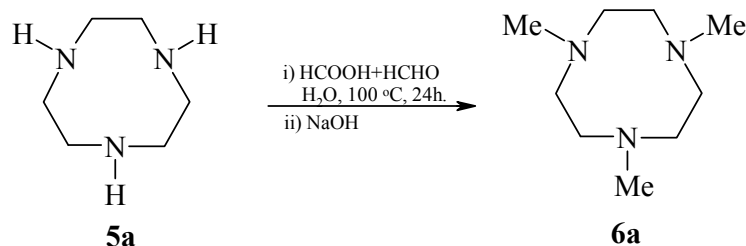
Scheme 2.15

1,4,7,10-Tetraazacyclododecane (cyclen)

Preparation of 1,4,7,10-Tetratosyl-1, 4, 7,10-tetraazacyclododecane (4b)
[22]; Route-1 (Scheme 2.16). To a solution of **2b** (6.09 g, 10 mmol) in dry DMF (30

ml) heated to 100°C was added a solution of **3b** (5.7 g, 10 mmol) in dry DMF (20 ml)

slowly with stirring through a syringe over a period of 2h. After the addition was over,

heating was continued for another 5 h and then the reaction mixture was cooled to room

temperature. The solution was added to vigorously stirred water (400 ml), the

precipitate was filtered-off, washed with water (50 ml), dried at 100°C and crystallized

from acetone/ethanol. Yield 89% (7.0 g).

2b   **3b**   **4b**

Scheme 2.16

Route-2 (Scheme 2.17). To the solution of **2b** (6.09 g, 10 mmol) in dry DMF (30 ml) heated at 100°C was added a solution of **3d** (2.96 g, 10 mmol) in dry DMF (20 ml) slowly with stirring through a syringe over a period of 2 h. After the addition was over the heating was continued for 10 h and the reaction mixture was cooled to room temperature. The solution was then added to vigorously stirred water (400 ml), the precipitate was filtered-off, washed with water (50 ml) and dried at 100°C and crystallized from acetone/ethanol. Yield 59% (4.6 g). m.p. 289 °C (lit. [23] 289 °C).

Anal. (wt %): Found - C: 54.8, H: 5.6, N: 7.3, S: 16.6. Calcd. C: 54.8, H: 5.6, N: 7.1, S: 16.4.

^{1}H NMR (CDCl$_3$) δppm: 2.43 (s, 12H), 3.42 (s, 16H), 7.30 (d, 8H, J = 8 Hz), 7.65 (d, 8H, J = 8.3 Hz).

IR (Neat) cm^{-1}: 2954-2924, 1597, 1460, 1336,1160,1081, 975, 902, 715

Scheme 2.17

Preparation of 1,4,7,10-Tetraazacyclododecane (cyclen)(5b) (Scheme 2.18).
4b (4.0 g, 5 mmol) was dissolved in conc. H$_2$SO$_4$ (5 ml) and stirred at 110°C for 48h. The mixture was cooled to 0°C and 20-30 ml of ether was added slowly with constant stirring. The brown solid obtained was filtered, dissolved in minimum amount of water and the pH was adjusted to 10 with 10N NaOH at 0°C (sodium sulphate precipitated was filtered and washed repeatedly with chloroform). The cyclen in the solution was

extracted repeatedly with equal volumes of chloroform (6 x 10 ml). The extracts were

dried over Na_2SO_4 and evaporated to get a light yellow solid of **5b.** Yield 68.5 % (0.65

g). m.p. 103 ^{o}C (lit. [24], 103-109 ^{o}C).

^{1}H NMR (CDCl$_3$) δppm: 2.68 (s, 16H), 2.39(br, 4H).

IR (Neat) cm^{-1}: 3280, 2852-2924, 1560, 1350, 1110, 1036, 941, 759.

MS: M$^{.+}$ 170, 153, 136, 121, 104, 85, , 80, 56, 44 (base peak).

4b   **5b**
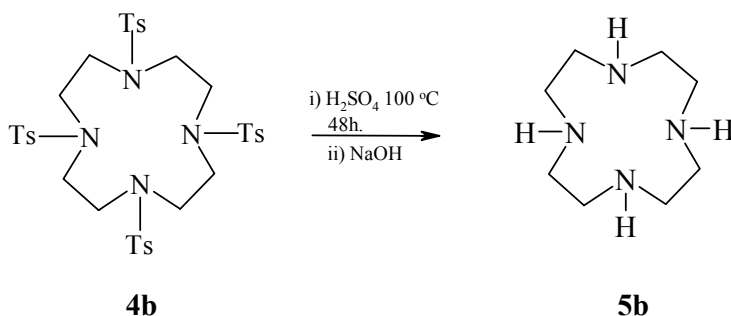
Scheme 2.18

1,4,7,10-Tetramethyl–1,4,7,10-Tetraazacyclododecane (tmcyclen) (6b) (Scheme 2.19)

In a modified reported procedure [25], **5b** (0.4 g, 3.1 mmol) was dissolved in

98% aqueous formic acid (4 ml), 37-40% aq. formaldehyde (4 ml) and water (2 ml).

The solution mixture was heated at 100°C for 24 h. The reaction mixture was cooled to

0°C and adjusted to pH = 10. The 1,4,7,10-tetramethyl–1,4,7,10-tetraazacyclononane

(tmcyclen) in solution was extracted repeatedly with chloroform. The liquid tmcyclen

6b obtained after evaporation of solvent was purified by a small filter column (silica

60-120 and pet. ether/MeOH = 80:20).

^{1}H NMR (CDCl$_3$) δppm: 2.49 (s, 12H), 2.79 (s, 16H).

IR (Neat) cm^{-1}: 2941-2848, 1598, 1365, 1195, 1118, 1070, 1029, 923, 729, 729.

MS: M$^{.+}$ 228, 213, 199, 186, 169, 149, 124, 113, 99, 82, 70, 58, 42 (base peak).

i) HCOOH+HCHO
H₂O, 100 °C, 24h.
ii) NaOH

5b

6b
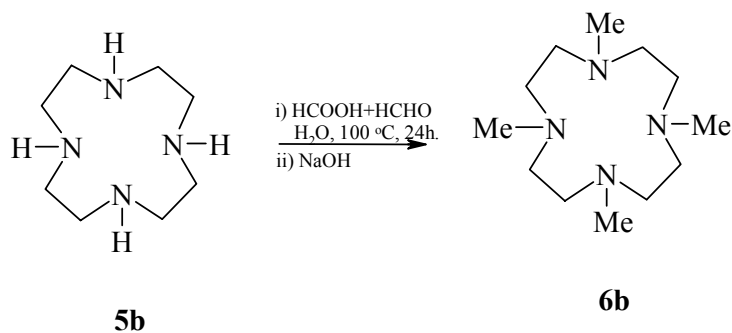
Scheme 2.19

1,4,8,11-tetrazacyclotetradecane (cyclam)

Tetratosylated cyclam was prepared first using N,N'-bis (*p*-tolylsulfonyl) propylenediamine and N, N'-ditosyl-1, 3-disodium-propylenediamine. It was then detosylated to get cyclam. Details of the synthesis are given below.

Preparation of N,N'-bis(*p*-tolylsulfonyl)propylenediamine (7) (Scheme 2.20). A solution of propylenediamine (2.2 g, 30 mmol) in pyridine (30 ml) was added slowly to a stirred solution of toluene-*p*-sulfonyl chloride (11.4 g, 60 mmol) in pyridine (30 ml) keeping the temperature below 50°C. The solution was heated at 60-70°C for 6 h. The reaction mixture was cooled and added to a beaker containing 350 g of ice and stirred well. The precipitate obtained was filtered after attaining room temperature, washed with ice-cold water and 50% ice-cold ethanol. It was dried at room temperature and recrystallised form ethanol to get 79.0% (9 g) yield of product **7**. m.p.163 °C (lit. [26], 165 °C).

EtONa
EtOH

7

Scheme 2.20

48
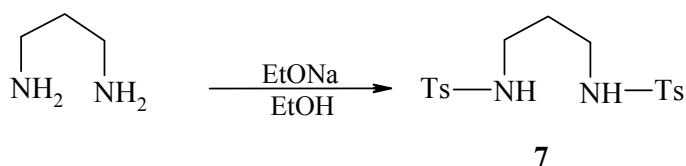
Anal. (wt %): Found - C: 53.5, H: 5.7, N: 7.1. Calcd.- C: 53.4, H: 5.7, N: 7.3, S: 16.7.

^{1}H NMR (CDCl$_3$) δppm: 1.67 (m, 2H), 2.43 (s, 6H), 3.01 (m, 4H), 5.15 (br, 2H), 7.27 (d, 4H, J = 8.4 Hz), 7.71 (d, 4H, J = 8.4 Hz)

IR (Nujol) cm^{-1}: 3267, 2850, 1595, 1325, 1155, 1074, 1024, 978, 860.

Preparation of N, N'-Ditosyl-1, 3-disodium-propylenediamine (8) (Scheme 2.21). A solution of sodium ethoxide (prepared from 0.46 g. of sodium in 15ml of dry ethanol) was added under dry conditions to the slurry of **7** (3.8 g, 10 mmol) in dry ethanol (45 ml) at 80°C and refluxed with efficient stirring for 2 hrs. The reaction mixture was kept at room temperature overnight, and the crystals were collected and dried to get the highly hygroscopic sodium salt **8.** Yield 99% (4.2 g).
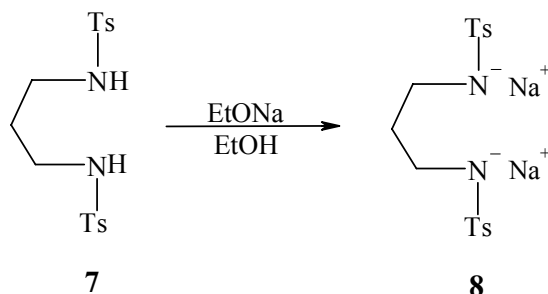
Scheme 2.21

Preparation of 1,4,8,11-Tetratosyl-1,4,8,11-tetrazacyclotetradecane (9)(Scheme 2.22). To a solution of **8** (6.09 g, 10 mmol) in dry DMF (80 ml) heated at 100°C was added slowly through a syringe a solution of **3a** (3.7g, 10mmol) in dry DMF (20 ml) with stirring over a period of 2 h. After the addition was over, heating was continued for 6 h and the mixture was cooled to room temperature. The solution was then added to vigorously stirred water (400 ml), the solid was filtered, washed with water (50 ml) and dried at 100°C. The compound **9** thus obtained was recrystallized from acetone/ethanol (80:20 v/v). Yield 76% (3.1 g). m.p. 256°C.

Anal. (wt %); Found - C: 55.8, H: 5.7, N: 66.8, S: 15.8. Calcd. C: 55.9, H: 5.9, N: 6.9, S: 15.7.

^{1}H NMR(CDCl$_3$) δppm: 1.99 (m, 4H), 2.43 (s, 12H), 3.35 (m, 16H), 7.29 (d, 8H, J = 7.8 Hz), 7.71 (d, 8H, J = 8.3 Hz)

IR (Neat) cm^{-1}: 2854-2950, 1600, 1334, 1159, 1093, 1039, 975, 813, 723.

8   **3a**   **9**
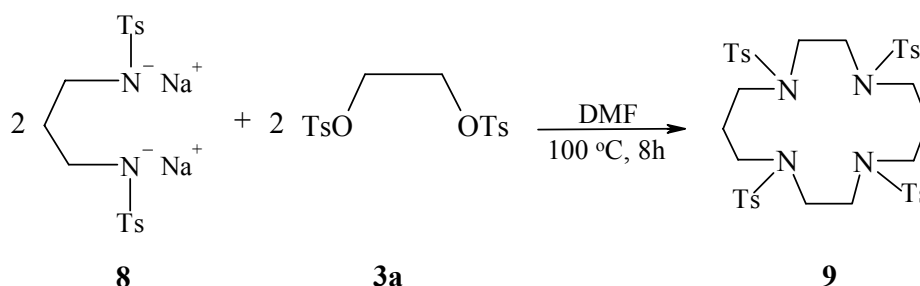
Scheme 2.22

Preparation of 1,4,8,11-Tetrazacyclotetradecane (cyclam) (10) (Scheme 2.23). 9 (3.0g, 3.7 mmol) was dissolved in conc. H$_2$SO$_4$ (5 ml) and stirred at 110°C for 48 h. It was cooled to 0°C and 20-30 ml of ether was added slowly with vigorous stirring. The brown solid obtained was filtered under nitrogen, dissolved in minimum amount of water and the pH was adjusted to 10 with 10N NaOH keeping in an ice bath (the sodium sulphate precipitated was filtered and washed repeatedly with chloroform). The cyclam in the solution was extracted repeatedly with equal volumes of chloroform (5 x 10 ml). The extracts were dried over Na$_2$SO$_4$ and evaporated to get 28.5% (0.21 g) of a light yellow solid **10**. m.p. 120°C.

9   **10**
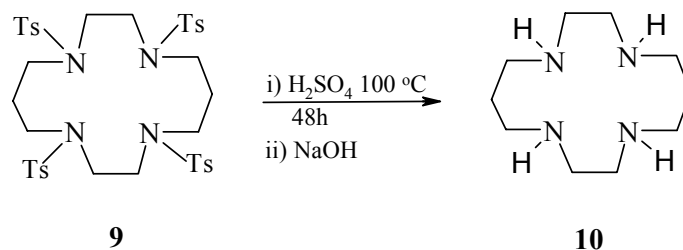
Scheme 2.23

^{1}H NMR (CDCl$_3$) δppm: 1.75 (m, 4H), 2.16 (s, 8H), 2.93 (m, 8H).

IR (Nujol) cm^{-1}: 3276, 2854-2960, 1468, 1370, 1205, 1126, 1070, 830.

The NMR spectra of representative peraza macrocyclic ligands are presented at the end of this chapter (Section 2.5).

These procedures reveal that cyclization of ligands could be achieved by different routes (see Scheme 2.22) [9, 11-13, 28, 29]. But the yields of the cyclized product varied with the route. Table 2.1 lists the yields of the cyclized product obtained by different routes. Cyclization using diol-ditosylates [9, 13] (Table 2.1; see route 3 for Ts-tacn and route 1 for Ts-cyclen) was found to be more efficient than the halide routes [28-30]. Again detosylation is a crucial step in the synthesis of cyclic peraza ligands as it had to be carried out under drastic conditions that can sometimes lead to ring opening. Among the various methods, detosylation using sulfuric acid was found to be superior. The cyclic amine was precipitated as the sulfate salt from the acidic mixture by the addition of ethanol/ether. In the sulfuric acid method, high yields of **5a** and **5b** were obtained by minimizing water. N-methylation of **5a** and **5b** with formic acid and

Table 2.1. Various cyclizations leading to tosylated cyclic amines

Tosylated Cyclic amine	*Disodium salt*	*Coupling reagent*	*Tosyalated cyclic amine*	*Cyclization Time (h)*	*Isolated Yield (%)*
Ts tacn-route 1	2a	3d	4a	12	47
Ts tacn-route 2	2b	3c	4a	14	64
Ts tacn-route 3	2b	3a	4a	6	96
Ts tacn-route 4	2a	3b	4a	8	55
Ts cyclen-route 1	2b	3b	4b	7	89
Ts cyclen-route 2	2b	3d	4b	16	59

formaldehyde afforded **6a** and **6b** in high yields. In the case of cyclam, the tosylation step yielded **9** in good yields. However, the yields in the detosylation step were very low (24%).

2.2.3.2. Synthesis of Neat Metal Complexes

Cu(tacn)(ClO₄)₂. In a modified procedure [27] to prepare $Cu(tacn)(ClO_4)_2$, to a solution of tacn (1 mmol, 0.13 g) in 3 ml methanol was added a solution of $CuCl_2$ $.2H_2O$ (1 mmol, 0.17 g) in 3 ml of methanol and $NaClO_4$ (1.5 mmol, 0.198 g) simultaneously and stirred at room temperature (25 ^oC) for 2 h. The reaction mixture was heated at 60^oC for 1 h. The solid obtained was filtered, washed with cold methanol (1-2 ml) and crystallized from methanol to get bluish green crystals. Yield 29% (0.142 g).

Anal. (wt%): Found - C: 25.4, H: 4.7, N: 14.6. Calcd. - C: 25.3, H: 4.4, N: 14.8.

IR (Nujol) cm^{-1}: 3284, 3192, 2854-2924, 1232, 1020, 966, 858, 623.

Cu(tmtacn)(ClO₄)₂, Cu(cyclen)(ClO₄)₂.2CH₃OH, Cu(tmcyclen)(ClO₄)₂ and Cu(cyclam)(ClO₄)₂. The copper complexes of tmtacn, cyclen, tmcyclen and cyclam were prepared using $Cu(NO_3)_2$ $.2.5H_2O$ / $CuCl_2.2H_2O$ as the source of copper.

Cu(tmtacn)(ClO₄)₂: Yield 27%. Anal. (wt%): Found - C: 24.5, H: 5.1, N: 10.0. Calcd. - C: 24.9, H: 4.8, N: 9.7. IR (Nujol) cm^{-1}: 2852, 1298, 1251, 1020, 958, 623.

Cu(cyclen)(ClO₄)₂.2CH₃OH: Yield - 42 %. Anal. (wt%): Found - C: 24.2, H: 6.3, N: 11.3. Calcd. - C: 24.0, H: 5.7, N: 11.2. IR (Nujol; cm^{-1}): 3240, 2854-2960, 1305, 1244, 1012, 974, 624.

Cu(tmcyclen)(ClO₄)₂: Yield 66% (crystallized from acetonitrile / chloroform).

Anal. (wt%): Found - C: 28.3, H: 6.3, N: 11.0. Calcd. - C: 29.3, H: 5.7, N: 11.4.

IR (Nujol) cm^{-1}: 2854-2960, 1350, 1294, 1278, 1018, 966, 756, 623.

Cu(cyclam)(ClO₄)₂: Yield 67% (crystallized from acetonitrile / chloroform).

Anal. (wt%): Found - C: 26.2, H: 5.2, N: 11.8. Calcd. - C: 25.9, H: 5.2, N: 12.1.

IR (Nujol) cm^{-1}: 3242, 2854-2924, 1370, 1299, 1040, 964, 625.

Mn(cyclen)(ClO$_4$)$_2$.3CH$_3$OH. In a typical procedure to prepare Mn(cyclen)(ClO$_4$)$_2$.3CH$_3$OH a solution of Mn(NO$_3$).4H$_2$O (0.8 mmol, 0.2 g) in 3 ml of methanol was added to a solution of cyclen (0.8 mmol, 0.14 g) in 3 ml of methanol and stirred at room temperature for 2 h. To this, was added an excess of NaClO$_4$ (2.4 mmol, 0.35 g) and the reaction mixture was refluxed for 1 h. The green solid obtained was filtered and washed with cold methanol (1-2 ml). All the manipulations were done under argon atmosphere. The complex was crystallized from acetonitrile. Yield 29% (0.098 g).

Anal. (wt%): Found- C: 26.0, H: 5.6, N: 9.8. Calcd. - C: 55.9, H: 5.9, N: 6.9.

IR (Neat) cm^{-1}: 3200, 2854-2924, 1278, 1018, 752, 624.

Mn(tmcyclen)(ClO$_4$)$_2$.2CH$_3$OH and Mn(cyclam)(ClO$_4$)$_2$. In a similar manner, manganese complexes of tmcyclen and cyclam were also prepared.

Mn(tmcyclen)(ClO$_4$)$_2$.2CH$_3$OH: Yield 23 % (crystallized from acetonitrile). Anal. (wt.%): Found - C: 31.6, H: 6.7, N: 10.7. Calcd. C: 30.8, H: 6.6, N: 10.2. IR (Neat)cm^{-1}: 2854-2924, 1294, 1286, 1026, 968, 750, 623.

Mn(cyclam)(ClO$_4$)$_2$: Yield 47% (crystallized from acetonitrile). Anal. (wt.%): Found - C: 27.1, H: 4.8, N: 12.0. Calcd. - C: 26.5, H: 5.2, N: 12.3. IR (Neat) cm^{-1}: 3249, 2854-2924, 1282, 1026, 752, 624.

Mn$_4$O$_6$(tacn)$_4$(ClO$_4$)$_4$.H$_2$O. To a solution of tacn (1.35 mmol, 0.175 g) in methanol (4 ml) were added Mn(NO$_3$)$_2$.4H$_2$O (1.35 mmol, 0.34 g) in water (2 ml), sodium oxalate (1.49 mmol, 0.199 g) in water (4 ml) and NaClO$_4$ (2 mmol, 0.285 g; 1.5 equiv). The suspension was heated at 60$^{\rm o}$C for 3 h. To the mixture, 1M NaOH solution was added till the pH was 10. The brown colored solution obtained was filtered and kept

for crystallization at room temperature. Flake like brittle crystals were obtained overnight. Yield 42% (0.175 g).

Anal. (wt%): Found - C: 23.9, H: 5.4, N: 13.5. Calcd. - C: 22.7, H: 5.4, N: 13.2.

IR (Neat) cm^{-1}: 3300, 2854-2924, 1228, 1030, 975, 950, 725, 623.

Mn(O)(tmtacn)SO₄.H₂O. MnSO₄ (1 mmol) dissolved in 2 ml of water was added to tmtacn (1 mmol) in 4 ml of methanol and the mixture was stirred well at room temperature and then warmed at 40°C for 2 h. It was filtered and kept for evaporation for 2-3 days to obtain the Mn(O)(tmtacn)SO₄. Solubility – water; yield - 55 % (0.208 g).

Anal. (wt %): Found- C: 30.6, H: 6.4, N: 11.7. Calcd.- C: 30.3, H: 6.9, N: 11.8.

IR (Neat) cm^{-1}: 2954-2924, 1647, 1300, 1285, 1083, 1012, 968, 939, 854, 721, 609.

2.2.3.3. *Preparation of Encapsulated Peraza Macrocyclic Complexes*

The encapsulated complexes of Cu and Mn tacn, tmtacn, cyclen, tmcyclen and cyclam were prepared by the "flexible ligand synthesis method" as described below. The Cu and Mn catalysts are designated as:

Cu(tacn)-Y, Cu(tmtacn)-Y, Cu(cyclen)-Y, Cu(tmcyclen)-Y, Cu(cyclam)-Y and Mn(tacn)-Y, Mn(tmtacn)-Y, Mn(cyclen)-Y, Mn(tmcyclen)-Y, Mn(cyclam)-Y, respectively.

In a typical preparation of the encapsulated complex, 2 g of Cu-Y or Mn-Y (1.2 % Cu or Mn) (prepared as in Section 2.2.2.3.) was initially evacuated and then mixed with the corresponding perazamacrocyclic ligand in methanol (ligand: metal = 4:1 mole). The mixture was heated in a specially designed glass reactor under nitrogen atmosphere to 100°C for 1 h. Then, the temperature was slowly raised to 200°C and heated for 6 hrs. It was cooled and the unreacted ligand and the complex on the surface were removed by Soxhlet extraction with acetonitrile and acetone for 8-10 h. The

zeolite encapsulated Cu and Mn peraza macrocyclic complex thus obtained was dried at 110 $^{\circ}$C for 5 h and used in the characterization and catalytic activity tests.

2.3. CHARACTERIZATION TECHNIQUES

The formation, integrity and purity of the materials prepared were confirmed by a variety of physicochemical characterization techniques. Details of these techniques, experimental conditions and sample preparation are as follows.

2.3.1. Chemical Analysis

The exact composition of the materials and their molecular formula were estimated from elemental analysis (C, H & N) and atomic absorption spectroscopy (AAS). The C, H & N analyses of the samples were done on a Carlo Erba EA 1108 elemental analyzer. In a typical analysis, about 3 - 5 mg of sample was used to estimate the percentage C, H and N contents. The metal ion composition (Cu and Mn) in zeolite-encapsulated materials was determined using a Varian Spectr SF-220 atomic absorption spectrometer. For AAS analysis, a solution was prepared by dissolving a 40 mg of the zeolite-encapsulated catalyst in minimum amount of HF. It was diluted to 25 ml using demineralised water. The sample solution, thus prepared, was injected into the sample port of the spectrometer. The metal ion content (in ppm) was estimated from the optical absorption values and the calibration plot made using standard solutions of different concentrations.

2.3.2. X-Ray Diffraction (XRD)

Powder XRD is used to study the cation distribution inside the zeolite matrix. An empirical relationship exists between the relative peak intensities of (331), (311), and (220) reflections and the location of small cations in NaY zeolite [31]. It also provides information on the phase purity and crystallinity of the materials. The studies

were conducted using a computer-controlled automatic Rigaku Miniflex X-ray diffractometer (Model D-MAX II VC, Japan). Ni-filtered Cu-Kα radiation (λ = 1.5404 Å) was used with a curved graphite crystal monochromator and a NaI scintillator. XRD data at 298 K were collected in the 2θ range of 5 - 50° at a scan rate of 4°/min or lower. After the background correction, the peak positions were marked and the d-values and relative intensities (I/I_o) of the peaks were estimated. Finely powdered and sieved (170 mesh) solid catalysts were used for the XRD analysis. The samples were prepared as thin layers on metal or glass slides.

2.3.3. Sorption Studies

Sorption experiments provide evidence for the presence of the metal complex inside the zeolite cavities. The extent of pore blocking can be ascertained from the decrease in the surface area or pore volume in the encapsulated metal complexes. BET surface area was drastically reduced when phthalocyanine and porphyrin complexes were incorporated into zeolite X and Y [32]. The surface areas of the samples were determined from the N_2 adsorption isotherms measured at -100°C by a Coulter (Omnisorb 100 CX) instrument.

2.3.4. Fourier Transform Infrared (FT-IR) Spectroscopy

This is an important "fingerprint" technique used for the determination of the molecular structure of metal complexes (both "neat" and encapsulated), by analyzing the characteristic vibrational bands arising from the functional groups. The FT-IR spectra were recorded on a Shimadzu 8201 PC spectrophotometer in the range of 4000-400 cm^{-1}. The spectra for the solutions were recorded using a ZnSe ATR circle cell. In the case of solids, samples were prepared as Nujol mulls and the spectra were recorded in the transmittance (%T) mode. In a typical IR sample preparation procedure, 10 - 25 mg of the sample was mulled in Nujol. The mull was evenly spread over an oval quartz

plate and then subjected to FT-IR analyses. The characteristic vibrational bands of Nujol were observed at 2925, 2854, 1465 and 1377 cm^{-1}. The spectra of the encapsulated complexes were measured in the reflectance mode.

2.3.5. UV-Visible Spectroscopy

UV-visible absorption spectroscopy, being dependent on the electronic structure and the environment of the absorbing chromophore, allows the effective characterization or identification of the metal complex. UV-visible spectra were recorded on Shimadzu UV-2550 spectrophotometer in the region 200 – 900 nm. The spectra of the liquid samples were measured in the normal absorption mode. Diffuse reflectance mode was used in the measurement of the solid samples. The UV-visible spectroscopy provided information about the changes in the electronic structure of metal complexes after they are encapsulated in zeolites. The effect of the macrocyclic ring and substitution is manifested on the electronic spectra of the compounds.

2.3.6. Electron Paramagnetic Resonance (EPR) Spectroscopy

EPR spectroscopy provides information about the molecular electronic structure of the metal complexes. In ideal cases it differentiates the encapsulated metal complexes from the surface adsorbed species. It also provides information about the electron spin density distribution and structural changes in the metal complex when it is encapsulated inside the zeolite pores [33, 34]. The EPR spectra of the "neat" and zeolite-Y-encapsulated complexes were recorded on a Bruker EMX X-band spectrometer operating with a 100 kHz field modulation. Frequency calibration was done using a microwave frequency counter fitted in an ER 041 XG-D microwave bridge. Measurements at low temperatures were performed using a Bruker BVT 3000 temperature controller. The spectra at -100°C were recorded using a quartz insert Dewar. Spectral simulations and manipulations were done using the Bruker Simfonia

and WINEPR software packages. The measurements for liquid samples at 298 K were

done using a quartz aqueous cell.

2.4. REFERENCES

1.   Lindoy, L.F. *The Chemistry of Macrocyclic Ligand Complexes,* Cambridge University Press, Cambridge, **1989**.

2.   Dietrich, B.; Viout, P.; Lehn, J.-M. *Macrocyclic Chemistry. Aspects of Oganic, Inorganic and Supramolecular Chemistry,* VCH, Weinhiem, **1993**.

3.   Canali, L.; Sherrington, D.C. *Chem. Soc. Rev.* **1999**, *28,* 85.

4.   Ito, Y.N.; Kastuki, T. *Bull. Chem. Soc. Jpn.* **1999**, *72,* 603.

5.   Srinivasan, K.; Michaud, P.; Kochi, J.K.   *J. Am. Chem. Soc.* **1986**, *108,* 2309.

6.   Coleman, W.M.; Boggess, R.K.; Hughes, J.W.; Taylor, L.T. *Inorg. Chem.* **1981**, *20,* 700.

7.   Bailes, R.H.; Calvin, M. *J. Am. Chem. Soc.* **1947,** *69*, 1886.

8.   Poon, C. K.; Tobe, M. L. *J. Chem. Soc. A,* **1968**, 1549.

9.   Kula, R. J.; Barefield, E. K.; Wagner, F.; Herlinger, A. W.; Dahl, A. R. *Inorg. Synth.* **1976**, *16,* 220.

10.   Richmann, J. E.; Atkins, T.J. *J. Am. Chem. Soc.* **1974**, *96*, 2268.

11.   Richmann, J. E.; Orttle, W.F. *Org. Synth.* **1978**, *58*, 86

12.   Stetter, H.; Mayer, K. H. *Chem. Rev.* **1961**, *94,* 1410.

13.   Barefield, E. K.; Wagner, F. *Inorg. Chem.* **1973**, *12,* 2436.

14.   Armarego, W.L.F.; Perrin D.D. *Purification of Laoratory Chemicals* 4th Edn. Butterworth-Heinemann Publishres, Oxford, **1996**.

15.   Kirsanov, A. V.; Kireannova, N. A. *Zh. Obshch. Khim.* 1962, *32,* 887. *Chem. Abstracts* **1962**, *58,* 3341c.

16.   Searle, G.H.; Geue, R.J. *Aust. J. Chem.* **1984**, *37*, 959.

17.   Gao, J.; Feng, Y.; Kang, J. *Synth. Comm.* **1997**, *27,* 3219.

18.   Qian, L.; Sun, Z.; Mertes, M.P.; Mertes, K.B. *J. Org. Chem.* **1991**, *56,* 4904.

19.   Teixidor, F.; Romerosa, A.M.; Rius, J.; Miravitlles, C.; Casabo´, J.; Vinas, C.; Sanchez, E. *J. Chem. Soc. Dalton. Trans.* **1990**, 525.

20.   Yang, R. Zompa J. *Inorg. Chem.* **1976**, *15*, 1499.

21.   McAuley, A.; Norman, P.R.; Olubuyide, O. *Inorg. Chem.* **1984**, *23*, 1938.

22. Lukyanenko, N.G.; Basok, S.S.; Filonova, L.K. *J. Chem. Soc. Perk. Trans. I*, **1988**, 3141.

23. Stetter, H.; Mayer, K.- H. *Chem. Ber.* **1961**, *94*, 1410.

24. Weisman, G.R.; Reed, D.P. *J. Org. Chem.* **1996**, *61,* 5185

25. Coates, J.S.; Hadi, D.A.; Lincoln, S.F. *Aust. J. Chem.* **1981***, 35,* 903.

26. Gentgens, C.; Bienz, S.; Hesse, M. *Helv. Chim. Acta.* **1997**, *80*, 1133.

27. Yan, H.-L. *Pol. J. Chem.* **1999**, *73*, 753.

28. Graham, P. G.; Weather burn, D. C. *Aust. J. Chem.* **1983**, *36,* 2349.

29. Koyama, H.; Yashino, T. *Bull. Chem. Soc. Jpn.* **1972**, 45481.

30. Martin, L. Y.; Sperati, C. R.; Busch, D. H. *J. Am. Chem. Soc.* **1977,** *99*, 2968.

31. Quayle, W.H.; Lunsford, J.H. *Inorg.Chem,* **1982**, *21*, 97

32. Diegruber, P.J.; Plath, P.J.; Schulz-Elkoff, E.G.; Mohl, M. *J. Mol. Catal.* **1984,** *24*, 115.

33. Deshpande, S.; Srinivas, D.; Ratnaswamy, P. *J. Catal.* **1999**, *188,* 261.

34. Chavan, S.; Srinivas, D.; Ratnasamy, P. *Topics Catal.* **2000**, *11/12*, 359.

2.5. SPECTRA OF PERAZA MACROCYCLIC COMPLEXES
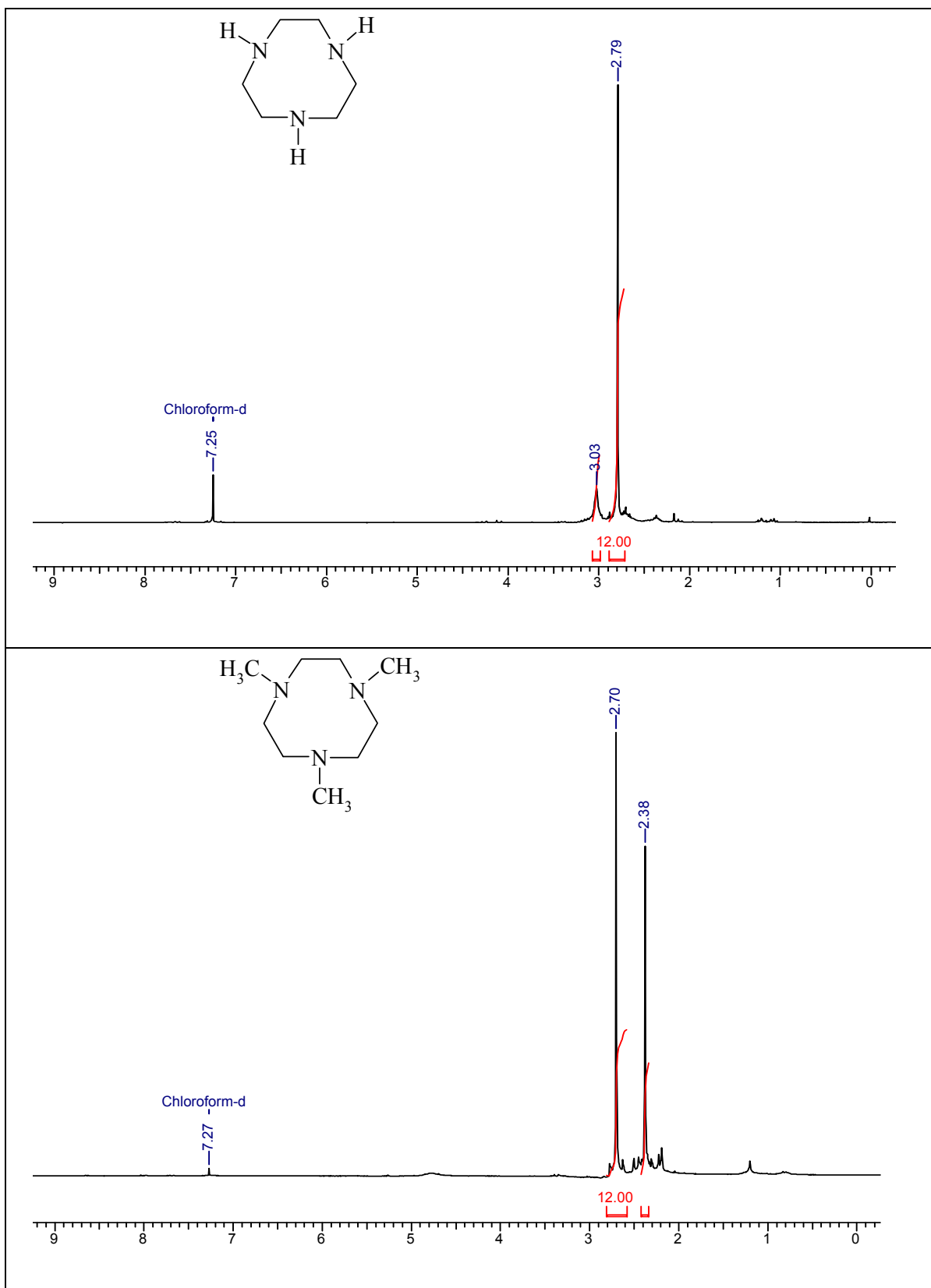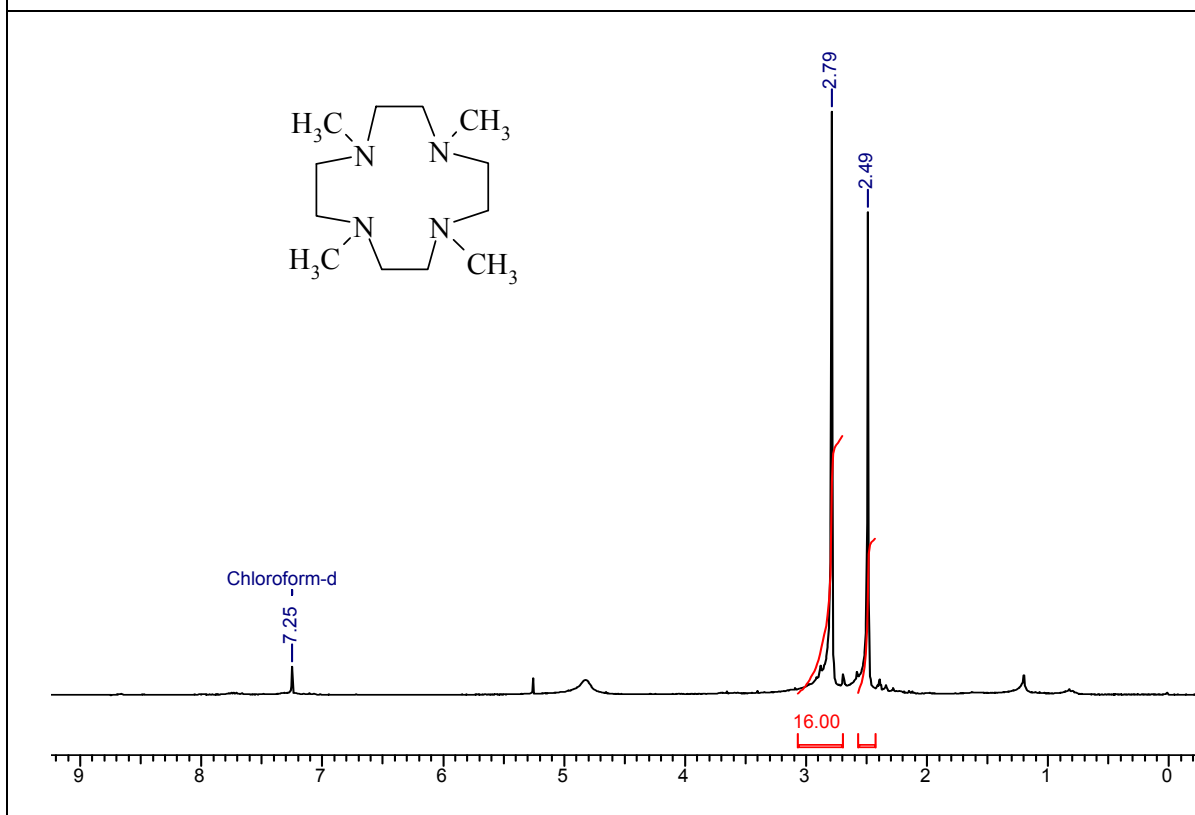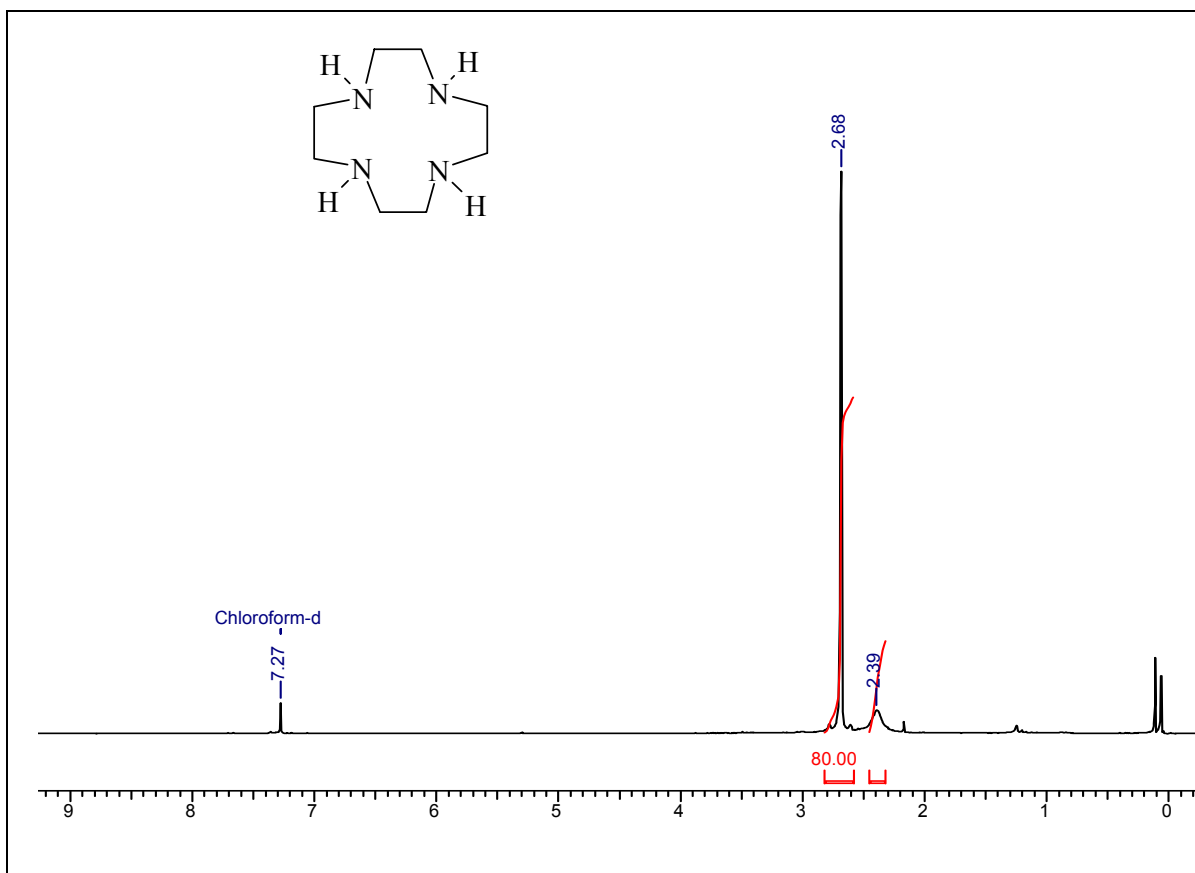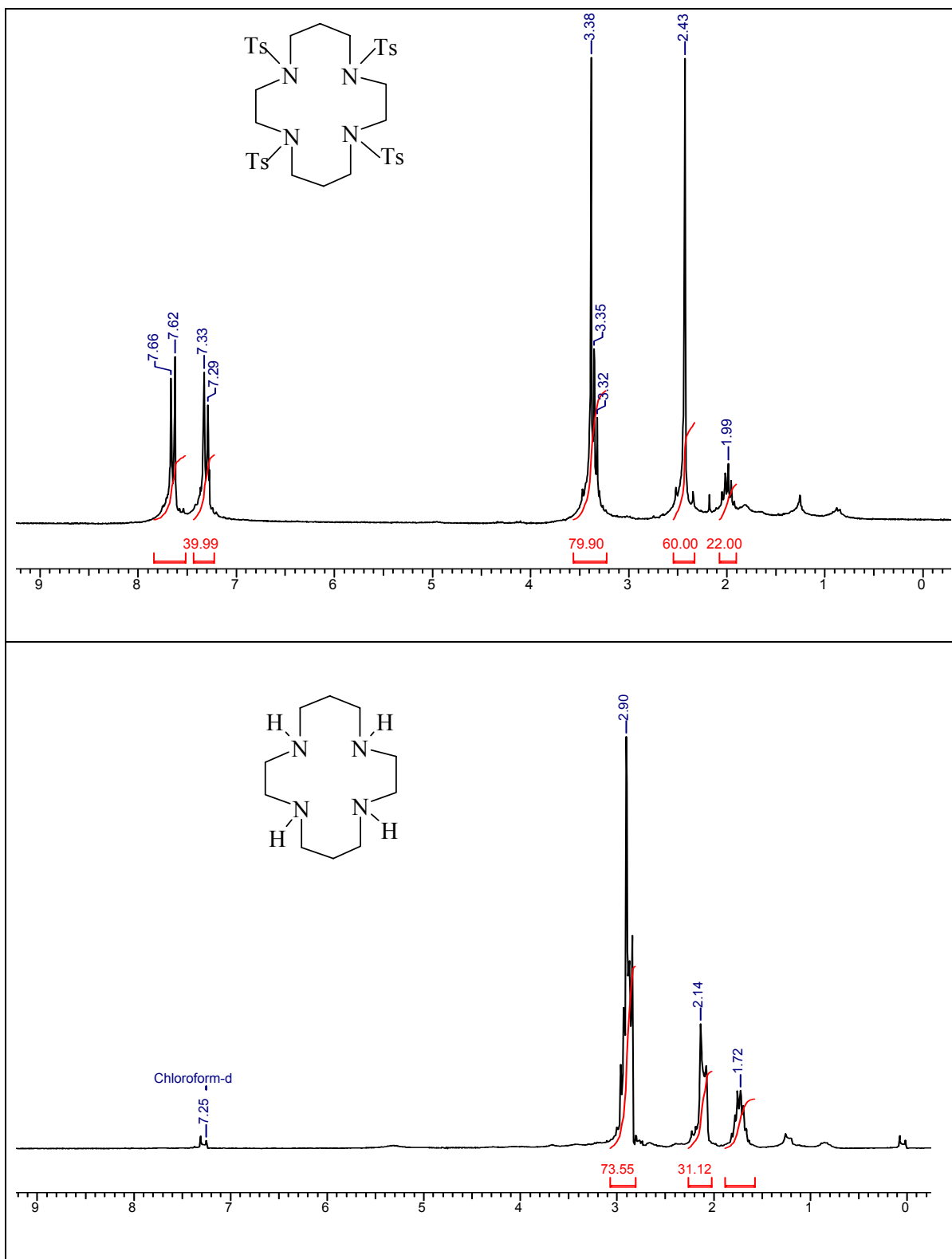
Chapter 3. CHARACTERIZATION AND CATALYTIC ACTIVITIES OF Cu AND Mn SCHIFF BASE AND PERAZA MACROCYCLIC COMPLEXES

_____

3.1. INTRODUCTION

Selective catalytic oxidation of hydrocarbons by transition metal complexes in homogeneous and heterogeneous phases is of great interest [1, 2]. These catalytic entities (metal complexes) can possibly reproduce or mimic the activity of heme-enzymes (cytochrome P-450 catalases and peroxidases). The transformation of hydrocarbons through the action of metal complexes has often been found to be efficient [3]. There have been significant developments in the synthesis, characterization and understanding the structure-activity relationships of metal complexes and also intrazeolite organometallics [4-6]. Many metal complexes, when trapped in zeolites exhibit high activity and selectivity in the oxidation of hydrocarbons [7]. Mn(II)-amine complexes trapped inside zeolite cages possess very good activity for hydrocarbon oxidation with TBHP [8, 9]. Many copper salts and copper complexes have been reported as biomimetic catalysts for hydrocarbon oxidations [10]. Unlike Schiff base complexes, the use of peraza macrocyclic complexes in biomimetic catalysis is very recent, though they have been known for many decades. This chapter concerns with the characterization and catalytic activity of neat and encapsulated copper and manganese complexes of Schiff base and peraza macrocyclic ligands synthesized in Chapter 2. The catalytic activities of the complexes in epoxidation and benzylic oxidation under mild conditions are explored.

Epoxides are an important and versatile class of organic compounds and as a result the selective epoxidation of alkenes is a major area of research [11, 12]. Many

epoxides are versatile building blocks in organic synthesis [13]. Both Mn(III) and Mn(II) salen complexes [13, 14] and Mn-peraza macrocyclic complexes [15] have been reported as good catalysts for epoxidation of olefins (Scheme 3.1). However, reports on the use of either homogeneous or heterogeneous Cu- peraza macrocyclic complexes for epoxidation are scarce.

R, R^1 = Ph, CH$_2$-, etc.
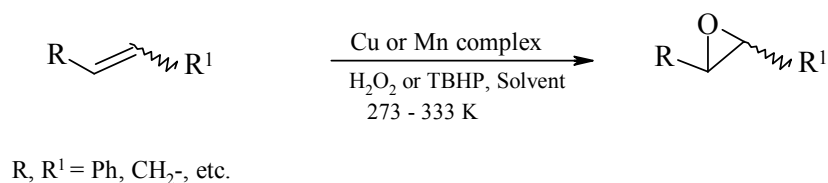
Scheme 3.1

Benzylic oxidation is a fundamental synthesis transformation, which converts alkyl aromatics to alcohols, aldehydes, ketones or acids depending upon the reaction conditions and catalysts [16]. For e.g., benzylic methylene or methyl groups have been converted into carbonyl groups by using cerium ammonium nitrate in hot acetic acid, or HNO$_3$. Enantioselective benzylic hydroxylation has been carried out with chiral oxoruthenium porphyrins [17]. Mild conditions and efficient catalysts are always preferred in benzylic oxidations [18]. It is now found that Cu and Mn Schiff base and peraza macrocyclic complexes are good catalysts for benzylic oxidation under mild conditions (Scheme 3.2).
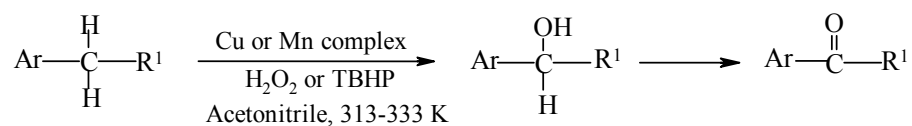
Ar = Ph, Naphth, etc.
R^1 = H, CH$_3$, Aryl, etc.

Scheme 3.2

64

3.2. EXPERIMENTAL

3.2.1. Materials and Instrumentation

The catalysts used in the reactions were prepared as reported in Chapter 2. The solvents acetonitrile, acetone, methanol and ethylene dichloride (EDC) used in this work were of A.R. grade and procured from s. d. fine Chem., India. The reagents styrene and ethylbenzene (99.9% purity) were obtained from Aldrich, USA. The oxidant H_2O_2 was obtained as a 50% aqueous solution from Merck, India and the exact concentration was determined by iodometric titration. TBHP (50%) in EDC was prepared from 70% aqueous TBHP (procured from Merck, India) according to the procedure reported in the literature [19, 20]. The experimental techniques used in the characterization of the metal complexes have already been described in Chapter 2 (Section 2.3).

3.2.2. Preparation of Anhydrous *tert*-Butyl Hydroperoxide (TBHP) (50%) in Ethylene Dichloride

To a 1 litre flask, 70% aqueous TBHP (286 ml) and ethylene dichloride (200 ml) were added and the mixture was refluxed for 1 – 2 h with efficient stirring. This was cooled and transferred to a 1 litre separatory funnel. About 50 ml of water was removed and the organic layer separated was transferred to a 1 litre two necked flask equipped with a Dean-Stark trap and a reflux condenser. The solution was refluxed using a heating mantle. Water accumulated in the arm of Dean-Stark apparatus was removed from time to time. When water stopped accumulating, the solution was cooled under nitrogen and kept over activated 3A molecular sieves. The composition of the TBHP solution was determined by standard titrimetric methods. The solution was found to be 5.0 M in TBHP.

3.2.3. Catalytic Activity Studies

3.2.3.1. Procedure for Styrene Epoxidation

Epoxidation with H_2O_2

The catalyst [Mn(O)(tmtacn)]SO$_4$ (0.7 mg, 0.2 mol%) was added to a solution of styrene (0.104 g; 1 mmol) in acetonitrile / acetone (1 ml) solvent. The reaction mixture was cooled to 273 K in an ice bath. The reaction was carried out by adding aq. H_2O_2 (38%; 0.25 ml, 0.2 ml of solvent) dropwise to the reaction mixture with stirring at 273 K for at least 20 min. The progress of reaction was monitored by GC (Varian 3400; CP-SIL8CB column; 30 m x 0.53 mm) and the products were identified by GC-MS (Shimadzu QP 5000; DB 1 column; 30 m x 0.25 mm) and GC-IR (Perkin Elmer 2000; BP-1 column; 25 m x 0.32 mm).

Epoxidation with TBHP

In a typical oxidation, styrene (0.104 g; 1 mmol), catalyst (0.2 mol% - in case of "neat" complexes and 0.02 g – in case of encapsulated complexes), TBHP (50% in ethylene dichloride; 0.42 ml) and CH$_3$CN (1 ml) were mixed in a 25 ml two-necked round bottom flask, fitted with a water cooled condenser. The reaction was carried at 333 K for 10 – 12 h by placing the flask in a thermostatted oil bath. The reaction was monitored by GC and the products were analysed by GC-MS and GC-IR.

3.2.3.2. Procedure for Oxidation of Ethylbenzene

Oxidation with H_2O_2

To the solution of ethylbenzene (0.053 g; 0.5 mmol) in acetonitrile (1 ml), the catalyst [Mn(O)(tmtacn)]SO$_4$ (0.7 mg, 0.4 mol%) was added. This was followed by the dropwise addition of 38% aqueous H_2O_2 (0.3 ml, 0.3 mmol) in acetonitrile (0.2 ml) for a period of 20-30 min keeping the temperature of the oil bath at 333 K. The

reaction was continued at 333 K and the progress of the reaction was monitored by GC. The products were analysed by GC-MS and GC-IR.

Oxidation with TBHP

In a 25 ml glass round bottom flask placed in a thermostatted oil bath and fitted with a water cooled condenser, were taken ethylbenzene (0.106 g, 1 mmol), catalyst (0.2 mol% of ethylbenzene – in case of "neat" complexes and 0.02 g – in case of encapsulated complexes), TBHP (50% in ethylene dichloride, 0.42 ml) and CH_3CN (1 ml) and the reaction was conducted at 333 K for 10 h with efficient stirring. The progress of the reaction was monitored by GC and the products were analysed by GC-MS and GC-IR.

Test for Heterogeneity of Reaction

Ethylbenzene (0.106 g, 1 mmol), the catalyst (encapsulated complex; 0.02 g), TBHP (50% in ethylene dichloride, 0.42 ml) and CH_3CN (1 ml) were mixed in a 25 ml round bottom flask and the reaction mixture was heated at 333 K. After 3 h of heating, the catalyst was separated by filtration and the reaction was continued further. The reaction was monitored by GC and the products were analysed by GC-MS and GC-IR.

3.3. RESULTS AND DISCUSSION

3.3.1. Characterization of Neat and Encapsulated Metal Complexes

3.3.1.1. *Copper and Manganese Schiff Base Complexes*

The elemental compositions and IR spectra of the copper and manganese complexes with salen ligands (Tables 3.1-3.3) confirmed the stoichiometry and structure. In the case of the encapsulated complexes, the % H values (Table 3.3) have contributions also from the zeolite hydroxyl and water molecules. The compositions of the encapsulated complexes were, therefore, confirmed from the C / N ratio (Table 3.3).

67

The experimental values are in good agreement with the calculated values. The copper and manganese contents of the encapsulated zeolite catalysts are presented in Table 3.3.

No major changes, except a marginal reduction in peak intensity, were observed in the X-ray diffraction patterns of zeolite-Y upon formation and encapsulation of metal complexes inside the zeolite cavities. The results indicate that the encapsulation of the complexes did not alter the zeolite framework structure. Also, encapsulation is believed to have occurred as there was a decrease in the BET surface area of the encapsulated complexes due to occupation of the pores by the complexes (Table 3.3).

3.3.1.1.1. FT-IR Spectroscopy

The "neat" complexes showed a sharp band in the range $1600 - 1650$ cm^{-1} attributed to the stretching mode of the azomethine group $\nu(C=N)$. A strong band corresponding to $\nu(C=C)$ appeared in the range $1577 - 1597$ cm^{-1}. The ring vibrations and C-O stretching modes appeared in the ranges $1440 - 1541$ cm^{-1} and $1284 - 1340$ cm^{-1}, respectively. The additional phenyl ring in M(saloph) compared to M(salen) complexes enhances electron delocalization in the molecule. These differences are more apparent in the spectra of the copper complexes. In Cu(saloph) the band corresponding to C=N is shifted from 1647 cm^{-1} (in salen) to 1608 cm^{-1}. Similar low energy shifts were observed for C=C and the ring vibrational modes. The band corresponding to C-O vibration shifted from 1304 cm^{-1} in Cu(salen) to 1339 cm^{-1} in Cu(saloph). These shifts in band positions are consistent with the reported changes in X-ray structural parameters [21, 22]. The IR spectra reveal that the band due to C-O shifts to lower values in manganese compared to copper complexes. These results reveal that the metal-ligand bond is more covalent in Cu(II) than in Mn(II) complexes.

Table 3.1. Chemical composition and IR stretching frequencies of neat copper and manganese Schiff base complexes

Complex	Color	Chemical composition (%)[a]				IR data (cm^{-1})			
		C	H	N	C/N	v (C=N)	v (C=C)	Ring	v (C-O)
Cu(salen).CH$_3$OH[b]	Green	56.0	4.7	7.5	7.5	1647,	1596	1541,	1304
		(56.4)	(5.0)	(7.7)	(7.3)	1629		1496	
Cu(saloph).0.5CH$_3$OH	Brick red	62.4	4.4	7.2	8.7	1608	1577	1521,	1339
		(62.3)	(4.1)	(7.1)	(8.6)			1460	
Mn(salen)	Brown	60.0	4.4	8.2	7.3	1627	1598	1541,	1284
		(59.8)	(4.4)	(8.7)	(6.9)			1496	
Mn(saloph).CH$_3$OH	Reddish	61.1	4.4	6.4	9.5	1627	1597	1541,	1284
	brown	(60.0)	(4.5)	(6.9)	(8.6)			1496	

[a]Calculated values are given in parentheses.
[b]Complex is associated with one molecule of CH$_3$OH as solvent of crystallization.

Bands corresponding to the zeolite framework dominated the IR spectra of the encapsulated complexes. Those of the metal complex were weak and masked by the zeolite bands due to the low concentration of the former.

3.3.1.1.2. Electronic Absorption Spectra

The electronic spectra of both the " neat" (acetonitrile solutions) and encapsulated complexes (Tables 3.2 and 3.3) showed strong absorption bands in the UV-region 220-290 nm which can be attributed to intraligand (IL) $\pi \to \pi^*$ transitions. The ligand-to-metal charge transfer (LMCT) transition in which the electron is excited from a predominantly ligand centered orbital to a predominantly metal centered orbital were found in the UV-region 300-400 nm. The bands due to d-d transition and metal to ligand charge transfer transition (MLCT) were observed in the visible region, 400-570 nm.

Table 3.2. Electronic spectral data of copper and manganese salen complexes (0.025 x 10^{-3} M) in acetonitrile

Complex	λ_{max} /nm (ε, l mol^{-1} cm^{-1})		
	d-d / MLCT	*LMCT*	*IL*
Cu(salen)	565 (2400)	362 (76800)	271 (200000), 228 (249600)
Cu(saloph)	420 (2000)	340 (288800)	290 (401600), 230 (194400)
Mn(salen)	408 (12800)	312 (62400)	252 (14400), 225 (249600)
Mn(saloph)	440 (6400)	335 (16000)	248 (29600), 220 (21600)

Table 3.3. Chemical composition, surface area (S.A.) and DRUV-vis data of zeolite-Y encapsulated copper and manganese Schiff base complexes

| Complex | Chemical composition (%) | | | | Metal | S. A. | DRUV-vis. |
	C	H	N	C/N ^{a}	%	m^2/g	λ_{max}/nm
Cu-Y; Pale blue	---	---	---	---	0.96	540	205
Cu(salen)-Y; Brick red	9.05	2.18	1.37	6.6 (6.8)	0.75	253	460, 325, 261
Cu(saloph)-Y; Brick red	10.1	1.3	1.6	6.4 (6.8)	0.80	248	440, 300, 249
Mn(salen)-Y; Brick red	10.8	1.4	1.2	9.0 (8.6)	0.76	229	445, 267, 243
Mn(saloph)-Y; Yellowish green	11.6	1.2	1.2	8.5 (8.6)	0.58	230	450, 326, 250

^{a}Calculated values are given in parentheses.

3.3.1.1.3. EPR Spectroscopy

EPR of Cu(II) and Mn(II) exchanged NaY

The EPR spectrum of Cu(II) (1.2 wt.%) exchanged NaY revealed two types of Cu(II) species: Species I (with g_x = 2.083, g_y = 2.095 and g_z = 2.373 and $A_x = A_y$ = 14.5 and A_z = 118.4 G) corresponding to Cu(II) ions located at the hexagonal prism and species II (with g_{av} = 2.181, exhibiting dynamic Jahn-Teller effect) corresponding to the ions in the supercages (Fig. 3.1a) [22]. Mn(II) (1.2 wt.%) exchanged Na-Y showed a six line spectrum (centered at g = 2.0; Fig. 3.1b) arising from the transitions between $|+1/2\rangle$ and $|-1/2\rangle$ electron spin levels of manganese and due to coupling of electron spin with ^{55}Mn nucleus spin (S = 5/2, I = 5/2). The other fine structure transitions corresponding to m_s : $|\pm5/2\rangle \leftrightarrow |\pm3/2\rangle$ and $|\pm3/2\rangle \leftrightarrow |\pm1/2\rangle$ were not resolved, but contributed to the background upon which the six major hyperfine resonances were

superimposed. The five weak doublets (marked by arrows; Fig. 3.1c) occurring between the sextet components corresponding to m_s : $|-1/2> \leftrightarrow |+1/2>$ are attributed to $\Delta M_I = \pm 1$ (forbidden) transitions and a low symmetry molecular environment at Mn(II).
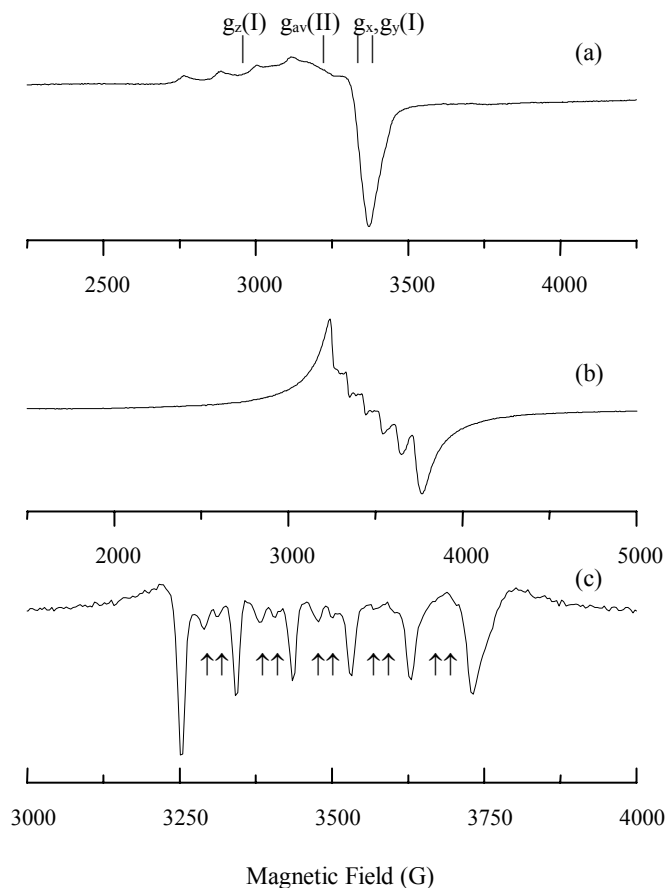
Figure 3.1. *X-band EPR spectra of Cu(II) and Mn(II) exchanged NaY (1.2 wt.%) at 298 K: (a) Cu-Y, (b) Mn-Y and (c) second derivative plot of Mn-Y. Arrows represent forbidden transitions.*

The spectra of both Cu(II) and Mn(II) exchanged NaY reveal the location of the metal ions in the hexagonal prisms of the faujasite framework [23]. At higher exchange

levels more metal ions reside in the supercages resulting in a featureless isotropic signal.

EPR of Neat and Encapsulated Copper Complexes

The powder samples of "neat" Cu(salen) and Cu(saloph) showed spectra characterized by axial g tensors (Fig. 3.2a and Fig. 3.2b, respectively). The hyperfine features due to copper ($S = \frac{1}{2}$, $I = 3/2$) could not be resolved, even at 77 K, due to intermolecular spin-spin interactions of the dimeric molecules in the solid state [21, 22]. The geometry of Cu(salen) is square pyramidal while Cu(saloph) is square planar. The g anisotropy ($\Delta g = g_{//} - g_{\perp}$) is lower in Cu(saloph) (Table 3.4).

The intermolecular spin-spin interactions were removed in frozen solutions and as a consequence of this, the copper hyperfine splitting was resolved. Typical spectra for Cu(saloph) in $CHCl_3$ and pyridine are shown in Figs. 3.3a and 3.3b, respectively. The well resolved superhyperfine features (Fig. 3.3a) are due to two equivalent nitrogen nuclei of the saloph ligand in the frozen $CHCl_3$ solution. These features could not be resolved in strong donor solvents like pyridine (Fig. 3.3b). The saloph complex adopts a planar geometry in $CHCl_3$ and in strong donor solvents it has a square pyramidal geometry [22, 23].

The spin Hamiltonian parameters for frozen solutions of Cu(II), obtained after spectral simulations, are listed in Table 3.4. Solvents exerted a marked effect on the g and A values of the complexes. The $g_{||}$ value increases while $A_{||}$ decreases with increasing σ-donation capacity of the solvent. For example, the $g_{||}$ value of 2.183 for Cu(saloph) in $CHCl_3$ increases to 2.227 in pyridine. In strong donor solvents like DMF and pyridine, the solvent molecule coordinates to Cu(II) forming a square pyramidal geometry around Cu(II). A comparison of values for Cu(salen) and Cu(saloph) reveal that due to the additional phenyl ring, Cu(saloph) forms a more stable square pyramidal

g|| = 2.191

|g⊥ = 2.084

(a) "Neat" Cu(salen)

g|| = 2.127

|g⊥ = 2.083

(b) "Neat" Cu(saloph)

2500   3000   3500   4000

Magnetic Field (G)

(a) CHCl₃

(b) Pyridine

*
(c) Encapsulated

2.54   2.33   2.15   2.00

g-value
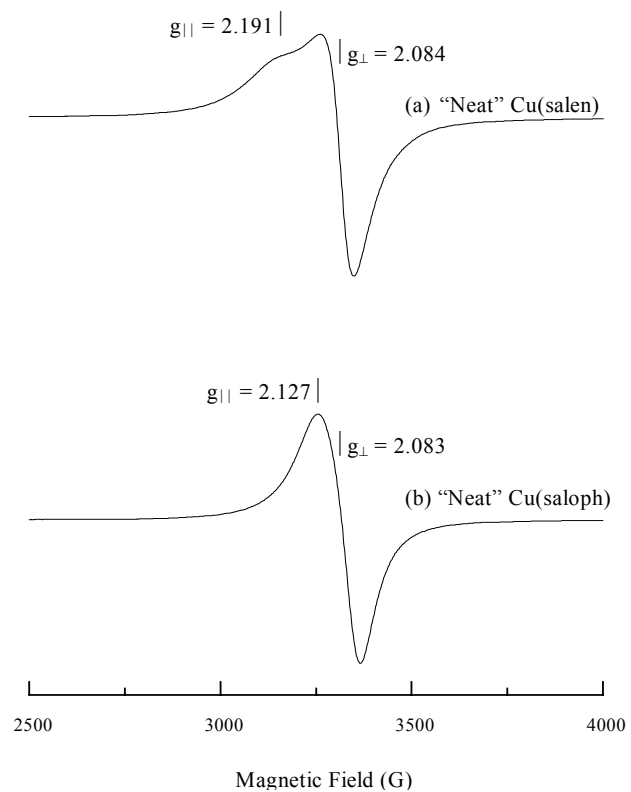
Figure 3.2. *EPR Spectra (at 298 K) for the polycrystalline samples of neat Cu(salen) (a) and Cu(saloph) (b).*
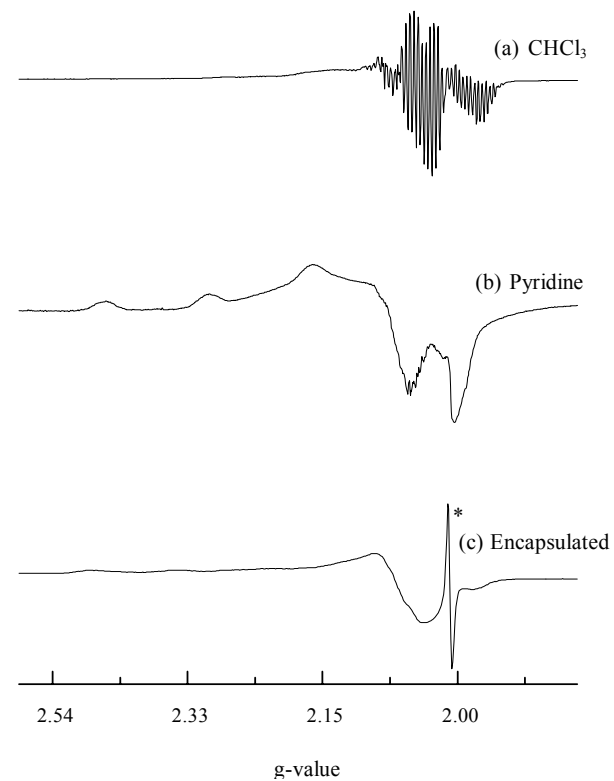
Figure 3.3. *EPR Spectra of Cu(saloph) at 77 K: (a) in CHCl₃, (b) in pyridine, and (c) zeolite-encapsulated Cu(saloph). Asterisk corresponds to signal due to free radical.*

complex than Cu(salen) ($g_{||}$ value for DMF and pyridine solutions varies in the order Cu(saloph) > Cu(salen)). The $A_{||}$ value in pyridine solvent varies in the order Cu(saloph) < Cu(salen)) indicating the greater electron delocalization to ligand orbitals in Cu(saloph) than in Cu(salen).

The spectra for the zeolite-Y-encapsulated copper complexes, Cu(salen)-Y and Cu(saloph)-Y are characterized by an axial spin Hamiltonian. A typical spectrum for Cu(saloph)-Y at 298 K is shown in Fig. 3.3. Comparison of Fig. 3.3(a) and Fig. 3.3(c) confirms that all the exchanged Cu(II) ions in the zeolite were complexed with Schiff base ligands. There are no "free" Cu(II) ions in the material. The spectra of the encapsulated complexes (Fig. 3.3c) resemble those of the frozen solutions (Fig. 3.3b) rather than the "neat" complexes (Fig. 3.2). The resolution in the copper hyperfine features confirms that the encapsulated metal complexes were isolated and present as monomeric species. The higher $g_{||}$ (2.269 for Cu(salen)-Y and 2.282 for Cu(saloph)-Y) and lower $A_{||}$ (163.3 G for Cu(salen)-Y and 160.0 G for Cu(saloph)-Y) values of the encapsulated complexes suggest that copper has a square pyramidal geometry. While the Schiff base (salen or saloph) ligand provides quadridentate coordination, the zeolite framework (hexagonal prism) provides the fifth coordination. The spectrum for the surface–adsorbed copper complex is almost similar to the neat complex (Fig. 3.2). Hence, EPR spectroscopy can be used to differentiate the zeolite-encapsulated complexes from the surface-adsorbed complexes.

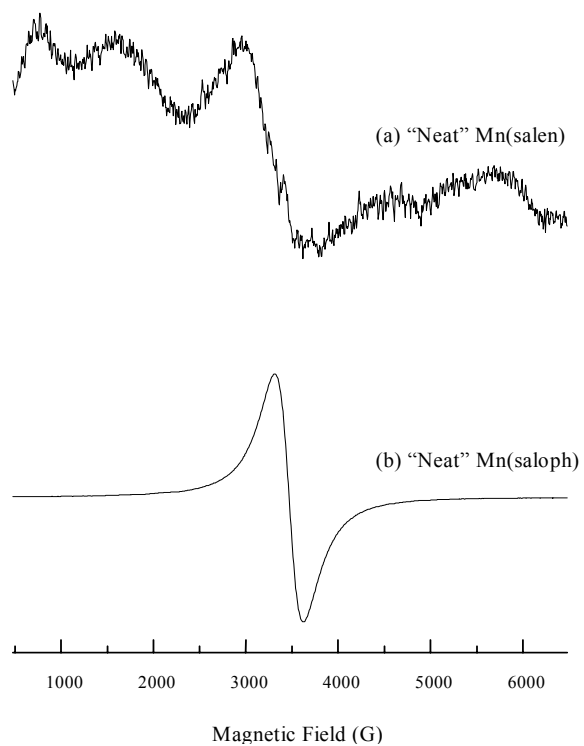### *EPR of Neat and Encapsulated Manganese Complexes*

Fig. 3.4 depicts the EPR spectra of "neat" Mn(II) complexes. Mn(salen) exhibits five signals corresponding to the zero-field transitions. From the spectrum the zero-field splitting parameter (D) was estimated to be 0.12 cm^{-1}. Unlike in Mn-Y, the manganese hyperfine features could not be resolved. In contrast, Mn(saloph), showed

a single isotropic resonance at g = 2. The intermolecular exchange interactions in Mn(saloph) are, hence, larger than the zero-field interactions (> 0.12 cm^{-1}). These interactions in Mn(salen) are an order of magnitude lower than that in Mn(saloph) (> 0.009 cm^{-1}).

Frozen solutions showed resolved Mn(II) hyperfine features. Typical spectra for Mn(saloph) in methanol and pyridine are shown in Figs. 3.5(a) and 3.5(b), respectively. The forbidden transitions ($\Delta m_S = \pm 1$ and $\Delta M_I = \pm 1$) are also visible. In pyridine solution, the zero-field transitions (marked by arrows) are more prominent than in methanol, probably due to higher zero-field interactions (D = 0.087 cm^{-1}) and the tetragonally elongated square pyramidal geometry. It is interesting to note that the intensity of the Mn(II) signal decreased in pyridine solution, probably due solvent promoted Mn(II) to Mn(III) oxidation.

Before the complexation, Mn-Y samples showed a spectrum with the characteristic sextet pattern of manganese with a total spectral width of 520 G (Fig. 3.1(b)). After complex formation the spectrum extends over a wider field range and displays fine splitting (marked by arrows; Fig. 3.5(c)). The spectra of the zeolite-encapsulated Mn(II) Schiff base complexes are similar to those of frozen solutions (Figs. 3.5(b) and 3.5(c)). The weak sharp signal at 1600 G corresponds to Fe(III) impurity in NaY while the intense signal (deonoted by an asterisk) overlapping with the Mn sextet lines corresponds to a free radical. The similarity of zeolite-encapsulated complexes and frozen Mn(II) solutions (as in the case of copper complexes) suggests that manganese complexes encapsulated in zeolites are isolated and present as monomers. The hyperfine coupling constants of zeolite-encapsulated and pyridine solvated Mn(II) complexes are lower than that observed in methanol solution and Mn-

(a) "Neat" Mn(salen)

(b) "Neat" Mn(saloph)

1000   2000   3000   4000   5000   6000

Magnetic Field (G)

(a) CH₃OH

(b) Pyridine

(c) Encapsulated

1000   2000   3000   4000   5000   6000

Magnetic Field (G)

Figure 3.4. *EPR spectra of the polycrystalline samples (at 298 K); (a) Mn(salen) and (b) Mn(saloph).*
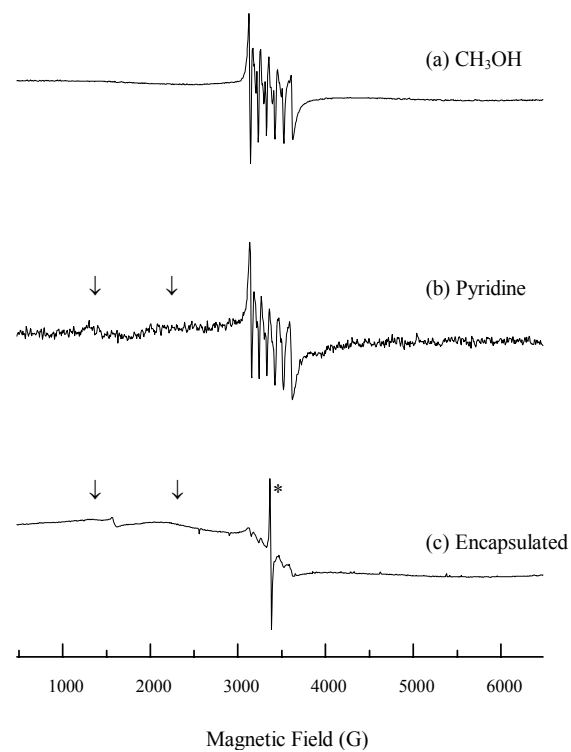
Figure 3.5. *EPR spectra of Mn(saloph) at 77 K: (a) in CH₃OH, (b) in pyridine, (c) zeolite-encapsulated Mn(saloph) complex. Asterisk corresponds to signal due to free radical.*

Table 3.4. EPR spin Hamiltonian parameters of neat and zeolite-encapsulated Cu(II) and Mn(II) Schiff base complexes at 77 K (NR: not resolved; $A^N_{||}$: parallel component of the superhyperfine coupling due to nitrogen)

Complex	State	$g_{||}$	$G_\perp$	$-A_{||}$ (G)	$-A_\perp$ (G)	$A^N_{||}$ (G)	g_{av} (G)	A_{av} (G)	D cm^{-1}
Cu(salen)	Neat	2.191	2.084	NR	NR	NR			
	CHCl$_3$/CH$_3$OH(1:3)	2.199	2.067	199.4	26.0	10.8			
	DMF	2.210	2.053	195.3	30.3	NR			
	Pyridine	2.225	2.053	191.3	24.0	NR			
Cu(salen)-Y	Encapsulated	2.269	2.051	163.3	28.6	NR			
Cu(saloph)	Neat	2.127	2.083	NR	NR	NR			
	CHCl$_3$	2.183	2.032	115.0	15.0	15.2			
	CH$_3$OH	2.223	2.066	193.0	15.3	NR			
	DMF	2.216	2.060	197.0	31.5	12.6			
	Pyridine	2.227	2.065	187.3	22.6	NR			
Cu(saloph)-Y	Encapsulated	2.282	2.061	160.0	29.1	NR			
Mn-Y							2.000	97.6	
Mn(salen)	Neat						2.000	__	0.12
Mn(saloph)	Neat						2.012	NR	__
	CH$_3$OH						1.998	96.0	__
	Pyridine						1.999	92.4	0.09
Mn(saloph)-Y	Encapsulated						1.997	94.6	0.08

Y. The zero-field splitting parameter (D) for the encapsulated complexes is similar to that of the pyridine-solvated complex suggesting that the geometry of Mn(II) complexes in pyridine solutions and in zeolite-Y is distorted. The Mn-ligand bond is more covalent, the metal electron density being partially delocalized onto the ligand orbitals.

Electronic Structure and Bonding Parameters

The molecular symmetry of the metal salen and saloph complexes is as low as C_{2v}. In such a case, the EPR spectrum of these complexes should be characterized by three g parameters g_x, g_y and g_z. However, as seen in the previous section, the spectra of copper complexes are characterized only by axial *g* and hyperfine tensors ($g_{||}$ and $g_\perp$ & $A_{||}$ and $A_\perp$). This implies that although the molecular symmetry is low, the electronic symmetry at the site of the metal ion is as high as C_{4v}. The g values for the copper complexes, with $g_{||} > g_\perp$ indicate that the unpaired electron of Cu occupies the

Table 3.5. Molecular orbital coefficients and electronic d-d transition energies for neat and zeolite-Y encapsulated copper Schiff base complexes

Complex	State	MO Coefficients				d-d transition energies (cm^{-1}) $E_{xy} - E_{x^2-y^2}$
		α^2	α'^2	β^2	$\delta^2/\Delta E_{xz/yz}$ x 10^5	
Cu(salen)	CH$_3$Cl/ CH$_3$OH	0.836	0.249	0.661	4.91	17,730
	DMF	0.832	0.253	0.687	3.86	17,361
	Pyridine	0.839	0.249	0.705	3.83	16,750
Cu(salen)-Y	Encapsulated	0.812	0.277	0.910	3.82	17,391
Cu(saloph)	CH$_3$OH	0.847	0.236	0.734	4.76	17,825
	DMF	0.845	0.236	0.701	4.31	17,793
	Pyridine	0.835	0.250	0.699	5.44	16,420
Cu(saloph)-Y	Encapsulated	0.821	0.266	__	4.54	__

$3d_{x^2-y^2}$ orbital. The ground state electronic wave function and the bonding parameters were evaluated using the ligand field approach described in the literature [24]. Here, α and β are the metal d-orbital coefficients for the MOs b_{1g} and b_{2g} representing the in-plane σ and π bonding, respectively; δ is the coefficient for the MO e_g representing the out-of-plane π bonding; α' is the coefficient for the ligand orbitals forming b_{1g} molecular orbital. The MO coefficients estimated from the experimental g and A values are listed in Table 3.5.

The MO coefficients are in general, smaller than unity indicating the covalent nature of of the bonding between the metal and the ligand orbitals. UV-vis spectra showed a band in the range 16,420-17,825 cm^{-1} corresponding to the excitation transition of $B_{1g} \leftarrow A_g$. The band corresponding to $B_{1g} \leftarrow E_g$ could not be resolved. Thus the value of δ (coefficient for the out-of-plane bending) could not be estimated, but evaluated in units of energy separation.

In general, MO coefficients varied in the order $\beta < \alpha$ suggesting that the in-plane π bonding (between $3d_{xy}$ and p_π orbitals) is more covalent than in-plane σ-bonding (between $3d_{x^2-y^2}$ and p_σ orbitals). The MO coefficients are modified considerably on encapsulation. The coefficient α, characteristic of in-plane σ-bonding, decreases while β, characteristic of in-plane π-bonding, increases on encapsulation. These results reveal the structural changes undergone by the metal complex on encapsulation. The higher in-plane covalency as indicated by smaller values of α for the encapsulated metal complexes (α changes from 0.836 to 0.812 for Cu(salen) and 0.847 to 0.821 for Cu(saloph)) reveals a larger depletion of electron density at the site of the metal in encapsulated complexes than in the neat complexes. This depletion in turn is likely to facilitate nucleophilic attacks by reagents like the *tert*-butyl

hydroperoxide or hydrogen peroxide anions at the metal center. Since the transition metal hydroperoxides are transient species in oxidation catalysis, an enhancement in their rates of formation will increase the catalytic activity. The in-plane covalency appears to be higher in salen than in saloph complexes. Even in the Mn complexes, the hyperfine coupling constant decreases from 97.6 to 94.6 G on encapsulation suggesting a similar depletion of spin density at the site of the metal ion in encapsulated complexes. Hence, a smaller value of α, increased in-plane covalency and reduced hyperfine coupling constants are the likely causes for the enhanced catalytic activity of the encapsulated copper complexes (Section 3.3.2). The distortion in molecular geometry arising out of encapsulation and the consequent depletion of electron density at metal center site are the probable causes for the enhanced catalytic activity of the zeolite-encapsulated manganese complexes (Section 3.3.2).

3.3.1.2. Copper and Manganese Peraza Macrocyclic Complexes

Various copper and manganese perazamacrocyclic complexes (neat and encapsulated) were prepared and the stoichiometry was confirmed by elemental analysis (Tables 3.6, 3.7, 3.11 and 3.12).

3.3.1.2.1. FT-IR Spectroscopy

Neat Complexes

Selected IR frequencies of the complexes are presented in Tables 3.6 and 3.7. The complexes showed a weak band in the range 1200 – 1300 cm^{-1} that can be attributed to the stretching mode of the ring C-N bond. Compared to the free ligands, there was a red shift of this band by about 10-15 cm^{-1} after complex formation. The extent of the shift depends on the nature of the co-ordination between the metal and the ligand. In addition to these bands, intense bands around 1070 and 624 cm^{-1}, the characteristic frequencies of ClO$_4$ [25] were also observed. In all the non-methylated

Table 3.6. Chemical composition and IR stretching frequencies of copper complexes with peraza macrocyclic ligands

Complex[a]	Chemical composition[b] (%)				IR data (cm^{-1})		
	C	H	N	C/N	v(C-N)	v(C-C)	v (N-H)
[Cu(tacn)](ClO$_4$)$_2$.2CH$_3$CN; Green	25.4 (25.3)	4.7 (4.4)	13.8 (14.8)	1.7 (1.7)	1232	1020	3284
[Cu(tmtacn)](ClO$_4$)$_2$; Green	35.9 (35.7)	6.9 (6.9)	12.8 (13.8)	2.8 (2.8)	1251, 1298	1020	----
[Cu(cyclen)](ClO$_4$)$_2$. 2CH$_3$OH ; Blue	24.2 (24.0)	6.6 (5.7)	11.3 (11.2)	2.2 (2.1)	1244	1012	3240
[Cu(tmcyclen)](ClO$_4$)$_2$; Deep Blue	28.3 (29.3)	6.3 (5.7)	11.0 (11.4)	2.5 (2.5)	1278, 1294	1018	----
[Cu(cyclam)](ClO$_4$)$_2$; Red	26.2 (25.9)	5.2 (5.2)	11.8 (12.1)	2.2 (2.1)	1299	1040	3242

[a]Some complexes are associated with solvent of crystallization.   [b]Calculated values are given in parentheses.

Table 3.7. Chemical composition and IR stretching frequencies of manganese complexes with peraza macrocyclic ligands

Complex[a]	Chemical composition (%)[b]				IR data (cm^{-1})		
	C	H	N	C/N	v(C-N)	v(C-C)	v(N-H)
[Mn$_4$O$_6$(tacn)$_4$](ClO$_4$)$_4$; Brown **(A)**	23.9 (23.2)	5.1 (5.3)	13.5 (13.5)	1.8 (1.7)	1228	1030	3300
[Mn(O)(tmtacn)]SO$_4$; Pale yellow **(B)**	30.6 (30.3)	6.4 (6.9)	11.7 (11.8)	2.6 (2.5)	1285, 1300	1012	----
[Mn(cyclen)](ClO$_4$)$_2$. 3CH$_3$OH; Green	26.0 (25.3)	5.6 (6.1)	9.8 (9.2)	2.7 (2.8)	1278	1018	3200
[Mn(tmcyclen)](ClO$_4$)$_2$ 2CH$_3$OH; Brown	31.6 (30.8)	5.7 (6.6)	10.7 (10.2)	3.0 (3.0)	1286, 1294	1026	----
[Mn(cyclam)]ClO$_4$; Green	27.1 (26.5)	4.8 (5.2)	12.0 (12.3)	2.3 (2.2)	1282	1026	3250

[a]Some complexes are associated with molecule solvent of crystallization. [b]Theoretical values are given in parentheses.

ligands the medium intense band at 3240-3300 cm^{-1} was due to N-H stretching. In the case of manganese oxo complex **A**, the IR peak at 725 cm^{-1} is characteristic of Mn_4O_6 skeleton [26]. For the terminal-oxo complex **B,** the peak at 721 cm^{-1} is the characteristic $Mn^{IV} = O$ stretching [27] (Table 3.7).

3.3.1.2.2. *Crystal Structure of [Mn$_4$O$_6$(tacn)$_4$](ClO$_4$)$_4$*

The molecular structure of complex **A** isolated as the oxo-bridged Mn-tmtacn complex has been confirmed by single crystal X-ray analysis. Single crystals of the complex were grown by slow evaporation of acetonitrile solution. A dark brown-colored thin needle of size 0.21 x 0.13 x 0.02 mm was used for the data collection on a Bruker SMART APEX CCD X-ray diffractometer using Mo K$_\alpha$ radiation. (50 kV and 40 mA). An ORTREP drawing of the complex is shown in Fig. 3.6. The complex crystallizes in a monoclinic, space group P2$_1$/n, with unit cell parameters being a = 24.214 (12) Å, b = 11.310 (6) Å, c = 36.080 (18) Å, β = 91.020 (9) °, V = 9879(9) Å^3, Z = 4, D$_c$ = 1.691mg / m^{-3}, μ (Mo–K$_\alpha$) = 1.304 mm^{-1}, T = 298 (2) K. Selected bond lengths and bond angles of the complex cation of **A** are given in Table 3.8. Mn has an octahedral geometry with +4 oxidation state. The Mn atoms are linked forming an adamantine-like structure. The ligand tacn acts as the capping unit.

Table 3.8. Selected bond lengths [Å] and angles [°] of Mn$_4$O$_6$(tacn)$_4$(ClO$_4$)$_4$.H$_2$O

Mn(1)-O(1)	1.797(7)
Mn(1)-O(5)	1.811(7)
Mn(1)-O(4)	1.824(7)
Mn(1)-N(2)	2.125(9)
Mn(1)-N(3)	2.126(9)
Mn(1)-N(1)	2.135(9)
O(1)-Mn(1)-O(5)	98.8(3)
O(1)-Mn(1)-N(2)	89.2(4)
N(2)-Mn(1)-N(3)	80.3(4)
Mn(1)-O(1)-Mn(2)	128.5(4)
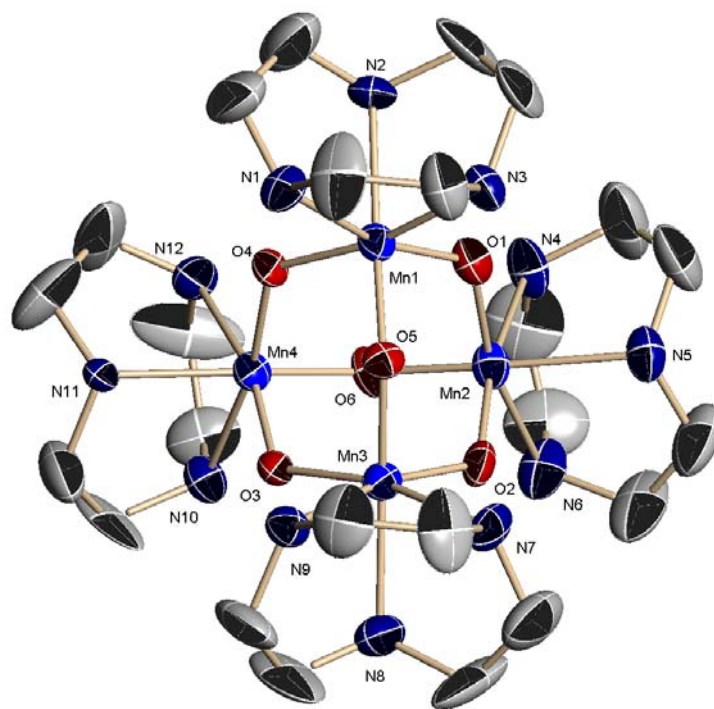
Figure 3.6. *ORTREP view of the bridged oxo-tetranuclear Mn(IV) complex cation* *[Mn₄O₆(tacn)₄]⁴⁺.*

Encapsulated Complexes

Bands corresponding to the zeolite framework dominated the IR spectra of the encapsulated complexes; so the peaks due to the metal complexes were weak and masked by the zeolite bands due to the low concentration of the former (Fig. 3.7).

3.3.1.2.3. Electronic Spectroscopy

Neat Complexes

The copper complexes exhibited a weak absorption band in the visble range 500-640 nm attributable to d-d transitions. A strong ligand-to-metal charge transfer (LMCT) transition was found in the UV-region 250-300 nm (Table 3.9, Fig. 3.8). The size of the macrocyclic ligand and N-methylation affected the structure. There was a

red shift in the d-d transition band with an increase in the number of nitrogens and ring size. As a consequence of this, the d-d band shifted from 640 nm in $[Cu(tacn)]^{+2}$ to 500 nm in $[Cu(cyclam)]^{2+}$ (Fig. 3.8; see inset). The LMCT band also shifted from 268 nm in $[Cu(tacn)]^{+2}$ to 255 nm in $[Cu(cyclam)]^{+2}$. The shift in band position to higher energy side indicates that the tetraaza ligand (cyclam) provides higher stability than the triaza ligand (tacn) and the ligand field is stronger in cyclam than in tacn complexes. Red shift in band position was observed in the with N-methylated complexes suggesting a decrease in their stability due to steric strain induced by the methyl groups [28].

The Mn complexes of cyclen and cyclam exhibited d–d transitions in the range 550 – 635 nm and LMCT transitions in the range 270-380 nm (Table 3.10). The d-d bands of oxo- Mn complexes could not be detected, as they might be very weak. This also suggests that Mn has high symmetry. X-ray structure of **A** confirms this hypothesis.

Table 3.9. Electronic spectral data of copper peraza macrocyclic complexes (0.025-0.1 x 10^{-3} M) in acetonitrile

Complex	λ_{max}/nm (ε, *l mol^{-1} cm^{-1}*)	
	d-d	*LMCT*
[Cu(tacn)](ClO$_4$)$_2$; Green (0.5 x 10^{-3}M)	640 (260)	268 (15800)
[Cu(tmtacn)](ClO$_4$)$_2$; Blue (0.1x10^{-3}M)	610 (40)	290 ((2990)
[Cu(cyclen)](ClO$_4$)$_2$.2CH$_3$OH; Deep blue	590 (2960)	273 (56800)
[Cu(tmcyclen)](ClO$_4$)$_2$ Fluorescent blue	585 (3880)	300 (51286)
[Cu(cyclam)](ClO$_4$)$_2$ Red	500 (1760)	255 (138800)
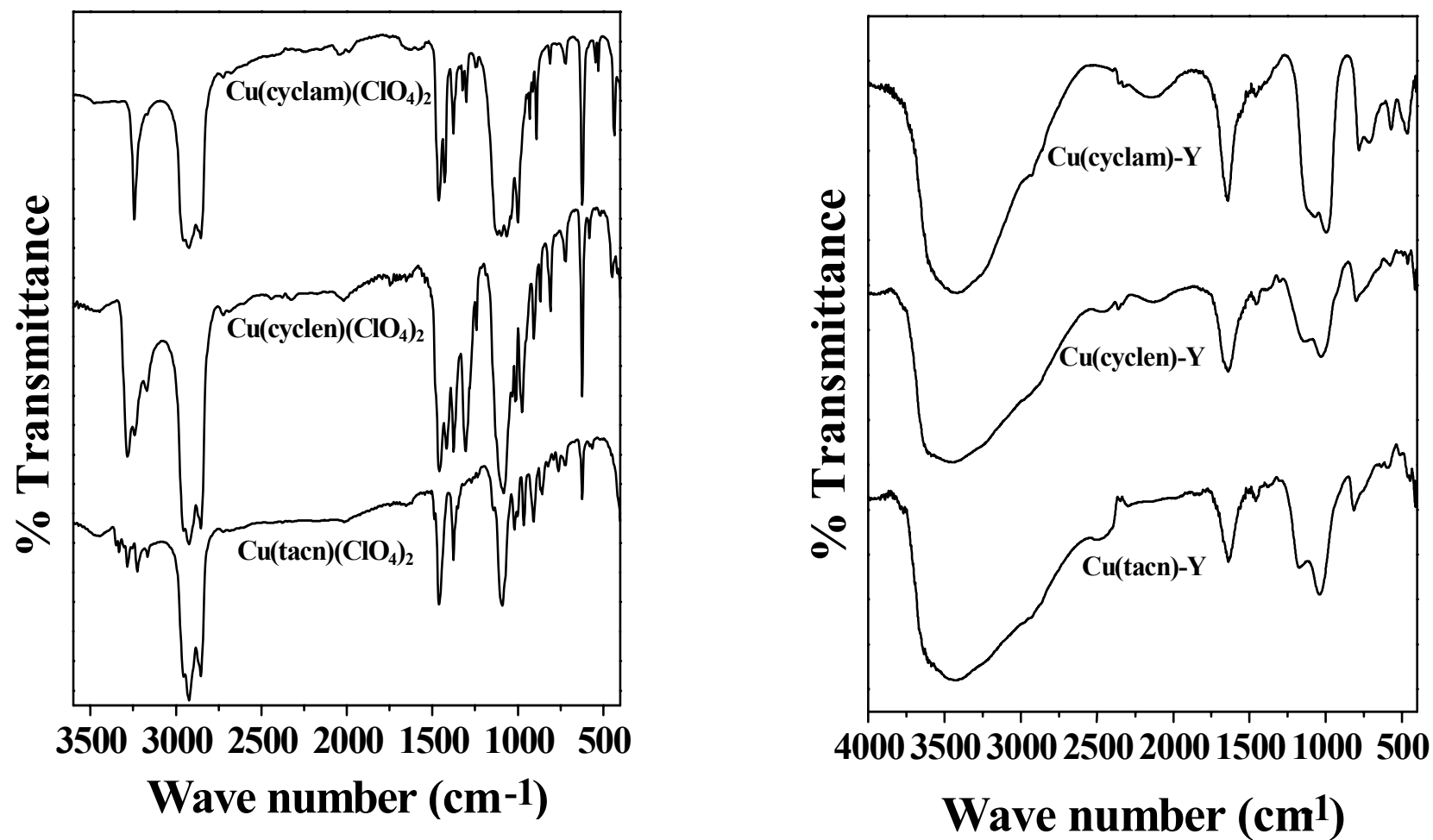
Figure 3.7. FT-IR spectra of "neat" and zeolite-Y-encapsulated Cu(II)-tacn, cyclen and cyclam complexes.
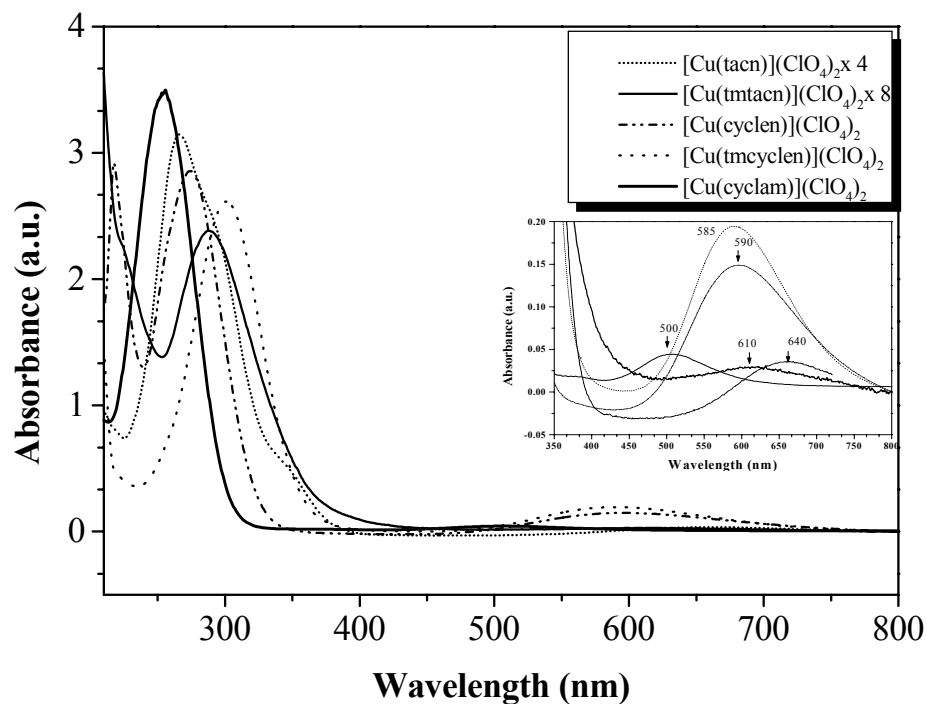
Figure 3.8. *UV-vis spectra of neat Cu peraza macrocyclic complexes in acetonitrile.*

Table 3.10. Electronic spectral data of manganese peraza macrocyclic complexes $(0.0125 \times 10^{-3}\,M)$ in acetonitrile

Copper Complex	λ_{max}/nm $(\varepsilon,\ l\ mol^{-1}\ cm^{-1})$		
	d-d	*LMCT*	*IL*
$[Mn_4O_6(tacn)_4]4ClO_4.H_2O$	-----	340 (400)	224 (7200)
Deep brown			
$[Mn(O)(tmtacn)]SO_4$ [a]	-----	300 (490)	245 (2760)
Pale yellow			
$[Mn(cyclen)](ClO_4)_2.3CH_3OH$	635 (4160),	380 (28000),	220 (296000)
Green	555 (3200)	270 (170400)	
$[Mn(tmcyclen)](ClO_4)_2.2CH_3OH$ [b]	-----	277 (1516)	220 (3860)
Brown			
$[Mn(cyclam)](ClO_4)_2.$	635 (12000),	380 (27200),	225 (174400)
Green	550 (12800)	290 (137600)	

[a] 0.5×10^{-3} M in H_2O. [b] 0.5×10^{-3} M in acetonitrile.
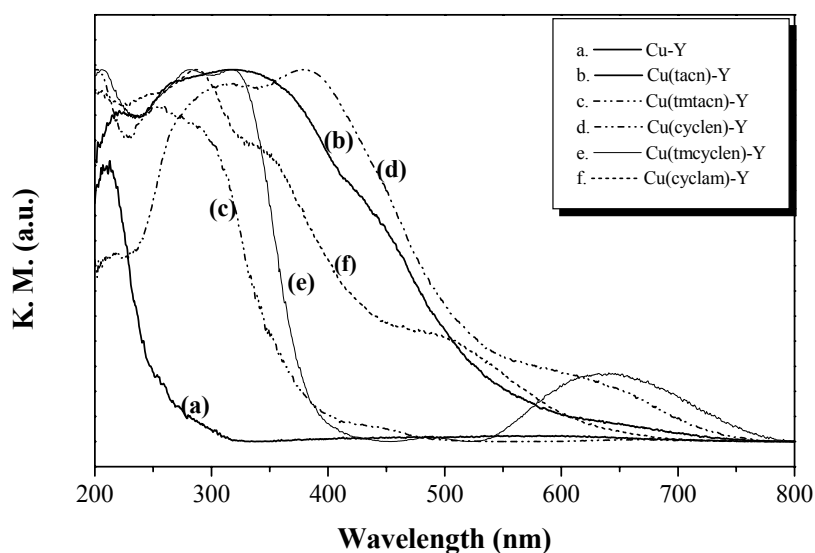
Encapsulated Complexes

When the complexes were encapsulated in zeolite-Y, again the d-d band shifted to the higher energy side (by 15 nm in cyclam and 20 nm in tacn complexes) (Table 3.11; Fig. 3.9). Thus, the stability of the complexes is enhanced when they are encapsulated in the pores of the zeolite-Y. The position of the d-d band corresponds to a square pyramidal geometry for $[Cu(tacn)]^{2+}$ and a square planar geometry for $[Cu(cyclen)]^{2+}$ and $[Cu(cyclam)]^{2+}$ [29].

Similar to that observed in the copper complexes, the Mn complexes also showed a red shift in both d-d or LMCT band positions with an increase in the size of the ligand and N-methylation, consistent with increasing stability.

Table 3.11. Chemical compositions, surface area (S.A.) and DRUV-vis data of zeolite-encapsulated copper peraza macrocyclic complexes

Complex	*Chemical composition (%)*				*Metal*	*S. A.*	*DRUV-vis.*
	C	*H*	*N*	*C/N[a]*	*(%)*	*m^2/g*	*λ_{max}/nm*
Cu-Y; Pale blue	---	---	---	---	0.96	540	205
Cu(tacn)-Y; Yellowish green	4.2	1.5	2.0	2.1 (1.7)	0.59	498	435, 320, 280, 208
Cu(tmtacn)-Y; Yellow	3.8	1.9	1.5	2.5 (2.5)	0.65	490	450, 280, 250, 205
Cu(cyclen)-Y; Green	5.4	2.4	2.2	2.5 (1.7)	0.77	485	610, 382, 300, 212
Cu(tmcyclen)-Y; Blue	3.2	2.0	1.0	3.1 (2.6)	0.76	460	638, 315, 280, 210
Cu(cyclam)-Y Pink	2.7	2.1	1.0	2.7 (2.1)	0.82	405	485, 342, 282, 215

[a]Theoretical values are given in parenthesis.

Figure 3.9. *DRUV-vis spectra of Cu-peraza macrocyclic complexes encapsulated in zeolite-Y.*

Table 3.12. Chemical compositions, surface area (S.A.) and DRUV-vis data of zeolite-encapsulated manganese peraza macrocyclic complexes

Complex	Chemical composition (%)				Metal	S. A.	DRUV-vis
	C	H	N	C/N[a]	%	m^2/g	λ_{max}/nm
Mn-Y; Pale pink	---	---	---	---	0.88	550	242, 265
Mn(tacn)-Y; Red	3.5	2.2	1.5	2.3 (1.7)	0.57	472	625, 520, 405, 315
Mn(tmtacn)-NaY; Yellow	5.2	2.4	1.6	3.2 (2.8)	0.52	468	565, 420, 336, 285
Mn(cyclen)-Y; Yellow	4.4	2.2	1.7	2.5 (1.7)	0.54	470	590, 488, 395, 300
Mn(tmcyclen))-Y; Yellow	4.2	2.1	1.5	2.8 (2.6)	0.62	456	560, 428, 325, 280
Mn(cyclam)-Y; Yellow	3.9	3.2	1.2	2.3 (2.1)	0.64	337	510, 430, 325, 285

[a]Theoretical values are given in parenthesis.
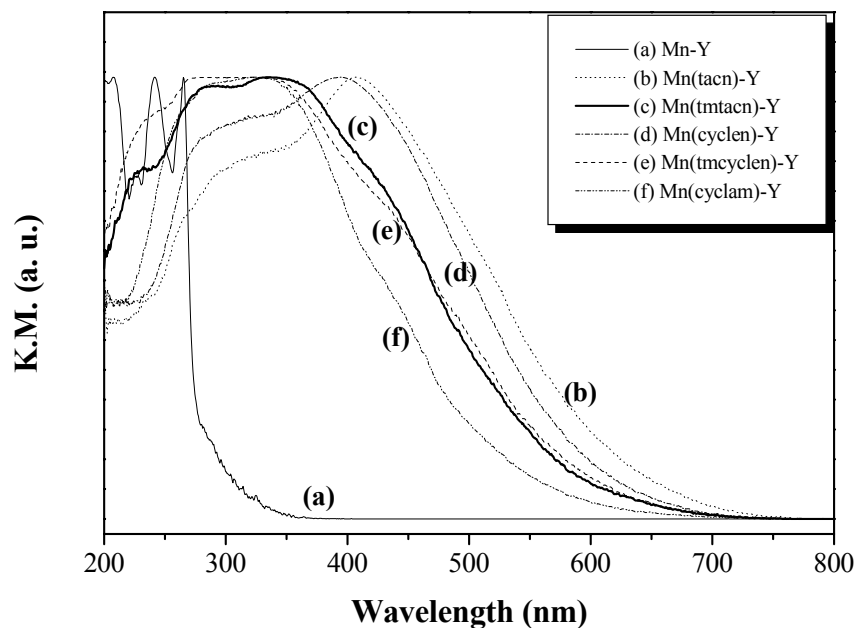
Figure 3.10. DRUV-vis spectra of Mn-peraza macrocyclic complexes encapsulated in zeolite-Y.

3.3.1.2.4. BET Surface Area

Surface area (S_{BET}) of the encapsulated complexes decreased systematically with an increase in the molecular dimensions of the macrocyclic ligand (Tables 3.11 and 3.12). S_{BET} decreased from 540 m^2/g (for Cu-Y) to 498 m^2/g for Cu(tacn)-Y, 485 m^2/g for Cu(cyclen)-Y and 405 m^2/g for Cu(cyclam)-Y. The surface area decreased also due to methyl substitution (Table 3.11). This is one of the direct evidences to show that the complexes are encapsulated in the cages of zeolite-Y. The decrease in S_{BET} is smaller in the present case compared to that observed for the encapsulated copper phthalocyanine complexes (203 m^2/g) [30]. This is perhaps due to the smaller dimensions of the peraza complexes (5.5 – 8 Å) compared to the phthalocyanine complexes (> 12 Å).

3.3.1.2.5. EPR Spectroscopy

Cu(cyclam)$^{2+}$ in CH$_3$CN showed a EPR spectrum at 77 K characteristic of axial symmetry (Fig. 3.11). Hyperfine features due to copper were resolved in the parallel region. Polycrystals of "neat" Cu(cyclam)$^{2+}$ did not show such resolved copper hyperfine features (Fig. 3.11) due to the intermolecular interactions that were obviously avoided in frozen solutions and also in the encapsulated complexes. The similarity in the EPR spectra of frozen solution and encapsulated Cu(cyclam)$^{2+}$ complexes reveals
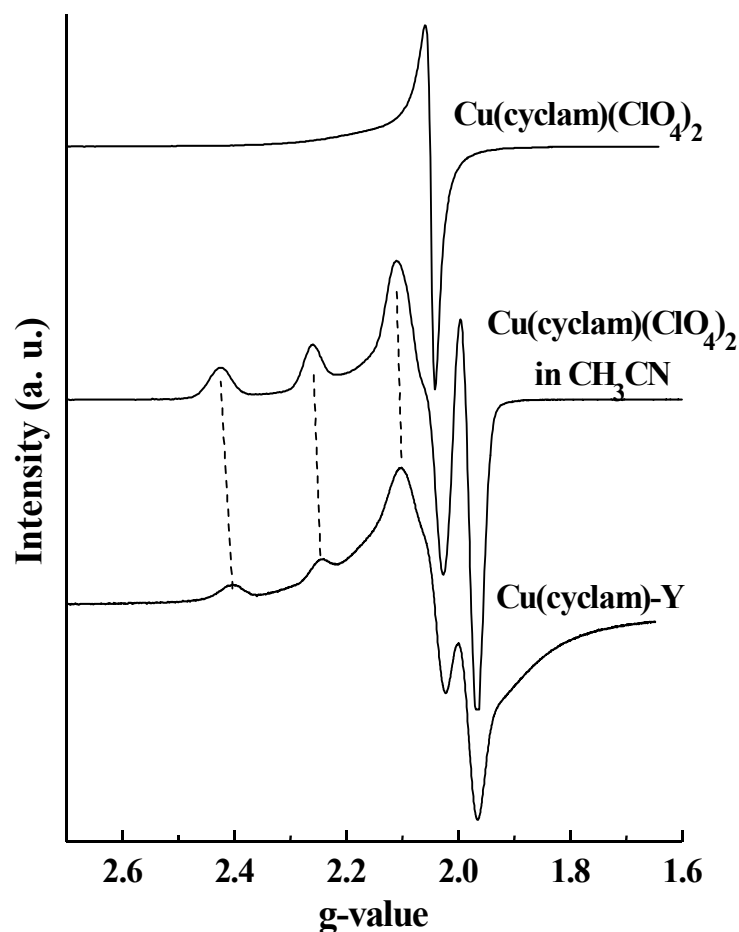
Figure 3.11. *EPR spectra of [Cu(cyclam)](ClO$_4$)$_2$. at 100 K (a) polycrystals, (b) frozen CH$_3$CN solution and (c) Zeolite –Y encapsulated complex.*

that (Fig. 3.11) the geometry of the complex does not change significantly upon encapsulation. Fig. 3.12 shows the EPR spectra of the "neat" and frozen methanolic spectra of Cu complexes.
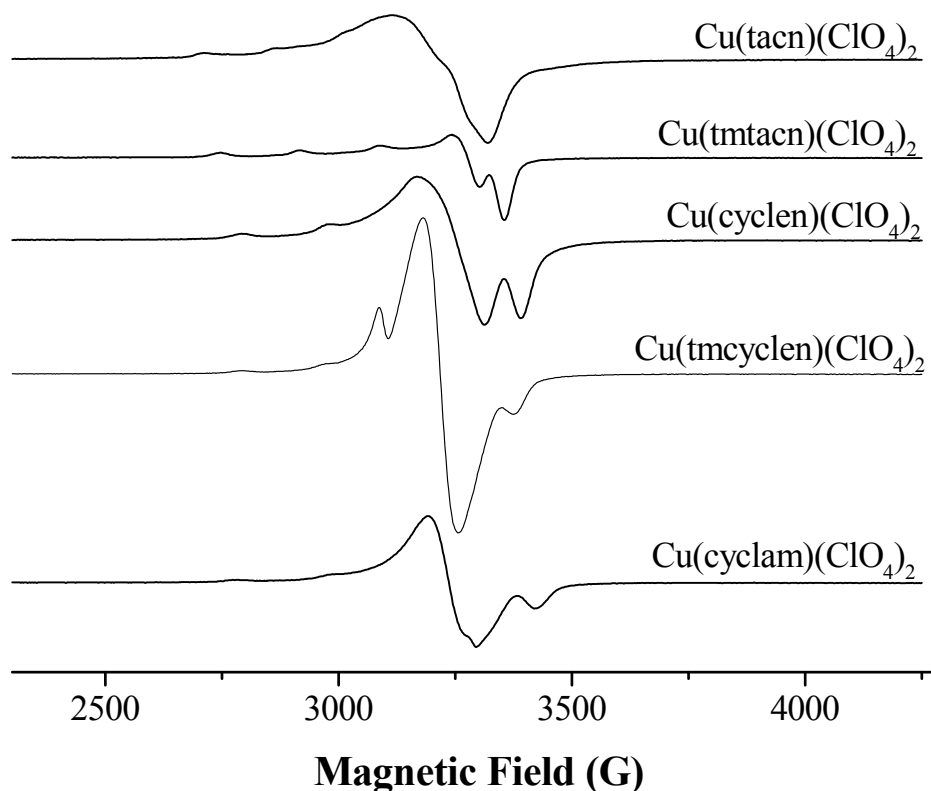
Figure 3.12. *EPR spectra of neat copper peraza macrocyclic complexes 298 K.*

Fig. 3.13 shows the EPR spectra of copper exchanged Y and the encapsulated complexes. Cu-Y exhibitd a spectrum characterized by spin Hamiltonian parameters of $g_{||} = 2.395$, $g_\perp = 2.083$ and $A_{||}(Cu) = 126.4$ G. These signals due to exchanged Cu ions were absent in the spectra of encapsulated tmtacn, cyclen, tmcyclen and cyclam indicating that nearly all the exchanged Cu(II) ions formed the complexes. A small quantity of uncomplexed Cu(II) ions were noticed in Cu(tacn)-Y. Spectral simulations revealed a considerable change in the g and A(Cu) parameters of the different Cu

92

complexes (Table 3.13). The spectrum of Cu(cyclam)$^{2+}$ corresponds to that of a square planar complex and that of Cu(cyclen)$^{2+}$ and Cu(tmcyclen)$^{2+}$ are attributable to weakly pentacoordinated structures. The high $g_{||}$ and low $A_{||}$ values of Cu(tacn)$^{2+}$ and Cu(tmtacn)$^{2+}$ indicate square pyramidal geometry and depletion of electron density at the site of Cu(II). The latter can happen if the geometry is distorted and Cu is out of the basal plane. X-ray structures of Cu(tacn)Cl$_2$ [31] and Cu(tacn)Br$_2$ [32] reveal a distorted square pyramidal geometry wherein the cyclic triamine occupies two equatorial sites and one axial site. The Cu atom is raised by about 0.2 Å from the basal plane toward the axial nitrogen atom. Such a distortion in the geometry can lead to small hyperfine coupling parameters. The shift in the d-d band position (Fig. 3.9) also
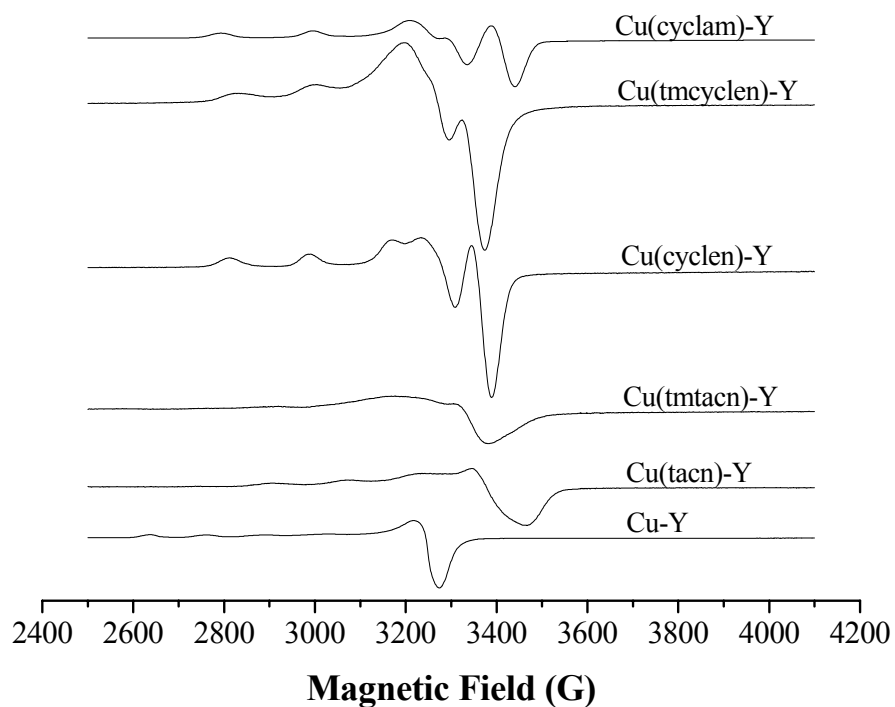
Figure 3.13. *EPR spectra of Cu-Y and encapsulated peraza macrocyclic complexes at 298 K.*

93

parameters are observed when the complexes are encapsulated in the pores of zeolite-Y, again revealing that the structure of the complexes is not changed due to encapsulation.

Mn peraza macrocyclic complex **A** showed a broad EPR signal (line width 825 G) with g = 2.00 indicating intramolecular manganese interactions. Complex **B** showed a signal at g = 2.00 having line width 436 G. All other Mn complexes also showed a broad signal centered at g = 2.00 and line width of about 450 G, characteristic of a high spin mononuclear manganese ion. Mn-Y samples showed a sextet pattern with g_{iso} = 1.99 and |A| = 96 G indicating an octahedral geometry for Mn. After complex formation there was a decrease in manganese hyperfine coupling constant (A) value consistent with a decrease in the symmetry (Table 3.14; Fig. 3.14). Unlike rest of the complexes, Mn(tacn)-Y showed zero field transitions at 2280, 2912, 3466 and 4372 G. The Mn hyperfine features could not be resolved. The spectral features indicate a distorted geometry.

Table 3.13. EPR parameters of neat and zeolite-Y encapsulated copper peraza macrocyclic complexes

Catalyst[a]	$g_{//}$	$g_{\perp}$	$A_{//}$ (G)	$A_{\perp}$ (G)
Cu(tacn)(ClO$_4$)$_2$ .2CH$_3$CN	2.288	2.098	155.5	35.0
Cu(tmtacn)(ClO$_4$)$_2$	2.245	2.045	170.0	13.0
Cu(cyclen)(ClO$_4$)$_2$.2CH$_3$OH	2.192	2.068	170.0	13.0
Cu(tmcyclen)(ClO$_4$)$_2$	2.200	2.095	182.9	10.0
Cu(cyclam)(ClO$_4$)$_2$	2.180	2.081	207.0	25.0
Cu(tacn)-Y	2.229	2.056	166.9	
Cu(tmtacn)-Y	2.305	2.067	148.4	
Cu(cyclen)-Y	2.205	2.057	180.4	
Cu(tmcyclen)-Y	2.207	2.063	173.7	
Cu(cyclam)-Y	2.178	2.047	202.0	
Cu-Y	2.395	2.083	126.4	

[a] For neat samples spectra are recorded in methanol at 77 K.

Table 3.14. EPR parameters of neat and zeolite −Y encapsulated manganese peraza macrocyclic complexes

Complex	g_{av}	$A_{av}(G)$
$Mn_4O_6(tacn)_4(ClO_4)_4$ (**A**)	2.00	NR
$Mn(O)(tmtacn)SO_4$ (**B**)	2.00	NR
$Mn(cyclen)(ClO_4)_2$	2.00	NR
$Mn(tmcyclen)(ClO_4)_2$	2.00	NR
$Mn(cyclam)(ClO_4)_2$	2.00	NR
Mn(tacn)-Y	2.00	NR
Mn(tmtacn)-Y	2.00	94.6
Mn(cyclen)-Y	2.00	93.6
Mn(tmcyclen)-Y	2.00	93.6
Mn(cyclam)-Y	2.00	93.2
Mn-Y	1.99	96.0

(f) Mn(cyclam)-Y

(e) Mn(tmcyclen)-Y

(d) Mn(cyclen)-Y

(c) Mn(tmtacn)-Y

(b) Mn(tacn)-Y

(a) Mn-Y

Magnetic Field (G)
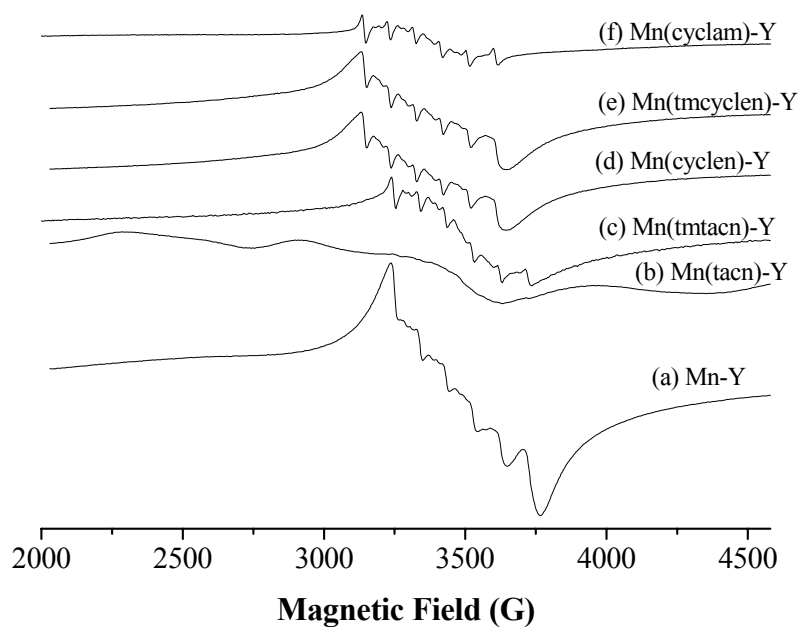
Figure 3.14. *EPR spectra of Mn-Y and Mn-peraza macrocyclic complexes encapsulated in zeolite –Y.*

95

3.3.2. Catalytic Activity of the Complexes

3.3.2.1. Epoxidation of Styrene

3.3.2.1.1. Schiff Base Complexes as Catalysts

Schiff base complexes of Cu(II) and Mn(II) exhibited good activity in the epoxidation of styrene with TBHP (Table 3.15). The reaction did not occur when H_2O_2 was used as the oxidant in place of TBHP. The activity was low when the reactions were carried out at 298 – 313 K (conversion = 13.4%, selectivity 18% for epoxide and 64.6% for benzaldehyde at 298 K). Hence the epoxidation were carried at higher temperature, 333 K. Heterogenization has amarked effect on the activity and product selectivity. The encapsulated complexes are more active than the neat complexes (Table 3.15). Selectivity for benzaldehyde is more over the encapsulated complexes

Table 3.15. Oxidation of styrene with neat and zeolite – Y encapsulated Schiff base Cu and Mn complexes

Catalyst	Conv.	Selectivity (%)				TON
	%	PhCHO	Ph.Oxirane	PhCH$_2$CHO	Others^a	
Cu(salen)	32.3	42.3	32.4	3.7	21.6	16.1
Cu(salen)-Y	48.8	44.2	33.4	5.6	16.8	20.3
Cu(saloph)	29.7	38.4	35.6	2.8	23.2	14.9
Cu(saloph)-Y	45.5	50.3	19.2	---	30.5	19.0
Mn(salen)	30.7	37.6	37.4	2.9	22.1	15.4
Mn(salen)-Y	44.4	53.3	26.2	---	20.5	15.8
Mn(saloph)	24.6	39.6	34.3	4.5	21.6	12.3
Mn(saloph)-Y	33.3	56.9	17.2	3.4	22.5	15.2

Reaction conditions: Styrene (1 mmol); catalyst, neat (0.2 mol%) and encapsulated (20 wt%); TBHP (1.5 equivalents); temp. (333 K); solvent = acetonitrile (1 ml); time (10 h). TON = number of moles of styrene converted per mole of the metal complex. ^{a}Includes products arising form ring opening and over oxidation.

compared to neat complexes. The Cu complexes possess a slightly larger activity than the Mn complexes. For the Cu complexes, the epoxide yield increases on encapsulation inspite of lower selectivity; for the Mn case, epoxide yield is not affected for salens but decreases in the case saloph on encapsulation.

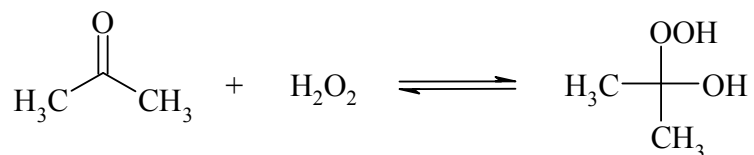*3.3.2.1.2. Peaza Macrocyclic Complexes as Catalysts*

Peraza macrocyclic copper and manganese complexes (except Mn-tmtacn) were also not active as catalysts with hydrogen peroxide for the oxidation of styrene. When the homogeneous reaction with $[Mn(O)(tmtacn)]SO_4$ was carried out without buffer in acetonitrile solvent only vigorous a decomposition of the oxidant was observed giving a very low yield of epoxide (4.0% in 3 h). However, a higher conversion (23.2%) was obtained in the presence of oxalate buffer. Solvent plays an important role in the reaction for both homogeneous and heterogeneous catalysts (Table 3.16). The

Table 3.16. Epoxidation of styrene with H_2O_2 catalyzed by neat and zeolite-Y encapsulated Mn-tmtacn complexes in different solvents

Catalyst	Solvent	Time (h)	Conv %	Selectivity %		TON
				Phenyl oxirane	*PhCHO*	
$[Mn(O)(tmtacn)]SO_4$	Acetonitrile	3	4.0	67.2	31.1	20
$[Mn(O)(tmtacn)]SO_4$ + Oxalate buffer	Acetonitrile	3	23.2	90.0	6.5	116
	Acetone	4	48.3	92.0	5.9	241
Mn(tmtacn)-Y	Acetonitrile	8	4.4	96.3	2.1	23
(No buffer)	Acetone	8	14.2	93.8	2.8	74

Reaction conditions: Styrene (1 mol); solvent (1 ml); $[Mn(tmtacn)]SO_4$ (0.2 μmol); oxalate buffer: oxalic acid (3 μmol), sodium oxalate (3 μmol); H_2O_2 (2 mmol, 40 % aqueous solution gradually added for 20-25 min along with 0.2 ml of solvent); temp. 273 K. For heterogeneous reaction with 1.2 % Mn(tmtacn)-Y same reaction conditions were chosen. TON = number of moles of styrene converted per mole of the metal complex.

encapsulated complex was not much active in acetonitrile but was active in acetone. No buffer was used with the encapsulated complexes. The encapsulated catalyst was not better than homogeneous catalyst except for a marginal improvement in selectivity and the ease of catalyst recovery. Though the N-methylated tacn Mn-tmtacn complex catalyzed styrene epoxidation, only the decomposition of H_2O_2 was observed with Mn-tacn complex. However, with Mn-cyclen and Mn-tmcyclen neither epoxidation nor decomposition of H_2O_2 was observed. The catalytic activity of Mn(tmtacn) encapsulated in NaY is found less than that of homogeneous Mn(tmtacn) catalyst (with buffer). Acetone was found to be the better solvent with H_2O_2 as oxidant in both neat and encapsulated complexes. This is attributed to the formation of 2- hydroxy-2-hydroperoxy propane (Scheme 3.3), an intermediate oxidant [33].

Scheme 3.3. Hydroperoxide intermediate formed during the oxidation with acetone solvent.

The other copper and manganese peraza macrocyclic complexes were active catalysts with TBHP as oxidant (Tables 3.17 and Table 3.18). Most of the homogeneous catalysts gave epoxide in very low selectivity (less than 20%). However, Cu(cyclam) gave a better selectivity (31.8 %) (Table 3.17). The formation of of benzaldehyde (about 50 – 60% selectivity) was observed in all the cases with a small amount of phenyl acetaldehyde. A higher turnover number was achieved with Cu-tacn complexes. Conversion was observed to decrease with increase in ring size and N-methylation of the ligand. Cu^{+2} exchanged NaY also catalyzes the epoxidation

98

(Table 3.17) to a considerable extent [9]. The dependence of catalytic conversion and selectivity on temperature in the case of Cu(cyclam) catalyst is presented in Fig. 3.16 and Fig. 3.17. The optimum temperature was found to be 333 K (Fig. 3.16) for the
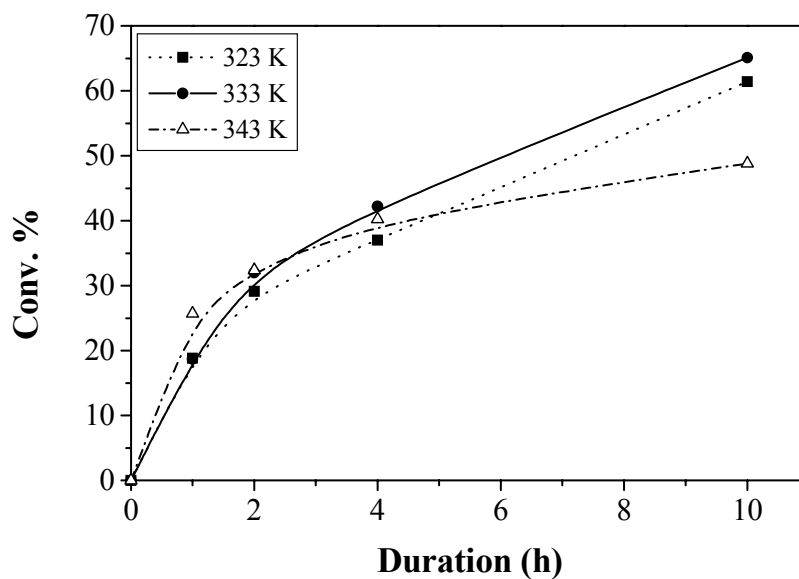
Figure 3.15. *Epoxidation of styrene over [Cu(cyclam)](ClO$_4$)$_2$ at different temperatures with TBHP oxidant.*
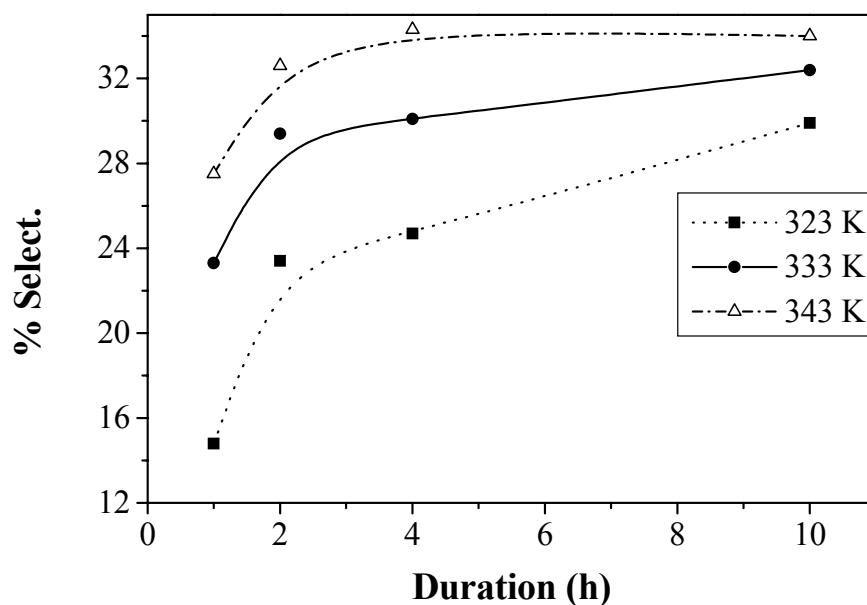
Figure 3.16. *Effect of temperature on epoxide selectivity in the epoxidation of styrene over [Cu(cyclam)](ClO$_4$)$_2$ and TBHP oxidant.*

epoxidation.   Selectivity was found to be lower at lower conversions with the formation of much benzaldehyde but it increased at higher conversions. It is noticed that the selectivity also increases with increase in temperature (Fig. 3.16). Conversion tends to increase very slowly (beyond 40 %) after about 4 h run duration at 343 K, but continues to rise to about 65 % in 10 h at 333 K. This is attributed to slower TBHP decomposition at lower temperature and its less availability for reaction.

Table 3.17. Epoxidation of styrene with TBHP over neat and Na-Y encapsulated Cu-peraza macrocyclic complexes

Catalyst	Conv.	TOF	Selectivity (%)			
	%	(h^{-1})	Phenyl oxirane	PhCHO	$PhCH_2CHO$	Others[a]
$[Cu(tacn)](ClO_4)_2$	96.0	48.0	18.5	23.9	1.0	56.6
$[Cu(tmtacn)](ClO_4)_2$	51.2	25.6	10.1	56.4	10.2	23.3
$[Cu(cyclen)](ClO_4)_2$	69.0	34.5	16.0	40.4	12.2	31.4
$[Cu(tmcyclen)](ClO_4)_2$	33.6	16.8	15.2	60.1	1.9	22.8
$[Cu(cyclam)](ClO_4)_2$	65.1	32.5	31.8	42.7	3.7	21.8
Cu(tacn)-Y	61.2	32.9	10.3	43.2	5.1	41.4
Cu(tmtacn)-Y	27.6	13.8	9.6	58.4	8.1	23.9
Cu(cyclen)-Y	44.3	18.2	13.6	59.3	9.3	17.8
Cu(tmcyclen)-Y	38.7	16.0	10.8	55.1	11.7	22.4
Cu(cyclam)-Y	35.8	13.8	22.0	51.5	8.3	18.2
Cu-Y	27.4	8.4	13.0	58.7	4.1	24.2

Reaction conditions: Styrene (1mmol); catalyst: neat (0.2 mol %) and encapsulated in Zeolite –Y (20 wt.%); TBHP (1.5 equivalents); temp. (333 K); acetonitrile (1 ml); time =10 h. TOF = number of moles of styrene converted per mole of the metal complex per hour. [a]Includes products arising from ring opening and over-oxidation.
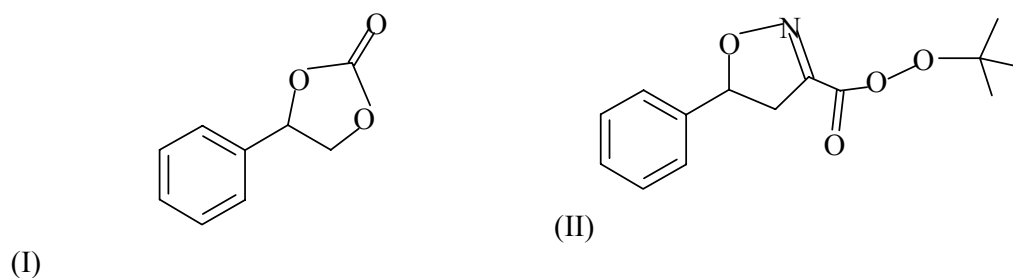
The epoxide selectivity is generally found to be small in the case of Mn complexes (Table 3.18). Only 4.6% selectivity for epoxide is observed with the isolated $[Mn_4O_6(tacn)_4](ClO_4)_4$ complex (Section 3.3.1.2.2). The reaction proceeds in an uncontrolled way producing many byproducts such as 1-phenyl-1,2-ethylene carbonate (I) and *tert*-butyl-4,5-dihydro-3-isooxazole carboperoxoate (II) (Scheme 3.4) other than benzaldehyde (identified by GC-MS and GC-IR). These products are probably formed from the oxidation of the solvent (acetonitrile) and epoxide ring opening.

Table 3.18. Epoxidation of styrene over neat and Zeolite –Y encapsulated Mn-peraza macrocyclic complexes

Catalyst	Conv %	TOF	Selectivity (%)			
			PhCHO	Phenyloxirane	PhCH₂CHO	Others[a]
$Mn_4O_6(tacn)_4(ClO_4)_4$	18.4	9.2	36.1	4.6	2.6	43.3
Mn(tacn)-Y	38.5	18.3	49.5	21.3	2.3	26.9
$Mn(cyclen)(ClO_4)_2$	36.6	18.3	55.9	18.9	8.5	16.7
Mn(cyclen)-Y	58.1	27.9	49.0	16.0	8.2	26.8
$Mn(tmcyclen)(ClO_4)_2$	22.7	11.4	61.8	15.8	5.9	16.5
Mn(tmcyclen)-Y	32.3	16.1	53.0	7.3	4.0	35.7
$Mn(cyclam)(ClO_4)_2$	43.9	22.0	58.5	15.9	5.2	20.4
Mn(cyclam)-Y	29.8	12.4	55.9	25.8	6.5	11.8
Mn-Y	24.0	7.3	56.4	18.4	2.9	22.3

Reaction Conditions: EB (1 mmol); catalyst: neat (0.2 mol %) and encapsulated in Zeolite –Y (20 % by wt.); TBHP (1.5 equivalents); temp.(333 K); acetonitrile (1 ml); time (10 h). TOF = number of moles of styrene converted per mole of the metal complex per hour. [a]Includes products arising form ring opening and over oxidation.

(I)   (II)

Scheme 3.4. *Side products observed during styrene epoxidation.*

3.3.2.2. Oxidation of Ethylbenzene

3.3.2.2.1. Schiff Base Complexes as Catalysts

Schiff base complexes were not active catalysts for ethylbenzene oxidation with H_2O_2 oxidant. However, with TBHP they could catalyze the oxidation under mild conditions. The results are presented in Table 3.19. An enhancement in the catalytic

Table 3.19. Oxidation of EB with TBHP over neat and zeolite –Y encapsulated Cu and Mn Schiff base complexes

Catalyst	Conv.	Time	Selectivity (%)			TOF
	%	(h)	AcPh	p- Hydroxy AcPh	Others[a]	
Cu(salen)	35.3	8	68.0	2.4	29.6	11
Cu(salen)-Y	37.1	10	88.7	1.1	10.2	15
Cu(saloph)	47.6	10	71.6	5.3	23.1	12
Cu(saloph)-Y	38.6	10	93.3	0.8	5.9	14
Mn(salen)	37.2	9	89.9	4.3	5.8	10
Mn(salen)-Y	31.8	9	93.7	0.6	5.7	11
Mn(saloph)	44.0	10	96.7	3.2	3.3	13
Mn(saloph)-Y	35.7	10	96.1	----	3.9	16

Reaction conditions: EB (1 mmol); catalyst: neat (0.4 mol %) and encapsulated in Zeolite –Y (20% by wt.); TBHP (1.5 equivalents); temp. (333 K); acetonitrile (1 ml); time (10 h). TOF = number of moles of styrene converted per mole of the metal complex per hour. [a]Includes peroxo compounds, benzaldehyde, styrene etc.

activity of the complexes (based on TOF) is noticed when encapsulated. This enhancement may be due to the isolation of complex molecule inside the pores and the environment provided by the zeolite framework as seen in the EPR studies.

3.3.2.2.2. Peraza Macrocyclic Complexes as Catalysts

Only [Mn(O)(tmtacn)]SO$_4$ was active catalyst for the oxidation of ethyl benzene with H$_2$O$_2$. The results are presented in Table 3.20 and Fig. 3.17. Acetophenone and 1-phenyl ethanol were the benzylic products obtained. About 5% ring hydroxylated products were also obtained as side products. The side products were benzaldehyde and styrene. Most of the conversion was obtained during the first 2 h and it remained constant thereafter. This may be due to decomposition of the catalyst or the H$_2$O$_2$. The selectivity was constant throughout the reaction.

Table 3.20. Oxidation of ethylbenzene with Mn(O)(tmtacn)SO$_4$ catalyst using H$_2$O$_2$

Time	Conv.	Benzylic Sel.	Hydroxy AcPh		Others[a]
(h)	%	%	o-	p-	
1	38.4	67.5	10.2	11.2	11.1
2	47.1	52.9	4.4	4.5	38.2
4	50.6	57.6	5.2	3.6	33.6
6	51.5	56.8	5.4	4.3	33.5
10	56.7	63.2	5.2	5.2	26.4

[a]Includes peroxo compounds, benzaldehyde, styrene etc.
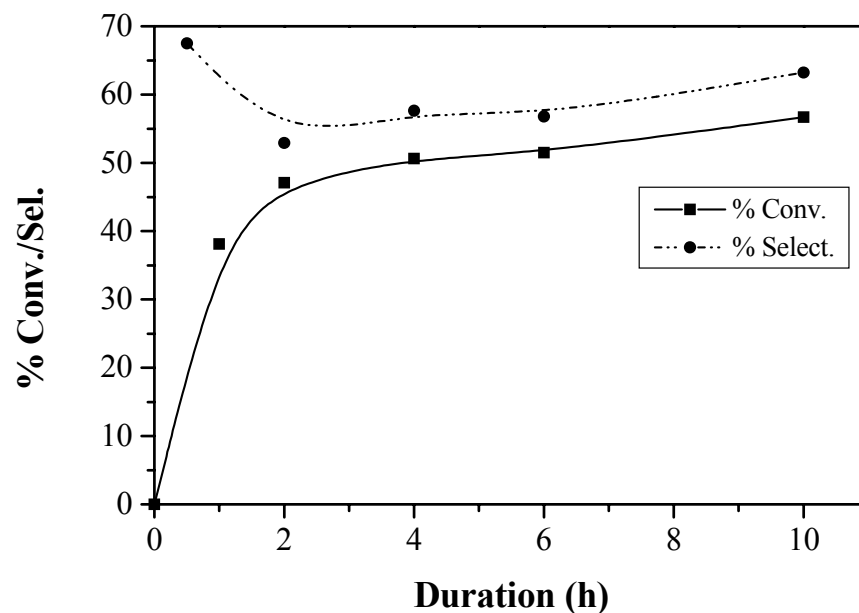
Figure 3.17. *Oxidation of ethylbenzene to AcPh with H₂O₂ oxidant using [Mn(O)(tmtacn)]SO₄.*

Peraza macrocyclic Cu complexes exhibit good activity in the oxidation of ethylbenzene using TBHP (Table 3.21). The reaction does not proceed in the absence of metal complexes. Also no reaction occurs when aqueous H_2O_2 was used in place of TBHP, as the oxidant. Acetophenone (AcPh) is the major product. Hydroxyacetophenones and other products such as benzaldehyde and styrene are also formed in small quantities. In the case of neat complexes, formation of 5 – 6% of EB-peroxide is observed which is not seen in encapsulated complexes. The type of the macrocyclic ring affects the product selectivity. Aromatic ring hydroxylation is more with "neat" tetraaza macrocyclic complexes than with the triaza complex. It decreas with different peraza ligands in the order: tmcyclen > cyclen > cyclam > tacn > tmtacn. Aromatic ring hydroxylation is suppressed significantly when the reactions are

104

conducted using the encapsulated complexes. The encapsulated complexes show enhanced selectivity for AcPh. The extent of selectivity enhancement (for AcPH) is more in the case of tetraaza complexes (13 – 16%) than with the triaza complex (6%).

Table 3.21. Oxidation of EB with various neat and zeolite –Y encapsulated Cu-cyclic amine complexes

Catalyst	Conv.	Time	TOF	Selectivity (%)		
	%	(h)		AcPh	p-Hydroxy AcPh	Others[a]
[Cu(tacn)](ClO$_4$)$_2$	49.6	10	24.8	91.0	3.7	5.3
Cu(tacn)-NaY	37.0	10	19.8	97.0	2.9	0.1
[Cu(tmtacn)](ClO$_4$)$_4$	24.5	10	12.3	79.8	5.5	14.7
Cu(tmtacn)-NaY	11.2	10	6.6	76.0	3.7	20.3
[Cu(cyclen)](ClO$_4$)$_2$	19.0	8	11.8	64.2	8.0	27.8
Cu(cyclen)-Y	30.5	10	12.6	80.2	4.3	15.5
[Cu(tmcyclen)](ClO$_4$)$_2$	35.1	10	17.6	71.0	13.5	15.5
Cu(tmcyclen)-Y	27.8	10	11.2	85.9	6.3	7.8
[Cu(cyclam)](ClO$_4$)$_2$	44.5	10	11.1	85.9	7.8	6.3
Cu(cyclam)-Y	44.4	10	17.1	98.0	2.0	0.0

Reaction Conditions: EB (1 mmol); catalyst: neat (0.4 mol %) and encapsulated in Zeolite –Y (20 wt%); TBHP (1.5 equivalents); temp. (333 K); acetonitrile (1 ml); time (10 h). TOF = Number of moles of reactant converted per mole of catalyst per hour. [a]Includes butyl peroxo compound, benzaldehyde, styrene etc.

Mn complexes are less active than Cu complexes in ethyl benzene oxidation. Both the turn over number and selectivity are comparatively smaller (Table 3.22). Ring hydroxylated products are also more. Higher conversion is observed with the complex [Mn$_4$O$_6$(tacn)$_4$](ClO$_4$)$_4$; however, benzylic selectivity is not good. Considering the turn

over frequency per Mn atom in this complex, it can be stated that the activity was comparable to that of encapsulated Mn(tacn) complex. Except for the Mn(tmcyclen) case, the activities of the neat and encapsulated complexes are less than those of neat complexes (Table 3.22). However, significant improvement in selectivity for AcPh is observed on encapsulation. Thus encapsulation does not have any advantage in these complexes.

Table 3.22. Oxidation of EB with various neat and zeolite –Y encapsulated Mn-cyclic amine complexes

Catalyst	Conv. (%)	*Time* (h)	*AcPh*	*Hydroxy AcPh*		*Others*[a]	*TOF*
				o-	*p-*		
[Mn$_4$O$_6$(tacn)$_4$](ClO$_4$)$_4$	56.6	10	49.1	----	4.1	46.8	14.2
Mn(tacn)-Y	16.0	10	44.3	---	18.0	37.7	3.2
Mn(tmtacn)-Y	19.0	10	51.0	---	11.2	37.8	9.4
Mn(cyclen)(ClO$_4$)$_2$	33.6	10	62.8	2.6	8.4	21.2	8.4
Mn(cyclen)-Y	16.9	12	73.2	---	14.5	12.7	7.0
Mn(tmcyclen)(ClO$_4$)$_2$	22.6	10	75.6	3.2	12.2	10	5.7
Mn(tmcyclen)-Y	37.7	12	77.7	---	17.0	5.3	13.0
Mn(cyclam)(ClO$_4$)$_2$	24.4	12	53.8	12.7	10.1	24	5.0
Mn(cyclam)-Y	17.6	8	51.9	---	16.8	41.3	8.0

Reaction Conditions: EB (1 mmol); catalyst: neat (0.4 mol %) and encapsulated in Zeolite –Y (20 wt%); TBHP (1.5 equivalents); temp. (333 K); acetonitrile (1ml); time (10 h). TOF = Number of moles of reactant converted per mole of catalyst per hour. [a]Includes butyl peroxo compound, benzaldehyde, styrene etc.

3.3.2.2.3. Leaching Test for Encapsulated Complexes

Experiments are conducted over the active copper catalysts to confirm the heterogeneous nature of the reaction over the encapsulated complexes. The results of the experiments carried out without separation and after separation of the catalyst are presented in Table 3.23. The studies show that the metal complexes leach into the solution during the reaction to different extents (Table 3.23). The extent of leaching is

Table 3.23. Leaching test for encapsulated Cu perazamacrocyclic complexes in EB oxidation

Catalyst	Time	Conv.	TON	Selectivity (%)			
	(h)	*%*		*AcPh*	*p*- Hydroxy AcPh	*Peroxide*	*Others[a]*
Cu(tacn)-Y	3	19.1	102	75.7	---	5.5	18.8
After separation ✳	10	37.7	201	85.2	0.8	3.9	10.1
Cu(tacn)-Y ✳✳ Without separation	10	37.0	198	97.0	2.9	0.1	0.0
Cu(cyclen)-Y	3	9.2	42	61.2	---	6.6	62.0
After separation ✳	10	19.3	79	67.9	4.8	4.9	18.8
Cu(cyclen)-Y ✳✳ Without separation	10	30.5	126	80.2	4.3	0.2	15.5
Cu(cyclam)-Y	3	16.5	63	78.0	---	6.0	16.0
After separation ✳	10	27.7	106	83.4	2.6	4.8	14.0
Cu(cyclam)-Y✳✳ Without separation	10	44.4	171	98.0	2.0	0.0	0.0

Reaction Conditions: EB (1 mmol); Catalyst: Zeolite –Y encapsulated catalyst (20 wt%); TBHP (1.5 equivalents); temp. (333 K); acetonitrile (1ml); time (10 h). TON = Number of moles of reactant converted per mole of catalyst. ✳ Catalyst separated after 3 h and reaction continued with clear solution for further 7 h. ✳✳ Reaction carried out for 10 h with the catalyst. [a]Includes butyl peroxo compound, benzaldehyde, styrene etc.

more with the smaller ligands. Considering the activity of the encapsulated complexes and the conversions (Table 3.23), the leaching appears to be in the order tacn > cyclen

> cyclam. The results suggest that most of the Cu(tacn) complex will be leached out during 3 hour reaction time. Based on turnover numbers of the different reactions it appears that nearly about half of the catalyst is leached out in the case of cyclen and cyclam complexes.

3.3.3. Mechanism

3.3.3.1. Styrene Epoxidation

The mechanism of epoxidation with Mn^{+2} salen is believed to involve the same species as that of Mn^{+3} salen complexes [34]. Based on the literature, a plausible mechanism for the reaction can be given as follows (Scheme 3.5). First, from the oxidant and complex an oxo species **(i)** is formed through peroxo species (Mn-OOR, R= H, *t*-Bu) in the case of Mn complexes. Subsequently, the oxygen atom is transferred to the olefin in a concerted or two step mechanism and a Mn^{II} complex is released with formation of the epoxide. The existence of Mn=O intermediate is well established in literature [34-36]. Two possible pathways have been proposed, as shown in Scheme 3.5 (route a or b) and the matter of concerted *vs* non-concerted reaction mechanisms has been the subject of discussion [34-38]. If a stepwise mechanism (route b) operates, rotation around the former double bond (in **6**) can cause isomerization during reaction leading to the formation of *trans*-epoxides from *cis*-olefins. A common side reaction in the catalyzed epoxidation of styrene is the formation of benzaldehyde. A possible mechanism of formation of benzaldehyde involves the reaction of the Mn^{III}-species, in case of Mn-complexes. Many reaction intermediates are suggested in the case of Cu catalyzed oxidations [39]. And many biomemetic oxo-complexes have been found to be active for the epoxidation. Though it is difficult to propose likely mechanism in the case of Cu – complexes, many species like Cu^{III}-O· or Cu^{IV}=O have been proposed to be involved in hydrocarbon oxidations (epoxidation) [40 – 43].
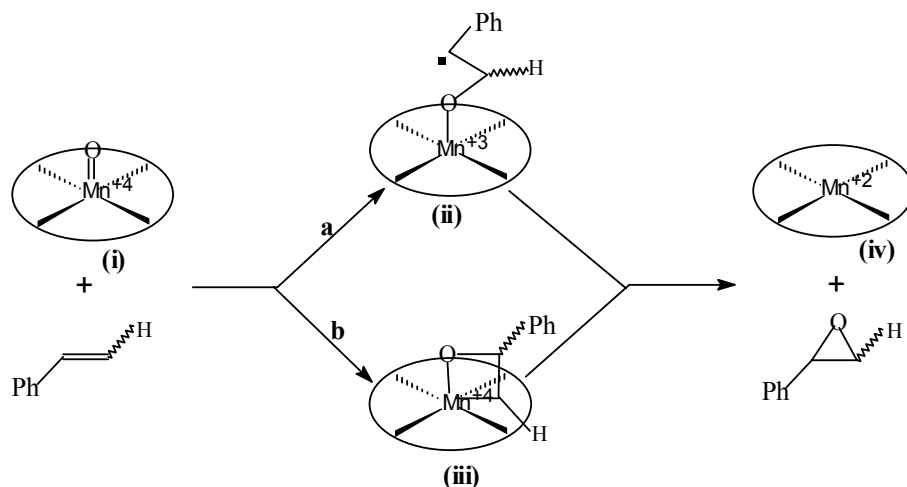
Scheme 3.5. *Possible mechanism for styrene epoxidation catalyzed by Schiff base and peraza macrocyclic Mn complexes.*

3.3.3.2. Ethylbenzene Oxidation

Assuming that the active catalytic species in the reaction is the metal oxo species, the possible mechanism can be proposed as follows (Scheme 3.6). Groves et al. [44] have proposed the oxygen rebound mechanism for the benzylic oxidation. Abstraction of hydrogen from benzylic position to form a benzylic radical intermediate followed by its hydroxylation to give alcohol are the major steps. Alcohol will be
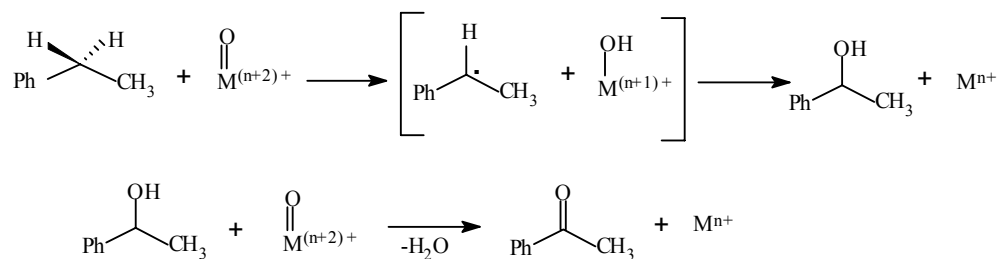
Scheme 3.6. *Possible mechanism for benzylic oxidation (M = Cu, Mn and n = 2).*

oxidized further to ketone by simultaneous abstraction of geminal and alcoholic hydrogen by metal oxo species.

This difference in the catalytic activity/selectivity of the peraza complexes in the "neat" form and when encapsulated in zeolites is probably due to the formation of different "active" copper-oxygen complexes. At least three types of "active" $Cu-O_2$ species viz., side-on peroxo-Cu_2^{II} (μ-η^2,η^2), bis-μ-oxo-Cu_2^{III} and mononuclear Cu^{II}-hydroperoxide (Scheme 3.7) have been identified in the binding, activation and reduction of oxygen to water by copper proteins [40]. Tyrosinase, a dinuclear copper protein, catalyzes the aromatic ring hydroxylation involving dimeric Cu-species such as side-on peroxo-Cu_2^{II} and probably, bis-μ-oxo-Cu_2^{III} intermediates [43]. Dopamine β-monooxygenase that catalyzes side chain hydroxylation forms a mononuclear Cu(II)-hydroperoxo intermediate [40]. Such types of oxo intermediates are formed in the present system also. Side-on peroxo-Cu_2^{II} and bis-μ-oxo-Cu_2 dimers (responsible for ring hydroxylation) are the more feasible forms in homogeneous solutions with the "neat" complexes. In fact, bis-μ-oxo-Cu_2-tacn complexes were isolated from the homogeneous oxygenated solutions and structurally characterized [45]. The possibility of forming such dimers is less likely in the case of encapsulated complexes, as the individual molecules are well separated and confined to the cavities. Thus, a significant suppression in ring-hydroxylated products is observed in catalysis by the encapsulated
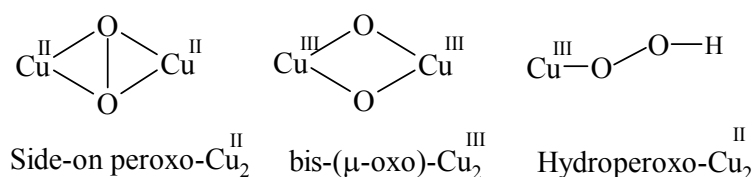

Scheme 3.7. *Active copper species involved in oxidations.*

complexes. Steric effects, weak electrostatic interactions and the synergism due to interactions with the zeolite framework are the other possible reasons for the differences in the reactivity of the encapsulated complexes. When the reaction is conducted at 313 K instead of 333 K, higher amounts of aromatic ring hydroxylated products are formed and the selectivity for acetophonone is low indicating that the stability of the binuclear side-on peroxo complexes is higher at low temperatures (313 K).

Controlled UV-vis and EPR experiments were performed to investigate the different "active" copper-oxygen species formed with the "neat" and encapsulated complexes upon contacting TBHP. Fig. 3.18(i) shows the UV-vis spectra of "neat" $Cu(tacn)(ClO_4)_2$ complexes in acetonitrile before (curve a) and after interacting with TBHP (curve b). The complexes showed an absorption band attributable to d-d transitions at 650 nm. Upon contacting with TBHP a new band was observed at about 462 nm and the intensity of the d-d transition decreased (curve b). The new band at 462 nm is attributed to bis-μ-oxo dimeric complex. This band for related substituted tacn complexes [39] and for the binuclear Cu model system containing N,N,N',N'-tetra (2-pyridylethyl)-3,5-di-(aminomethyl)phenyl [40] occurs at 430 – 448 nm. The characteristic charge transfer band due to Cu-hydroperoxide should appear at around 600 nm [40]. This band, supposed to be weak, could not be separated as it perhaps overlapped with the broad d-d band (curve b). EPR spectroscopy provided evidence for the formation of Cu-hydroperoxide species (Fig. 3.5(ii)). Significant changes in the spectra were observed upon contact with TBHP. In $Cu(cyclam)^{2+}$, the spectrum characterized by the signals with $g_{||} = 2.187$, $g_{\perp} = 2.053$ and $A_{||} = 202$ G due to the original complex (curve a) were replaced by the signals due to two new paramagnetic Cu(II) species I and II (curves b and c). Species I is characterized by $g_{||} = 2.419$, $g_{\perp} =$

2.081 and A$_{||}$ = 117 G. Species II is characterized by g$_{||}$ = 2.333, g$_\perp$ = 2.081 and A$_{||}$

= 102 G). The overall spectral intensity decreased indicating that part of the Cu ions

upon contacting with TBHP are the Cu^{II}-hydroperoxo species. Solomon and co-workers

reported based on detailed spectroscopic and theoretical studies that mononuclear

copper(II) alkyl and hydroperoxo complexes show EPR spectrum with large g values

and small hyperfine splitting features [46]. Indeed the large g$_{||}$ value (2.419 and 2.333)

and small A$_{||}$ values (117 and 102 G) for species I and II indicate the formation of Cu-
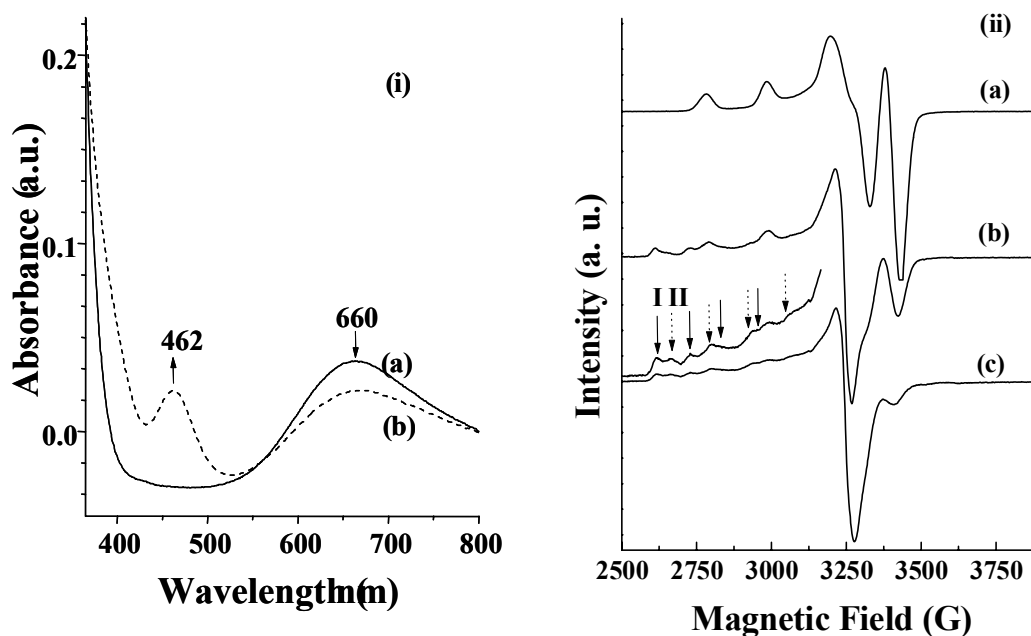
Figure 3.18. *(i) UV-vis spectra of Cu(tacn)(ClO$_4$)$_2$: (a) before and (b) after adding TBHP. (ii) EPR spectra of Cu(cyclam)(ClO$_4$)$_2$. (a) before, (b) after 4 h and (c) after 10 h of adding TBHP. Parallel hyperfine features due to Cu-hydroperoxide species I and II are marked.*

hydroperoxide species. Thus, based on the combined UV-vis and EPR spectroscopic

studies it can be concluded that both copper-oxo and hydroperoxo species are formed in

the interaction of copper-tri and tetraaza complexes with TBHP. The difference in their

relative concentration is presumably responsible for the difference in the selectivity behavior.

3.4.CONCLUSIONS

Neat complexes of Cu and Mn Schiff base and peraza macrocycles were characterized using various physicochemical techniques. The complexes were heterogenized by encapsulating them in cages of zeolite-Y. The effect of encapsulation is manifested on molecular, structural and geometrical changes as seen by UV-vis and EPR spectroscopy. EPR spectroscopy has been used to provide an unequivocal evidence for the encapsulation of complexes inside the super cages of zeolite-Y. The catalytic activities of the neat and encapsulated complexes were evaluated in epoxidation of styrene and ethyl benzene oxidation. Only Mn-tmtacn complexes were efficient oxidation catalysts with H_2O_2 as oxidant for both styrene epoxidation and ethylbenzene oxidation. The other complexes were found to be active with TBHP as oxidant. The complexes were active catalysts for the epoxidation of styrene but the epoxide selectivity was not high. Schiff base complexes were found to be better for epoxidation. The encapsulated complexes have shown enhanced activity and selectivity in the oxidation reactions. The "neat" and zeolite-Y-encapsulated copper tri- and tetraaza macrocyclic complexes have exhibited efficient catalytic activity in the regioselective oxidation of ethylbenzene using TBHP. C-H activation has occurred at both the benzylic and aromatic ring carbon atoms. The difference in the activity of the neat and encapsulated complexes is due to different active Cu-oxygen species involved in the reaction and their different concentration.

3.5. REFERENCES

1. Sheldon, R.A.; Kochi, J.K. (Eds.), *Metal Catalyzed Oxidations of Organic Compounds,* New York, **1981.**

2. Jacobsen, E.N.; Pflatz, A.; Yamamoto, H. (Edt.) *Catalytic Asymmetric Synthesis Vol I and Vol. II* Springer – Verlag Berlin Heidelberg **1999**.

3. Murahashi, S.-I. *Angew. Chem. Int. Ed. Engl.* **1995**, *34,* 2443.

4. Wieghardt, K.; Bossek, U.; Nuber, B.; Weiss, J.; Bonvoisin, J.; Corbella, M.; Vitols, S.E.; Girerd, J.J. *J. Am. Chem. Soc.* **1988,** *110,* 7398.

5. White, M.C.; Doyle, A.G.; Jacobsen, E.N. *J. Am. Chem. Soc.* **2001,** *123,* 7194.

6. Bein, T.; De Vos, D.E.; Meinershagen, J.L. *Angew. Chem. Int. Ed. Engl.* **1996**, *35,* 2211.

7. Holderich, W.; Kollmer, F. *Pure Appl. Chem,* **2000**, *72*, 1273.

8. Niassary, M.S. Farzaneh, F.; Ghandi, M.; Turkian, L. *J. Mol. Catal. A: Chemical,* **2000***, 157,* 183.

9. Ferzaneh. F.; Sadeghi, S.; Turkian, L.; Ghandi, M.; *J. Mol. Catal. A: Chemical,* **1998,** *132,* 255.

10. Komiya, N.; Naota, T.; Oda, Y.; Murahashi, S. -I. *J. Mol. Catal. A: Chemical* **1997**, *117*, 21 and references cited there in.

11. Gorzynski S. J. *Synthesis* **1984**, 629.

12. Bonini, C.; Righi, G. *Synthesis* **1994**, 225.

13. Ojima, I. (Ed.) *Catalytic Asymmetric Synthesis,* VCH, New York, **1993**.

14. Choudary, B.M.; Kantam, M.L.; Bharati, B.; Sreekanth, P.; Figueras, F. *J. Mol. Catal. A: Chemical,* **2000,** *159,* 417 and references cited there in.

15. De Vos, D.E.; Bein, T. *Chem. Comm.* **1996**, 917.

16. Molander, G.A. *Chem. Rev.* **1992**, *92*, 29.

17. Zhang, R.; Yu, W-Y.; Lai, T-S.; Che, C-M. *Chem. Comm.* **1999**, 1791.

18. Hamachi, K.; Irie, R.; Katsuki, T. *Tet. Lett.* **1996**, *37*, 4979.

19. Hill, J.G.; Rossiter, B.E.; Sharpless, K.B. *J. Org. Chem.* **1983**, *48,* 3607

20. Sharpless, K.B.; Verhoeven, T.R. *Aldrichimica Acta* **1979**, *12,* 63.

21. Bhadbhade, M.M.; Srinivas, D. *Inorg. Chem.* **1993,** *32,* 5458.

22. Suresh, E.; Bhadbhade, M.M.; Srinivas, D. *Polyhedron,* **1996**, *15*, 4133.

23. Barry, T.I.; Lay, L.A. *Nature,* **1965,** *208,* 1312.

24. Deshpande, S.; Srinivas, D.; Ratnasamy, P. *J. Catal.* **2000**, *188*, 359.

25. Pavakovic, S.F.; Meck, D.W. *Inorg. Chem.* **1965**, *4*, 1091.

26. Bossek, U.; Wieghardt, K.; Gebert, W. *Angew. Chem. Int. Ed. Engl.* **1983,** *32,* 328.

27. Groves, J.T.; Stern, M.K. *J. Am. Chem. Soc.* **1988,** *110*, 8628.

28 Thom, V.J.; Hosken, G.D.; Hancok, R.D. *Inorg.Chem.* **1985,** *24,* 3378

29. Hathaway, B.J. in Sir G. Wilkinson, Gillard, G.D.; McCleverty, J.A. (Ed.) *Comprehensive Coordination Chemistry,* Pergamon Press, Oxford, *Vol. 5*, **1987**, Ch. 53, 533.

30. Seelan, S.; Sinha, A.K.; Srinivas, D.; Sivasanker, S. *J. Mol. Catal. A: Chemical* **2000**, *15*, 163.

31. Schwindinger, W.F.; Fawcett, T.G.; Lalancette, R.A.; Potenza, J.A.; Schugar, H.J. *Inorg. Chem.* **1980,** *19,* 1379.

32. Bereman, R.D.; Churchill, M.R.; Schaber, P.M.; Winkler, M.E. *Inorg. Chem.* **1979**, *18,* 22.

33. Sauer, M.V.C.; Edwards, J.O. *J. Phys. Chem.* **1971**, *75*, 3004.

34. Srinivasan, K.; Michaud, P.; Kochi, J.K. *J. Am. Chem. Soc.* **1986,** *108*, 2309.

35. Solomon, E.I.; Tuczek, F.; Root, D. E.; Brown, C.A. *Chem. Rev.* **1994**, *94*, 827.

36. Feichtinger, D.; Plattner, D.A. *Angew. Chem. Int. Ed. Engl.* **1997,** *36,* 1718.

37. Finney, N.S.; Pospisil, P.J.; Chang, S.; Palucki, M.; Konsler, R.G.; Hansen, K.B.; Jacobsen, E.N. *Angew. Chem. Int. Ed. Engl.* **1997,** *36,* 1720.

39. Linde, C.; Arnold, M.; Norrby, P-O.; Akermark, B. *Angew. Chem. Int. Ed. Engl.* **1997,** *36,* 1723.

40. Solomon, E. I.; Chen, P.; Metz, M.; Lee, S-K.; Palmer, A.E. *Angew. Chem. Int. Ed. Engl.* **2001,** *40*, 4570.

41 William, A.L; Bruice, T.C. *J. Am. Chem. Soc.* **1985,** *107*, 513.

42 Barton, D.H.R.; Bévíéne, S.D.; Chawasiri, W.; Csuhai, É.; Doller, D.; *Tetrahedron* **1992,** *25*, 504.

43 Karlin, K.D.; Hayes, J.C.; Gultneh, Y.; Cruse, R.W.; McKnown, J.W.; Hutchinson, J.P.; Zubieta, J. *J. Am. Chem. Soc.* **1984,** *106,* 2121.

44. Groves, J.T.; Viski, P. *J. Am. Chem. Soc.* **1989,** *111*, 8537.

45. Mahapatra, S.; Halfen, J.A.; Wilkinson, E.C.; Pan, G.; Wang, X.; Young, V.G. Jr.; Cramer, C.J.; Que, L. Jr.; Tolman, W.B. *J. Am. Chem. Soc.* **1996,** *118,* 11555.

46. Chen, P.; Fujisawa, K.; Solomon, E.I. *J. Am. Chem. Soc.* **2000**, *122*, 10177.

SELECTIVE OXIDATIONS WITH Mn-TMTACN-H$_2$O$_2$ System:

INFLUENCE OF CARBOXYLATE BUFFER

AND ACTIVE Mn SPECIES

4.1. INTRODUCTION

Manganese complexes have been widely studied in the oxidation of hydrocarbons [1-5]. The Mn complexes of porphyrins, Schiff bases and peraza macrocycles constitute a class of biomimetic catalysts and have been known to perform several oxidation reactions stereoselectively [6-10]. Hydroxylation and hydroperoxidation of poorly reactive hydrocarbons have been achieved with these complexes in acetic acid [11]. Recently, the Mn complexes of 1,4,7-trimethyl-1,4,7-triazacyclononane (tmtacn; Fig. 4.1) have been reported to exhibit remarkable catalytic activity for the oxidation of alkenes and alcohols with a cheap and environmentally friendly oxidant H$_2$O$_2$, at ambient temperatures [12, 13]. It has been reported that the catalytic activity is enhanced significantly in the presence of a carboxylate buffer such as oxalate [14-16]. In this chapter, the effect of different carboxylate buffers on the catalytic benzylic oxidation of aromatics with Mn-tmtacn-H$_2$O$_2$ system is investigated. Epoxidation of electron deficient terminal/non-terminal olefins and dienes is also investigated. The catalyst system (Mn-tmtacn complex) is prepared *in situ* by mixing
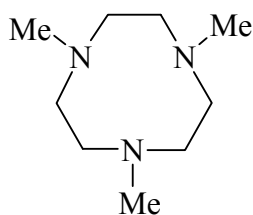
Figure 4.1. *Molecular structure of tmtacn*

known quantities of MnSO$_4$, tmtacn and a carboxylate buffer. H$_2$O$_2$ is used as the oxidant. The buffers used are acetate, oxalate, tartarate, malonate, citrate and ascorbate. These buffers, not only provide different pH to the reaction medium, but may also coordinate with the metal complex, in a variety of coordination modes. Although it has been reported that the catalytic activity of the Mn-tmtacn system is enhanced in the presence of oxalate buffer, the structure of the reactive Mn- intermediate generated upon contact with H$_2$O$_2$ is not reported so far. In this study, *in situ* FT-IR, UV-vis and EPR spectroscopic techniques are used to investigate the structure of active Mn species formed during the reaction. A possible replacement of the expensive tmtacn ligand with cheaper peraza macrocyclic ligands and Mn by iron and vanadium ions is also examined.

4.2. EXPERIMENTAL

4.2.1. Materials and Instrumentation

The peraza macrocylic ligands including tmtacn were synthesized as described in Chapter 2. MnSO$_4$.H$_2$O, carboxylic acids (acetic, malonic, oxalic, tartaric, citric, and ascorbic acids) and CH$_3$CN (A.R. grade) were obtained from s. d. fine Chem. Ltd., India.   The sodium salts of the carboxylic acids were prepared by reacting the corresponding carboxylic acid with stoichiometric amounts of NaOH.   Hydrogen peroxide (38 % or 50% aqueous) was obtained from Merck, India. The substrates used in the catalytic reactions viz., ethyl benzene, allyl acetate, 1-hexene, 1-octene, 1-decene, cyclohexene, styrene, cyclooctene, cis or trans- stilbene etc. were procured from Aldrich. The catalyst system is characterized by EPR, UV-Vis and FT-IR spectroscopies.

4.2.2. Reaction Procedures

4.2.2.1. Epoxidation of Olefins

In a general procedure for epoxidation of olefins, $MnSO_4.H_2O$ (1 µmol) dissolved in 0.1 ml of water was taken in a 25 ml double-necked round bottomed flask fitted with a water-cooled condenser. To this, 8.4 µL of 0.22 M tmtacn stock solution in CH_3CN (net 1.5 µmol of tmtacn) and 1.5 µmol of buffer (carboxylic acid + Na-salt of carboxylic acid (1:1)) were added. Then 1 mmol of olefin was added followed by 0.8 ml of CH_3CN. The reactor was cooled to 273 K using an ice bath. The reaction was carried out by adding drop-wise 0.3 ml of aq. H_2O_2 (38%, 3 mmol) diluted with 0.2 ml of CH_3CN over a 20 min period. The reaction was monitored by GC and the products were identified by GC-MS and GC-IR.

In the epoxidation of dienes, 1 ml of acetone was used as the solvent. The catalyst amount was doubled ($MnSO_4.H_2O$ (2 µmol) dissolved in 0.1 ml water + 16.4 µL of 0.22 M tmtacn stock solution (3 µmol) in CH_3CN + 3 µmol of buffer) and 0.6 ml of H_2O_2 was added over a 30 – 40 min period.

4.2.2.2. Oxidation of Cyclohexane

The catalyst system was prepared in a similar manner as described above in a 25 ml round bottomed flask. To it, cyclohexane (1 mmol) followed by 0.8 ml of CH_3CN were added. The reaction was carried out at 298 K by adding drop-wise 0.4 ml of aq. H_2O_2 (38%, 2 mmol) diluted with 0.2 ml of CH_3CN over a 20 min period. The reaction was monitored by GC and the products were identified by GC-MS and GC-IR.

4.2.2.3. Benzylic Oxidation of Aromatics

In the oxidation of ethylbenzene, the catalyst system was prepared *in situ*. $MnSO_4.H_2O$ (2 µmol) dissolved in 0.1 ml of water was taken in a 25 ml double-necked round bottomed flask fitted with a water-cooled condenser. To this, 16.8 µL of a 0.22 M

tmtacn stock solution in CH_3CN (net 3 μmol of tmtacn) and 3 μmol of buffer were added. Then 0.5 mmol of ethylbenzene was added followed by 0.8 ml of CH_3CN. The flask was placed in an oil bath. The reaction was conducted at a desired temperature (273 – 333 K) by adding drop-wise 0.3 ml of aq. H_2O_2 (38%, 3 mmol) diluted with 0.2 ml of CH_3CN over a 20 min period. The reaction was monitored by GC (Varian 3400; CP-SIL8CB column, 30 m x 0.53 mm) and the products were identified by GC-MS (Shimadzu QP 5000; DB1 column, 30 m x 0.25 mm) and GC-IR (Perkin Elmer 2000; BP-1 column, 25 m x 0.32 mm).

4.2.3. Measurement of pH of the Buffer

The solution of a carboxylate buffer for measuring its pH was prepared as follows: Na salt of a carboxylic acid (18 μmol) was dissolved in a minimum amount of water (0.2 ml) and the corresponding acid (18 μmol) was added. It was then diluted to 8 ml with 75 : 25 acetonitrile : water solution.

4.2.4. *In Situ* Spectroscopic Studies

The structures of the Mn complexes formed during the reactions were investigated using EPR, UV-vis and FT-IR spectroscopic techniques. The solutions for the spectroscopic studies were prepared as follows. $MnSO_4.H_2O$ (6 μmol) was dissolved in 0.2 ml of water and it was diluted with 5 ml of acetonitrile : H_2O (75:25) mixture. To it, 50.4 μL of 0.22 M tmtacn stock solution in CH_3CN (i.e., 15 μmol of tmtacn) was added followed by 12 μmol of carboxylate buffer. Then, the substrate (0.005 mmol) was added with the help of a micro syringe followed by 10 μL of H_2O_2. The spectra were recorded after each step of these additions.

## 4.3. RESULTS AND DISCUSSION

4.3.1. Catalytic Activity Studies

4.3.1.1. Epoxidation of Olefins

De Vos et al [12] have reported that the Mn-tmtacn-H_2O_2 system is efficient for the epoxidation of olefins in the presence of oxalate buffer (Scheme 4.1). Here, the influence of different buffers on the activity of the Mn catalyst system is investigated.

4.3.1.1.1. Epoxidation of Allyl Acetate

It is inferred (Table 4.1) that the carboxylate buffers enhance the catalytic activity of Mn-tmtacn complex to different extents. Selectivity to epoxide is also improved when buffers are used. Among all the buffers, oxalate and ascorbate are found to be the best. Complete conversion of allyl acetate (with 98% epoxide selectivity) was achieved in 0.3 h itself in the presence of oxalate and ascorbate buffers. It took 1 h for the same to be achieved in the presence of citrate and malonate buffers (Table 4.1). In the presence of acetate and tartarate buffers the reaction had to be conducted for almost 5 h for the complete conversion of the substrate. Hence, the reactivity (turnover frequency; TOF) of the Mn-tmtacn system in the presence of different buffers varies in the order: tartarate < acetate < citrate ≤ malonate < ascorbate ≤ oxalate. This variation in activity follows to some extent the variation in the pH of the different buffers: acetate (4.5) < citrate (5.0) < oxalate (5.4) < ascorbate (5.9). However, tartarate (5.3) and malonate (6.0) deviate from the pH-reactivity correlation. Hence, apart from pH, the type of Mn species formed in the presence of buffers is also responsible for the activity of the Mn-tmtacn system. A minimum of 2 equivalents of H_2O_2 was needed to get complete conversion of allyl acetate. With 1 equivalent of H_2O_2, only 37% conversion was obtained with 96.5% selectivity. The conversions with the Mn complexes of tacn, cyclen, tmcyclen and cyclam were negligible. Also, the

120

corresponding cobalt, iron and vanadium complexes were poorly active. Having found that the Mn-tmtacn system is highly active in the presence of oxalate buffer, the rest of the epoxidation reactions were carried out in the presence of oxalate buffer only.
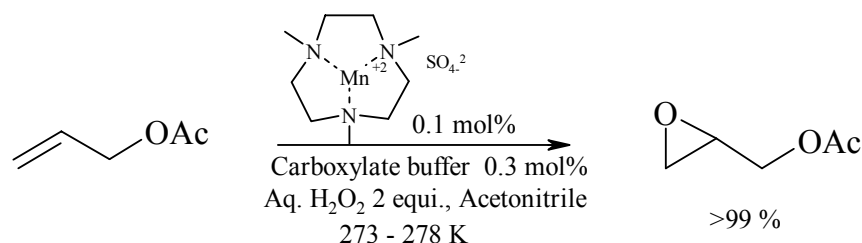
Scheme 4.1

Table 4.1. Catalytic activity data of Mn-tmtacn-H_2O_2 system in different buffers

Buffers	Time (h)	Conv %	Sel. %	TOF^a
No buffer	3	56	94	187
Acetate	3	72	86	286
Citrate	1	98	98	980
Malonate	1	98	98.5	980
Ascorbate	0.3	99	98	1980
Tartarate	5	99	98	198
Oxalate	0.3	99	99	1980
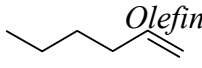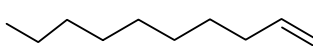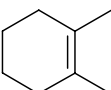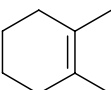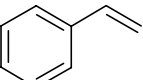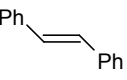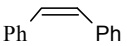
[a]Number of moles of reactant converted per mole of catalyst per hour.

4.3.1.1.2. *Epoxidation of Terminal and Non-termianl Olefins*

The catalyst system, Mn-tmtacn-oxalate, is effective for the epoxidation of a variety of terminal and non-terminal olefins (Table 4.2). In the case of bulkier substrates like 1-octene, longer time is necessary to achieve complete conversions. However, in the case of s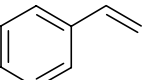ubstrates with more number of carbon atoms, due to poor solubility of the substrate (lipophilic nature) in the reaction medium containing water, low conversions and selectivities were observed. To improve the solubility of the

substrate acetone was used in place of acetonitrile. The rate of H_2O_2 addition has a great effect on the conversion, slow addition of H_2O_2 being desirable for higher conversions. Oxidation of solvent was observed in some cases. Reactions at elevated temperatures and for longer hours led to ring opened products. The studies revealed that the epoxidation with Mn-tmtacn-carboxylate buffer system is stereoselective, *E* and *Z* olefins gave the epoxides without change in the configuration. Epoxidation of cyclohexene at room temperature

Table 4.2. Selective epoxidation of olefins with Mn-tmtacn-oxalate-H_2O_2 system.

Olefin	*Solvent*	*Time (h)*	*Conv. %*	*Epoxide Selectivity %*	*TOF[a]*
	Acetonitrile	0.5	99.0	99.0	1980
	Acetone	2	91.0	90.0	455
	Acetone	5	49.1	88.0	98
	Acetonitrile	1	99.0	82.5	990
	Acetone	4	67.2	65.0	163
	Acetonitrile	1	98.5	98.0	985
	Acetone	6	38.0	87.0	63
	Acetone	4	16	89.3	40
	Acetone	2	22.3	70.1	112
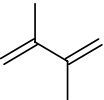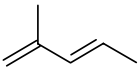
[a]Number of moles of reactant converted per mole of catalyst per hour.

gave *E*-1,2-cyclohexanediol; ^{1}H NMR (CDCl$_3$) δppm: 1.26 (m, 4H), 1.69 (br s, 2H), 1.96 (br s, 2H), 3.36 (s, 2H), 3.9 (br s, 2H), GC-IR cm^{-1}: 3630, 2944, 2874, 1454, 1265, 1064, 849 and GC-MS: M^{+} at 116 [19]. This implies that during the reaction *Z*-epoxide is formed, the ring opening of which yields E-1,2-cyclohexane diol.

Some reports are available on asymmetric epoxidation using triazacyclononane manganese complexes [17-18]. Also many co-ligands have been screened for inducing asymmetry during the epoxidation [16].   However, epoxidation of styrene in the presence of (+)-tartaric acid or (-)-ascorbic acid buffers did not yield enantiomerically rich styrene epoxide in the use of Mn-tmtacn.

4.3.1.1.3. Epoxidation of Dienes

Table 4.3. Epoxidation of Dienes with Mn-tmtacn-oxalate-H$_2$O$_2$ system

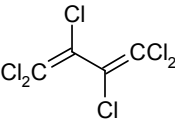| Diene	Time (h)	Conv. %	Epoxide Selectivity %		TON
			Mono	Di	
	6	76.0	29.1	38.2	380
(Cl$_2$C / Cl / CCl$_2$ / Cl)	8	-	-	-	0
	6	70.2	36.0	44.1	350
	4	58	17.1	56.7	290
	6	35.1	78.6	6.3	180

[a] Number of moles of reactant converted per mole of catalyst

Mn-tmtacn-oxalate buffer-H_2O_2 system was also found effective for the epoxidation of (conjugated or non conjugated) dienes (Table 4.3). Both the mono and diepoxides were formed, though the selectivities to diepoxide were not appreciable.

The monoepoxide (*Z-cis*-1, 2-epoxy-5-cyclooctene) was the major product in the epoxidation of *Z*-cyclooctadiene; NMR (CDCl$_3$), δppm: 1.99-2.06 (m, 4H), 2.42 (m, 2H), 2.86-3.02 (m, 4H), 5.55-5.60 (m, 2H), GC-IR cm^{-1}: 3018-2914 (C-H), 1659 (C=C), 1450, 1038 (C-O), 937, 861 and GC-MS: M$^{.+}$ at 124 [20]. No epoxidation was observed in the case of hexachloro-1,3-butadiene due to the highly electronegative chlorine atoms attached to olefinic bond.

4.3.1.2. C-H Bond Activation of Alkanes

4.3.1.2.1. Cyclohexane Oxidation

Catalytic oxidation of alkanes under mild conditions is a difficult process due to the lack of reactivity of alkanes [21, 22]. Mn-tmtacn-oxalate buffer system is investigated for the oxidation of cyclohexane with H_2O_2 under mild conditions. The
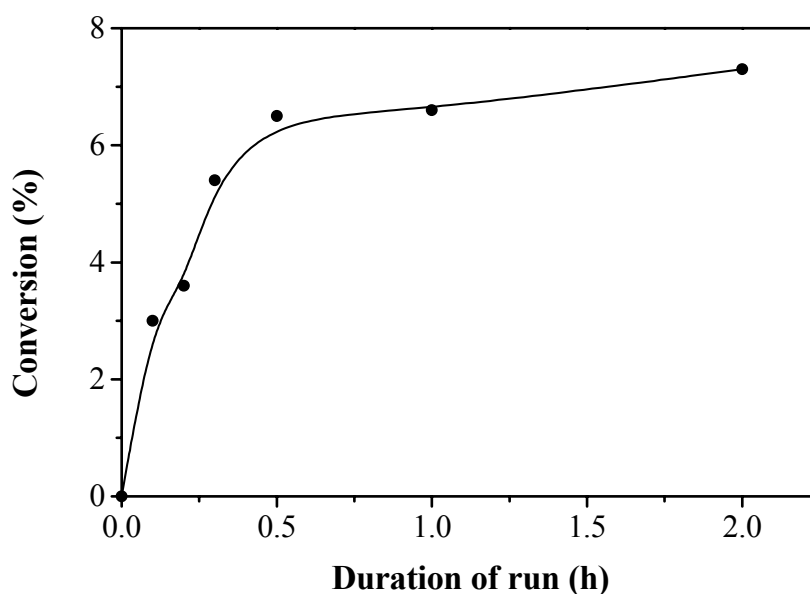
Figure 4.2. *Oxidation of cyclohexane using Mn-tmtacn-oxalate-H$_2$O$_2$ system at 298 K.*

system exhibited low activities (TOF (h^{-1}) ~ 5). Selectivity for cyclohexanone is very high (99%). Increasing the reaction temperature 298 to 313 K did not improve the conversion much. Thus the system is not efficient enough for oxidation of non-reactive C-H bonds. The results of the oxidation at room temperature are shown in Fig. 4.2.

4.3.1.2.2. Benzylic Oxidation

R^1= Aryl
R^2 = H, CH_3, Aryl, etc.

Scheme 4.2

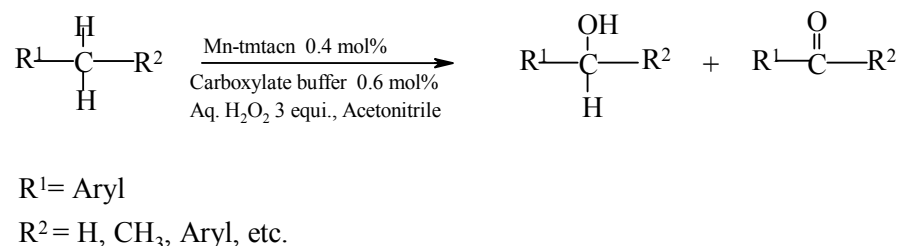The catalytic activity of Mn-tmtacn-oxalate buffer-H_2O_2 system in the epoxidation of olefins and oxidation of alcohols was reported by De Vos and coworkers and Shulpin and coworkers [10-12, 14, 15]. Here, the activity of this system in benzylic oxidation of aromatics is investigated for the first time (Scheme 4.2). Many benzylic oxidation products are commercially important as fragrance materials and in the preparation of optically active α-amino acids. The observations presented in the following section reveal that Mn-tmtacn-H_2O_2 system is unique for benzylic C-H bond oxidation of aromatics compared to the earlier reported catalysts [23-28], in that, it is efficient even at ambient temperatures. Commercial processes for C-H bond activation use cobalt-bromide ion catalyst in acetic acid medium and the reactions are carried out at a high temperature (~498 K) and oxygen pressure (~30 bar) [23]. The C-H bond oxidation reactions when carried out with cerium ammonium nitrate in hot acetic acid, HNO_3 and $HClO_4$, Ce(IV)-triflate with water and oxo-Ru-porphyrin catalysts give only low yields of the intermediate oxidation products [24-27]. Choudary et al. have obtained high yields of benzylic products by using Cr-PILC catalysts and tert-butyl

hydroperoxide. H_2O_2 is used as the oxidant in this study and the reactions are performed at low temperatures (273 – 333 K) [29]. Unlike porphyrin metal complexes attention has not been given in the literature for benzylic oxidation using tmtacn complexes [28, 30].

Oxidation of Ethylbenzene

Catalytic activity data (Table 4.4) reveal that Mn-tmtacn-H_2O_2 system is efficient and selective for benzylic C-H bond oxidation of ethylbenzene (EB). No β-C-H bond oxidation was noticed. 1-Phenylethanol (PhEtOH) and acetophenone (AcPh) were the major oxidation products. *Ortho*- and *para*-ring hydroxylated products were also observed. The reaction did not proceed in the absence of Mn-tmtacn complex. $VOSO_4$ and $FeSO_4$ failed to replace $MnSO_4$ in the catalyst system. The Mn system with no methyl substitution in the cyclic triaza ligand (Mn-tacn) was much less active (13 wt.% EB conversion in 8 h at 313 K with 43.5 wt.% benzylic selectivity in oxalate buffer) compared to Mn-tmtacn (Table 4.4). There was no change in the conversion and selectivity when other manganese salts like $MnCl_2$ were used in the place of $MnSO_4$.

Effect of temperature. Fig. 4.3 shows the effect of temperature on EB oxidation activity of Mn-tmtacn-H_2O_2 system in the presence of oxalate buffer. The conversion of EB was low at 273 K (3.8 wt.%) and 301 K (14.5 wt.%), but the benzylic product selectivity was high at these temperatures (88.4 wt.%). The conversion increased with temperature up to 313 K and then decreased on a further increase in the temperature (Fig. 4.3). At 333 K, both the conversion (27 wt.%) and product selectivity (55 wt.%) were low due to decomposition of H_2O_2 and formation of ring hydroxylated products, respectively. Higher activity and selectivity were observed at 313 K. Thus, all the reactions discussed in the following sections were carried out at 313 K only.
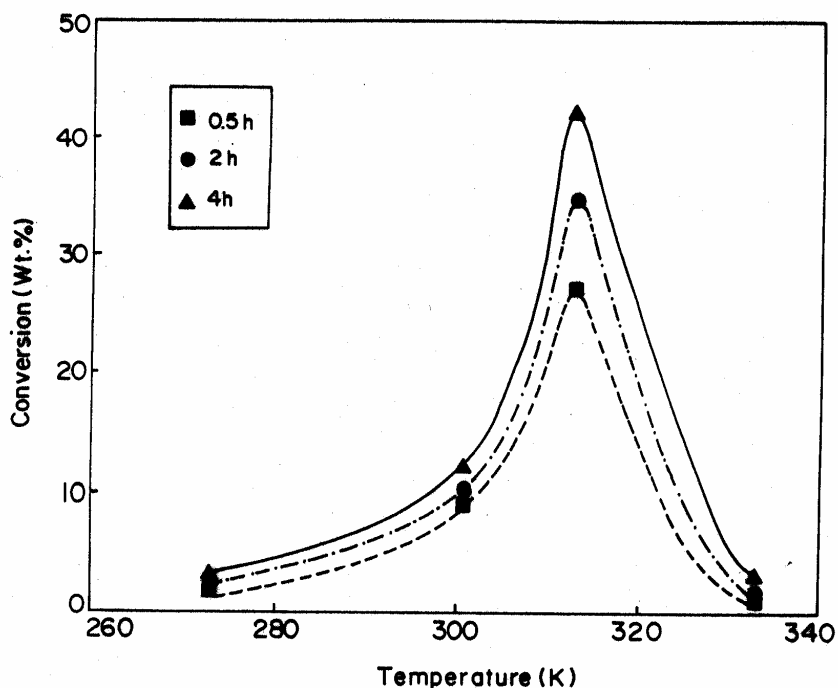
Figure 4.3. *Effect of temperature on the catalytic activity of Mn-tmtacn-oxalate-H_2O_2 system.*

Effect of Carboxylate Buffer. The catalytic activity of Mn-tmtacn-H_2O_2 system for EB oxidation was studied in the presence of different carboxylate buffers viz., acetate, malonate, oxalate, tartrate and citrate and the non-carboxylate ascorbate buffer. The results are listed in Table 4.4. Figs. 4.4a and 4.4b show respectively, the conversion of EB and benzylic product selectivity obtained in different buffers as a function of run duration. It may be noticed that the conversion was rapid during the first 0.5 h (nearly 40 − 70% of the total conversion in 10 h was obtained during this period). The conversion was small in the absence of any buffer (Table 4.4). The activity of the catalyst system (EB conversion and turnover frequency (TOF)) at 0.5 h in different buffers varied in the following order: acetate < tartrate < malonate < oxalate ≤

127

Table 4.4. Catalytic activity of Mn-tmtacn-H$_2$O$_2$ in the oxidation of ethylbenzene[a]

Buffer	*Reaction time (h)*	*Conv. (wt.%)*	*TOF[b]*	*Benzylic[c] selectivity (wt.%)*	*Selectivity (wt.%)[d]*	
					PhEtOH	*AcPh*
Acetate	0.5	8.7	44	76.7	25.7	51.0
	10	18.8	4.7	68.4	21.5	46.9
Tartrate	0.5	14.7	74	84.4	23.5	60.9
	10	27.9	7.0	79.9	20.7	59.2
Malonate	0.5	26.2	130	85.0	0.0	85.0
	10	54.4	13.6	83.2	0.0	83.2
Oxalate	0.5	27.0	136	57.3	12.3	45.0
	10	69.0	17.3	60.2	19.4	40.8
Ascorbate	0.5	27.6	138	91.0	0.0	91.0
	10	59.1	14.8	83.5	0.0	83.5
Citrate	0.5	37.4	188	83.9	0.0	83.9
	10	52.3	13.0	85.2	17.9	67.3
No buffer	0.5	1.5	8	32.6	0.0	32.6
	10	6.5	1.6	70.3	0.0	70.3

[a]Reaction conditions: Ethylbenzene = 0.5 mmol; aq. H$_2$O$_2$(38%) = 5 mmol; CH$_3$CN =1 ml; H$_2$O = 0.1 ml; MnSO$_4$ = 2 μM; tmtacn = 3 μM; buffer = carboxylic acid (3 μM) + corresponding Na salt (3 μM); temp. = 313 K.
[b] Number of moles of ethylbenzene converted per mole of catalyst per hour.
[c]Combined selectivity of PhEtOH and AcPh. Rest are ring hydroxylated products.
[d] PhEtOH = 1-phenylethanol; AcPh = acetophenone.

ascorbate < citrate. The increase in EB conversion after 0.5 h was smaller in acetate, tartrate and citrate buffers than in oxalate and malonate buffers. At the end of 6 h, a higher conversion was observed in the oxalate buffer than in the other buffers. The system with oxalate buffer showed lower benzylic product selectivity (57 wt.%) compared to the other buffers (76 – 91 wt.%; 0.5 h; Table 4.4; Fig. 4.4b). The benzylic product selectivity decreased marginally after 1 – 4 h (depending on the buffer) due to an increase in the rate of other reactions and decomposition of buffer/complex (Fig.

4.4b).   The malonate and ascorbate buffers were unique to yield only AcPh as the

selective benzylic product while the rest of the buffers yielded both PhEtOH and AcPh

(Table 4.4). This suggests that with the malonate and ascorbate buffers, the intermediate

alcohol is rapidly oxidized to the ketone or a different type of oxidation mechanism is

involved.   In the absence of any buffer, the conversion of EB was smaller (6.5% at 10
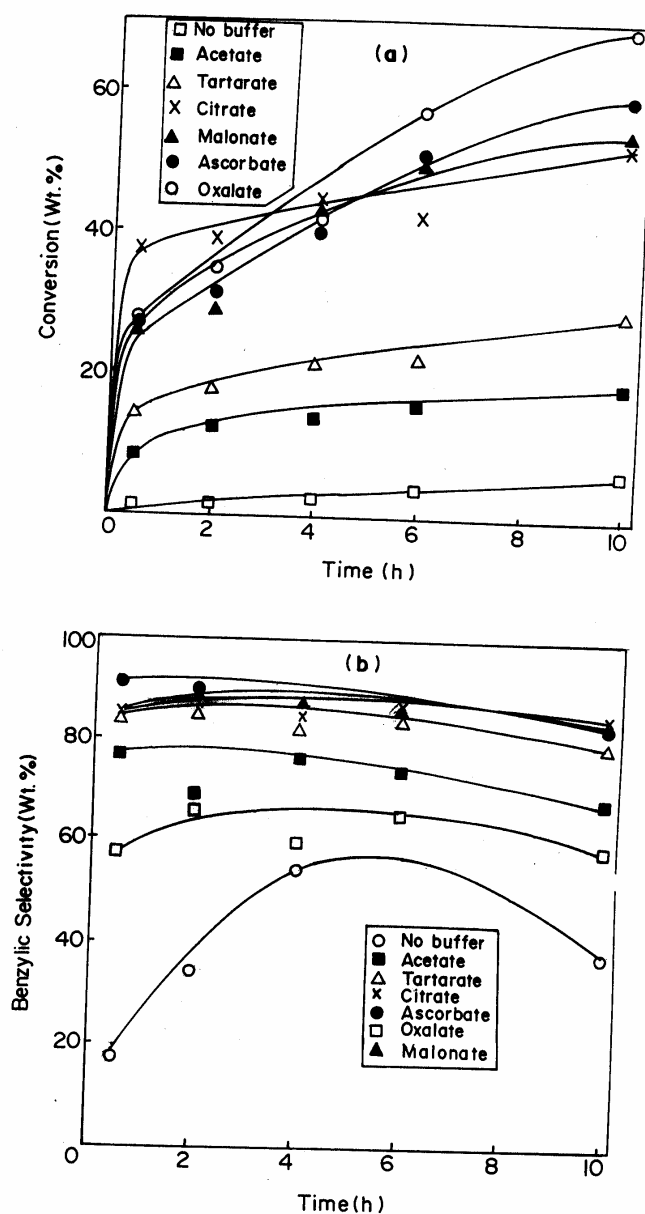
Figure 4.4.   *Influence of carboxylate buffer on the activity of Mn-tmtacn-H₂O₂ system in the oxidation of ethylbenzene.*

h) and the ketone was the only product (Fig. 4.4 and Table 4.4). Formation of EB-hydroperoxide (10 – 12%) was observed in the case of oxalate buffer, which was not seen in any other buffer. This suggests that the reaction probably goes through the formation of hydroperoxide as the intermediate product.

Oxidation of Aromatic Compounds

Table 4.5. Benzylic oxidation of aromatic compounds by Mn-tmtacn-H_2O_2 system in oxalate and citrate buffers

Substrate	Buffer	Time (h)	Conv. (wt.%)	TOF	Benzylic selectivity (wt.%)	Benzylic product Distribution (wt.%)
DEB	Oxalate	0.5	25.1	125.4	67.8	A-31.4; B-36.4
		10	49.6	12.4	55.9	A-25.3; B-30.6
	Citrate	0.5	32.1	160.6	81.0	A-33.1; B-47.8
		10	35.1	8.8	78.5	A-29.5; B-49.0
OX	Oxalate	0.5	20.1	100.8	39.4	C-13.9; D-25.5
		10	77.4	19.3	44.9	C-19.3; D-25.6
	Citrate	0.5	14.5	71.8	55.0	C-17.6; D-37.4
		10	53.3	13.3	50.2	C-10.2; D-40.0
MPT	Oxalate	0.5	8.7	43.4	81.8	E-30.9; F-41.3; G-9.7
		6	15.3	6.3	50.8	E-19.0; F-31.8; G-6.0
	Citrate	0.5	7.4	37.0	72.1	E-23.2; F-42.7; G-6.2
		10	12.2	3.0	80.5	E-28.9; F-41.5; G-10.1
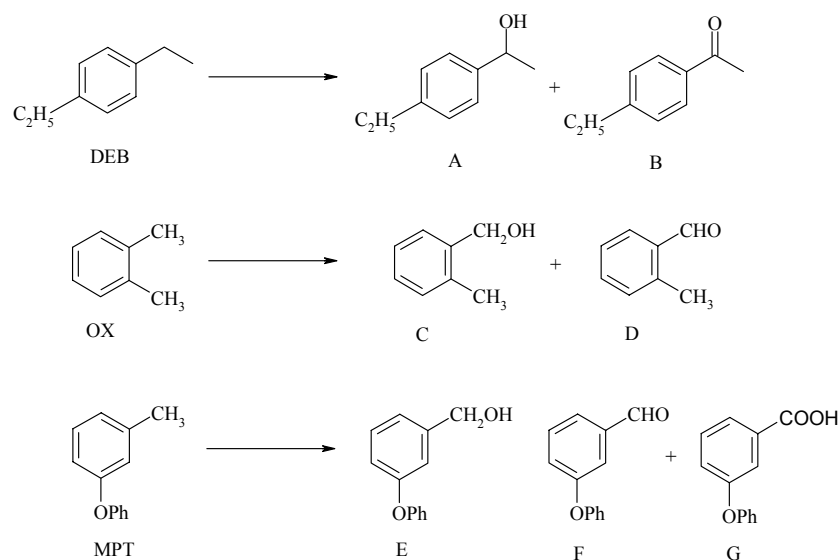
The catalytic activity data for the oxidation of diethylbenzene (DEB), *ortho*-xylene (OX) and *meta*-phenoxytoluene (MPT) in oxalate and citrate buffers are presented in Table 4.5. A maximum conversion of 77.4 wt.% was observed for OX, 49.6 wt.% for DEB and 15.3 wt.% for MPT in the oxalate buffer. Only one of the alkyl groups in DEB and OX could be oxidized. The ring hydroxylated products were more in OX oxidation. Substrate conversion was, in general, more in oxalate than in the citrate buffer, though the benzylic product selectivity was lower than in the latter buffer.

4.3.2. *In situ* Spectral Studies

The reasons for the differences in the activity observed in different carboxylate buffers perhaps arise from the differences in the structures of the active Mn intermediates formed in the oxidation reactions. In this section, the structure of the active Mn intermediates in different buffers is identified by *in situ* UV-vis, FT-IR-attenuated total reflectance (FT-IR-ATR) and EPR spectroscopic studies.

4.3.2.1. *UV-Vis Spectroscopy*

UV-Vis spectra of Mn-tmtacn-H_2O_2 were recorded in the presence of acetate and oxalate buffers (Figs. 4.5(i) and 4.5(ii)). The Mn-tmtacn complex in CH_3CN-H_2O mixture showed broad, partially resolved UV bands of ligand origin at around 300 and 360 nm (Fig. 4.5(i), curve a). The intensity of these bands decreased in the presence of acetate buffer (Fig. 4.5(i), compare curve b with curve a). Upon adding H_2O_2 to Mn-tmtacn- acetate system, a new, intense band was observed at 280 nm (Fig. 4.5(i), curve c), in addition to three weak bands at 390, 480 and 520 nm (Fig. 4.5(i); inset). The former (at 280 nm) is attributed to carboxylate to Mn charge transfer band and those bands at 480 and 520 nm are due to d-d transitions. Soon after adding the oxalate buffer, a marked change was noted in the spectrum of Mn-tmtacn (Fig. 4.5(ii), compare
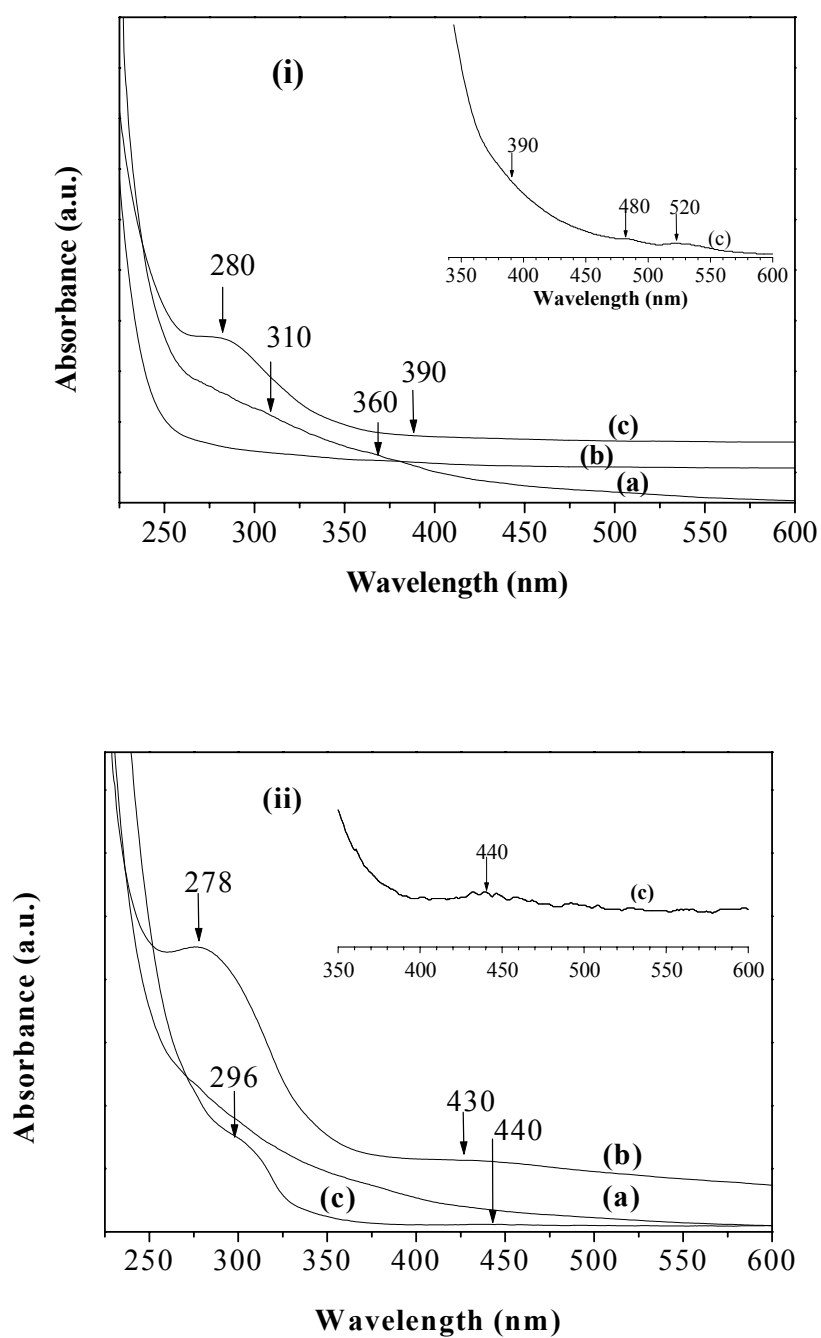
Figure 4.5. *UV-vis spectra in CH₃CN-H₂O: (i) – (a) MnSO₄ + tmtacn, (b) MnSO₄ + tmtacn + acetate buffer, (c) MnSO₄ + tmtacn + acetate buffer + H₂O₂; (ii) – (a) MnSO₄ + tmtacn, (b) MnSO₄ + tmtacn + oxalate buffer, and (c) MnSO₄ + tmtacn + oxalate buffer + H₂O₂. Inset shows the blow-up of traces (c).*

curves b and a); a strong band at 278 nm and a weak, broad band at 430 nm were observed. Such bands were not seen in acetate buffer indicating the formation of a different kind of Mn-tmtacn complex in oxalate compared to that in acetate buffer. This is further substantiated by EPR spectroscopy (*vide infra*). However, on adding H_2O_2 these bands disappeared and two new bands appeared at 296 and 440 nm (Fig. 4.5(ii), curve c and inset). A comparative study with similar Mn complexes [31, 32] reveals that the weak band at 440 nm in Mn-tmtacn-oxalate-H_2O_2 is due to the formation of a terminal-oxo manganese complex, (tmtacn)(oxalate)Mn=O and the band at 390 nm in Mn-tmtacn-acetate-H_2O_2 is due to μ-oxo manganese complex, (μ-O)(μ-acetato)$_2$Mn$_2$(tmtacn)$_2$. The different oxo-manganese species account for the difference in activity of the Mn-tmtacn system in different buffers. The formation of oxo-manganese complexes was confirmed also from FT-IR-ATR and EPR investigations.

4.3.2.2. FT-IR-ATR Spectroscopy
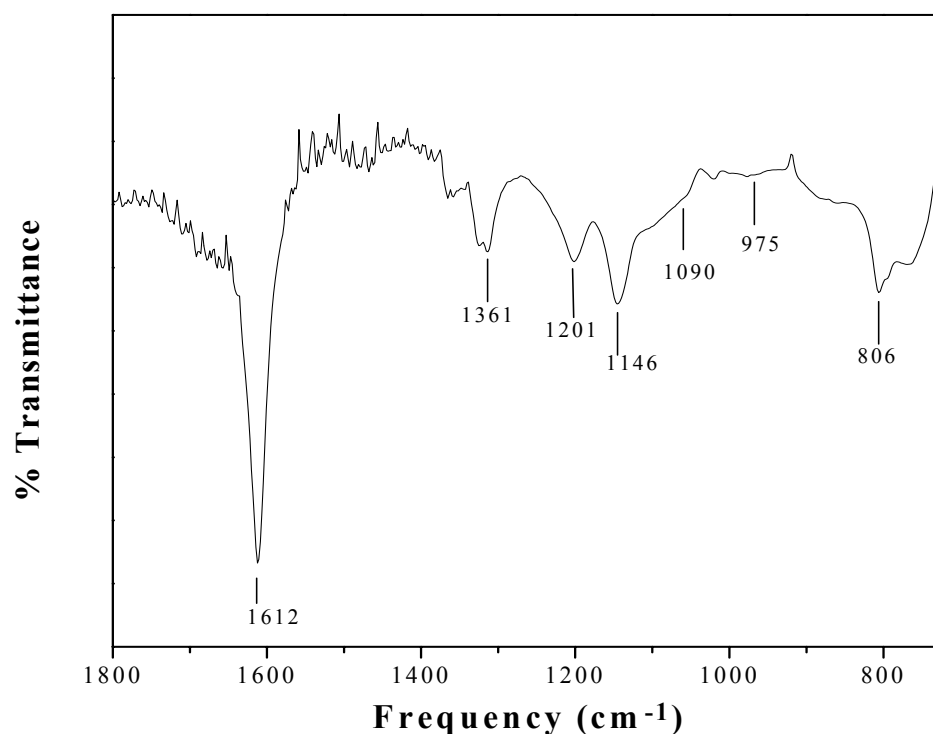
Figure 4.6. *FT-IR-ATR spectrum of MnSO$_4$-tmtacn-oxalate buffer-H$_2$O$_2$ in CH$_3$CN-H$_2$O solution.*

The FT-IR-ATR spectrum of Mn-tmtacn-oxalate-H_2O_2 in CH_3CN-H_2O is shown in Fig. 4.6. The coordinated oxalate exhibits characteristic IR bands at 1612 and 1361 cm^{-1} due to carboxylato stretching modes. The bands at 1146 and 1201 cm^{-1} are due to SO_4^{2-} ions. Upon adding H_2O_2 to Mn-tmtacn-oxalate, weak partially resolved bands were observed at around 1090, 975 and 806 cm^{-1}. Similar optical features (at 412 nm in UV-visible and 979 cm^{-1} in FT-IR) were reported earlier for terminal oxo-Mn-porphyrin complexes [33, 34].

4.3.2.3. EPR Spectroscopy
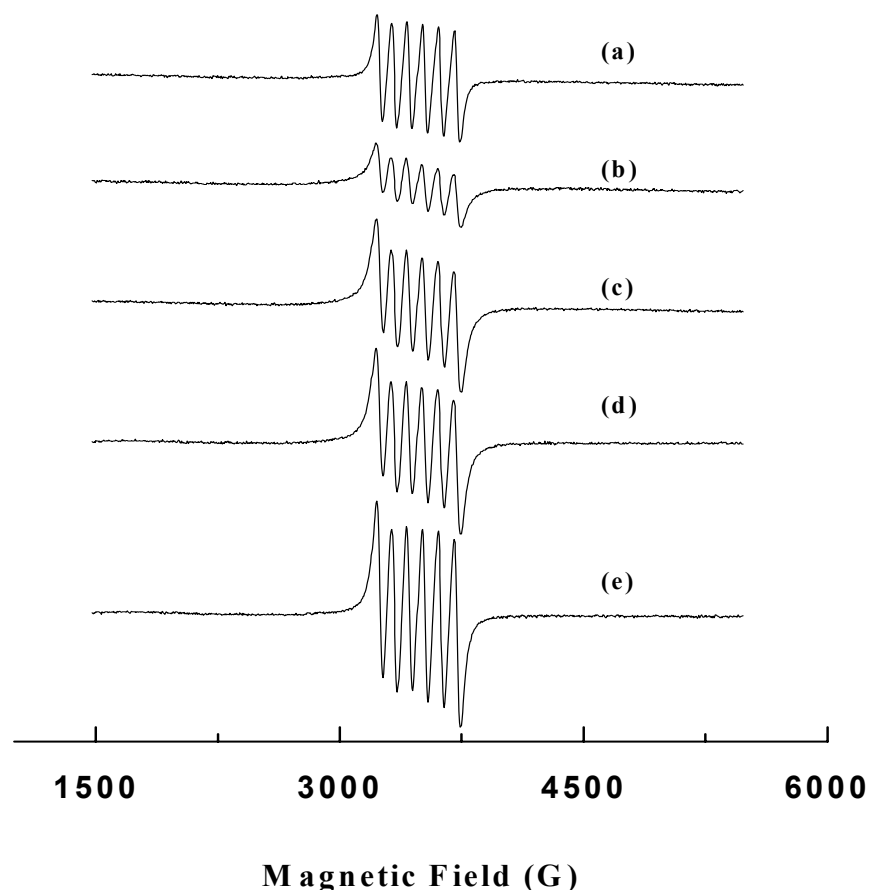
Figure 4.7. EPR spectra in CH_3CN-H_2O at 298 K: (a) $MnSO_4$, (b) $MnSO_4$ + tmtacn, (c) $MnSO_4$ + tmtacn + acetate buffer, (d) $MnSO_4$ + tmtacn + acetate buffer + ethylbenzene, and (e) $MnSO_4$ + tmtacn + acetate buffer +ethylbenzene + H_2O_2.

134

$MnSO_4$ dissolved in CH_3CN-H_2O mixture showed characteristic, well resolved Mn hyperfine features centred at g_{iso} = 2.002 (A_{iso}(Mn) = 95.6 G; line width (ΔH_{pp}) = 32 G; Fig. 4.7a). The intensity of the Mn signals decreased on adding tmtacn ligand (Fig. 4.7b). However, on adding acetate buffer to the Mn-tmtacn solution, the original spectral intensity (Fig. 4.7c) was regained (ΔH_{pp} = 55 G). Addition of substrate (EB) had little effect on the spectrum (Fig. 4.7d), but, when H_2O_2 was added, the line width of the Mn signals decreased to 40 G (Fig. 4.7e). The EPR results are interpreted as follows. When $MnSO_4$ and tmtacn were mixed Mn(II)-tmtacn complex was formed. This was highly reactive towards aerial oxygen. A part of it was converted into an EPR-silent Mn(III) species and as a consequence of this, the overall spectral intensity of $MnSO_4$-tmtacn decreased. The line width of Mn(II)-tmtacn (60 G) was more than that of $MnSO_4$ solution (32 G) (Fig. 4.7b) suggesting weak intermolecular interactions in the former solution. In acetate buffer, Mn was in +2 oxidation state as Mn(II)-tmtacn-acetate complex. However, on adding H_2O_2, a binuclear μ-oxo-manganese(IV) (designated as species A) was formed. Such μ-oxo-Mn complexes were isolated and structurally characterized by Wieghardt and co-workers [33-35] and Koek et al [36].

Marked changes were observed in the spectra of Mn-tmtacn complex in oxalate buffer. Mn-tmtacn with oxalate buffer exhibited an intense signal at g_{iso} = 2.0012 with ΔH_{pp} = 33.6 G (Fig. 4.8a); no Mn hyperfine features were observed. The origin of this signal was due to a radical attached to Mn(III) center. The intensity of the radical signal decreased on adding EB (Fig. 4.8b) and weak Mn(II) hyperfine could be seen due to interaction of the radical species with EB. On adding H_2O_2 the radical species disappeared and a signal with ΔH_{pp} = 190 G (Fig. 4.8c) due to teminal-oxo-Mn(IV) complex (designated as species B) appeared.

Figure 4.8. EPR spectra in CH₃CN-H₂O at 298 K. (a) MnSO₄ + tmtacn + oxalate buffer, (b) MnSO₄ + tmtacn + oxalate buffer + ethylbenzene, and (c) MnSO₄ + tmtacn + oxalate buffer +ethylbenzene + H₂O₂.

In other buffers, on adding H_2O_2, spectra corresponded to both species A and B (exhibiting overlapped Mn hyperfine features with the broad signal). The relative amounts of these species were different in different buffers. Fig. 4.9 shows the experimental and simulated spectra of the system in the presence of malonate buffer. The EPR signal intensity variations of species A and B in different buffers are shown in Fig. 4.10.
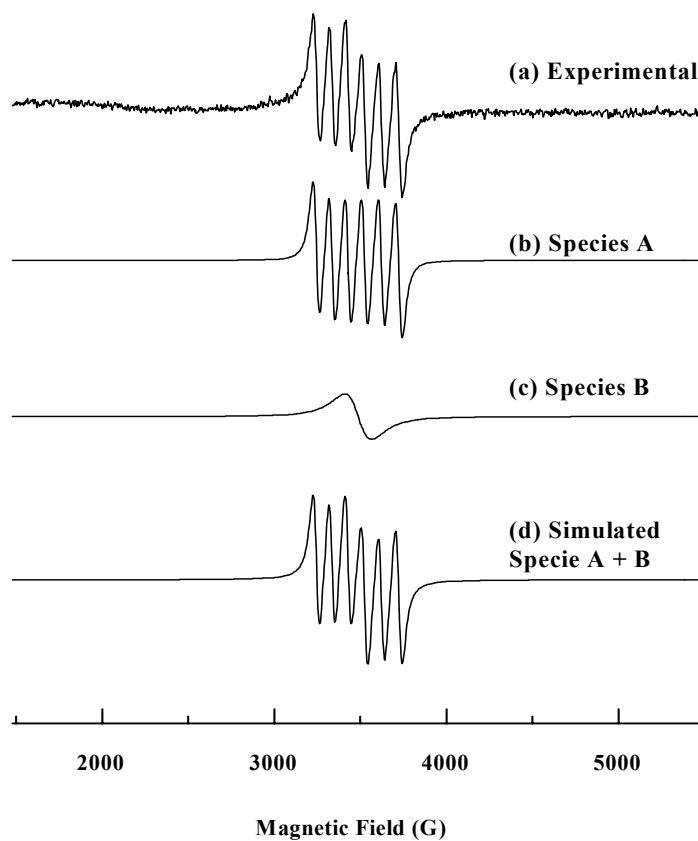
Figure 4.9. *Experimental and simulated EPR spectra of MnSO$_4$-tmtacn-malonate-ethyl benzene-H$_2$O$_2$ system in CH$_3$CN-H$_2$O mixture at 298 K.*

4.3.3. Structure- Activity Relationship

The following conclusions are drawn from the *in situ* spectroscopic studies. Carboxylic acid acts as a co-ligand in addition to acting as a buffer. Carboxylato-bridged complexes have been identified as active sites in metalloenzymes [37]. The nature of the carboxylic acid group and mode of coordination influence the redox behavior of the Mn site. In the presence of acetate, malonate and tartrate, Mn-tmtacn forms carboxylato-bridged complexes of type (I) shown in Fig. 4.11 [33 – 35].

However, in oxalate buffer, Mn(II) is oxidized to Mn(III) with a concomitant reduction of oxalate yielding (tmtacn)Mn^{III}(oxalate$^{-\bullet}$) radical complex (II; Fig. 4.11). Such radical intermediates were identified also in the oxidation reactions involving metal porphyrins [38]. Addition of H_2O_2 forms μ-oxo- (species A) and terminal-oxo- (Species B) Mn(IV) complexes (Fig. 4.10). The former type of complexes are characterized by resolved Mn hyperfine pattern (Fig. 4.7e) while the latter by a broad EPR signal at g ~ 2 at 298 K (Fig. 4.8c). In acetate, malonate and citrate buffers both A and B were co-existent. In the oxalate buffer, species B was most predominant (Fig. 4.10) while species A was dominant in solutions containing acetate and tartrate buffers. The distinctive behavior of oxalate buffer is attributed to (i) its capability to influence the redox behavior of manganese, (ii) intramolecular electron transfer resulting in the formation of the carboxylato radical intermediates and (iii) formation of terminal-oxo-Mn(IV) species.
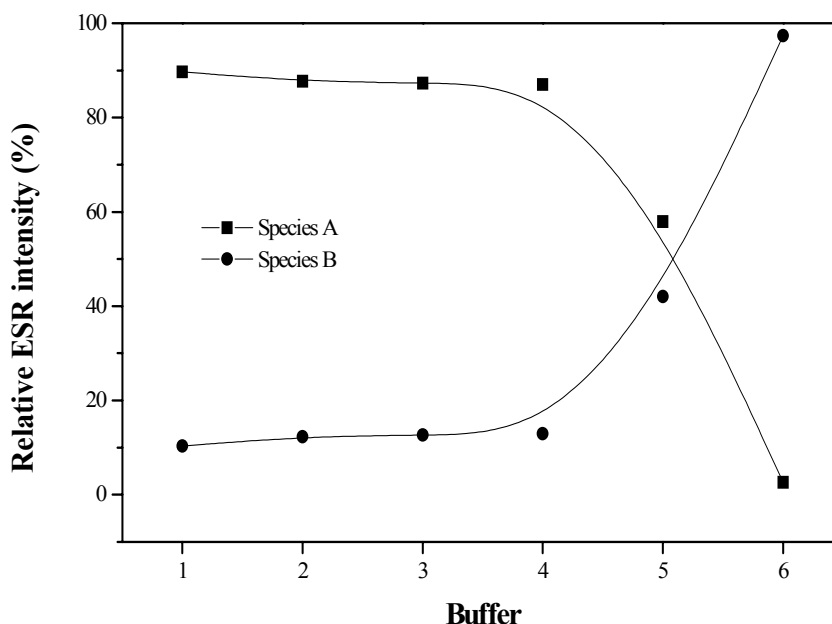
Figure 4.10. *EPR signal intensity (%) of species A and B in Mn-tmtacn-H_2O_2 in the presence of carboxylic acid buffers: 1 – acetate; 2 – citrate; 3 – ascorbate; 4 – tartrate; 5 – malonate; 6 – oxalate.*

It is interesting to note that Mn-tmtacn exhibits good activity even in the presence of a non-carboxylic acid ascorbate buffer. This suggests that ascorbate too can influence the redox behavior of Mn and form the active Mn species required for the benzylic oxidation. Based on the EPR and UV-vis studies two types of oxo-manganese complexes, (μ-oxo)(μ-carboxylato)-[Mn^{IV}-tmtacn]$_2$ (species A) and terminal-oxo-Mn^{IV}-tmtacn (species B) can be identified in the solutions after reactions with H_2O_2. Tentative structures of these oxo-manganese complexes are shown in Fig. 4.11. Although the teminal oxo-manganese complexes (species B) appeared to be the active species for benzylic oxidation, no linear correlation in catalytic activity with the concentration of A or B was noted. This suggests that other factors such as the structure of the buffer and its mode of coordination also play an important role in the activity of the oxo-manganese species.

4.3.4. Mechanism

Many studies have been done in order to elucidate the mechanism of hydrocarbon oxidation reactions [39-43]. Based on the conclusions drawn from the *in situ* spectroscopic studies that terminal oxo-Mn^{IV}-tmtacn is the active species in the
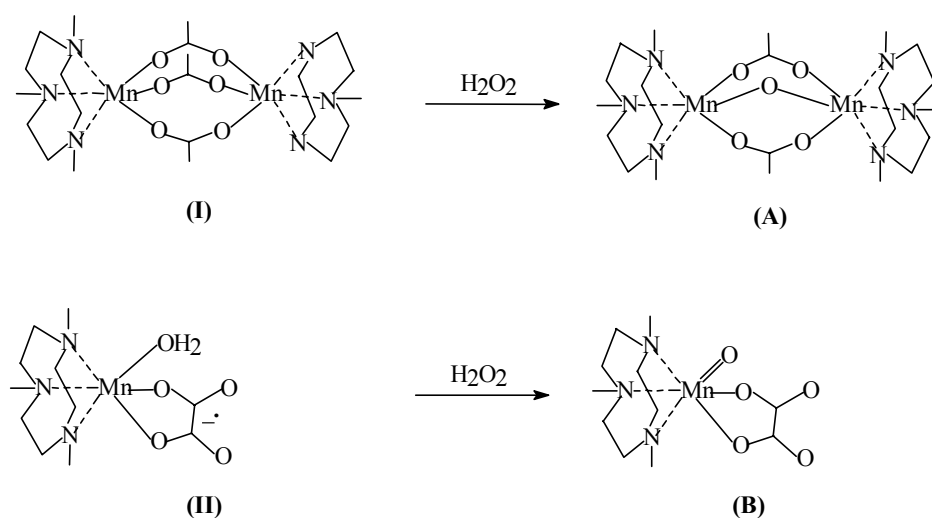
Figure 4.11. *Active Mn-tmtacn species in the presence of acetate and oxalate buffers.*

benzylic oxidation and epoxidation reactions, a plausible mechanism for the oxygen

transfer and insertion is given in the following sections. This mechanism is in analogy

with that proposed for Mn(III) porphyrin catalyzed oxidations [43].

4.3.4.1.Epoxidation

It is observed that epoxidation occurs with retention in the stereochemistry of

olefin. In a plausible mechanism oxygen atom transfer takes place *via* formation of a

metal-oxo-olefin intermediate (Scheme 4.3). Epoxidation of olefin takes place

stereoselectively without formation any carbon radical.
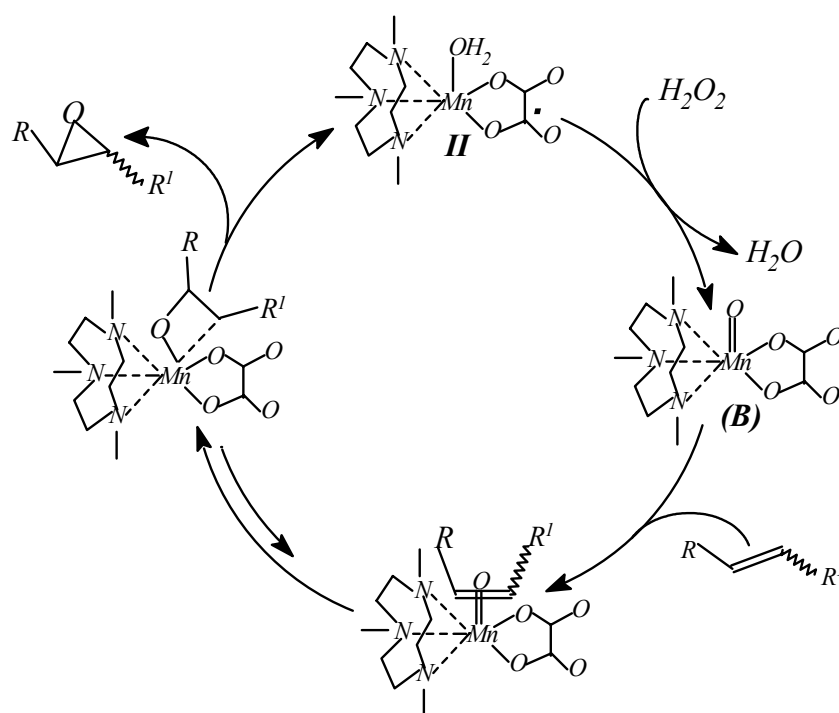
Scheme 4.3. *Proposed mechanism for epoxidation with Mn-tmtacn-oxalate-*
H_2O_2 system.

4.3.4.2.Benzylic Oxidation

The high valent oxo-Mn species have been invoked as intermediates in the

oxidations by Mn-porphyrins [44] and cytochrome P-450 and other biomimetic

analogous [6, 45]. Accordingly, the benzylic oxidation reaction can proceed in two pathways: (a) where the abstraction of hydrogen from benzylic carbon and its hydroxylation are concerted and (b) the formation of peroxide as intermediate product. The alcohol will be oxidized further to ketone (Scheme 4.4). Thus formation of all the products in the reaction can be explained.

Scheme 4.4. *Mechanism for benzylic C-H bond oxidation with Mn-tmtacn-oxalate-H_2O_2 system.*

4.4. CONCLUSIONS

The Mn-tmtacn complex exhibits superior activity for the epoxidation of terminal and non-terminal olefins. The activity of the Mn complex is enhanced in the presence of carboxylate buffers. Benzylic C-H bond of aromatics is selectively oxidized with the catalyst system under mild conditions. *In situ* spectroscopic studies reveal that

oxo-manganese complexes are the active species. The nature of the buffer and its mode of coordination have a definite role in the activity of the oxo-manganese complexes.

4.5. REFERENCES

1. Jerry Mrach, *Advanced Organic Chemistry: Reactions, Mechanisms and Structure,* 4th Edition, Wiley, New York, **1992.**

2. Shelodn, R.A.; Kochi, J.A. *Metal Catalyzed Oxidation of Organic Compounds*, Academic press, New York, **1981.**

3. Hage, R.; Iburg, J.E.; Kerschner, J.; Koek, J.H.; Lempers, E.L.M.; Martens, R.J.; Racherla, U.S.; Russell, S.W.; Swarthoff, T.; van Vliet, M.R.P.; Warnaar, J.B.; van der Wolf, L.; Krijnen, B. *Nature* **1994**, *369*, 637.

4. Larrow, J.F.; Jacobsen, E.N.; Gao, Y.; Hong, Y.; Nie, X.; Zepp, C.M. *J. Org. Chem.* **1994**, *59*, 1939.

5. Hosoya, N.; Hatayama, A.; Yanai, K.; Fujii, H.; Irie, R.; Katsuki, T. *Synlett* **1993**, 641.

6. Meunier, B. *Chem. Rev.* **1992**, *92*, 1411.

7. Sheldon, R.A. (Ed.) *Metalloporphyrins in Catalytic Oxidations,* Marcel Dekker, New York, **1994**.

8. Katsuki, T. *Coord. Chem. Rev.* **1995**, *140*, 189.

9. Groves, J.T.; Viski, P. *J. Org. Chem.* **1990**, *55*, 3628.

10. Smith, J.R.L; Shulpin, G.B. *Tet. Lett.* **1998**, *39*, 4909.

11. Shulpin, G.B.; S-F, Georg; Smith, J.R.L. *Tetrahedron* **1999**, *55*, 5345.

12. De Vos, D.E.; Bein, T. *Chem. Commun*. **1996**, 917.

13. Zondervan, C.; Hage, R.; Feringa, B. L. *Chem. Commun*. **1997,** 419.

14. Shul'pin, G.B.; Süss-Fink, G.; Shul'pina, L.S. *J. Mol. Catal. A: Chemical*, **2001**, *170*, 17.

15. De Vos, D.E.; Sels, B.F.; Reynaers, M.; Subba Rao, Y.V.; Jacobs, P.A. *Tet. Lett.* **1998**, *39*, 3221.

16. Berkessel, A.; Sklorz, C.A. *Tet. Lett.* **1999**, *40*, 7965.

17. Bolm, C.; Meyer, N.; Raabe, G.; Weyhermüller, T.; Bothe, E. *Chem. Comm.* **2000**, 2435.

18. Bolm, C.; Kadereit, D.; Valachhi, M. *Synlett* **1997**, 687.

19. Davies, S.G.; Polywka, M.E.C.; Thomas, S.E. *J. Chem. Soc. Perkin Trans. 1* **1986**, 1277.

20. Jaeqlym B.(Ed.) *Aldrich Library of ^{13}C and ^{1}H FT NMR Spectra* ED. 1 **1993**, *Vol.1,* 242B.

21. Shilov, A.E.; Shulpin, G.B. *Chem. Rev.* **1997**, *97*, 29.

22. Shulpin, G.B. *J. Mol. Catal. A: Chemical* **2002**, *189*, 39.

23. Sheldon, R.A.; van Santen. (Eds.), *Catalytic Oxidation-Principles and Applications*, World Scientific, Singapore **1995**.

24. Molander, G.A. *Chem. Rev.* **1992**, *92*, 2879.

25. Ho, T.L. *Synthesis* **1973**, 347.

26. Nair, V.; Mathew, J.; Prabhakaran, J. *Chem. Soc. Rev.* **1997**, 127.

27. Laali, K.K.; Herbert, M.; Cushnyr, B.; Bhat, A.; Terrano, D. *J. Chem. Soc. Perkin Trans*. 1, **2001**, 578.

28. Zang, R.; Yu, W-Y.; Lai, T-S.; Che, C-M. *Chem. Comm.* **1999**, 1791.

29. Choudary, B.M.; Durgaprasad, A.; Bhuma, V.; Swapna, V. *J. Org. Chem.* **1988**, *110*, 7398.

30. Groves, J.T.; Viski, P. *J. Am. Chem. Soc.* **1989**, *111*, 8537.

31. Groves, J.T.; Watanabe, Y. *Inorg. Chem.* **1986**, *25*, 4808.

32. Collins, T.J.; Powell, R.D. Slebodwick, C.; Uffelman, E.S. *J. Am. Chem. Soc.* **1990**, *112*, 897.

33. Wieghardt, K.; Bossek, K.U.; Nuber, B.; Weiss, J.; Bouvoisin, J.; Corbella, M.; Vitols, S.E.; Girerd, J.-J. *J. Am. Chem. Soc.* **1988**, *110*, 7398.

34. Bossek,] K.; Wieghardt, K.; Nuber, B.; Weiss, J. *Inorg. Chim. Acta* **1989**, *165*, 123.

35. Hartman, J.R.; Rardin, R.L.; Chaudhuri, P.; Pohl, K.; Wieghardt, K.; Nuber, B.; Papaefthymion, G.C.; Frankel, R.B.; Lippard, S.J. *J. Am. Chem. Soc.* **1987**, *109*, 7387.

36. Koek, J.H.; Russell, S.W.; van der Wolf, L.; Hage, R.; Warnaar, J.B.; Spek, A.L.; Kerschner, J.; DelPizzo, L. *J. Chem. Soc. Dalton Trans*. **1996**, 353.

37. Mehrotra, R.C.; Bohra, R. *Metal Carboxylates,* Academic Press, New York **1983**.

38. Meunier B. (Ed.), *Metal-oxo and Metal-peroxo Species in Catalytic Oxidations,* Springer-Verlag, Berlin, Structure and Bonding, *Vol. 97*, **2000**.

39. Arasasingham, R.D.; He, G-X.; Bruice, T.C. *J. Am. Chem. Soc.* **1993**, *115*, 7985.

40. Waldemar, A.; Cordula, M-K.; Chantu, R. S-M.; Herderich, M. *J. Am. Chem. Soc.* **2000**, *122*, 9685.

41. Namo, W.; Valentine, J.S. *J. Am. Chem. Soc.* **1993**, *115*, 1772.

42. Barton, D.H.R. *Tetrahedron* **1998**, *54*, 5805.

43. Collman, J.P.; Brauman, J.I.; Brnard, M.; Hayashi, T.; Kodadek, T.; Raybuck, S.C. *J. Am. Chem. Soc.* **1985**, *107*, 2000.

44. Barton, D.H.R.; Doller, D. *Acc. Chem. Res.* **1992**, *25*, 504.

45. Meunier, B.; Bernardou, J. *Topics in Catal.* **2002**, *21*, 47.

Chapter 5. **CARBON-CARBON BOND FORMING REACTIONS**
OVER PALLADIUM (II) CONTAINING HYDROTALCITES

_____

5.1. INTRODUCTION

Transition metal catalyzed carbon-carbon bond formation reactions are among the important reactions in synthetic organic chemistry [1]. Palladium catalyzed Heck reaction, Suzuki coupling and Sonogashira reaction are versatile methods practiced in various chemical syntheses in both academic research and chemical industry [2-5]. Generally, these reactions involve the use of homogeneous palladium catalysts containing *phosphine ligands* to couple (i) aryl or alkyl halides with vinyl functionality (Heck reaction), (ii) aryl halides with aryl boronic acids (Suzuki coupling) and (iii) aryl halides with acetylenes (Sonogashira reaction) [6]. Palladium phosphine complexes are notorious for air and moisture sensitivity, they deactivate fast and it is tedious and not economical to recover and recycle the catalyst. The increasing environmental and economic concerns have resulted in attempts to develop clean and high performance catalysts [7, 8]. Much attention has been paid to heterogeneous catalysts due to their easy recovery and recyclability [9,10]. Efforts have been done to support palladium on metal oxides, polymers, clays like montmorillonite (K-10), palladium grafted on MCM-41 and other supports [11-15]. Ni and Mn containing hydrotalcite catalysts have also been tried for the Heck reaction [16].

5.1.1. Heck Reaction

The palladium catalyzed Heck reaction of aryl halides and olefins is an important C-C bond forming reaction in organic synthesis (Scheme 5.1) [17]. The reaction is generally catalyzed by either Pd(0) or Pd(II) complexes in solution [6]. In order to facilitate the recovery of the precious metal catalyst, immobilization of

homogeneous catalysts has been the research goal for many years [18]. Thus, the use of supported metal catalysts has now become a viable alternative to the commonly used homogeneous catalysts [8-10]. Here we report the use of Pd-hydrotalcite as a new efficient catalyst for the Heck reaction.

$$Ar-X \; + \; =\!\!\!\!\diagdown^R \quad \xrightarrow[\text{Base}]{\text{Pd catalyst}} \quad Ar\diagup\!\!=\!\!\diagdown^R$$
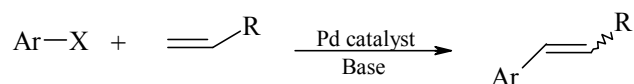
where Ar = Aryl, X = I, Br
$R = CO_2CH_3, C_6H_5$ etc.

Scheme 5.1

5.1.2. Suzuki Coupling

Suzuki coupling is a well-established method of coupling organoboran compounds with aryl or alkenyl halides in the presence of a palladium catalyst (Scheme 2) [19]. The reaction represents an alternative C-C coupling method over other methods using organomtallics because organoboranes are air and moisture stable with relatively low toxicity. Recently, many heterogeneous catalysts have been reported in the literature for Suzuki reaction [20, 21].

$$Ar-X \; + \; B(OH)_2\!-\!\!\bigcirc \quad \xrightarrow[\text{Base}]{\text{Pd catalyst}} \quad Ar\!-\!\!\bigcirc \; + \; BX(OH)_2$$
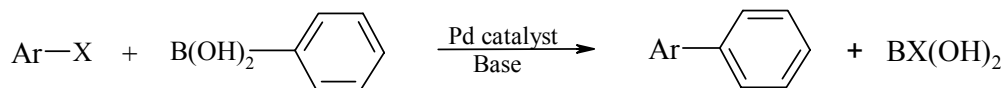
X= I, Br
R_1= OCH_3, CH_3, Cl, etc.

Scheme 5.2

5.1.3. Sonogashira Reaction

Sonogashira reaction is another interesting palladium catalyzed carbon-carbon bond formation reaction, which couples terminal acetylenes with aromatic halides

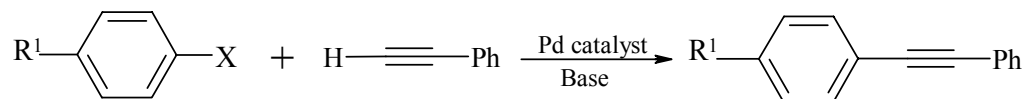(Scheme 3) [22]. Not many heterogeneous catalysts have been reported for this reaction [23, 24].

Scheme 5.3

5.1.4. Hydrotalcites as Catalysts

In the recent years, layered double hydroxides (LDH) or hydrotalcite like anionic clays have gained interest as catalysts in organic synthesis [25]. They have the general formula, $[M^{(II)}_{(1-x)} M^{(III)}_x (OH)_2]^{x+} [(A^{n-})_{x/n} yH_2O]^{x-}$, where $x = M^{(III)} / M^{(III)} + M^{(II)}$ (0.1 to 0.33) , $M^{(II)}$ = Mg, Cu, Ni, Co, and Mn, $M^{(III)}$ = Al, Fe, Cr, and Ga and A^{n-} is an interlayer anion such as CO_3^{2-}, NO_3^- and SO_4^{2-}. The layered structure is composed of positively charged single octahedral sheets called brucite layers separated by interlayer galleries containing organic or inorganic anions and water molecules. Positive charge is developed by occupancy of the nominally octahedral sites by metals of different charges. Various elements that are expected to act as active sites of catalysts can be introduced in the brucite layer [26]. Hydrotalcites containing metals like Ni, Cu, Pd etc., have already been reported in the literature [27, 28]. Narayanan et al. [29] studied the hydrogenation of phenol to cyclohexanone over Pd(II) containing Mg-Al hydrotalcites. Kaneda et al. [30] reported Ru-Co-Al-CO_3 HT for oxidation of alcohols. Choudhary et al. [31] found the application of Ni-Al hydrotalcite in the oxidation of alcohols using molecular oxygen. Velu et al. [32] incorporated zirconium ions into the layers of hydrotalcites and carried out the selective oxidation of phenol to catechol. In view of the growing interest to prepare new heterogeneous catalysts for

carbon-carbon bond forming reactions like Heck reaction, palladium-containing hydrotalcites have been synthesized, characterized and evaluated.

5.2. EXPERIMENTAL

5.2.1. Materials

Pd(CH$_3$COO)$_2$ was procured from Sigma-Aldrich Corporation, USA. Mg(NO$_3$)$_2$.6H$_2$O, Al(NO$_3$)$_3$.6H$_2$O and all other chemicals used for the catalyst preparation were obtained by Merck, India. All aryl iodides used in the reactions were prepared via diazotization of the corresponding amines (Sandmeyer reaction) [33]. Aryl bromides, aryl chlorides, methyl acrylate and styrene used as substrates in the reactions were obtained from Aldrich, USA. The solvents, acetonitrile, dimethyl formamide (DMF) and N-methylpyrrolidinone (NMP) (A.R. grade) obtained from s. d. fine Chem. India, were dried using standard procedures [34].

5.2.2. Preparation of Pd-containing hydrotalcites

In a modified procedure [35] for preparation of the catalyst Pd-HT(25) (Table 1), a solution of 20 mmol of Mg(NO$_3$)$_2$.6H$_2$O and 10 mmol of Al(NO$_3$)$_3$.6H$_2$O in 15 ml of demineralized (DM) water was added dropwise to a solution of 285 mmol of NaOH and 38 mmol of Na$_2$CO$_3$ in 60 ml of water over a period of 0.5 h with vigorous stirring. When the addition was half done, 1mmol of Pd(CH$_3$COO)$_2$ was added in one lot and the addition was continued. The solution was then heated at 50ºC for 18 h with stirring. Later the contents were cooled and filtered. The precipitate obtained was washed repeatedly with water till the filtrate was neutral to litmus and dried at 110ºC for 24 h. Other samples were prepared by varying the amount of Pd(CH$_3$COO)$_2$ added with respect to magnesium.

5.2.3. Characterization

Powder X-ray diffraction patterns of all the samples were recorded using a Rigaku (Model D-MAX II VC, Japan) X-ray diffractometer with Ni-filtered Cu-Kα radiation (λ = 1.540 Å). The atomic absorption spectroscopic (AAS) analyses of the samples were done on a Varian Spectra AA 220 instrument. UV-vis spectra of the reaction mixtures were recorded on a Shimadzu UV-2101 PC spectrophotometer in the region 200 – 900 nm. FT-IR spectra were recorded on a Shimadzu 8201 PC spectrophotometer in the region 400 – 4000 cm^{-1}. Thermal analyses of the samples were performed on an automatic derivatograp (Setaram TG/DTA-92). The surface areas of the samples were calculated from N_2 sorption isotherms using the BET procedure (NOVA, Model 1200). Scanning Electron Microscope (SEM) (Model JSM 5200, JEOL, JAPAN) equipped with Energy Dispersive X-ray analysis (EDX) was used to determine the crystallite size and morphology of the samples. X-ray photoelectron spectra were recorded on a VG Microtech Multilab Electron Spectroscopy for Chemical Analysis (ESCA) 3000 equipped with a twin anode of Al and Mg. The reactions were monitored by GC (HP-5880A; capillary column HP1, 50 m x 0.2 mm; FID detector). NMR spectra of the products were recorded at room temperature on a 200 MHz Bruker spectrometer.

The samples were dried at 110ºC for 12 h before their characterization by physicochemical methods. To obtain the chemical composition (Pd, Mg and Al) by AAS, weighed amounts of the samples (ca. 20 mg) were dissolved in a few drops of conc. HCl and diluted with DM water to 50 ml. The carbonate content was determined by elemental analysis. The surface areas of the samples were measured by N_2 adsorption (BET method) after activation at 200ºC.

149

5.2.4. Heck reaction

5.2.4.1. General Procedure for Heck reaction

A typical reaction was carried out by combining, under argon atmosphere, 3 mmol of iodobenzene, 3.9 mmol of methyl acrylate, 3.6 mmol of triethyl amine (1.2 equiv.) and Pd-HT (20 wt% with respect to iodobenzene) in dry DMF (8 ml). The stirred mixture was heated at 140°C. The reaction was monitored by GC/TLC. After the reaction was over it was quenched with 5 ml of water and the catalyst was filtered. Water (50 ml) was added to the filtrate and the product was extracted with ethyl acetate (50 ml x 2). The organic layer was given dil. HCl, water and brine wash and was dried over Na_2SO_4. The product **3a** (Table 5.4, Scheme 5.5) obtained after evaporation of the solvent was purified by column chromatography. Yield 0.399 g (82 %).

(3a) (E)- Methyl-3-phenyl propenoate (Table 5.4, Scheme 5.5)

^{1}H NMR (CDCl₃) δppm: 3.80 (s, 3H), 6.40 (d, 1H, J =16Hz), 7.37 (m, 3H), 7.50 (m, 2H), 7.65 (d, 1H, J =14Hz).

IR (Neat) cm⁻¹: 2923, 2854, 1724, 1637, 1450, 1313, 1169, 978, 767.

(3b) (E)-1,2-Diphenylethene

m.p.: 122°C

^{1}H NMR (CDCl₃) δppm: 7.16 (s, 2H), 7.41 (m, 6H), 7.55 (d, 4H, J = 6Hz).

IR (Neat) cm⁻¹: 834, 1598, 1492, 1440, 1368, 1069, 970, 762.

(3c) (E)-1-(4-Methyl phenyl)-2-phenylethene

m.p.: 118-19°C

^{1}H NMR (CDCl₃) δppm: 2.35 (s, 3H), 7.07 (s, 2H), 7.18-7.52 (m, 9H).

IR (Neat) cm⁻¹: 2924, 2854, 1599, 1508, 1448, 1377, 970, 806, 750, 690.

(3d) (E)-Methyl-3-(4-Methoxyphenyl)-propenoate

m.p.: 96°C

^{1}H NMR (CDCl$_3$) δppm: 3.81 (s, 3H), 3.85 (s, 3H), 6.29 (d, 1H, J = 8Hz), 6.90 (d, 2H, J = 8Hz), 7.47 (d, 2H, J = 8Hz), 7.63 (d, 1H, J = 8Hz).

IR (Neat) cm^{-1}: 2950, 1714, 1637, 1602, 1512, 1465, 1286, 1167, 1026, 983, 767.

(3e) (E)-Methyl-3-(4-chlorophenyl)-propenoate

m.p.: 84°C

^{1}H NMR (CDCl$_3$) δppm: 3.81 (s, 3H), 6.37 (d, 1H, J = 16Hz), 7.38-7.46 (m, 4H), 7.62 (d, 1H, J = 8Hz).

IR (Neat) cm^{-1}: 2923, 1705, 1633, 1591, 1488, 1433, 1315, 1193, 1080, 939, 732.

(3f) (E)-1-(4-Methoxyphenyl)-2-phenylethene

m.p.: 134°

^{1}H NMR (CDCl$_3$) δppm: 3.85 (s, 3H), 6.90 (d, 1H, J = 8Hz), 7.02 (d, 1H, J = 8Hz), 7.47-7.82 (m, ArH).

IR (Nujol) cm^{-1}: 2923, 2854, 1602, 1446, 1377, 1251, 1029, 968, 750, 814.

(3g) (E)-1-(4-Acetylphenyl)-2-phenylethene

m.p.: 136°C

^{1}H NMR (CDCl$_3$) δppm; 2.62 (s, 3H), 7.18 -7.62 (m,10H), 7.95 (d, 2H, J = 8Hz).

IR (Nujol) cm^{-1}: 2922, 2852, 1678, 1600, 1560, 1456, 1361, 1267, 966, 734, 690.

(3h) (E)-Methyl-3-(1-naphthyl)-propenoate

^{1}H NMR (CDCl$_3$) δppm: 3.85 (s, 3H), 6.49 (d, 1H, J = 16 Hz), 7.51 (m, 3H), 7.87 (m, 3H), 8.17 (d, 1H, J = 8Hz), 8.50 (d, 1H, J = 14Hz).

IR (Neat) cm^{-1}: 3058, 2949, 1716, 1635, 1575, 1510,1435, 1346, 1307, 1269, 1168, 1039, 978, 777.

5.2.4.2. Test for heterogeneity of reaction

The catalyst Pd-HT(25) (Table 5.1), iodobenzene and triethyl amine (except olefin) were mixed in dry DMF (6 ml) and heated at 140°C under argon atmosphere with constant stirring for 4 – 5 h. The catalyst was filtered off quickly under argon, methyl acrylate was added to the filtrate followed by 10% more of the triethyl amine base and the reaction was continued for another 4 h at 140°C. Analysis by GC did not reveal any product formation. This showed that the reaction did not proceed on the removal of the solid catalyst and the reaction was heterogeneous. However, the catalyst recovered after the reaction did reveal a small amount of Pd loss (< 10%). Apparently the Pd lost (or leached out from the catalyst) was not significantly responsible for the catalytic activity.

5.2.4. Suzuki Coupling

In a typical Suzuki coupling, iodobenzene (2 mmol), phenyl boronic acid (2.6 mmol, 1.3 equiv), K_2CO_3 (3.0 mmol) and Pd-HT(25) (20 wt% with respect to iodobenzene) were mixed in dry DMF (6 ml) solvent under argon atmosphere. The reaction mixture was heated at 140°C with efficient stirring.   The reaction was monitored by TLC. After the reaction was over, it was quenched with 5ml of water, the catalyst was filtered, 50ml of water was added to the filtrate and the product was extracted with ethyl acetate (50 ml x 2). The organic layer was given dil. HCl, water and brine wash and was dried   with Na_2SO_4. The product, biphenyl **6a** (Table 5.5, Scheme 5.66) obtained after evaporation of the solvent was purified by column chromatography. Yield 0.241 g (79%).

(6a) Biphenyl (Table 5.5, Scheme 5.6)

m.p.: 68 °C

^{1}H NMR (CDCl3) δppm: 7.47(m, 6H), 7.61 (d, 4H, J = 6Hz).

IR (Neat) cm^{-1}: 3060, 1638, 1456, 1210, 898, 698, 728.

(6b) 4-Methoxybiphenyl

m.p.: 86 °C

^{1}H NMR (CDCl$_3$) δppm: 7.47(m, 6H), 7.61 (d, 4H, J = 6Hz).

IR(Nujol)cm^{-1}: 2923, 2854, 1606, 1488, 1450, 1251, 1201, 1184, 1035, 835, 759, 688.

(6c) 4-Chlorobiphenyl

m.p.: 77 °C

^{1}H NMR (CDCl$_3$) δppm: 7.38-7.61(m, 9H).

IR (Neat) cm^{-1}: 2923, 1463, 1377, 1095, 831, 758, 694.

(6d) 4- Phenyltoluene

m.p.: 45°C

^{1}H NMR(CDCl$_3$) δppm: 2.39 (s, 3H), 7.22-7.59 (m, 9H).

IR (Nujol) cm^{-1}: 2923, 2852, 1490, 1448, 821, 756, 696.

(6e) 4-Acetylbiphenyl

m.p.: 116°C

 ^{1}H NMR (CDCl$_3$) δppm: 2.6 (s, 3H), 7.44 (m, 3H), 7.66 (m, 4H), 7.79(d, 2H, J = 8Hz).

IR (Nujol) cm^{-1}: 2938, 2874, 1720, 1598, 1377, 1260, 1192, 950, 762.

(6f) 1-Phenylnaphthtlene

^{1}H NMR (CDCl$_3$) δppm: 7.39-7.48 (m, 9H), 7.85 (m, 3H).

IR (Neat) cm^{-1}: 3057, 1591, 1496, 1492, 1446, 1394, 1029, 802, 779, 704, 569.

5.2.6. Sonogashira Reaction

In a general procedure, 3.0 mmol of iodobenzene, 3.0 mmol of phenyl acetylene, 3.6 mmol of K$_2$CO$_3$ and Pd-HT(25) (10 wt% with respect to iodobenzene) were mixed in dry DMF (6 ml) under argon atmosphere. The reaction mixture was heated at 140°C

with efficient stirring. The reaction was monitored by TLC and was over by 10 h. The reaction was quenched with 5 ml of water, the catalyst was filtered, 50ml of water was added to the filtrate and the product was extracted with ethyl acetate (50 ml x 2). The organic layer was given dil.HCl, water and brine wash and was dried with Na_2SO_4. The product diphenyl acetylene obtained after evaporation of the solvent was purified by column chromatography. Yield 0.4 g (79 %).

(9a) Diphenylacetylene (Table 5.6, Scheme 5.7)

Yield: 0.399 g (79 %)

m.p.: 57 °C

^{1}H NMR (CDCl$_3$) δppm: 7.3 (m, 6H), 7.5 (m, 4H).

IR (Neat) cm^{-1}: 3024, 2350, 1597, 1490, 1443, 1074, 1028, 760.

(9b) 1-(4-Methoxyphenyl)-2-phenylacetylene

Yiled: 0.49g (81 %)

^{1}H NMR (CDCl$_3$) δppm: 3.85 (s, 3H), 6.9 (d, 2H, J = 8.5Hz), 7.5-7.71 (m, 7H).

IR (Neat) cm^{-1}: 3057, 2108, 1597, 1487, 1443, 1242, 1028, 882.

Selected NMR spectra of the products obtained are shown in Section 5.6

5.3. RESULTS AND DISCUSSION

Various Pd-containing Mg-Al hydrotalctites were synthesized from soluble salts of the metals in the right atomic ratio by co-precipitation from a solution containing a slight excess of Na_2CO_3 at pH ~10 [35]. The different Mg/Al and Pd/Mg ratios selected were Mg/Al = 2-3 and Pd/Mg = 0.01- 0.05. The catalysts were designated according to the Pd/Mg and Mg/Al ratios used for the preparation. For e.g., Pd - hydrotalcite with Pd/Mg = 1/100 and Mg/Al = 2 is designated as Pd-HT(21).

5.3.1. Characterization

5.3.1.1. Chemical Composition

The chemical composition of the samples derived from elemental analysis (C and H) and AAS estimation (Pd, Mg and Al) are summarized in Table 5.1. The molar compositions of Pd are always less than expected. This may be due to the lower tendency of Pd to enter the brucite sheets. The water content was well within the expected values; the maximum number of water molecules in the interlayer per formula of hydrotalcite like anionic clay $[M^{(II)}_{(1-x)}, M^{(III)}_x (OH)_2]^{x+} [(A^{n-})_{x/n} .yH_2O]^{x-}$ would be y < 2-3x/2 [36]. When the catalyst recovered was estimated for palladium, the amount of palladium was found to have decreased only by about 10 %.

Table 5.1. Chemical compositions of various palladium containing hydrotalcites

Catalyst /[mol % of Pd used for incorporation][a]	Composition (atomic)[b] Pd : Mg : Al	Chemical Composition [d]
Pd-HT(20)/ [0]	0.00 : 100.00 : 41.20	$Pd_{0.0}Mg_{0.60}Al_{0.25}(OH)_{1.8}(CO_3)_{0.14}.0.3H_2O$
Pd-HT(21)/ [1]	0.68 : 100.00 : 40.85	$Pd_{0.004}Mg_{0.60}Al_{0.24}(OH)_{1.8}(CO_3)_{0.15}.0.1H_2O$
Pd-HT(22)/ [2]	1.52 : 100.00 : 40.67	$Pd_{0.009}Mg_{0.60}Al_{0.24}(OH)_{1.8}(CO_3)_{0.16}.0.4H_2O$
Pd-HT(23)/ [3]	2.76 : 100.00 : 39.31	$Pd_{0.016}Mg_{0.60}Al_{0.24}(OH)_{1.8}(CO_3)_{0.15}.0.4H_2O$
Pd-HT(24)/ [4]	3.35 : 100.00 : 41.02	$Pd_{0.02}Mg_{0.60}Al_{0.25}(OH)_{1.8}(CO_3)_{0.145}.0.2H_2O$
Pd-HT(25)/ [5]	4.13 : 100.00 : 39.80	$Pd_{0.025}Mg_{0.60}Al_{0.24}(OH)_{1.8}(CO_3)_{0.15}.0.4H_2O$
Pd-HT(26)/ [6]	4.20 : 100.00 : 41.33	$Pd_{0.025}Mg_{0.60}Al_{0.25}(OH)_{1.8}(CO_3)_{0.14}.0.4H_2O$
Pd-HT(35)/ [5] [c]	4.37 :100.00 : 27.72	$Pd_{0.026}Mg_{0.60}Al_{0.17}(OH)_{1.8}(CO_3)_{1.5}.0.5H_2O$

[a] Pd used in the preparation is given inside square brackets as mol % with respect to Mg. [b] As estimated by AAS; Mg/Al for all the samples $\cong 2.5$. [c] Mg/Al $\cong 3.6$. [d] Formula derived based on the C, H, N and AAS analysis.

5.3.1.2. X-Ray Diffractions and BET Surface Area

Powder XRD patterns of the various samples (Fig. 5.1A) (2θ range from 0° to 80°) showed sharp reflections for (003), (006), (110) and (113) planes, which are characteristic of a well crystallized HT phase [37]. This suggests that most of the Pd^{+2}
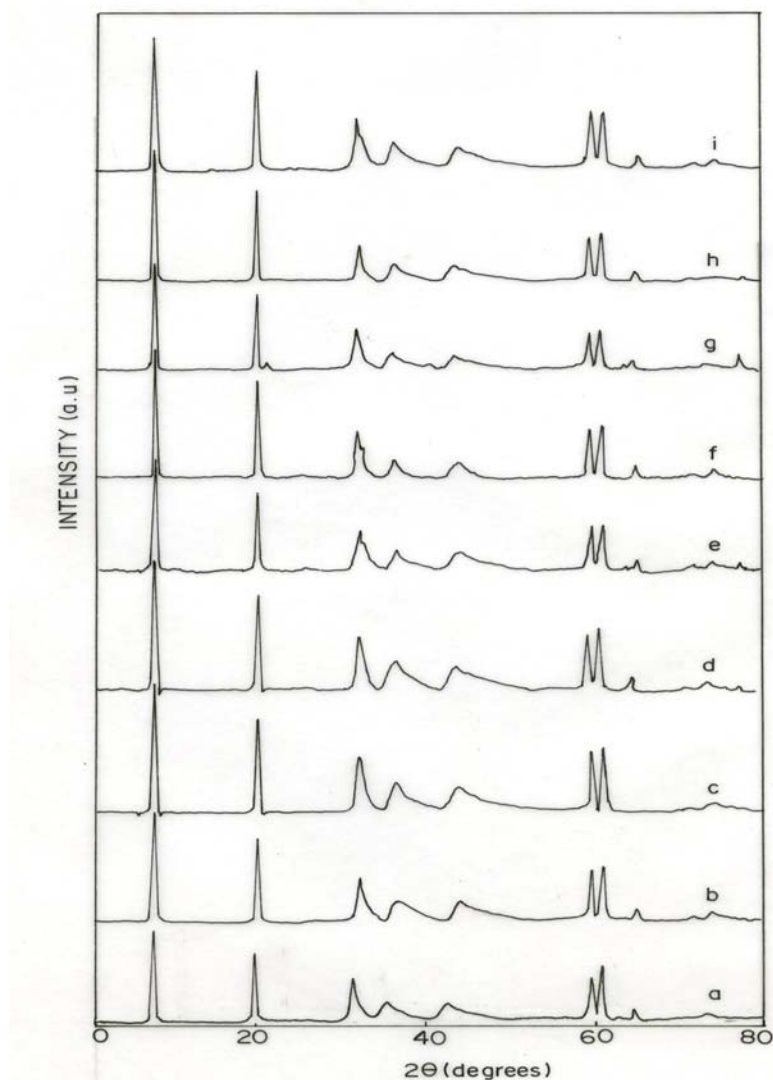
Figure 5.1A. *XRD patterns of hydrotalcite samples prepared (a) Pd-HT(20) (b) Pd-HT(21) (c) Pd-HT(22) (d) Pd-HT(23) (e) Pd-HT(24) (f) Pd-HT(25) (g) Pd-HT(30) (h) Pd-HT(35) (i) recovered Pd-HT(25) [Pd-HT(rec)].*

ions substitute Mg^{+2} in the brucite layer of the hydrotalcite, although palladium favours square planar coordination [38]. The lattice constants were determined by PDP 11-Package least-squares refinement programme, from the well defined position of the most intense peaks. Hydrotalcite belongs to a hexagonal crystal system and the lattice parameters *a* and *c* calculated are presented in Table 5.2. It is noticed that there is an overall increase in the values of both the parameter '*c*' and interlayer spacing d_{003} with increase in both the Pd/Mg and Mg/Al ratios [from Pd-HT(20) to Pd-HT(35), Table 5.2]. The increase in the value of '*a*' is less evident. The surface areas were determined after activating the catalyst at 200°C for 2 h. The change in the BET surface area with the change in chemical composition (Table 2) was too small to make any definite conclusion.

Table 5.2. Cell parameters and surface areas of various Pd-containing hydrotalcites.

Catalyst designation	*Pd/Mg[a]*	$x^b = \dfrac{Al^{(III)}}{Al^{(III)} + Mg^{(II)}}$	*Surface Area (m^2/gm)*	*d [A°]*	*Cell parameters*	
					a (A°)	*c (A°)*
Pd-HT(20)	0.000	0.29	22.3	7.53	3.0368	23.7673
Pd-HT(21)	0.068	0.29	20.0	7.54	3.0384	22.7612
Pd-HT(22)	0.152	0.29	20.0	7.62	3.0438	22.9502
Pd-HT(23)	0.276	0.29	23.0	7.62	3.0425	22.9014
Pd-HT(24)	0.335	0.29	19.0	7.64	3.0419	22.8101
Pd-HT(25)	0.413	0.29	15.8	7.75	3.0555	23.1984
Pd-HT(26)	0.420	0.29	15.0	7.74	3.0475	23.1844
Pd-HT(35)	0.437	0.21	24.0	7.65	3.0476	23.0595

[a] Atomic ratio. [b] As estimated by AAS.

It is observed that the XRD patterns of the catalyst recovered after the reaction [Pd-HT(rec)] was coincident (both in peak position and peak intensity) with the original catalyst (a = 3.05(A°) and c = 22.97(A°)) (Fig. 5.1B). This indicates that the layer structure of the catalyst remains intact even after the reaction.
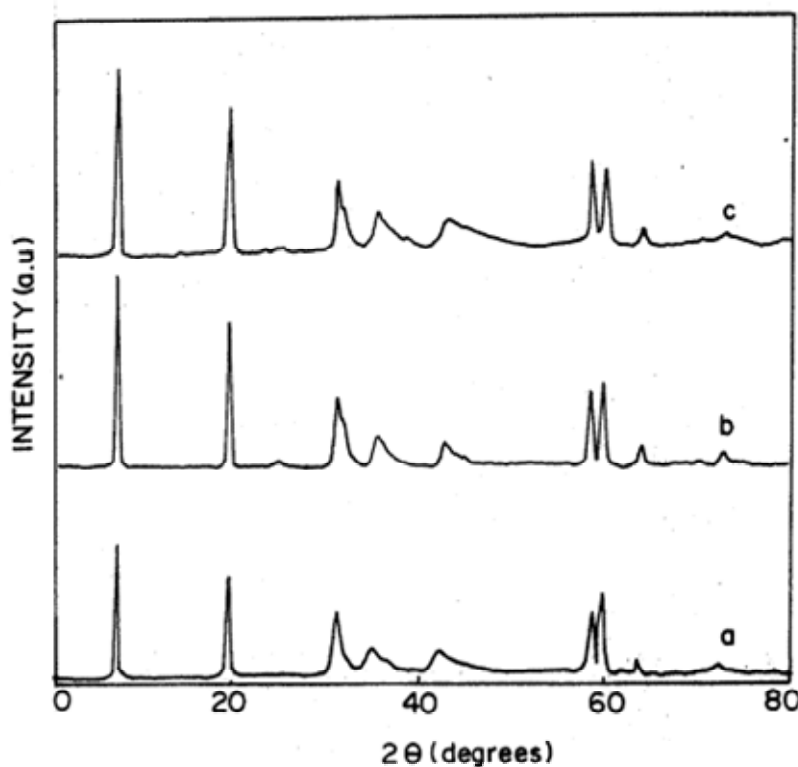

Figure 1B. *XRD patterns of hydrotalcites. (a) hydrotalcite [Pd-HT (20)]; (b) Pd-hydrotalcite [Pd-HT(25)]; (c) recovered Pd-HT(25) [Pd-HT(rec)].*

5.3.1.3. *UV-visible Spectroscopy*

Fig. 5.2 shows the UV-visible reflectance spectra of selected samples. Pd(II) in [Pd-HT(25)] shows a band in the region of 300 – 500 nm having different environment

of cations and anions in the brucite layer [26, 39, 40]. For the recovered sample [Pd-HT(rec)], the intensity of absorbance was less partly due to the small leaching of Pd^{+2} from the structure and mainly due to its partial reduction to Pd(0) (evident from XPS analysis) which is not observed in the spectrum.
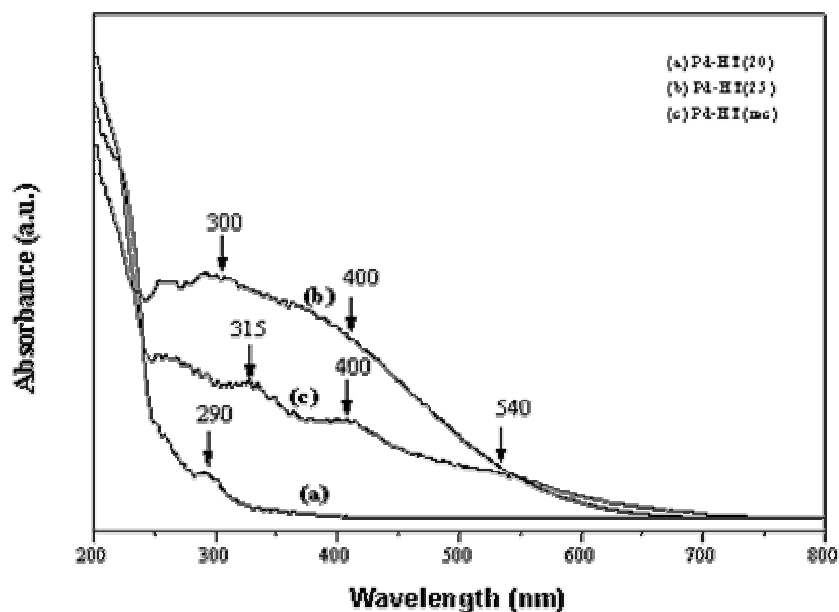
Figure 5.2. *UV-visible reflectance spectra of (a) Pd-HT(20), (b) Pd-HT(25) and (c) Pd-HT(rec).*

.

5.3.1.4. FT-IR Spectroscopy

The FT-IR spectra of selected samples are as shown in Fig. 5.3. The asymmetric intense peak at 3450 cm^{-1} is attributed to the OH stretching vibrations [41, 42]. The presence of the carbonate anion is inferred from the characteristic IR bands at 850, 1050, and 1372 cm^{-1} [25]. The weak band at around 1630 cm^{-1} is due to the bending vibration of adsorbed interlayer water [43]. The bands below *ca*. 800 cm^{-1} are due to metal-oxygen vibration modes.
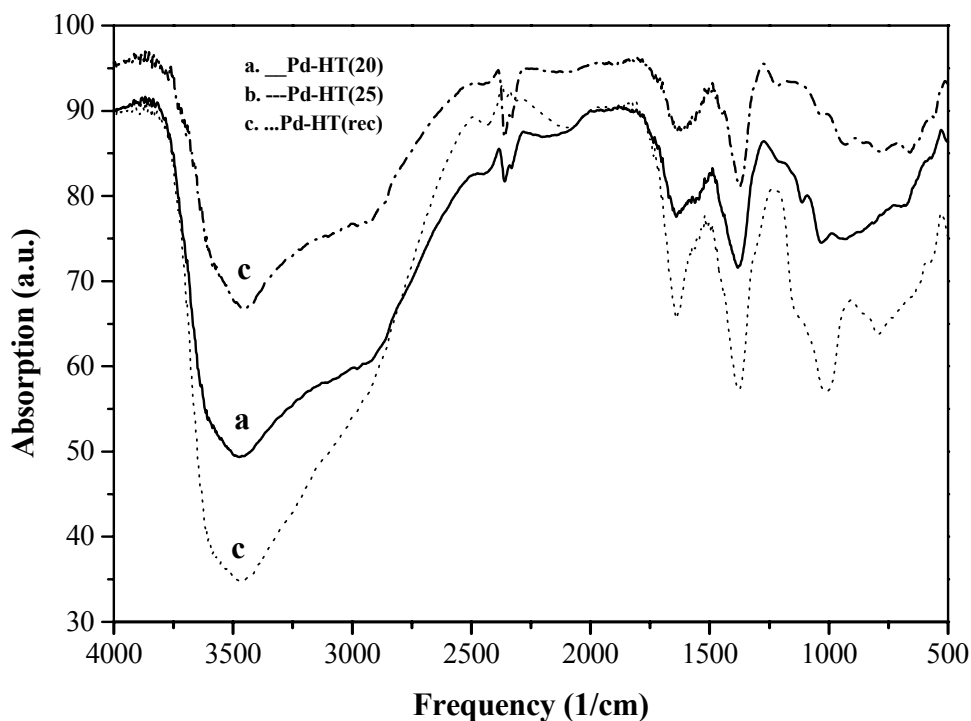
Figure 3. *FT-IR diffused reflectance spectra of (a) Pd-HT(20), (b) Pd-HT(25) and (c) Pd-HT(rec).*

5.3.1.5. Thermal and XPS Analyses

TG-DTA profiles of the selected samples between 20 and 1000°C in the presence of air are shown in Fig. 5.4. The sharpness of the peaks reflects the high degree of crystallanity. The weight loss is observed in two well-differentiated stages. An endothermic peak in the first stage (75 - 260°C) corresponds to the loss of water in the interlayer space. The broad peak in the second stage (300 – 480°C) is related to the weight loss due to dehydroxylation and decarbonylation processes.

X-ray photoelectron spectrum of Pd-HT(25) is as shown in Fig. 5.5. It is clear that all the palladium is present (presumably in the framework of the hydrotalcite) as
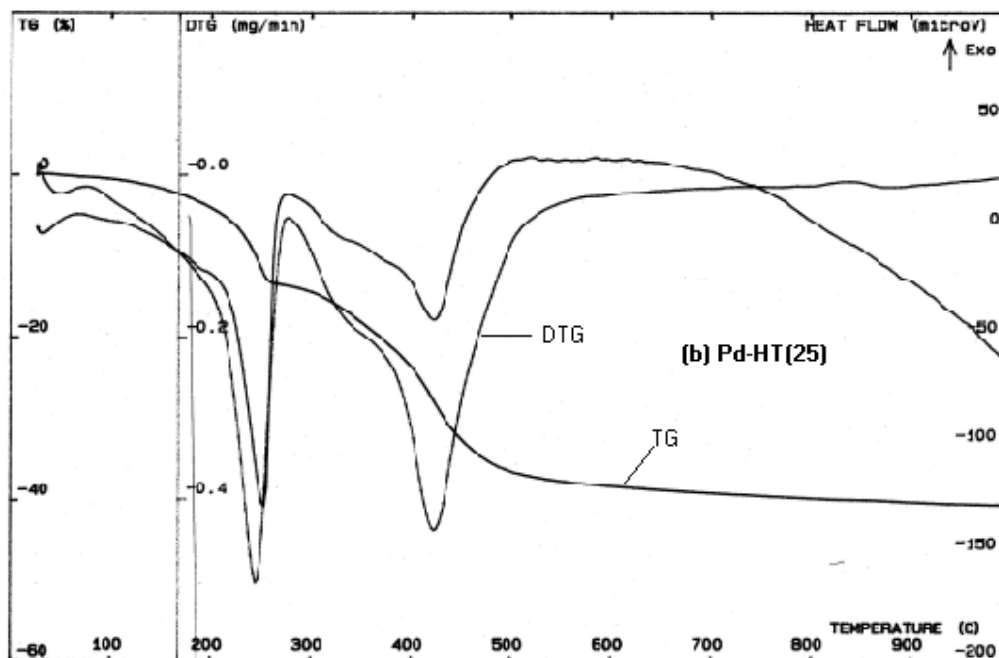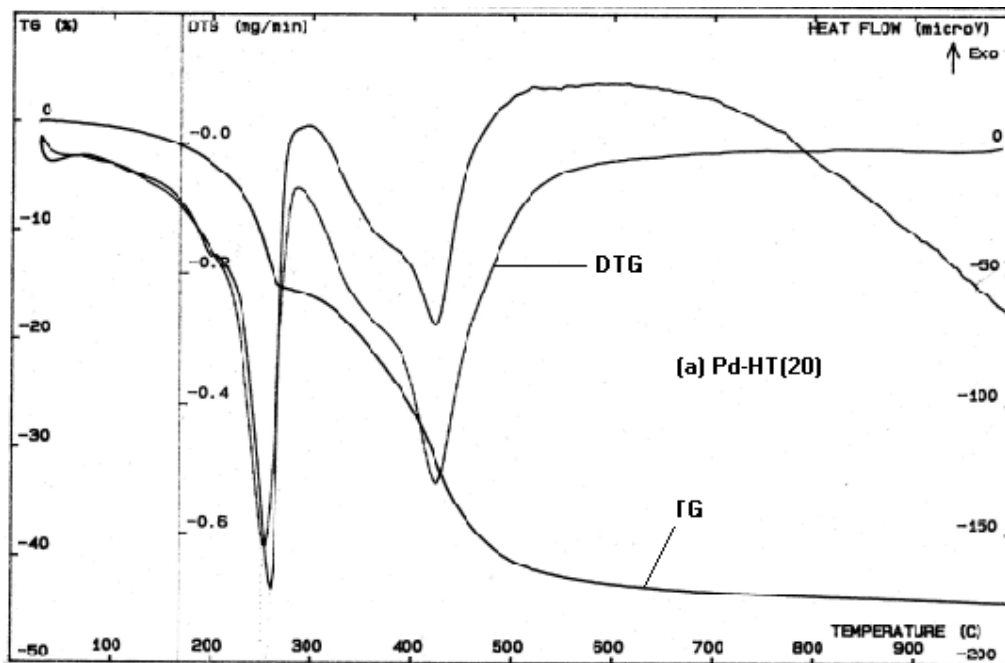
Figure 5.4. *TG-DTA plots of (a) Pd-HT(20); (b) Pd-HT(25).*

161

Pd(II). The binding energies for the 3d levels of Pd(II) are 336.4 eV(3d$_{5/2}$) and 341.7

eV(3d$_{3/2}$). These values are comparable with the observed binding energies for Pd(II)

salts (336.1 eV(3d$_{5/2}$) for PdO, 338.7 eV(3d$_{5/2}$) for Pd(OAc)$_2$ and 337.9 eV(3d$_{5/2}$) for

PdCl$_2$) [44]. Pd(0) palladium has a binding energy of 335.7 eV (3d$_{5/2}$). Two types of

the palladium species with a little difference in their binding energies were observed in

spent catalyst. One is the Pd(II) and the other is the newly formed Pd(0) with binding

energies 336.6 eV(3d$_{5/2}$) and 341.8 eV(3d$_{3/2}$)respectively. The reduction of about 50%

of the Pd(II) to Pd(0) was noticed from the XPS spectra of the recovered catalyst.


Figure 5. X-ray photoelectron spectrum (XPS) of palladium containing hydrotalcite [Pd-HT(25)].

5.3.1.6. SEM Studies

SEM structures of a fresh sample and a recovered after the reaction are presented in Figs. 5.6a and 5.6b respectively. It is seen that the fresh sample (Fig. 5.6a) is made up of crystals of hexagonal platelets of about 0.5 - 1 μm diameter. During the

162

reaction, the crystals break into finer particles (presumably due to the stirring) (Fig. 5.6b). The formation of smaller crystals may be responsible for the increase in surface area observed on usage.
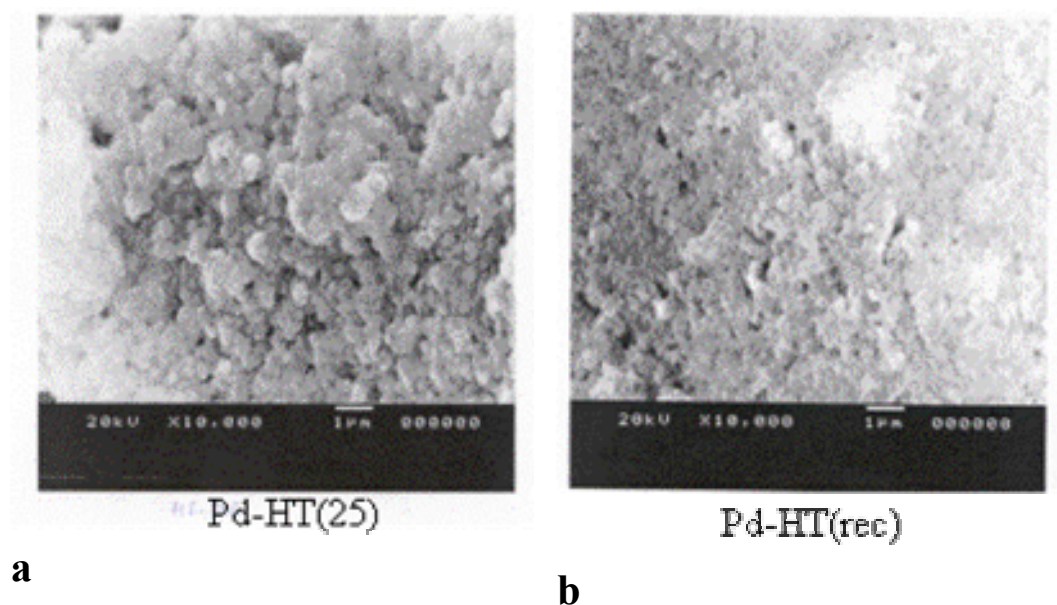
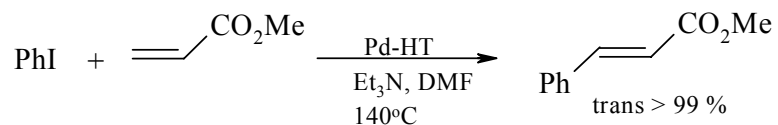*Figure 5.6.* *Scanning electron microscopy (SEM) of (a) Pd-HT(25) and (b)Pd-HT(rec) (Pd-HT(25) recovered after one reaction cycle).*

5.3.2. Pd-HT as Catalyst for C-C Bond Forming Reactions

5.3.2.1. Heck Reaction

Heck reaction of iodobenzene with methyl acrylate was carried out using various palladium containing hydrotalcites (Table 5.1) after activation at 120°C for 6 h (Scheme

Scheme 5.4

5.4). It was found that the yield of methyl cinnamate increased with Pd loading.

Catalysts with a Pd loading of ~ 4% with Mg/Al $\cong$ 2.5 appeared to be the most active

(Table 5.3). Pure HT without Pd did not produce methyl cinnamate even after 36 h.

When the reaction was carried out with 0.1 mol % of Pd(OAc)$_2$ as the catalyst, the

product yield was 14 %. Surprisingly, the Pd-HT sample prepared with Mg/Al $\cong$ 3.6

was not as active as the other Pd-HT samples, Mg/Al $\cong$ 2.5 and Pd $\cong$ 3-4% (compare

Pd-HT(35) with Pd-HT(24-25), Table 5.3). In toluene and acetonitrile solvents no

reaction was observed under reflux conditions. Also the catalysts were not active in

DMF at temperatures below 140°C. So all the reactions were carried out at 140°C. The

reaction was found to be heterogeneous in nature [45].

Table 5.3. Heck reaction of iodobenzene with methyl acrylate over Pd-HT.

Catalyst /[mol % of Pd used for incorporation][a]	*Time* *(h)*	*Conv.*[b] *%*	*% Yield of methyl cinnamate (Isolated)*
Pd-HT(21)/ [1]	36	23	10
Pd-HT(22) / [2]	36	19	10
Pd-HT(23) / [3]	24	34	16
Pd-HT(24) / [4]	8	98	71
Pd-HT(25) / [5]	4	100	82
Pd-HT(26) / [6]	4	100	84
Pd-HT(35) / [5]	24	29	20

[a] Pd mol % with respect to Mg. [b] Conversion of Iodobenzene

Results of the Heck reaction between various aryl halides and olefins (Scheme

5.5) are presented in Table 5.4. It is obvious from the results that good yields of the

products could be obtained with all the aryl iodides with even 10% w/w of the catalyst.

164

The highest turn over number (TON) achieved was around 1000. Under similar experimental conditions, aryl bromides did not appear to be much reactive. Hence, the reaction conditions were modified; NMP (N-methyl pyrrolidinone) was used as the solvent, K_2CO_3 as the base, and the temperature was raised to 150°C.

$$Ar\!-\!X \;+\; =\!\!\!/^{R} \quad \xrightarrow[\text{Base}]{\text{Pd-HT(25)}} \quad Ar\diagup\!\!=\!\!\diagup^{R}$$

trans > 99 %

1   **2**

where Ar = Aryl, X = I, Br
R = CO_2CH_3, C_6H_5 etc.

3a. Ar = C_6H_5, R = CO_2CH_3
3b. Ar = C_6H_5, R = C_6H_5
3c. Ar = C_6H_5, R = p-$CH_3C_6H_4$
3d. Ar = p-$CH_3OC_6H_4$, R = CO_2CH_3
3e. Ar = p-ClC_6H_4, R = CO_2CH_3
3f. Ar = $CH_3OC_6H_4$, R = C_6H_5
3g. Ar = $CH_3COC_6H_4$, R = C_6H_5
3h. Ar = C_8H_{17}, R = CO_2CH_3
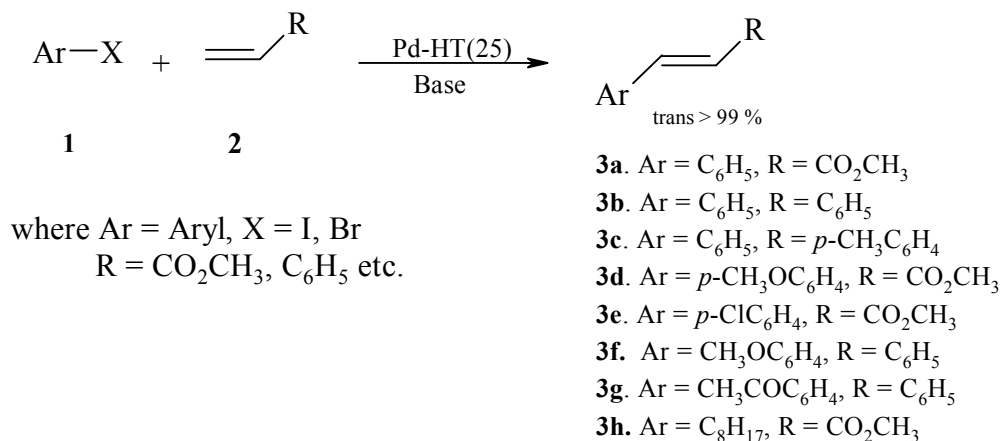
Scheme 5.5

Stilbene was isolated in good yield, under these conditions, from the reaction of bromobenzene and styrene (TON = 492). The reaction of 1-bromonaphthalene with methyl acrylate gave 45% yield of the product (Table 5.4). The catalyst, however, was not effective with the less reactive aryl chlorides. Chlorobenzene failed to react with methyl acrylate. Activated aryl chlorides like p-nitrochlorobenzene also gave low yields. Addition of NaI/CuI did not bring about any improvement. Intramolecular Heck reaction of 2-iodophenylallyl ether did not give any product.

The catalyst could be recycled after the activation at 100°C, though some loss was noticed in the yield of methyl cinnamate from the reaction between iodobenzene and methyl acrylate (Table 5.4). Interestingly, the reaction was faster over the recycled catalyst than over the fresh one, which could be attributed to the increase in surface area (65 m^2/g) of the catalyst.

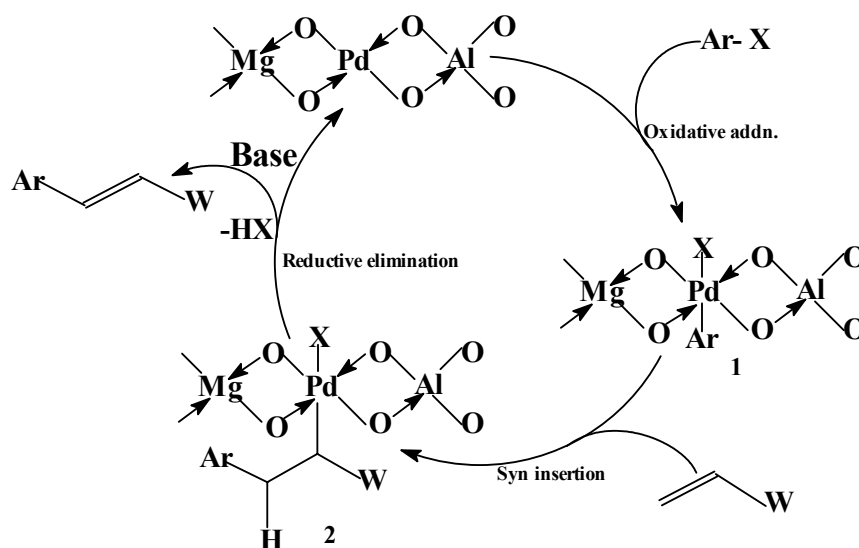**Table 5.4.** Heck reaction over heterogeneous catalyst: Pd- HT (25).

Ar	X	R	Amount of catalyst % w/w	Product Isolated[b]	Time (h)	Yield %	TON [c]
C_6H_5	I	CO_2CH_3	10	3a	8	82	928
C_6H_5	I	CO_2CH_3	10 [a]	3a	5	69	781
C_6H_5	I	C_6H_5	10	3b	8	87	985
C_6H_5	I	$p\text{-}CH_3C_6H_4$	10	3c	20	59	668
$p\text{-}CH_3OC_6H_4$	I	CO_2CH_3	10	3d	7	87	863
$p\text{-}ClC_6H_4$	I	CO_2CH_3	10	3e	7	88	852
C_6H_5	Br	CO_2CH_3	20	3a	20	35 [d]	257
C_6H_5	Br	C_6H_5	20	3b	12	67 [d]	492
$p\text{-}CH_3OC_6H_4$	Br	C_6H_5	20	3f	12	67 [d]	492
$p\text{-}CH_3COC_6H_4$	Br	C_6H_5	20	3g	12	48 [d]	277
C_8H_7	Br	CO_2CH_3	20	3h	12	45 [d]	259

[a] With the recovered catalyst (first recycle); surface area $65m^2/gm$. [b] All products gave satisfactory IR and NMR spectra. [c] Turn over numbers were calculated on the basis of amount of Pd estimated by AAS (TON = mol of product x mol^{-1} of catalyst-Pd). [d] N-Methyl pyrrolidinone solvent; K_2CO_3 base;150°C.

Though the Heck reaction is well known, it is still unclear whether the catalytic cycle involves Pd(0)/Pd(II) redox couple or Pd(II)/Pd(IV) [46]. Also, there are contradictory views concerning the mechanism and structure-activity relationships in heterogeneous catalysts. Based on some models like hydrogenation a surface mechanism is suggested (Scheme 5.6). However, the idea of soluble Pd species (release and recapture mechanism) cannot also be denied. A reasonable mechanism for the
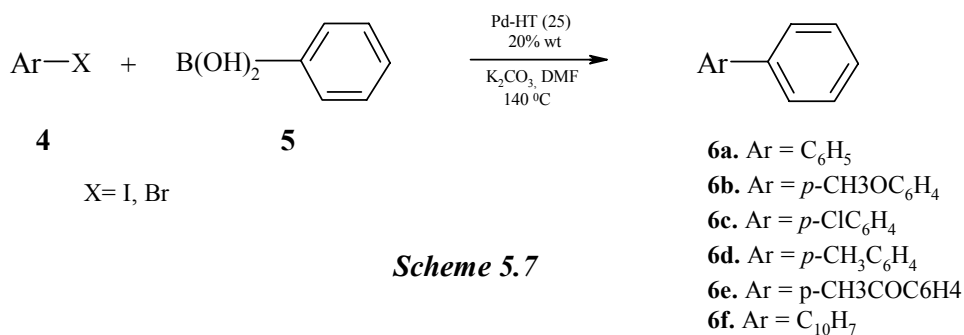
reaction involving Pd(II)/Pd(IV) can be suggested to be as follows: The $d_{(003)}$ basal spacing (7.78 Å) acts as a nano reactor.   Aryl halide is added oxidatively to Pd(II) present in the brucite layer to give Pd(IV) complex **1**. The *syn* insertion of the olefin to C-Pd bond results in the formation of σ- alkanyl-Pd complex **2**. The catalyst is regenerated after the reductive elimination of HX in the presence of a base giving the *trans* product. Thus palladium will be intact in the brucite structure. Oxidative addition of haloarenes can be taken as the rate determining step. The formation of Pd^0, observed by XPS analysis, in the recovered catalyst can be accounted for the partial structural damage at the reaction temperatures followed by *in situ* reduction of Pd(II) in the reaction medium.

Scheme 5.6.   *Proposed mechanism for Heck reaction over Pd-HT (O should be considered as hydroxy group).*

5.3.2.2. Suzuki Coupling

Palladium containing hydrotalcites could be good heterogeneous catalysts for Suzuki reaction (Scheme 5.7) giving high yields of products. The results of the reaction performed with Pd-HT(25) are presented in Table 5.5.

Ar—X   +   B(OH)$_2$—⟨benzene ring⟩ $\xrightarrow[\substack{K_2CO_3, DMF \\ 140\ ^0C}]{\substack{Pd-HT\ (25) \\ 20\%\ wt}}$ Ar—⟨benzene ring⟩

4   **5**

X= I, Br

Scheme 5.7

6a. Ar = C$_6$H$_5$
6b. Ar = *p*-CH3OC$_6$H$_4$
6c. Ar = *p*-ClC$_6$H$_4$
6d. Ar = *p*-CH$_3$C$_6$H$_4$
6e. Ar = p-CH3COC6H4
6f. Ar = C$_{10}$H$_7$

Table 5.5. Suzuki coupling of various aryl halides over Pd-HT(25) catalyst.

Aryl halide		Time (h)	Product	Yield	TON^a
Ar	X		(Isolated)	(%)	
C$_6$H$_6$	I	8	6a	79	447
p-CH$_3$O C$_6$H$_6$	I	6	6b	98	554
p-ClC$_6$H$_6$	I	12	6c	79	447
C$_6$H$_6$	Br	18	6a	66	373
p-CH$_3$ C$_6$H$_6$	Br	17	6d	58	328
p-CH$_3$CO C$_6$H$_6$	Br	14	6e	89	503
C$_{10}$H$_7$	Br	14	6f	85	481
C$_6$H$_6$	Cl	16	6a	23	130

^{a} TON = mol of product x mol^{-1} of Pd (estimated by AAS).

.

Here also, yields obtained with aryl iodides are excellent. But aryl bromides did not give high yields and the reaction with aryl chlorides was very slow.   Turnover numbers achieved (~500) was not as high as those obtained in the Heck reaction.

Though the rate determining step is the oxidative addition of aryl halides it involves another important transmetallation step.   The transmetallation between organopalladium(**II**) halides and organoboron compounds does not occur readily due to the low nucleophilicity of the organic group on boron atom. So, it is necessary to have a base, which increases the nucleophilicity of the boron [47]. The plausible mechanism for the reaction is shown in Scheme 5.7.
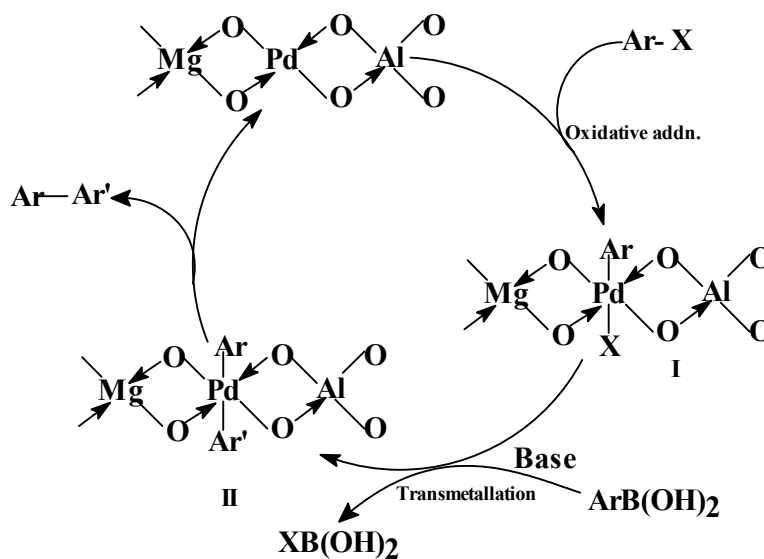
Scheme 5.8. *Proposed mechanism for Suzuki coupling over Pd-HT (O should be considered as hydroxy group).*

5.3.2.3. Sonogashira Reaction

Pd-hydrotacite could be a very good heterogeneous catalyst for the reaction providing good yields of products (Scheme 5.9; Table 5.6). However, the reaction is slow. The highest turn over numbers achieved is 900 in 10-12 h.
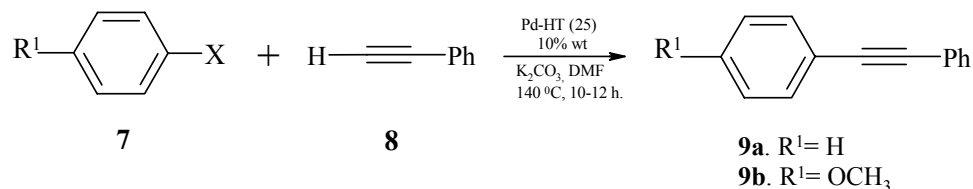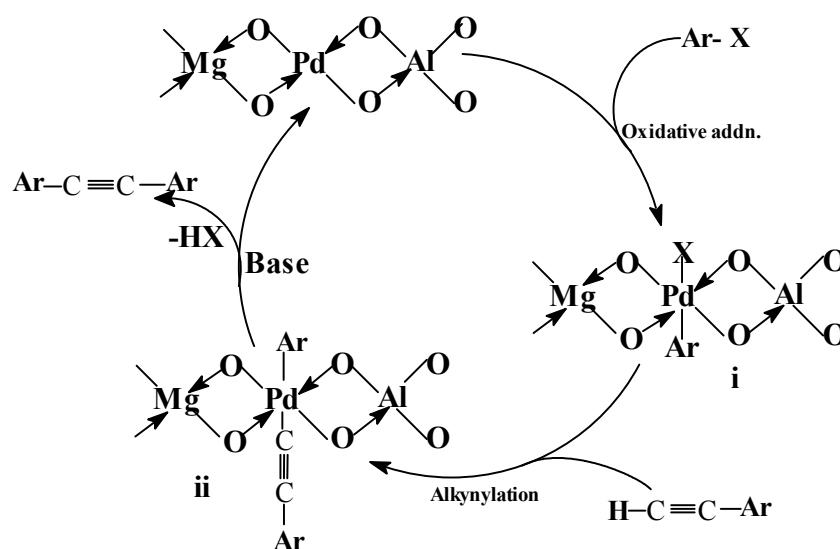

Scheme 5.9

The mechanism of the Sonogashira reaction can be anticipated very much similar to Suzuki coupling. The oxidative addition of aryl halide will be followed by an alkynylation, to give an aryl-alkynyl derivative of palladium (**ii**), which easily

regenerates the original palladium through the reductive elimination of the substitution

products (Scheme 5.10).

Table 5.6. Sonogashira coupling of various aryl halides over Pd-HT(25) catalyst.

Aryl halide		Time (h)	Product	Yield	TON^a
Ar	X		(Isolated)	(%)	
C_6H_6	I	12	9a	76	447
p-CH$_3$O C$_6$H$_6$	I	10	9b	81	554

^{a} TON = mol of product x mol^{-1} of Pd (estimated by AAS).

Scheme 5.10. *Proposed mechanism for Sonogashira reaction over Pd-HT (O should be considered as hydroxy group).*

5.4.   CONCLUSIONS

In conclusion, palladium containing hydrotalcites with various Pd/Mg and

Mg/Al ratio were prepared by a co-precipitation method and characterized by many

physicochemical techniques. X- ray powder diffraction patterns showed in all cases the

presence of a well crystallized HT phase which suggested that most of the Pd(II) was

aggregated into the brucite sheets of the hydrotalcite. Thus the palladium was anchored instead of being supported onto the surface. The versatility and efficiency of the Pd-hydrotalcite catalyst for carbon-carbon bond formation reaction is thus demonstrated. This *phosphine free* heterogeneous catalyst can be more advantageous to use than the other reported Pd-based catalysts for the reaction due to ease of separation and reuse besides good yields of the products. The recoverability of the catalyst with efficient recyclability coupled with high turn over numbers makes it a good candidate for C-C bond formation reactions.

5.5.   REFERENCES

1.   J. Tsuji, *Palladium Reagents and Catalysts: Innovations in Organic Synthesis,* Wiely, Chichister, **1995**.

2.   Stinson, S.C. *Chem. Engg. News* **1999**, 81.

3.   Ennis, D.S.; McManus, J; Wood-Kaczmar, W.; Richardson, J.; Smith, G.E.; Carstairs, A. *Org. Process Res. Dev.* **1999**, *3,* 248.

4.   Raggon, J.W.; Snyder, W.M. *Org. Process Res. Dev.* **2002**, *6,* 67.

5.   Baumeister, P.; Meyer, W.; Örtle, K.; Seifert, G.; Siegrist, H.; Steiner, H. *Chimia* **1997**, *51,* 144.

6.   Cornils, B.; Hermann, W.A. Applied *Homogeneous Catalysis with Organometallic Compounds,* VCH. Wienheim, **1996**.

7.   Beletskaya, I.P.; Cheperkov, A. V. *Chem. Rev.* **2000**, *100,* 3009.

8.   Biffis, A.; Zecca, M.; Basato, M. *J. Mol. Cat. A: Chemical* **2001,** *173,* 249.

9.   BlaserB, H.-U.; Indolese, A.; Schnyder, A.; Stiener, H.; Studer, M. *J. Mol. Cat. A: Chemical* **2001,** *173,* 3.

10. Bhange, B.M.; Arai, M. *Catal. Rev.* **2001**, *43*, 315.

11. Wagner, M.; Köhler, K.; Djakovitch, L.; Weinkauf, S.; Hagen, V.; Muhler, M. *Topics in Catal.* **2000**, *13*, 319.

12. Anderson, C. M.; Korebelas, K.; Awasti, A. K. *J. Org. Chem.* **1985**, *50*, 3891.

13. Ramachandani, R.K.; Uphade, B. S.; Vinod, M. P.; Wakharkar, R. D.; Choudhary, V. R.; Sudalai, A. *Chem. Comm.* **1997,** 2071.

14. Mehnert, C.P.; Ying, J. Y. *Chem. Comm.* **1997**, 2215.

15. Mubofu, E.B; Clark, J.H.; Macquarrie, D.J. *Green Chem.* **2001**, 3 23.

16. Ramani, A.; Yuvaraj, S.; Chanda, B.M.; Sivasanker, S. Unpublished results.

17. Heck, R. F. *Palladium Reagents in Organic Synthesis*, Academic Press, London, **1985**

18. Julia, M.; Duteil, M.; Grad, C.; Kuntz, E. *Bull. Soc. Chim. Fr.* **1973,** 2791.

19. Miyaura, N.; Suzuki, A. *Chem. Rev.* **1995**, *95*,2457.

20. LeBlond, C.R.; Andrews, A.T.; sun, Y.; Sowa, J.R. Jr. *Org. Lett.* **2001**, *3*, 1555.

21. Kabalka, G.W.; Namboodiri, V.; Wang, L. *Chem. Comm.* **2001,** 775.

22. Sonogashira, K. In *Compr. Org. Synth.* Trost, B.M; Fleming, I. Eds: Pergmon Press New Yark, **1991,** *Vol. 3,* 521.

23. Kabalka, G.W.; Wang, L.; Namboodiri, V.; Pagni, R.M. *Tetrahedron Lett*. . **2000**, *41*, 5151.

24. Quignard, F.; Larbot, S.; Goutodier, S.; Choplin, A. *J. Chem. Soc., Dalton Trans.* **2002**, 1147.

25. Cavani, F.; Trifiro, F.; Vaccari, A. *Catal. Today* **1991**, *11*, 173.

26. Basile, F.; Fernasar, G.; Gazzane, M.; Vaccari, A. *Appl. Clay Sci.* **2000**, *16*, 185

27. Labajos, F. M.; Rives, V.; Malet, P.; Centeno, M.A.; Ulibarri, M.A. *Inorg. Chem.* **1996**, *35*, 1154.

28. Trifiro, F.; Vaccari, A. in Atwood, J.L; Macwicol, D.D.; Davies, J.E.D.; Vogtles, F. (Eds.), *Comprehensive Supramolecular Chemistry* chapt. 7 V*ol.7* Pergmon press Oxford, **1995.**

29. Narayanan, S.; Krishna, K. *Chem. Comm.* **1997**, 1991.

30. Kaneda, K.; Yamashita, T.; Matsushita, T.; Ebitani, K. *J. Org. Chem.* **1998**, *63*, 1750.

31. Choudhary, B. M.; Kantam, M. L.; Rahman, A.; Reddy, Ch. V.; Rao, K. K. *Angew. Chem. Int. Ed. Engl.* **2001**, *40*, 763.

32. Velu, S.; Veda, R.; Ramani, A.; Chanda, B.M.; Sivasanker, S. *Chem. Comm.* **1997**, 2107.

33   Lucas, H.J.; Kennedy, E.R. In *Org. Synth. Coll. Vol.2* Blatt, A.H. (Ed.) John Wiley and Sons, Inc. New Yark, **1943**, 351.

34. Perrin, D.D.; Armarego, W.L.F.; Perrin, D.R. *Purification of Laboratory Chemicals,* Pergamon Press 2nd Edn. Oxford, **1980**.

35. Narayanan, S.; Krishna, K. *Appl. Catal. A: General* **1996**, *147*, L253.

36. Miyata, S. *Clays Clay Miner*. **1993**, *41*, 551.

37. Das, N.N.; Srivastava, S.C. *Bull. Mater. Sci.* **2002**, *25*, 283.

38. Greenwood, N.N.; Earnshow, A. *Chemistry of Elements*, Pergmon Press Oxford, **1989**, 125.

39. Rasmussen, L.; Jorgenson, C.K. *Acta. Chim. Scand.* **1968**, *22*, 879.

40. Lopez, T.; Villa, M.; Gomez, R. *J. Phys. Chem.* **1991**, *95*, 1691.

41. Rhodes, C.N.; Franks, M.; Parkes, G.M.B.; Brown, D.R. *J. Chem. Soc. Chem. Commun.* **1991**, 804.

42. Miyata, S. *Clays Clay Miner.* **1975**, *23*, 369.

43. Rhodes, C.N.; Brown, D.R. *Catal. Lett.* **1997**, *45*, 35.

44. Kumar, G.; Blackburn, J.R.; Albridge, R.G.; Moddeman, W.E.; Jones, M.M. *Inorg. Chem.* **1972**, *11*, 296.

45. Mehnert, C. P.; Weaver, D. W.; Ying, J. Y. *J. Am. Chem. Soc.* **1998**, *120*, 12289.

46. Catellani, M.; Fagnola, M.C.; *Angew. Chem. Int. Edn. Engl.* **1994,** *33*, 2421 and references cited there in.

47. Pelter, A.; Smith, K.; Brown, H. C. *Borane Reagents;* Academic: New York, **1988.**

5.6.   SPECTRA

173
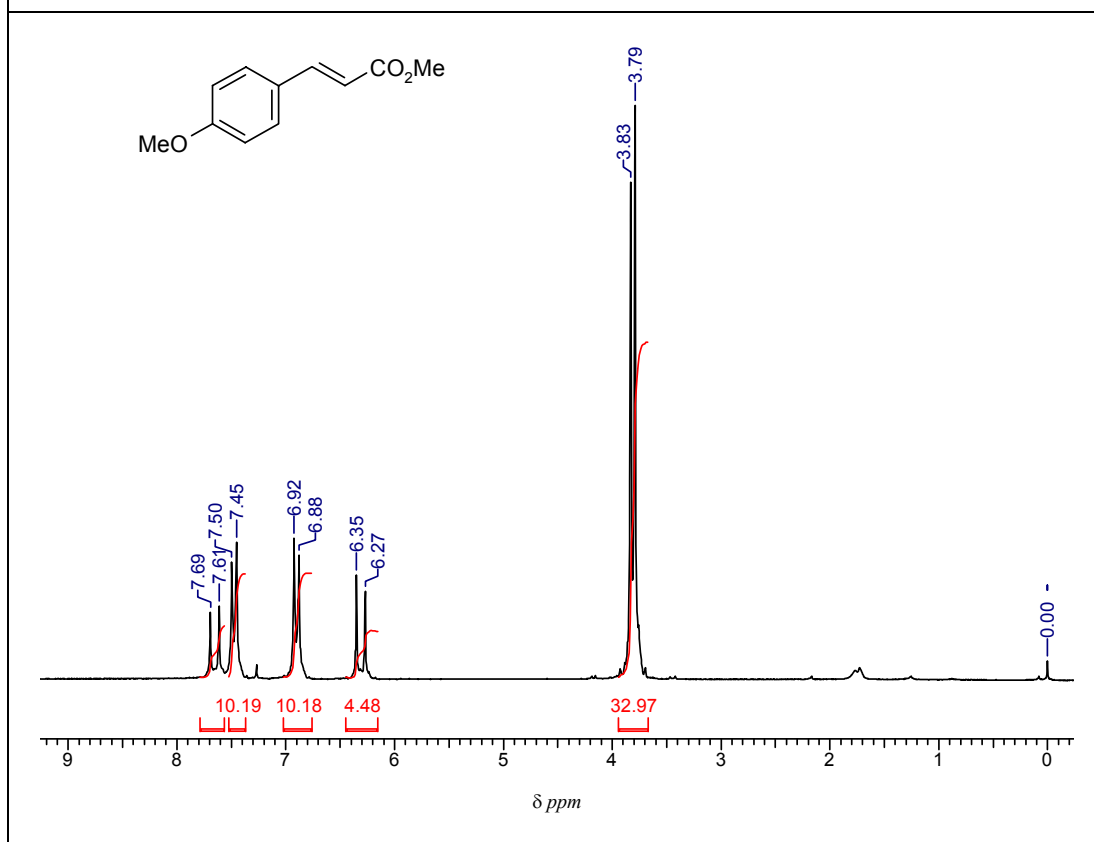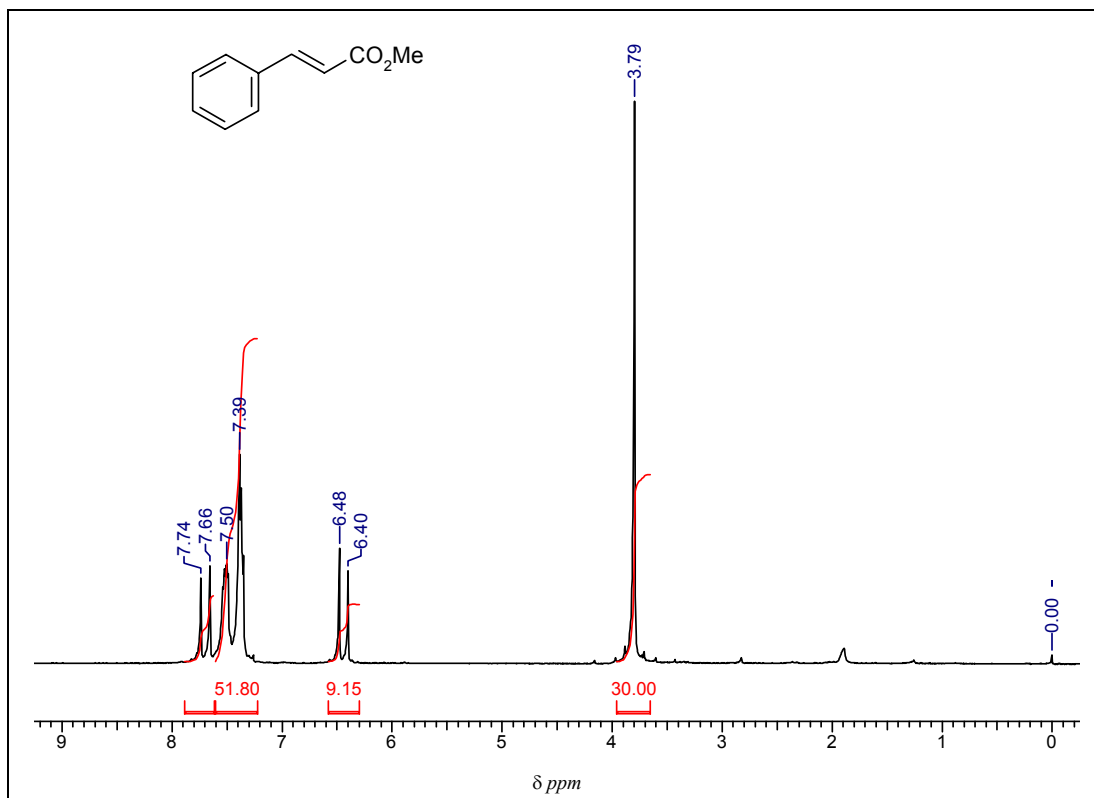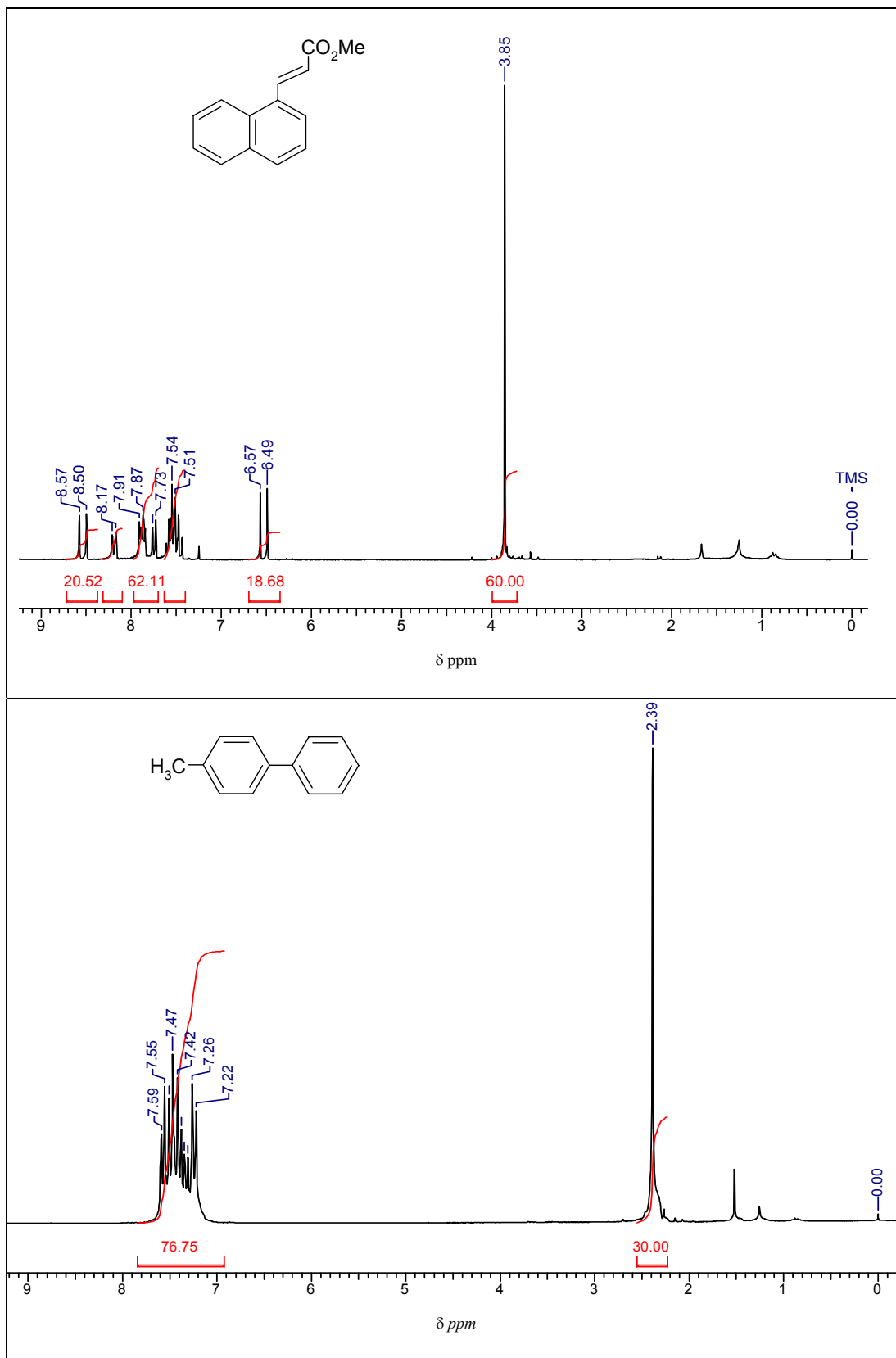
Chapter 6. SUMMARY AND CONCLUSIONS

_____

This thesis reports the investigations on the use of Cu and Mn Schiff base and peraza macrocyclic complexes as catalysts for selective oxidation of hydrocarbons viz., epoxidation, benzylic oxidation and cyclohexane oxidation. It also presents the studies carried out on the use of a new type of heterogeneous catalyst, Pd containing hydrotalcite, for carbon-carbon bond forming reactions viz., Heck reaction, Suzuki coupling and Sonogashira reaction.

6.1. Synthesis of Metal Complexes

SalenH$_2$ and salophH$_2$ are the acyclic Schiff bases used in the investigations, while tacn, tmtacn, cyclen, tmcyclen and cyclam are the peraza macrocycles chosen as the cyclic ligands. The synthetic method used for the preparation of the peraza macrocycles and their N-methylation has been generalized for tacn ([9]ane N$_3$), cyclen ([12]ane N$_4$) and cyclam ([14]ane N$_4$). The Cu and Mn peraza macrocyclic complexes have been prepared as their perchlorate salts. Efforts to isolate oxalate bridged Mn peraza macrocyclic complexes were not successful. Adamantane like [Mn$_4$O$_6$(tacn)$_4$]$^{+4}$ was isolated under basic conditions. Metal complexes were heterogenized by encapsulating them in zeolite –Y by the "flexible ligand" method.

6.2. Characterization of Metal Complexes

The complexes were characterized by elemental analysis, UV-visible, FT-IR and EPR spectroscopy. UV-visible and EPR spectra suggest that the stability of the metal complexes increases with increase in ring size of the macrocyclic ligand and decreases on its N-methylation. The effect of encapsulation on molecular association and geometry has been studied by UV-visible and EPR spectroscopic techniques. The

resolution in the hyperfine features in the EPR spectra reveals that isolated and monomeric complex species is present in the super cages of zeolite –Y. The higher $g_{||}$ values for Cu(salen) and Cu(saloph) (2.269 for Cu(salen)-Y and 2.282 for Cu(saloph)-Y) and lower $A_{||}$ values (163.3 G for Cu(salen)-Y and 160.0 G for Cu(saloph)-Y) confirm their square pyramidal geometry in zeolite cages with the zeolite framework providing the fifth coordination. Similar geometrical changes are observed with encapsulated Mn Schiff base complexes. In the case of the peraza macrocyclic complexes, the geometry of the metal complex depends on the size, number of nitrogen atoms and N-methylation. Comparing the EPR spectra of $[Cu(cyclam)]^{+2}$ in frozen solution and after encapsulation it is concluded that the square planar geometry of the complex does not change significantly upon encapsulation. UV-visible and EPR studies reveal $[Cu(cyclam)]^{+2}$ to be square planar, and $[Cu(cyclen)]^{+2}$ and $[Cu(tmcyclen)]^{+2}$ to be weakly pentacoordinated. The high $g_{||}$ and low $A_{||}$ values of $[Cu(tacn)]^{+2}$ and $[Cu(tmtacn)]^{+2}$ indicate a square pyramidal geometry for this complex. The shift in the d-d band to a lower wavelength supports such a molecular geometry. As no changes in the EPR parameters were noticed it is concluded that the structure of the complexes is unchanged on encapsulation. Except $[Mn(tacn)]^{+2}$, all the Mn complex molecules are monomers and isolated inside the zeolite cages. The retention of molecular geometry on encapsulation is also observed for Mn-peraza macrocyclic complexes. However, a lowering in symmetry of the complexes is observed.

6.3. Selective Oxidations with Metal Complexes as Catalysts

Catalytic activities of both neat and encapsulated Cu and Mn complexes have been evaluated for styrene epoxidation and ethylbenzene oxidation using H_2O_2 and *tert-*butyl hydroperoxide oxidants. Among all the complexes, only Mn(tmtacn) is catalytically active with H_2O_2 oxidant. An oxalate buffer is necessary to improve the

catalytic activity of [Mn(O)tmtacn]SO$_4$ during styrene epoxidation.   The oxalate buffer not only reduces the decomposition of H$_2$O$_2$ and but also helps in improving selectivity and conversion.   Since the other Mn-peraza macrocyclic complexes did not possess catalytic activity with H$_2$O$_2$, it appears that neither the ring size nor N-methylation that regulates the activation of H$_2$O$_2$ during the oxidation.   The other complexes are catalytically active with TBHP oxidant for styrene epoxidation and ethylbenzene oxidation. All the catalysts possess about 30% selectivity for styrene epoxide, 50 – 60% for benzaldehyde and 5-10% for phenylacetaldehyde. Under similar experimental conditions, Cu complexes are found to be more active and selective compared to Mn complexes. Also, there is an enhancement in the activity of the Schiff base complexes when encapsulated in zeolite – Y.   Among peraza macrocyclic complexes, better conversion and selectivity is observed only with [Cu(cyclam)]$^{+2}$ for the epoxidation of styrene with TBHP.

Oxidation of ethylbenzene with [Mn(O)(tmtacn)]SO$_4$ as the catalyst and H$_2$O$_2$ oxidant in the presence of an oxalate buffer occurs with turnover numbers of about 250 with acetophenone as the major product. Peraza macrocyclic Cu complexes exhibit good catalytic activity in ethylbenzene oxidation. The type of the macrocyclic ring affects the product selectivity. Ring hydroxylation is more with "neat" tetraaza complexes than with triaza complexes. It decreases with different peraza ligands in the order: tmcyclen > cyclen > cyclam> tacn > tmtacn.   Activity is suppressed and selectivity for AcPh is increased when the complexes are encapsulated.   Both conversion and selectivity are comparatively smaller in the case of the Mn-peraza complexes. Ring hydroxylation is also observed to be more. However, the selectivity for AcPh improves on encapsulation.

6.4. Selective Oxidations With *in situ* Prepared Mn-tmtacn Catalysts

The *in situ* prepared Mn-tmtacn complex exhibits excellent catalytic activity for the epoxidation of electron deficient, terminal and non-terminal olefins with H_2O_2. Enhancement in the catalytic activity is observed in the presence of carboxylate buffers. The nature of the buffer has a definite role in the activity of the complex. Ascorbate and oxalate buffers are found to increase the activity to a greater extent. Mn-tmtacn-oxalate buffer-H_2O_2 system is found to be efficient for benzylic oxidation of aromatics. A change of either metal ion or peraza macrocyclic ligand does not constitute a good system. Only decomposition of H_2O_2 is observed with the tacn complex and the other macrocycles do not exhibit any activity. The activity of *in situ* prepared Mn complexes is as good as isolated complexes. The Mn-tmtacn-oxalate buffer-H_2O_2 system is not efficient for the activation of the C-H bond of alkanes (cyclohexane). It is concluded from *in situ* spectroscopic studies that the oxo-manganese complexes are the active species involved in catalytic oxidation.

6.5. Pd-Hydrotalcite, a New Catalyst for Selective C-C Bond Forming Reactions

Pd(II) containing hydrotalcites, containing palladium in their structure, have been prepared with different Mg / Al and Pd / Mg ratios (Mg / Al = 2-3 and Pd / Mg = 0.01- 0.05) and characterized by elemental analysis, N_2 adsorption, powder XRD, etc. X- ray powder diffraction patterns reveal, in all the cases, the presence of a well-crystallized HT phase and most of the Pd(II) lying inside the brucite sheets of the hydrotalcite. The activity of the catalysts has been evaluated for Heck, Suzuki and Sonogashira reactions. The catalysts with a Pd loading of Pd / Mg $\cong$ 0.004 with Mg / Al $\cong$ 2.5 appear to be the most active ones with the turnover numbers exceeding 1000; these also underwent minimum leaching.

To conclude, in general, Cu and Mn complexes with Schiff base and peraza macrocyclic ligands can be good biomimetic catalysts for selective hydrocarbon oxidations. However, they have limited activity towards the oxidation of alkanes. Palladium containing hydrotalcites are a new type of heterogeneous catalysts for carbon-carbon bond forming reactions.

LIST OF PUBLICATIONS

_____

Papers Published / Communicated in International Journals

1. **T.H. Bennur**, D. Srinivas, P. Ratnasamy, "EPR spectroscopy of copper and manganese complexes encapsulated in zeolites", *Microporous and Mesoporous Materials* **2001,** *48,* 111.

2. **T.H. Bennur**, S. Sabne, S.S. Deshpande, D. Srinivas and S. Sivasanker, "Benzylic oxidation of aromatics with H_2O_2 catalyzed by manganese complexes of N, N', N"-trimethyl-1,4,7-triazacyclononane: Spectroscopic investigations of the active Mn species" *J. Mol. Catal: A Chem.,* **2002,** *185, 71.*

3. **T.H. Bennur**, A. Ramani, R. Bal, B.M. Chanda and S. Sivasanker**, "**Palladium (II) containing hydrotalcite as an efficient heterogeneous catalyst for Heck reaction" *Catal. Commun.* **2002,** *3,* 493.

4. **T.H. Bennur**, D. Srinivas and S. Sivasanker, "Regioselective oxidation of aromatics over neat and encapsulated Cu(II) tri- and tetraaza macrocyclic complexes" (*communicated).*

5. Nandkumar M. Patil, **T.H. Bennur,** Ashutosh A. Kelkar, D. Srinivas and R.V.Chaudhari, "Shape selective amination reaction using encapsulated copper complexes in Na-Y and MCM-41" *(manuscript under preparation).*

Posters Presented in National and International Conferences

1. **T.H. Bennur**, A. Ramani, S. Yuvaraj, B.M. Chanda and S. Sivasanker, "Heck reaction   catalyzed by transition metals containing hydrotalcite like anionic clays", poster presented at *International Symposium on Catalysis – CATSYMP-15 & IPCAT-2*, NCL Pune India, January **2000.**

2. **T.H. Bennur**, D. Srinivas and S. Sivasanker, "Selective Oxidation of Hydrocarbons with H_2O_2 Catalyzed by Manganese Complexes of N, N', N"-trimethyl-1,4,7-triazacyclononane" poster presented at *National Symposium in Chemistry 4,* NCL Pune India, February **2000**.

3. **T.H. Bennur**, V. Puranik, D. Srinivas and S. Sivasanker, "Structure and Spectroscopic Characterization of Cyclic Tri- and Tetraaza Mn Complexes: Catalytic Studies on Oxyfunctionalization of Hydrocarbons" poster presented at *16th National Symposium and 1st Indo-German Conference on Catalysis*, IICT Hyderabad, India February **2003**.